



International Energy Agency

*Energy Conservation in Buildings
and Community Systems Programme*

Annex 23: Multizone Air Flow Modelling

Evaluation of COMIS

Appendices

Edited by J.-M. Fürbringer
C.-A. Roulet
R. Borchellini

*Swiss Federal Institute of Technology, Lausanne
LESO.PB, Institute of Building Technology
1996*

INTERNATIONAL ENERGY AGENCY
Energy Conservation in Buildings and Community Systems Programme

Annex 23 : Multizone Air Flow Modelling

FINAL REPORT

EVALUATION OF COMIS

Appendices

Edited by

J.M. Fürbringer, LESO-PB, EPFL, CH-1015 Lausanne, Switzerland

C.A. Roulet, LESO-PB, EPFL, CH-1015 Lausanne, Switzerland

R. Borchiellini, Politecnico di Torino, Dipartimento di Energetica, Torino, Italy

WITH contributions from

F. Amara, INSA, France

A. Bossaer, BBRI, Belgium

E. Dascalaki, University of Athens, Greece

V. Dorer, EMPA, Switzerland

D. Ducarme, BBRI, Belgium

B. Geerinckx, BBRI, Belgium

F. Haghighat, Concordia University, Canada

F. Huck, EMPA, Switzerland

M. Orme, AIVC, UK

M. Santamouris, University of Athens, Greece

Y. Utsumi, Miyagi National College of Technology, Japan

A. Weber, EMPA, Switzerland

P. Wouters, BBRI, Belgium

H. Yoshino, Tohoku University, Japan

Y. Zhao, Tohoku University, Japan

TABLE OF CONTENT OF VOLUME 1

Preface	IV
IEA Executive committee members	V
Authors' Address list.....	VI
Summary	VII
How to get A23 documents, programs and data.....	VIII
Selection of some Annex 23 documents	IX
Introduction	1
1 Strategy, methods and tools.....	3
1.1 Strategy.....	3
1.2 Methods.....	7
1.3 Tools.....	13
1.4 References	18
2 Analytical evaluation.....	21
2.1 Introduction	21
2.2 A guide through the test cases	24
2.3 Conclusions from the analytical evaluation	35
2.4 References	36
3 Intermodel comparison.....	37
3.1 Introduction	37
3.2 Programs used for the comparisons.....	37
3.3 Comparison and results	42
3.4 Conclusion from the inter-model comparison.....	64
3.5 Algorithms for some of the air flow models used in 3.2.....	65
3.6 References	72
4 Experimental comparison.....	73
4.1 Introduction	73
4.2 OPTIBAT facility.....	79
4.3 Japan Solar House	83
4.4 Japanese Family House	87
4.5 LESO three storey office building.....	91
4.6 Belgian PASSYS cell.....	97
4.7 Belgian Flat	101
4.8 PASSYS Cell and large opening experiment in Greece.....	107
4.9 Italgas House	109
4.10 Conclusion of the comparison.....	113
4.11 References	114
5 User tests.....	115
5.1 Introduction	115
5.2 User tests on case 1	115
5.3 User tests on case 2	127
5.4 Conclusions	133
5.5 References	133
6 Synthesis.....	135
6.1 General results.....	135
6.2 Results from specific evaluation tasks	135
6.3 A few hints	137
6.4 Conclusion.....	137

TABLE OF CONTENT OF VOLUME 2

Preface.....	IV
IEA Executive committee members.....	V
Author's address list	VI
Summary.....	VII
How to get A23 documents, programs and data	VIII
Selection of some Annex 23 documents.....	IX
Introduction.....	1
A 1. LISA (Library for Sensitivity Analyses)	3
A 1.1 What is LISA?.....	3
A 1.2 Short description of functions.....	4
A 2. Multirun Interface for Sensitivity Analysis	7
A 2.1 Purpose of MISA	7
A 2.2 Required files	7
A 2.3 File structure	8
A 2.4 How to run MISA	12
A 3. The EMPA test cases.....	15
A 3.1 Structure of the test case data base.....	15
A 3.2 Content of the test case data base	15
A 4. Experimental evaluation.....	25
A 4.1 Introduction.....	25
A 4.2 The OPTIBAT facility	25
A 4.3 Japan Solar House.....	35
A 4.4 Japanese Family House.....	49
A 4.5 LESO three storey office building	61
A 4.6 Single sided ventilation in a 2-zone test cell.....	71
A 4.7 Namur Flat: Contaminant Spreading	93
A 4.8 PASSYS Cell In Greece.....	133
A 4.9 Large opening experiment in Greece	137
A 4.10 Italgas House.....	151
A 5. User Tests	169
A 5.1 Proposals for changes in the User Manual and COMVEN.....	169
A 5.2 Reference input file for case 2	170

PREFACE

International Energy Agency

In order to strengthen cooperation in the vital area of energy policy, an Agreement on an International Energy Programme was formulated among a number of industrialised countries in November 1974. The International Energy Agency (IEA) was established as an autonomous body within the Organisation for Economic Cooperation and Development (OECD) to administer that agreement. Twenty-two countries are currently members of the IEA, with the Commission of the European Communities participating under a special arrangement.

As one element of the International Energy Programme, the Participants undertake cooperative activities in energy research, development, and demonstration. A number of new and improved energy technologies which have the potential of making significant contributions to our energy needs were identified for collaborative efforts. The IEA Committee on Energy Research and Development (CRO), assisted by a small Secretariat staff, coordinates the energy research, development, and demonstration programme.

Energy Conservation in Buildings and Community Systems

As one element of the Energy Programme, the IEA encourages research and development in a number of areas related to energy. In one of these areas, energy conservation in buildings, the IEA is encouraging various exercises to predict more accurately the energy use of buildings, including comparison of existing computer programmes, building monitoring, comparison of calculation methods, as well as air quality and inhabitant behaviour studies.

The Executive Committee

Overall control of the R&D programme "Energy Conservation in Buildings and Community Systems" is maintained by an Executive Committee, which not only monitors existing projects but identifies new areas where collaborative effort may be beneficial. The Executive Committee ensures all projects fit into a predetermined strategy without unnecessary overlap or duplication but with effective liaison and communication.

Annex XXIII: Multizone Air Flow Modelling

The prediction and the control of the air flow patterns through the building is necessary to provide an efficient ventilation. Planning methods should allow that prediction from the earliest stage of a project, in order to enhance the comfort and the air quality while saving energy.

The general scope of the Annex XXIII is to provide a validated and user-friendly computer program, based on COMIS, for simulating air flow patterns in multizone buildings. This project has three subtasks:

- Subtask 1: Implementing new features in COMIS, including new models and user-friendly interface
- Subtask 2: Collecting data as well for input as for experimental comparison.
- Subtask 3: Evaluation of the code and its User Guide.

Countries participating to this annex are Belgium, Canada, France, Greece, Italy, Japan, the Netherlands, Switzerland, and USA. Moreover, IEA-ECB Annex V (Air Infiltration and Ventilation Centre) collaborated to this annex.

IEA EXECUTIVE COMMITTEE MEMBERS

Belgium	Prof. J. Lebrun
Canada	Dr. S. A. Barakat (chairman)
CEC	Mr. F. Conti
Denmark	Mr. P. Dorph-Petersen / O. Jensen
Germany	Mr. A. Le Marié
Greece	Mr. Malezious
Finland	Prof. R. Kohonen
France	Mr. P. Herant
Italy	Mr. C. Boffa / Mr. D. Malosti
Israel ()	Dr. J. Nowarski
Japan	Dr. Y. Kodama
Netherlands	Mr. P. Heijnen
New Zealand	Mr. P. Graham
Norway	Mr. J. Brunsell
Poland (Associate Member)	Prof. Mierzwinski
Sweden	Mr. J. Lagerstrom
Switzerland	Mr. Zimmermann (vice chairman)
Turkey	Prof. R. Oskay
UK	Dr. E. Perera / Mr. B. Austin / Mr. S. Irving
USA	Mr R. Karney

Chairman

Dr. S.A. Barakat, National Research Council of Canada, Building M-24, Ottawa, Ontario, Canada K1A 0R6, Fax: +1 613 954 3733

IEA Secretariat Liaison

Ms. Gudrun Maass, International Energy Agency, 2 rue Andre Pascal, 75016 Paris, France

EXECUTIVE SUMMARY

IEA-ECB&CS Annex 23 program intends to provide a validated and user-friendly computer code simulating air and contaminant flows in multizone buildings. When developing such a code, which intends to be a model of the reality, it is essential to check, at each step, its conformity with the model. At the other end, the claimed user-friendliness should also be checked with real users.

This evaluation task took a large part of the efforts and means put into Annex 23 by participating countries. The result is that COMIS was checked very carefully, using up-to-date strategies and tools. This report presents the methods used and the results of this huge validation task. The tools especially developed within this annex include the validation and user test strategy, methods and computer tools for sensitivity analysis of the code.

Simulation results were compared with more than 50 simple **benchmarks** or test cases, for which either an analytical or a numerical solution was obtained using classical tools (such as EXCEL or MATHEMATICA). Each of these test cases was created to check a particular feature of COMIS. This so-called analytical evaluation allowed the correction of several bugs which appeared in the early versions of COMIS.

Inter-model comparison with as much as 14 other simulation programs was performed by five different laboratories, using various objects. For each compared program, the objects were adapted or chosen in such a way that they could be modelled by the program. The result of these comparison is that all compared models provided the same results, within a very narrow dispersion band. This comes from the fact that these models all use similar algorithms and simulations were performed with identical input data. However, this also shows that, at least for the checked features, these models do not contain bugs.

The **experimental comparison** task conducted within Annex 23 is very likely the largest ever performed for a computer code. Nine different buildings were monitored for this purpose, each building offering several cases for comparison. For each case, a **sensitivity analysis** was performed, in order to know, not only the uncertainties on the measurements, but also the confidence intervals of the simulations, which result from uncertainties on input data. These were found to be very large. Therefore, the results from simulations and measurements were, in some cases, not significantly different. In other cases, however, important differences were found, showing errors in either the model or in the measurements.

The most significant differences were, however, found in the **user test**. Two cases were submitted to several different users and results were compared. One case was simple and clearly defined, with all essential input data provided. For this case, all users but one (who made a modelling error) provided the same results. The other case, however, was more realistic, since data were provided as usually available in practice: only building plans and some measurement results. The user not only had to design the network model, but also had to choose some essential input data, in particular the pressure coefficients. Very large differences in the results were found in this instance. Most discrepancies can be explained by modelling errors which are partly due to some unclear instructions in the draft User Guide, since corrected, and others from differences in input data.

The limits of applicability of COMIS were not found although they may exist. But other limitations were found by the user: the uncertainty of input data and the way a particular case is modelled have a large effect on the result. This Annex provides an important indication to the user on how the uncertainty of his result is related to the uncertainty of the input data.

AUTHORS' ADDRESS LIST

- J.-M. Fürbringer, NIST, Building Environment Division, Gaithersburg MD 20899, USA.
jean-marie.furbringer@nist.gov
- C.-A. Roulet, LESO, EPFL, CH-1015 Lausanne, Switzerland, claude.roulet@leso.da.epfl.ch
- R. Borchiellini, Politecnico di Torino, Dipartimento di Energetica, 24 C.so Duca degli
Abruzzi, I- 10129 Torino, Italy, borchiel@polito.it
- F. Amara, Insa, Rue Albert Einstein, Lyon, France
- A. Bossaer, BBRI, 21 Av. Pierre Holoffe, B-3142 Limelette, Belgium
- E. Dascalaki, University of Athens, Laboratory of Meteorology, Ippokratous 33, GR-10680
Athens, Greece
- V. Dorer, Empa, CH-8600 Dübendorf, Switzerland, dorer@empa.ch
- D. Ducarme, BBRI, 21 Av. Pierre Holoffe, B-3142 Limelette, Belgium
- B. Geerinckx, BBRI, 21 Av. Pierre Holoffe, B-3142 Limelette, Belgium
- F. Haghghat, Centre for Building Studies, Concordia University, 1455 de Maisonneuve Blvd.
W., Montreal, Quebec H3G 1M8, Canada
- F. Huck, Empa, CH-8600 Dübendorf, Switzerland, huck@empa.ch
- M. Orme, AIVC, University of Warwick Science Park, Sir William Lyons Rd., Coventry CV4
7EZ, UK, msorme@aivc.org
- M. Santamouris, University of Athens, Laboratory of Meteorology, Ippokratous 33, GR-10680
Athens, Greece
- Y. Utsumi, Miyagi National College of Technology, Dep. of Architecture, Medeshima Natori,
Miyagi 981-12, Japan
- A. Weber, Empa, CH-8600 Dübendorf, Switzerland, andreasweber@empa.ch
- P. Wouters, BBRI, 21 Av. Pierre Holoffe, B-3142 Limelette, Belgium
- H. Yoshino, Tohoku University, Sendai, Japan
- Y. Zhao, Tohoku University, Sendai, Japan

HOW TO GET A23 DOCUMENTS, PROGRAMS AND DATA

- Copies of this report can be obtained from:
C.-A. Roulet, LESO, EPFL, CH-1015 Lausanne, Switzerland,
claude.roulet@leso.da.epfl.ch
- as well as the following software:
 - MISA (Multirun Interface for Sensitivity Analysis), which is an interface for COMIS working on DOS, UNIX or VMS
 - LiSA (library for design of experiment), which runs within MATLAB
 - MATLAB which is a mathematical software can be obtained from:
The Math Works, Inc. 24 prime Park Way, Natick, Mass. 01760-1500, USA
On Netscape: <http://www.matworks.com>
E-mail: info@mathworks.com
 - COMIS (COMVEN) which is the multizone air flow program evaluated in this report can be obtained from:
H. Feustel, Lawrence Berkeley Laboratory, Building 90, Room 3074, 1 Cyclotron Road, Berkeley, CA 94720, USA. hefeustel@lbl.gov
The availability is submitted to IEA rules and you will probably be directed to your national contact (cf. IEA information at the beginning of this report).
 - Annex 23 Papers can be obtained from the authors
 - Evaluation data can be obtained from the authors

SELECTION OF SOME ANNEX 23 DOCUMENTS

The following documents have been selected by the editors to enlarge the view over the annex and especially over subtask 3. There are as well manuals of the Annex as working documents whose interest exceeds their status of internal documents but which have not yet been distributed more widely and whose content has not been reported in this report by care of conciseness. There are also publications which summarise the work. A comprehensive list of the Annex 23 documents and publications can be found in the operating agent report. The listed papers can be ordered to their author.

Borchiellini R.: The inverse problem theory applied to air flow estimation and experiment design in the multizone case. *Paper presented at International Symposium on Air Flow in Multizone Buildings, Technical University of Budapest, Hungary, September 8, 1992. IEA.ECB.A23/92.09.08/RB.*

COMIS: Fundamentals of the Multizone Air Flow Model - COMIS. *Technical Note AIVC 29, May 1990.*

COMIS: COMIS User Guide.

Fürbringer J.-M.: Evaluation procedure using sensitivity analysis of models and measurements. *Paper presented at International Symposium on Air Flow in Multizone Buildings, Technical University of Budapest, Hungary, September 8, 1992. IEA.ECB.A23/92.09.09/JMF*

Fürbringer J.-M., Dorer V.: Air flow simulation of the LESO building including comparison with measurements and sensitivity analysis. *Proc. INDOOR AIR '93, Finland, 1993.*

Fürbringer J.-M., Borchiellini R.: Technique of sensitivity analysis applied to an air infiltration multizone model. *ASHRAE trans. Vol. 100, part 2, pp. 683-691, 1994.*

Fürbringer J.M.: Comparison of the accuracy of detailed and simple models of air infiltration. *Proc. 15th AIVC conf. Buxton, Sept. 1994.*

Fürbringer J.M., Roulet C.-A.: Sensitivity analysis- an unavoidable step in the evaluation of simulation program. *Proc. European conf. on Energy Performance and indoor Climate in Buildings, Lyon, Nov. 1994.*

Fürbringer J.M., Roulet C.-A.: The evaluation of a multizone infiltration Computer Code, 2nd int. Conf. on IAQ and ECB, Montreal, May 10-12, 1995.

Geerinckx B., Wouters P.: Empirical methodology to validate energy related simulation programs. *Paper presented at International Symposium on Air Flow in Multizone Buildings, Technical University of Budapest, Hungary, September 8, 1992. IEA.ECB.A23/92.09.09/BG*

Pelletret R., Feustel H.: A23: General presentation. *Paper presented at The ExCo meeting in Sophia Antipolis, France, 2-4 June 1992, IEA.ECB.A23/92.06.01/RP*

Rao J., Haghghat F.: A procedure for sensitivity analysis of airflow in multizone buildings. *Paper presented at International Symposium on Air Flow in Multizone Buildings, Technical University of Budapest, Hungary, September 8, 1992. IEA.ECB.A23/92.09.09/JR*

Roulet C.-A., Fürbringer J.-M.: The evaluation of a multizone infiltration computer code. *Paper presented at International Symposium on Air Flow in Multizone Buildings, Technical University of Budapest, Hungary, September 8, 1992. IEA.ECB.A23/92.09.09/CAR*

Wouters P.: Validated simulation tools: possibilities and limitations. *Paper distributed at the Tokyo E.M. IEA.ECB.A23/94.09.19/PW.*

INTRODUCTION

This volume of the report on the evaluation of COMIS contains, as appendices to the main report, information which may be of interest to those readers who intend to go deeper in the topic.

Appendix 1 describes the Library for Sensitivity Analyses (LiSA) created within the frame of this annex to prepare and interpret sensitivity analyses. LiSA is at the prototype level, but can be used by newcomers after some learning. LiSA may therefore be of great help for researchers performing sensitivity analysis

Appendix 2 presents MISA, a package of computer code prepared to automatically perform sensitivity analysis on COMIS.

A detailed presentation of the benchmarks prepared by the EMPA is given in Appendix 3, together with the results obtained with COMSI on each of these benchmarks.

Appendix 4 is the main part of this volume. It contains the detailed description of all experimental comparisons, including a description of the measured objects, the measurement performed, the comparisons and the sensitivity analysis.

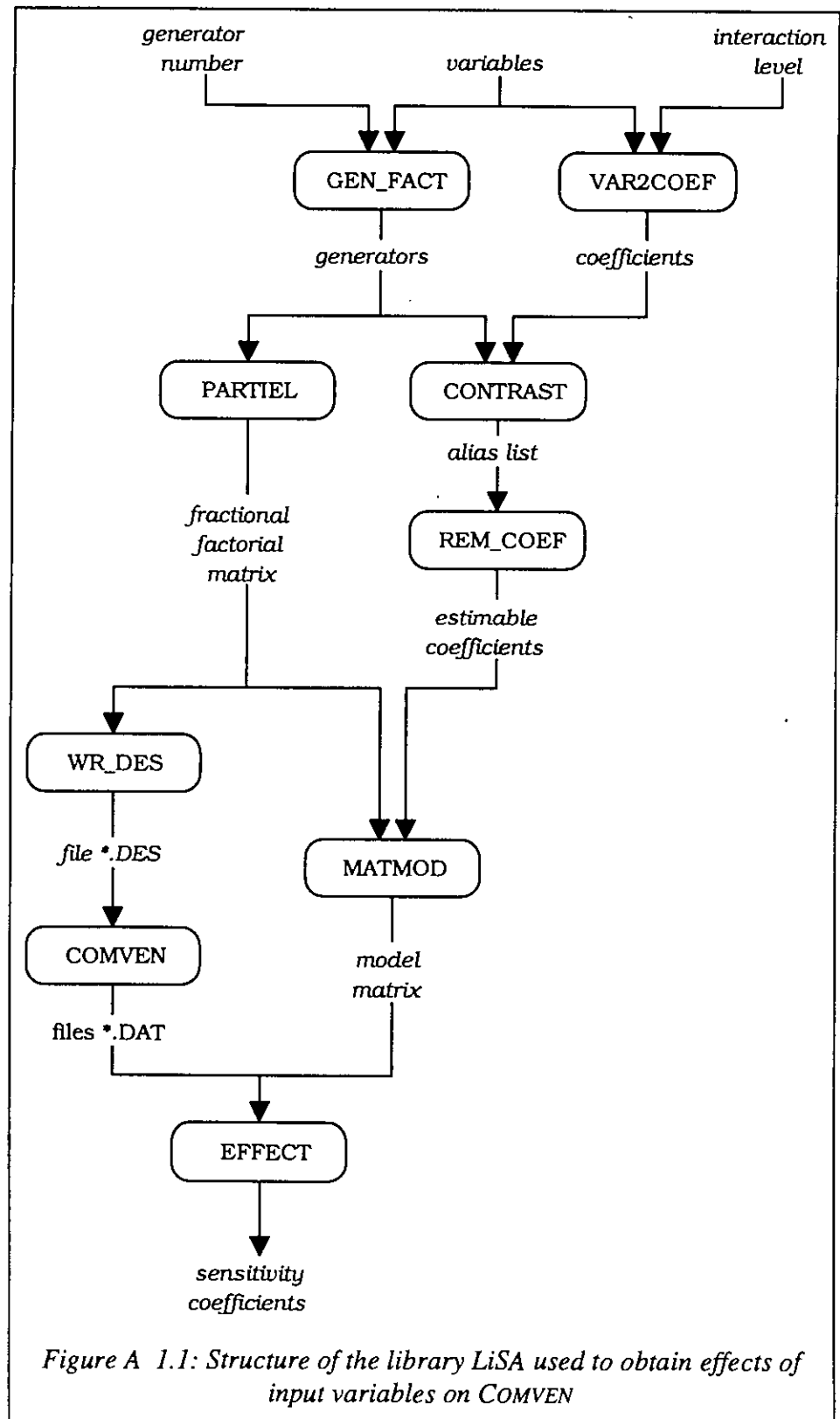
Appendix 5 is related to the User tests. It contains first a list of changes resulting from this test, and also the input file used as reference.

A 1. LISA (LIBRARY FOR SENSITIVITY ANALYSES)

A 1.1 What is LISA?

A library called LiSA (Library for Sensitivity Analyses) was devised within the mathematical software MATLAB for the design of simulations and their analyses. The list of the main functions is given below. The library is available for PC, UNIX or MACINTOSH from the LESO group (cf. p. 9).

Figure 1.5 shows how the functions are used. They can be linked through script files or used on-line one after the other. A short description of the main functions is given below. A minimum of knowledge of experiment planning theory is required to use them. For that we recommend reading one of these references: [Box et al. 1978, Gunter 1993, Goupy 1988 or Fürbringer 1994].



A 1.2 Short description of functions

alias.m	determines the aliases of a given matrix.
aliasrec.m	is a recursive function which gives aliases of the experiment matrix.
alias_tb.m	displays the table of aliases and generators.
ar.m	calculates the Archimedes number.
brevent.m	is an air infiltration model for houses from the BRE.
chi2.m	is the chi square function.
chi2test.m	is the test of the chi square.
coef_int	extracts the parameters from the index of the list of coefficients.
comb.m	is the combination of A objects by B: (A,B)
combine.m	is the recursive function providing the combinations of elements of a list k by k.
combine3.m	provides the combinations of n variables 3 by 3 without repeating any couples.
concat.m	concatenates two text strings. An optional growth argument allows one to complete the text string with blanks.
concat_s.m	concatenates two variable names with a separator.
contrast.m	provides the contrast series (by line in 'alias'). The coefficients are referred to by their indices in variable 'coef'.
corr.m	computes the correlation matrix from the matrix of the model.
des_ana.m	computes the related matrices of the model matrix X.
ef_ana.m	computes the sums of the squares of sensitivity coefficients.
effect.m	computes effects from the matrix of the model and the response vector. The algorithm computes $\text{inv}(X'X) X'\text{Rep}$.
ef_fract.m	computes effects from the matrix of the model and the response vector avoiding the matrix inversion.
ELA.m	computes the equivalent leakage area (ELA) from air tightness coefficients and for given pressure and temperature.
fact.m	computes the factorial of the input integer.
fact_mat.m	generates a full factorial matrix.
findcoef.m	provides the index in the list of coefficients of the combined coefficient.
findgen.m	provides a generator either from its list or from the generation function.
forec.m	is a recursive function providing the series of interaction coefficients of the level L. The strings are of the form 'Xi_Xj...'.
fracsens.m	computes effects of a fractional factorial design and draws the bar charts of the effects.
fracti4.m	generates a fractional factorial matrix of resolution IV for 2^k variables containing 2^{k+1} runs.

- g_gauss.m** is a generalised normal distribution.
- had2exp.m** transforms a Plackett-Burman matrix in a matrix of experiments. This function is used for defining blocs.
- had_jmf.m** generates an Plackett-Burman matrix from a generator (MATLAB has its own Plackett-Burman function which provides matrices only for 2^N variables).
- int_coef.m** provides all the interactions of k parameters till level L.
- invexp.m** inverts $(X'X)$ where X is a model matrix.
- lognorm.m** is a lognormal function of x for the mean μ and the standard deviation σ .
- matflow.m** reads flow matrix files (MAT_FLOW.DAT) of COMVEN_MISA
- matmod.m** computes the model matrix from the matrix of experiments and the coefficient vector.
- mat_mcf.m** merges a factorial matrix with a Monte-Carlo matrix with a given ratio between the range of the factorial and the Monte Carlo design.
- mergerow.m** merges two rows of a matrix, re-sizing it if necessary.
- mod_test.m** provides a response vector for a model $(Ax+Bxy+Cy+D)$.
- normal.m** is a normal distribution of x for the mean μ and the standard deviation σ .
- numerote.m** adds a first column corresponding to the number of the row to a given matrix.
- N_factIV.m** computes the optimal number of parameter for a given number of experiments when using fractional factorial $2^{(N-k)}$ of resolution IV
- partiel.m** generates a fractional factorial matrix for Nfact factors with the generator GEN having the form 5=123 (not I=1235).
- procol.m** computes the product of the columns i and j of a matrix.
- psychro.m** computes the density of air depending on temperature, pressure and humidity.
- recht.m** generates a 'Rechtschafner' design for n factors.
- rem_coef.m** provides the list of the remaining coefficients after cutting the aliases.
- subgen.m** cuts elements in a generator.
- test_id.m** tests if a vector is parallel to the identity vector.
- trier.m** sorts the coefficients corresponding to the index in the alias matrix. When necessary the classes are merged.
- trier_rec.m** is a recursive function for the screening of the generator. The function sorts the aliases found in the generator and in the coefficient list .
- VAR2COEF** creates the list of the coefficients from the list of the variables.

A 2. MULTIRUN INTERFACE FOR SENSITIVITY ANALYSIS

A 2.1 Purpose of MISA

This chapter constitutes a user guide for MISA which is available for PC, VMS and UNIX. MISA, which means Multirun Interface for Sensitivity Analysis, is the software used for the sensitivity analysis of COMVEN. At that stage of development no user friendly program is available to design the planning of the simulation nor to process the result files. These features will be available only with SAM (Sensitivity Analysis Module) to be included in COMIS 3.0.

MISA prepares a series of input files for COMVEN, according to proper experimental planning. It then runs COMVEN as many times as necessary and collects the resulting outputs.

A 2.2 Required files

Files and applications, necessary to run MISA, were provided (and could still be) by the LESO. As far as possible, source files are available to allow the user to adapt the code when necessary. The following files are required :

<i>Source</i>	<i>Executable</i>	<i>Language</i>	<i>compiler</i>
	INSTALL.BAT	DOS	
MISA.BAS	MISA.EXE	QUICK BASIC	
MISA.COM	-	DCL (VMS)	
MISA.csh	-	C-shell (UNIX)	
GENER.FOR	GENER.EXE	FORTRAN 77	WATCOM (PC)
UTIL.FOR			
UTIL77.FOR			
	COMVEN.EXE	FORTRAN 77	WATCOM (PC)
	COMIS.SET		
	DOS4GW.EXE		
MISA.FIL		text files	
TEST.RG			
TEST.DES			
ITAL32.REF			

The main program MISA.EXE is replaced on VMS by a command procedure in DCL (MISA.COM) and in UNIX by a script (MISA.csh) in C-shell. DOS4GW which is a high memory manager is no longer necessary on VMS or UNIX.

A 2.3 File structure

The exchange of files between the programs follows the scheme presented in Figure A 2.1.

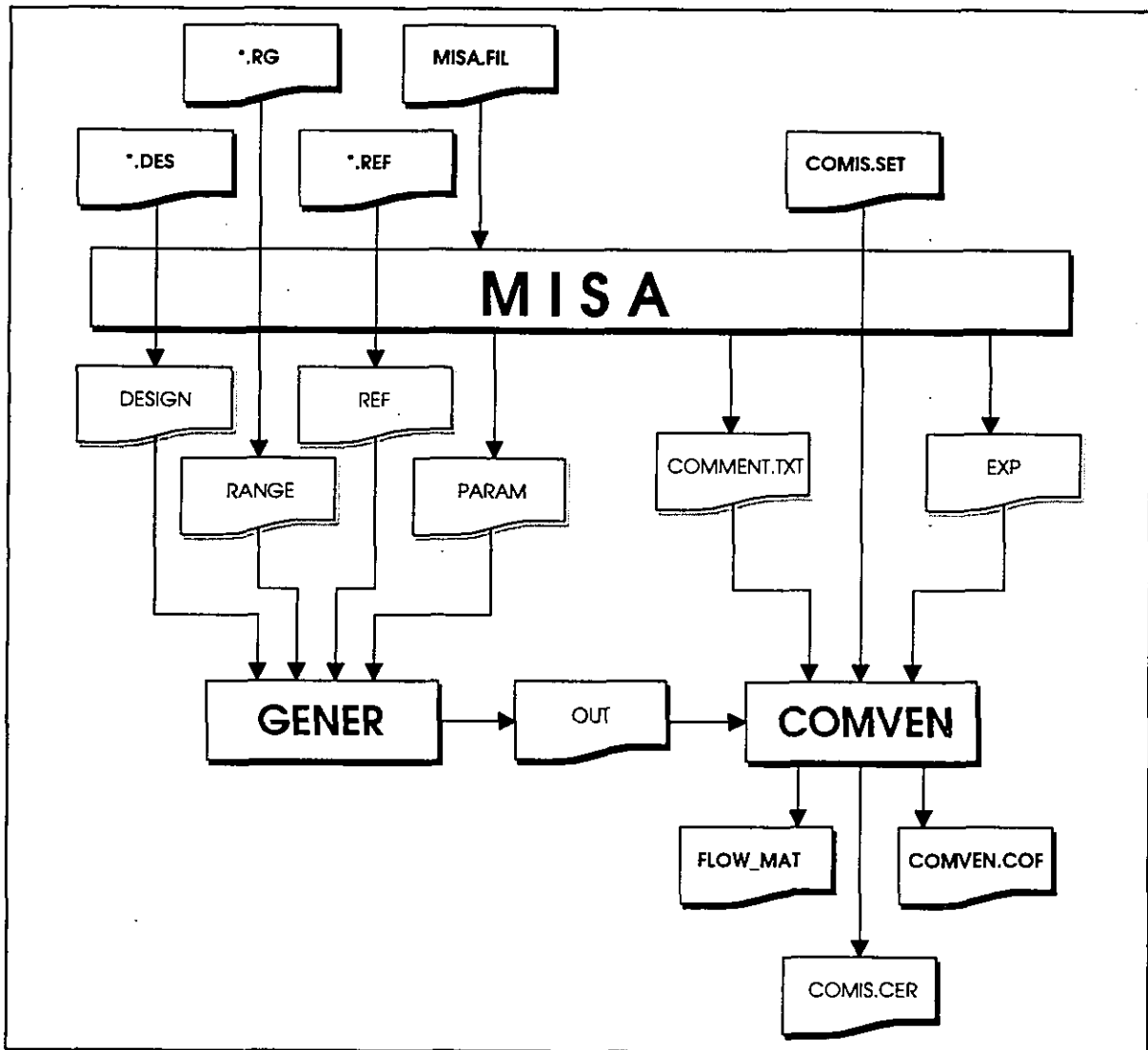


Figure A 2.1: Exchange of files between MISA, GENER and COMVEN

Here below is a short description of the main files:

- INSTALL.BAT** The installation program, written in DOS, creates a sub directory /MISA on a hard disk and copies the files from the diskette. Go in the (sub)directory which must contain MISA sub directory and type 'A: INSTALL' (or 'B: INSTALL').
- MISA.EXE** The executable of MISA, which manages the different runs of GENER and COMVEN. If the operating system is VMS MISA.COM must be used, and MISA.csh for UNIX. Type 'MISA' to run it. But it requires specific input files: MISA.FIL, *.RG, *.REF, *.DES
- MISA.COM**
- MISA.csh**

- GENER.EXE** The executable of GENER which produces the input file for COMVEN according to the requirement described in the files RANGE, REF, DESIGN and PARAM. These files are prepared by MISA.EXE. GENER produces a COMIS input file called OUT which is deleted each time by MISA before running GENER. This compiled version of GENER needs DOS-extender DOS4GW, so the corresponding command line included in MISA.BAS is 'DOS4GW GENER'. To be compiled, GENER.FOR needs subroutines included in UTIL.FOR. Another compiler could be also used, but if so the code in MISA must be changed. GENER has been designed to process any input file with the technique of the numbered flags.
- COMVEN.EXE** The executable of an adapted version of COMVEN. The changes with respect to the official version concern the output which provides some additional post processed data. The successive runs append the outputs to the preceding output files (comven.cof, flow_mat.dat). This compiled version needs the DOS-extender DOS4GW, so the corresponding command line included in MISA.BAS is 'DOS4GW COMVEN'. The COMIS.SET file has also been adapted.
- DOS4GW.EXE** A DOS extender for COMVEN.EXE which makes the use of a larger memory possible.
- MISA.FIL** This is a text file giving the names of the input files for GENER. The format is as follows:
- reference file name
 - range file name
 - nij file name (when any put 'any')
 - COMVEN input file name (OUT)
 - design file name
- ITAL32.REF** It is an example of a reference file with 32 variables. It is a *.CIF file where the values to be changed are replaced by numbered flags \$1, \$2, etc. There is no requirement regarding the order of the flags in this file. But of course, the number of each flag must correspond to the order of the variables in *.RG and *.DES.
- TEST.RG** It is an example of a range file. It is a text file. Each line corresponds to a variable, hence to a flag in the reference file. Clearly, the first line corresponds to the first flag \$1, the second to \$2 and so on.
- The format is as follows: 'Integer,tab,floating point number,tab,floating point number,tab,character'.
- Example:
- | | | | |
|---|------|------|-------------------------------|
| 3 | 1.2 | 2.6 | wind speed(m/s) |
| 4 | .001 | .002 | Cdoor (kg/s Pa ⁿ) |
- ↑ ↑ ↑ ↑
 order min max. comment

TEST.DES This is an example of a design file. It is a text file containing the matrix of experiments X_{ij} . Each line corresponds to a run i and each column to a variable j . Each line begins with a \$, a space and a number allowing the use of long lines. Then line i has the following structure:

$$\$ i \quad X_{i1} \quad X_{i2} \quad X_{i3} \quad X_{i4} \quad X_{i5} \quad \dots$$

As no user friendly software to build this matrix exists, the LESO provided, on request, suitable matrices for the sensitivity analysis. Random matrices can also be used to perform Monte Carlo analysis [Lomas *et al*, 1992].

If the directory is checked during the run of MISA, the following files can be seen:

COMMENT.TXT This is a comment file produced by GENER for COMVEN.

PARAM This is a file for parameter transmission between MISA and GENER.

REF The current reference, range and design files to be read by GENER.

RANGE MISA makes a copy of the files listed in MISA.FIL.

DESIGN

OUT The current COMIS input file produced by GENER and to be processed by COMVEN.

FLOW_MATDAT An additional output file of COMVEN giving the flow matrix Q_{ij} of the building with a semicolon to separate the fields.

```
***** FLOW MATRIX ***** Experiment 1
```

```
MISA asks for a comment (this is an example comment)
```

```
COMVEN puts it into the output files.
```

```
0.210780;-0.210780; 0.000000; 0.000000; 0.000000; 0.000000
0.000000; 0.421606; 0.000000; 0.000000; 0.000000; 0.000000
0.000000;-0.210780; 0.210780; 0.000000; 0.000000; 0.000000
-0.210780; 0.000000; 0.000000; 0.210780; 0.000000; 0.000000
0.000000; 0.000000; 0.000000;-0.210780; 0.421611;-0.210780
0.000000; 0.000000;-0.210780; 0.000000; 0.000000; 0.210780
```

```
***** FLOW MATRIX ***** Experiment 2
```

```
MISA asks for a comment (this is an example comment)
```

```
COMVEN puts it into the output files.
```

```
0.210780;-0.210780; 0.000000; 0.000000; 0.000000; 0.000000
0.000000; 0.421606; 0.000000; 0.000000; 0.000000; 0.000000
0.000000;-0.210780; 0.210780; 0.000000; 0.000000; 0.000000
-0.210780; 0.000000; 0.000000; 0.210780; 0.000000; 0.000000
0.000000; 0.000000; 0.000000;-0.210780; 0.421611;-0.210780
0.000000; 0.000000;-0.210780; 0.000000; 0.000000; 0.210780
```

nij file

Data file from tracer gas measurement. The n_{ij} values are the coefficients of the multilinear relation between the flows measured by the tracer gas method and the flows computed with COMIS. For details please see [Dorer et al]. The format of that file is:

```

Day          361.125    361.146    ...
Date        27-Dez     27-Dez     ...
Time        03h00     03h30     ...

[    5]  {    1}    3.30E-03  7.42E-03  ...
[    3]  {    1}    3.42E-03  7.88E-03  ...

```

When such a file is provided, COMVEN (MISA version) produces a QAI.DAT file whose flows can be compared with experimental data.

When not necessary just put 'any' in its place in MISA.FIL. COMVEN will produce a comment in the COMIS.CER file but the simulation will run correctly.

AIR_AGE.DAT: the age of air matrix for the building

```
***** AGE OF AIR MATRIX ***** Experiment 1
```

MISA asks for a comment (this is an example comment)
COMVEN puts it into the output files.

```

47.44    71.16    0.00    0.00    0.00    0.00
 0.00    71.16    0.00    0.00    0.00    0.00
 0.00    71.16   237.21    0.00    0.00    0.00
47.44    71.16    0.00    94.89    0.00    0.00
23.72    71.15   118.59    47.44   237.19   118.59
 0.00    71.16   237.21    0.00    0.00   237.21

```

```
***** AGE OF AIR MATRIX ***** Experiment 2
```

MISA asks for a comment (this is an example comment)
COMVEN puts it into the output files.

```

47.44    71.16    0.00    0.00    0.00    0.00
 0.00    71.16    0.00    0.00    0.00    0.00
 0.00    71.16   237.21    0.00    0.00    0.00
47.44    71.16    0.00    94.89    0.00    0.00
23.72    71.15   118.59    47.44   237.19   118.59
 0.00    71.16   237.21    0.00    0.00   237.21

```

MEAN_AGE.DAT : the mean age of air for each zone of the building

```
MISA asks for a comment (this is an example comment)
CONVEN puts it into the output files.
```

```
118.60    71.16    308.37    213.48    616.67    545.59
118.60    71.16    308.37    213.48    616.67    545.59
```

A 2.4 How to run MISA

A 2.4.1 Preparation phase

The starting point is a correct *.CIF file for the considered case, and then, the following files have to be built:

- the *.REF file: analysing your building, select the parameters you want to vary and replace them with numbered flags (\$1,\$2,etc.) in the *.CIF file. A safe way to do that is to put a '#' at the beginning of the line, changing it in a comment line and writing the new line with the flag just below. That allows you to rapidly eliminate a variable if necessary.
- the *.RG file: use a line editor to write this file in which you give a range for all the variables corresponding to flags (for the format, see the example).
- The suitable *.DES file was provided on request by the LESO. Fractional factorial designs are found in the literature for up to 11 groups of parameters. For higher numbers, they must be built. Grouping some variables allows a smaller number of simulations. In a group, all the variables vary in the same time, and in the same proportion. Designs for 12, 24 and 32 groups have now been built and studied, so as much as possible we will use them. For small range, if small interaction can be assumed, Plackett-Burman designs are available for the following numbers of variables: 8, 12, 16, 20, 21, 28, 32, 36, 40, 44, 48, 52, 56, 60, 64, 68, 72, 76, 80, 84, 88, 92, 96, 100. A Monte Carlo analysis can also be performed using a random generator to generate a matrix of experiments. As the values in the matrix of experiments are standardised, be sure to correctly interpret the parameters of the used distribution. Typically, the uniform distribution is given by its range and not its standard deviation.

A 2.4.2 Running phase

- Put the files (*.REF, *.RG,*.DES,) in the MISA sub directory
- Fill up the MISA.FIL file
- Type 'misa'

The program shows you the files it will process and asks :

- for the 'number of variables' which, strictly speaking, must be greater or equal to the number of flags in *.REF and smaller or equal to the number of lines in *.RG and the number of columns in *.DES. That allows you to rapidly eliminate (to fix) a variable using the same design and range files.

- for the 'number of the first run' which must be between 1 and the number of lines in the design file *.DES,
- for the 'number of the last run' which must be between 1 and the number of lines in the design file,
- if you want an echo of the created *.CIF file

MISA can also be started with those numbers as parameters: 'misa 32 1 20 0' which require 32 variables, from the run 1 to 20 of the design, without echo of the *.CIF file. (You may try that command as an example).

The program then asks for a comment to be put into the COMVEN output files. Eventually the program works by itself, performing the required simulation. However, this can take some time: have a coffee break.

If you have a problem of memory space on a PC, try to run MISA from a DOS window within WINDOWS.

A 2.4.3 Post processing phase

The post processing phase will be performed more easily on a worksheet.

The following operation should be done:

- to build the model matrix M from the matrix of experiments X with the routine 'mat-mod.m' of LiSA [F yrbringer,1992].
- to put the result to be analysed (same output parameter for each run) in a column vector R (for response)
- calculate the vector $\alpha = (M^T M)^{-1} M^T R$ with the routine 'ef_fract.m' or 'effect.m' of LiSA (but for factorial design $(M^T M)^{-1} = I_N / N$ where I_N is the identity matrix of dimension N), α is the vector containing the coefficients of the model corresponding to the matrix M :

$$R = \alpha_0 + \sum_i \alpha_i X_i + \sum_{i \neq j} \alpha_{ij} X_i X_j + \dots$$

One method of analysis is to plot in a bar chart the relative effects α_i / α_0 , α_{ij} / α_0 , ... to highlight the important parameters.

- The standard deviation $s(R)$ of the response can be used to estimate its confidence interval [F yrbringer,1994].

A 3. THE EMPA TEST CASES

A 3.1 Structure of the test case data base

Technical reports: 'Problem description and analytical results' on individual subjects:		
Report on Subject 1	- Subject 2	- Subject 3

Data Base: ASCII Files (at EMPA and on LBL Annex Information System)

SUMMARY FILE	TESTFILES.RES
List of subjects and list of the respective XX. RES files	subject:
For	subject
- Short description of the test subject	files
- List of CIF test files	
- Name of respective result summary file	

SUBJECT SUMMARY FILE	CPTST.RES	XX.RES	YY.RES
Subject 1 (e.g. Wind pressures)		Subject 2	Subject 3
- Subject description			
- Input file names			
- Parameters			
- Per test case:			
-- Analytical Results			
-- COMVEN Output			
-- Conclusions			
-- Actions			

XX.CIF	XX.COF	CIF	COF	CIF	COF
Input files	Output files	Input	Output		
(several versions)	(several versions)				

A 3.2 Content of the test case data base

The content of the test case data base is described according to the structure given below. The same information is given in the file 'Testfiles.res'.

SUBJECT-ACRONYM

- Description:** This part describes in a few words the aims and purposes of the specific tests contained under the relevant subject header.
- Input files:** The names of the individual *.CIF files contained in the database.
- Output files:** The names of the individual *.COF files contained in the database.
- Results:** The name of the respective *.RES summary file. This file contains input and output file names, gives the most important input values and describes the analytical solution by giving the equations used or by making reference to separate technical reports.
This files also contains the results of this analytical solution and the respective result values as calculated by the different COMVEN versions*). This file ends with the conclusions.
- Analytical:** Here reference is made to where the analytical solution is documented.
- Conclusions:** Here the most important findings from the testing are summarised. The conclusions might not be valid anymore for COMVEN versions issued after the compilation of this report.

*) *COMVEN version numbers refer to the EMPA numbering system, cross-references to LBL version numbers may be found on the AIS version file.*

CPTEST

- Description** In these test files a list of wind pressure coefficients is entered under the CP-VALUES keyword. Cp-values are given for the four facade-elements of a rectangular monozone building for different wind directions (relative to the building x-axis). With a set of files CPTTEST*.CIF is tested, whether the program correctly interpolates the Cp-values for different orientations of the building x-axis and for different wind directions (relative to north).
- Input files:** CPTTEST0.CIF, CPTTEST30.CIF, CPTTEST60.CIF
- Output files:** CPTTEST0.COF, CPTTEST30.COF, CPTTEST60.COF
- Results:** CPTTEST.RES
- Analytical:** Equations are given in the *.RES file
- Conclusions:** The calculation of wind pressure and mass flow for this simple example is done correctly. A change of the orientation of the building x-axis is considered correctly.

LAYLOPO

- Description** These files test whether COMVEN correctly calculates the time dependent concentration of a pollutant in a two room building, and whether the influence of the concentration difference between the two zones on the mass flow through a large opening between the zones, is calculated correctly. The same test is run for different time steps and the influence of

the step length on the final results for mass flow and concentration is investigated.

Input files: LAYLOPO1.CIF, LAYLOPO2.CIF, LAYLOPO3.CIF, LAYLOPO4.CIF, LAYLOPO5.CIF

Output files: LAYLOPO1.COF, LAYLOPO2.COF, LAYLOPO3.COF, LAYLOPO4.COF, LAYLOPO5.COF

Results: LAYLOPO.RES

Analytical: Equations are solved using MATHEMATICA

Conclusions: The calculation of the pollutant concentration in the zones is done correctly. The influence of the concentration difference on the mass flow through the large opening is calculated correctly. The final results of the concentrations depend significantly on the time step length chosen by the user. For those cases where the mass flows depend on the time dependent concentrations it is very important to choose a short enough time step (about 0.1 to 0.2 of the zone time constant) to avoid incorrect results.

METTEST

Description The subject of these files is to test, whether COMVEN correctly calculates the barometric pressure and the air-density at the altitude of the building. The tests are run for different altitudes of building and meteorisation and for different values of temperature, humidity and pressure (measured at the meteor station).

Input files: METTEST1.CIF, METTEST2.CIF, METTEST3.CIF, METTEST4.CIF, METTEST5.CIF

Output files: METTEST1.COF, METTEST2.COF, METTEST3.COF, METTEST4.COF, METTEST5.COF

Results: METTEST.RES

Analytical: Equations are given in the *.RES file

Conclusions: The values of pressure at building height and of density outside and inside are calculated correctly. The values entered under the SCH-METeo data keyword are related to the altitude of the meteor station. Temperature and humidity are constant for all altitudes. (Humidity is the ratio of mass of water to mass of dry air!), the changes of molar mass (and density) due to changes of humidity are calculated correctly (less humidity → higher molar mass).

S2ZOCR

Description Test cases for network and cracks: two zone building, layers, temperature-, humidity- and pollutant-gradients; cracks at different heights.

Input files: S2ZOCR_x.CIF (x = 1, 2, 3, 4, 5, 6, 7, 8a, 8b, 9a, 9b, 9c, 10, 11a, 11b, 12a, 12b, 12c, 12d, 13a, 13b, 13c, 13d, 13e, 13f)

Output files: S2ZOCR_x.COF (x = 1, 2, 3, 4, 5, 6, 7, 8a, 8b, 9a, 9b, 9c, 10, 11b, 12a, 12b, 12c, 12d, 13a, 13c, 13d, 13e, 13f)

Results: S2ZOCR.RES

Analytical: The analytical problem is documented in [Schauwecker, 1993 a]

Conclusions: Version 2 (cracks at start heights of layers): This case is calculated wrongly in COMVEN 1-8E. This bug has been fixed in COMVEN 1-3EA. Version 3: The parameters "flow to next layer factor" and "flow to zone factor" have no influence on the result. Version 4 (non horizontal links): In the MATHEMATICA calculation routine the non horizontal cracks are treated in the same way as horizontal cracks at link height in the zone the air is flowing into. This way of calculation may lead to an ambiguous solution, so the calculated values may be not the only solution. The following parameters seem to be treated correctly by COMVEN:

Keyword:	Parameters:
&-CR	Cs, Expn, Length
&-NET-ZON	Temp, Ref Height, Abs Hum
&-NET-ZL	Start Height, Temp Grad, Hum Grad Fact, Poll Grad Fact
&-NET-ZP	Init Conc
&-NET-LIN	From Height, To Height, Mul Fct (for crack), Zone Nr
&-POL-DES	Molar Mass

S2ZOWI

Description: Test cases for network and large openings: two zones building, layers, temperature-, humidity- and pollutant- gradients; large opening between the two zones.

Input files: S2ZOWI_x.CIF (x = 1, 2a, 2b, 2c, 3a1, 3a2, 3b, 3c, 3d, 4a, 4b, 4c, 4d, 4e, 4f, 4g, 4h, 4i, 4j, 4k, 5b, 5c, 5d, 5e, 5f)

Output files: S2ZOWI_x.COF (x = 1, 2a, 2b, 2c, 3a1, 3a2, 3b, 3c, 3d, 4a, 4b, 4c, 4d, 4e, 4f, 4g, 4h, 4i, 4j, 4k, 5b, 5c, 5d, 5e, 5f)

Results: S2ZOWI.RES

Analytical: The analytical problem is documented in [Schauwecker 1993 c]

Conclusions: Version 3a1 (start height of large opening at start height of a layer): This case is calculated incorrectly by COMVEN. The COMVEN results for the mass flow through a large opening between two zones can show significant deviations (version 4e: 25%) from the analytical solution, if there are layers in one or both zones.

Versions 3d, 5b, 5c, 5d, 5e, 5f: If the zones are not layered there is a good agreement between the COMVEN results and the analytical solution. The height of the neutral plane(s) is calculated correctly. (Exception: version 3a2. According to the COMVEN solution the pressure difference between the two zones has the same sign over the whole opening (no neutral plane within the opening), but air is flowing in both directions ($mfl1 > 0$ and $mfl2 > 0$!) →?)

Versions 3f, 3g: These versions are physically identical, but the COMVEN results for both versions are different due to a different way of density and pressure profile calculation in the presence and absence of layers.

SCRZ

- Description Test cases for non horizontal cracks:
 SCRZ_x.CIF: one zone building, no layers, no gradients.
 S2CRZ_x.CIF: two zones building, layers, temperature-, humidity- and pollutant-gradients.
- Input files: SCRZ_x.CIF (x = 1a...1h, 2a...2h), S2CRZ_x.CIF (x = 1a...1k, 2a...2k)
- Output files: SCRZ_x.COF (x = 1a...1h, 2a...2h), S2CRZ_x.COF (x = 1a...1k, 2a...2k)
- Results: SCRZ.RES
- Analytical: The analytical problem is documented in [Schauwecker, 1993 b]
- Conclusions: In COMVEN the non horizontal cracks are treated in the same way as horizontal cracks at link height in the zone into which the air is flowing. This approach may lead to some deviations from the correct result, if there is a density gradient in the zone from which the air is flowing out. The problems of convergence in the critical region, where the mass flow through the non horizontal crack is either ambiguous or not defined, seem to be solved in COMVEN 1-8E.

TESTLO

- Description These files test whether COMVEN correctly calculates the mass flow through a large opening between the two layered zones of a two zone building.
- Input files: TESTLO3A.CIF, TESTLO3B.CIF, TESTLO3C.CIF, TESTLO5A.CIF
- Output files: TESTLO3A.COF, TESTLO3B.COF, TESTLO3C.COF, TESTLO5A.COF
- Results: TESTLO.RES
- Analytical: Equations are solved using MATHEMATICA
- Conclusions: The calculation of the mass flows is done correctly for TESTLO3A,B,C.CIF, if in zone 2 (temp.grad. =0) a layer is defined. For the case TESTLO5A.CIF (2 layers in zone 1, layer boundary within the large opening) a deviation from the calculated values of 10-18% occurs, because COMVEN 1-8E calculates the mass flow through the large opening with only one gradient. (This has been improved in COMVEN 1-3EA).

TLAY1

- Description This test file is based on a single room building with cracks and a window to the outside. Under the NET-ZL-keyword five layers are defined for the single zone. For each layer a temperature gradient and a gradient factor for humidity and for one pollutant are entered. This file tests whether COMVEN correctly calculates pressure and density at the heights of the cracks.
- Input file: TLAY1.CIF
- Output file: TLAY1.COF
- Results: TLAY1.RES
- Analytical: Equations are given in the *.RES file

Conclusions: The approach with a linearised density profile seems to be exact enough. Only the single pollutant, for which a gradient factor is given in the layers definition, is taken into account for the calculation of the total molar mass and the effective density. The gradient factors of humidity and pollutant are relative values to the humidity and pollutant concentration at reference height.

TLO

Description These files test whether COMVEN correctly calculates the mass flow through a large opening between the two zones of a two zone building. The concentrations of a pollutant are calculated for the two zones.

Input files: TLO1.CIF, TLO1B.CIF, TLO_POL1.CIF

Output files: TLO1.COF, TLO1B.COF, TLO_POL1.COF

Results: TLO.RES

Analytical: Equations for the software package MATHEMATICA are given in the *.RES file '

Conclusions: The calculation of zone pressure, the mass flow and the concentration are done correctly. Pollutant concentration: in the MATHEMATICA calculations the sink value is interpreted as sink strength relative to the pollutant concentration. In COMIS 1 the sink value equals the absolute decrease of pollutant mass in the zone (zero if the concentration =0).

TPOL

Description These files test whether COMVEN correctly calculates the time dependent concentration of a pollutant in a two room building. Different values for start concentration, outside concentration, filter, source and sink in the rooms are given.

Input files: TPOL1.CIF, TPOL2.CIF, TPOL3.CIF, TPOL4.CIF, TPOL5.CIF

Output files: TPOL1.COF, TPOL2.COF, TPOL3.COF, TPOL4.COF, TPOL5.COF

Results: TPOL.RES

Analytical: Equations for the software package MATHEMATICA are given in the *.RES file '

Conclusions: The calculation of the pollutant concentration in the zones is done correctly. The filter value for the second pollutant is taken as the one for the first one. Calculation of wind pressure: the outside pollutant concentration is taken into account for the calculation of outside density and wind pressure, but not the concentration factor of the different facade elements.

WPTEST

Description The subject of these files is to test whether COMVEN correctly calculates the wind speed at the reference height for the Cp-values for different wind profile exponents.

Input files: WPTEST017.CIF, WPTEST025.CIF, WPEST033.CIF

Output files: WPTEST017.COF, WPTEST025.COF, WPEST033.COF

Results: WPTEST.RES

Analytical: Equations are given in the *.RES file

Conclusions: The calculation of wind speed at reference height, wind pressure and mass flow is done correctly. In COMIS 1.0 the wind speed calculations are restricted to the case of identical roughness values at the building site and at the meteo station site. Subsequent versions consider different roughness values for meteo station and site location.

1ZOHU

Description This file tests the influence of very high humidity on the mass flow due to stack effect and wind pressure in a single zone building. Two cracks on two different facade elements are defined, and a temperature difference of 16°C is given.

Input file: 1ZOHU.CIF

Output file: 1ZOHU.COF

Results: 1ZOHU.RES

Conclusions: The zone pressure and mass flow are calculated correctly.

1ZOPO1

Description This file tests whether COMVEN correctly calculates the time dependent concentration of a pollutant in a room with a constant mass flow. The outside concentration is constant, source and sink in the room are zero.

Input file: 1ZOPO1.CIF

Output file: 1ZOPO1.COF

Results: 1ZOPO1.RES

Analytical: Equations are given in the *.RES file

Conclusions: The calculation of the pollutant concentration in the zone is done correctly.

1ZOPO2

Description This file tests whether COMVEN correctly calculates the time dependent concentration of a pollutant in a room with a constant mass flow. The outside concentration, source and sink in the room are zero and an initial concentration is given.

Input file: 1ZOPO2.CIF

Output file: 1ZOPO2.COF

Results: 1ZOPO2.RES

Analytical: Equations are given in the *.RES file

Conclusions: as above

1ZOPOSO

Description With this file tests whether COMVEN correctly calculates the time dependent concentration of a pollutant in a room with a constant mass flow. The outside concentration is constant, sink and start concentration in the room are zero and a value for source is given.

Input file: 1ZOPOSO.CIF

Output file: 1ZOPOSO.COF

Results: 1ZOPOSO.RES

Analytical: Equations are given in the *.RES file

Conclusions: as above

1ZOST

Description These files tests whether COMVEN correctly calculates the mass flow due to stack effect in a single zone building. Two cracks (windows) on two different facade elements are defined, and a temperature difference of 20°C is given.

Input files: 1ZOSTCR.CIF, 1ZOSTWI.CIF

Output files: 1ZOSTCR.COF, 1ZOSTWI.COF

Results: 1ZOST.RES

Analytical: Equations are given in the *.RES file

Conclusions: The calculation of zone pressure, link pressure and mass flow is done correctly for the cracks as well as for the windows.

1ZOWI

Description This file tests whether COMVEN correctly calculates the mass flow due to stack effect through a large opening.

Input file: 1ZOWI.CIF

Output file: 1ZOWI.COF

Results: 1ZOWI.RES

Analytical: Equations are given in the *.RES file

Conclusions: The calculation of zone pressure and mass flow is done correctly.

1ZOWP

Description Test for the calculation of the mass flow in a single zone building with a crack in each facade. A list of Cp-values and the wind speed are given.

Input file: 1ZOWP.CIF

Output file: 1ZOWP.COF

Results: 1ZOWP.RES

Analytical: Equations are given in the *.RES file

Conclusions: The calculation of wind pressure and mass flow for this simple example is done correctly.

1ZOWPFA

Description This file tests whether COMVEN correctly calculates the mass flow in a single zone building with a fan and five cracks to the outside. A list of Cp-values is entered under the &-CP keyword. The fan curve is described by a second order polynomial.

Input file: 1ZOWPFA.CIF

Output file: 1ZOWPFA.COF

Results: 1ZOWPFA.RES

Analytical: Equations for the software package MATHEMATICA are given in the *.RES file '

Conclusions: The calculation of zone pressure and mass flow is done correctly.

1ZOWPST

Description This test file tests whether COMVEN correctly calculates the mass flow due to wind pressure and stack effect in a rectangular single zone building with a crack in each wall and two cracks in the roof. A list of C_p -values for wall and roof, a temperature difference of 20°C and the wind speed are given.

Input file: 1ZOWPST.CIF

Output file: 1ZOWPST.COF

Results: 1ZOWPST.RES

Analytical: Equations are given in the *.RES file

Conclusions: The calculation of zone pressure, link pressure and mass flow is done correctly for the cracks as well as for the windows.

2ZOFA

Description This file tests whether COMVEN correctly calculates the mass flow in a two zone building with a fan from one zone to the outside, a crack between the zones and one from the second zone to the outside. The fan curve is described by a second order polynomial.

Input file: 2ZOFA.CIF

Output file: 2ZOFA.COF

Results: 2ZOFA.RES

Analytical: Equations for the software package MATHEMATICA are given in the *.RES file '

Conclusions: The calculation of zone pressure and mass flow is done correctly.

2ZOPO

Description This file tests whether COMVEN correctly calculates the time dependent concentration of a pollutant in a two room building. A constant mass flow and a start concentration in one room is given. The outside concentration, source and sink in the rooms are zero.

Input file: 2ZOPO.CIF

Output file: 2ZOPO.COF

Results: 2ZOPO.RES

Analytical: Equations are given in the *.RES file

Conclusions: as 1ZOPO

2ZOPOFI

Description This file tests whether COMVEN correctly calculates the flow of pollutants through a crack with filter.

Input file: 2ZOPOFI.CIF

Output file: 2ZOPOFI.COF

Results: 2ZOPOFI.RES

Conclusions: For different filter values the calculation of the pollutant concentration in the zones is done correctly.

2ZOST

- Description This file tests whether COMVEN correctly calculates the mass flow due to stack effect in a two zone building. Cracks are defined between the zones and between the zones and the outside. Three different temperatures are given for the two zones and the outside.
- Input file: 2ZOST.CIF
- Output file: 2ZOST.COF
- Results: 2ZOST.RES
- Analytical: Equations are given in the *.RES file
- Conclusions: The calculation of zone pressure, link pressure and mass flow is done correctly for all cracks in both zones.

2ZOWP

- Description This file tests whether COMVEN correctly calculates the mass flow in a two zone building with cracks between the zones and the outside and a crack between the two zones. A list of Cp-values and the wind speed are given.
- Input file: 2ZOWP.CIF
- Output file: 2ZOST.COF
- Results: 2ZOWP.RES
- Analytical: Equations are given in the *.RES file
- Conclusions: The calculation of wind pressure, zone pressures and mass flows is done correctly.

3ZOST

- Description This file tests whether COMVEN correctly calculates the mass flow due to stack effect in a three zone building. Cracks are defined between the zones and between the zones and the outside. Different temperatures are given for the zones and the outside.
- Input file: 3ZOST.CIF
- Output file: 3ZOST.COF
- Results: 3ZOST.RES
- Analytical: Equations are given in the *.RES file
- Conclusions: as 2ZOST

A 4. EXPERIMENTAL EVALUATION

A 4.1 Introduction

This appendix describes in more details than in the main text (chapter 4) all experimental comparisons, including a description of each measured object, the measurement performed, the sensitivity analysis performed around each case, and the comparisons with simulations.

A 4.2 The OPTIBAT facility

A 4.2.1 Measured object

OPTIBAT is a real scale experiment consisting of an 108 m² four-room dwelling built in the laboratory hall at the INSA in Lyon (Figure A4.2.1). It is an exact replica of an existing apartment within an actual building located near Lyon. Climatic chambers are placed against the two facades of this dwelling to simulate the outdoor climate (temperature and pressure).

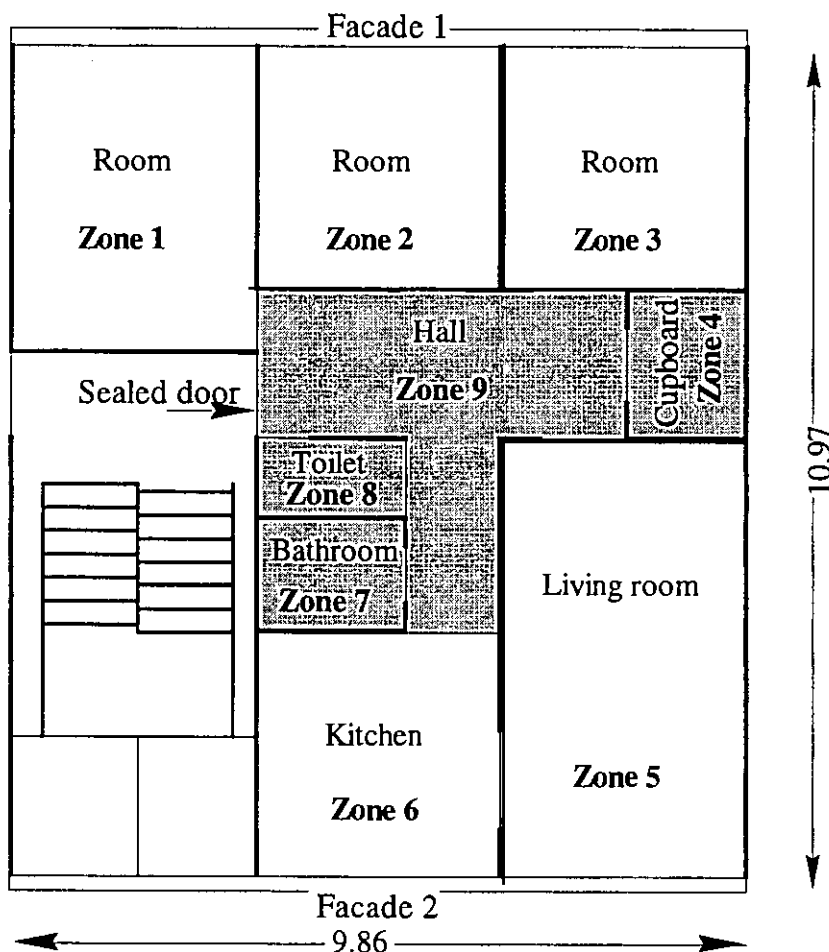


Figure A4.2.1: The OPTIBAT facility with the nine zones defined for the infiltration measurements.

Other climatic chambers are added on each face of the experimental cell, in order to control the boundary conditions. The two main facades (top and bottom on Figure A4.2.1) can be submitted to temperatures between -10 and 30°C, to relative humidity between 30 and 80% and to pressure differentially up to 180 Pa. The other four faces (two walls, floor and ceiling) have thermal and pressure guards, simulating the adjacent apartments.

This facility allows measurements of air permeabilities and air flows in a very well controlled environment. Simulations can also be performed with very well controlled boundary conditions. The comparisons between simulations and experiments made with this facility are therefore much more accurate than those performed on real buildings. Since real pressures on facades were directly input for simulations, the possible discrepancies resulting from the use of pressure coefficients are avoided.

A 4.2.2 Measurements performed

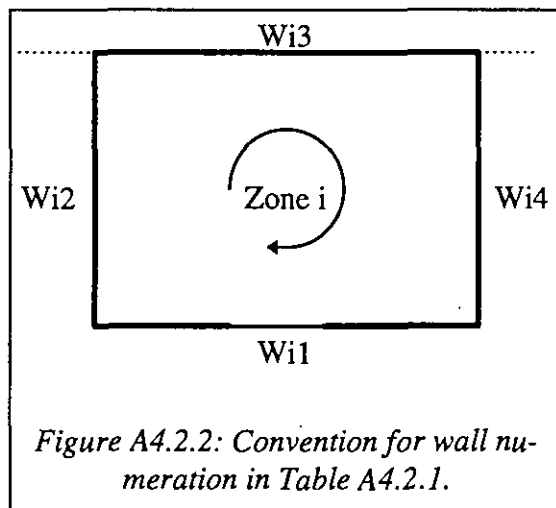
Air permeability characteristics of all inter-zonal links, including links to exterior, were measured using a guarding zone technique and a passive method [Amara, 1993], [Megri, 1993].

The guarded zone method employs two fans. The pressure difference across the outer walls of the primary zone is kept constant (i.e. at zero Pa), while the pressure in the secondary zone is varied between - 200 and + 200 Pa. The flow rates required to maintain the constant pressure difference across the external walls of the primary zone were recorded for different pressure levels in the secondary zone.

Table A4.2.1: Value of C and n for the internal components

Component	Active Method		Passive Method	
	$C[m^3/(h.Pa^n)]$	n	$C [m^3/(h.Pa^n)]$	n
W11 = W22	0.01 ± 0.02	0.95 ± 0.05	0.14 ± 0.001	0.90 ± 0.001
W21	19.30 ± 0.38	0.71 ± 0.01	20.22 ± 1.03	0.78 ± 0.05
W22	0.01 ± 0.02	0.95 ± 0.05	0.14 ± 0.001	0.90 ± 0.001
W24	0.08 ± 0.02	0.99 ± 0.01	0.17 ± 0.01	0.87 ± 0.01
W31	14.17 ± 0.03	0.66 ± 0.001	14.94 ± 1.26	0.59 ± 0.004
W32 = W24	0.08 ± 0.02	0.99 ± 0.01	0.17 ± 0.01	0.87 ± 0.01
W41	2.54 ± 0.22	0.92 ± 0.03	2.49 ± 0.16	0.84 ± 0.02
W42	2.89 ± 0.21	0.66 ± 0.01	2.97 ± 0.08	0.65 ± 0.01
W44	5.48 ± 0.04	0.51 ± 0.002	5.64 ± 0.02	0.51 ± 0.01
W51	14.67 ± 1.54	0.71 ± 0.03	15.03 ± 0.64	0.76 ± 0.01
W54 = W62	6.47 ± 0.02	0.64 ± 0.01	6.29 ± 0.02	0.64 ± 0.001
W61 = W72	1.76 ± 0.26	0.74 ± 0.05	1.24 ± 0.21	0.81 ± 0.02
W64	1.64 ± 0.06	0.77 ± 0.02	1.99 ± 0.27	0.69 ± 0.06
W71	4.59 ± 0.99	0.89 ± 0.04	4.83 ± 0.31	0.80 ± 0.02
W72	1.76 ± 0.26	0.74 ± 0.05	1.24 ± 0.21	0.81 ± 0.02
W74	0.34 ± 0.01	0.97 ± 0.01	0.34 ± 0.01	0.97 ± 0.01
W82 = W74	0.34 ± 0.01	0.97 ± 0.01	0.34 ± 0.01	0.97 ± 0.01
W12	Airtight Component		Airtight Component	
W13	Airtight Component		Airtight Component	
W14	12.62 ± 1.04	0.59 ± 0.03	13.43 ± 0.91	0.58 ± 0.02
W23	13.93 ± 0.84	0.57 ± 0.02	11.82 ± 1.4	0.60 ± 0.04
W33	9.37 ± 1.15	0.61 ± 0.03	10.02 ± 1.08	0.55 ± 0.04
W34	Airtight Component		Airtight Component	
W43	Airtight Component		Airtight Component	
W52	Airtight Component		Airtight Component	
W53	13.52 ± 1.6	0.55 ± 0.03	13.34 ± 0.21	0.57 ± 0.01
W63	6.79 ± 1.15	0.52 ± 0.05	5.86 ± 0.02	0.56 ± 0.005
W73	Airtight Component		Airtight Component	
W83	3.34 ± 0.59	0.65 ± 0.05	3.94 ± 0.54	0.59 ± 0.04

In the passive method, one blower door is employed with the interior and exterior openings kept either closed or opened. The blower door is installed in the door of the room containing the element to be measured. The advantage of this method is that it is cheaper than the active method and easy to use. However, it requires more time than the active method and the estimation of the flow coefficients is more difficult because it requires the solution of a set of non-linear equations coupled with statistical treatment [Amara, 1993].



A least square regression technique was used to estimate the flow coefficients, C and flow exponents, n . Table A4.2.1 gives the values of these parameters for each component. In order to identify the components, they have been numbered clockwise starting from the door. Thus, $Wi1$ is wall number 1 of zone number i , Figure A4.2.2.

The values of C and n obtained using active and passive techniques are not the same in all cases. The statistical error treatment however shows that, in most of the cases, the confidence intervals calculated using the two methods overlap with each other [Amara, 1993]. This good agreement

between the results indicates that the possible error between the actual values (C and n) and those used as input in the models has been minimised.

The air leakage from the inside doors is not determined by the fan pressurisation method, but estimated by $C = 0.83 \times S$, where S is the area of the crack [m^2], and $n = 0.5$.

A smoke test was also performed to accurately find the location of these cracks. They were mainly located above the windows near the shutters, where the electric cables crossed.

Several climatic conditions (cf. Table A4.2.2), including winter and summer, were simulated using the climate chambers. The wind effect was simulated by pressure differentials at the facades. The temperature and pressure drop were measured in the middle of the room at height of 1.2 m from the floor. The indoor air temperature was kept at 20 °C throughout the apartment.

Table A4.2.2: The different scenarii used for the measurements

Scenario	T_{Out} [°C]	T_{In} [°C]	$\Delta P1$ [Pa]	$\Delta P2$ [Pa]	$\Delta P3$ [Pa]
Summer 1	20 ± 0.5	20 ± 0.5	16 ± 1	-81 ± 2	-2.8 ± 0.5
Summer 2	20 ± 0.5	20 ± 0.5	54.1 ± 1.2	-122 ± 3	-13.4 ± 1
Summer 3	20 ± 0.5	20 ± 0.5	25 ± 1	-58.6 ± 2	-6 ± 1
Summer 4	20 ± 0.5	20 ± 0.5	1 ± 1	-43 ± 2	-0 ± 1
Winter 1	-1.3 ± 0.5	20 ± 0.5	15.7 ± 1	-79.6 ± 2	-2.5 ± 1
Winter 2	-1.1 ± 0.5	20 ± 0.5	52 ± 1	-121 ± 3	-12.6 ± 1
Winter 3	-1.7 ± 0.5	20 ± 0.5	21.5 ± 1	-42 ± 2	-4.8 ± 1
Winter 4	-1.5 ± 0.5	20 ± 0.5	1 ± 1	-42 ± 3	-0 ± 1

Air flow rates resulting from these boundary conditions were measured using multi-tracer gas technique and a Bayesian interpretation method.

The OPTIBAT flat was modelled using the network illustrated in Figure A4.2.3. Node 4 includes bathroom (zone 7), toilets (zone 8), hall (zone 9) and cupboard (zone 4). Interconnecting doors between these zones were opened for tracer gas measurements and simulations.

A 4.2.3 Sensitivity analysis

Global sensitivity analysis was performed using the Monte-Carlo technique: 100 runs were conducted, varying all parameters at random before each run. The random changes of the parameters were made following a uniform distribution, with maximum and minimum values as given in Table A4.2.3. For these calculations, COMVEN 1.3 was used, together with the MISA tool.

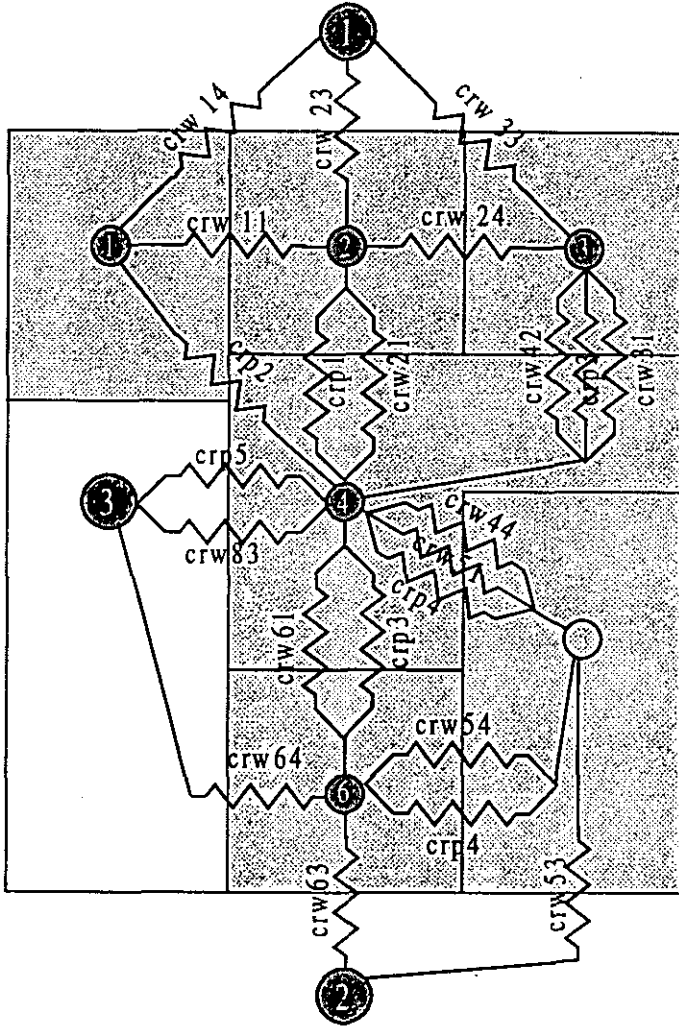


Figure A4.2.3: Network modeling the OPTIBAT flat. Door cracks are crp, while crw are wall cracks.

A 4.2.4 Results

Simulations were performed with COMIS 1.1, using as input the measured boundary conditions (pressure differentials, temperature and humidity) and the measured air permeability characteristics. Resulting inter-zonal flow rates are compared in Figure A4.2.5 to Figure 4.2.12, as explained in Figure A4.2.4.

Zone	1	2	3	4	5	6
1	Dark grey	Light grey	Empty	Light grey	Empty	Empty
2	Light grey	Dark grey	Light grey	Light grey	Empty	Empty
3	Empty	Light grey	Dark grey	Light grey	Empty	Empty
4	Light grey	Light grey	Light grey	Dark grey	Light grey	Empty
5	Empty	Empty	Empty	Light grey	Dark grey	Light grey
6	Empty	Empty	Empty	Light grey	Light grey	Dark grey

Figure A4.2.4: Explanation for Figure A4.2.5 to Figure 4.2.12. The diagonal blocks (dark grey zones) contain the total flow rate in each zone, including outdoor air. The other blocks contain inter-zone flow rates. Empty blocks correspond to non-existent air flows.

Table A4.2.3: Maximum and minimum values of parameters.

No	Crack	Flow coefficient C [$\text{m}^3/(\text{s}\cdot\text{Pan})$]		Exponent n	
		Minimum	Maximum	Minimum	Maximum
1	"CRW14"	3,477E-3	3,983E-3	0,56	0,6
3	"CRW23"	2,891E-3	3,669E-3	0,56	0,64
5	"CRW33"	2,48E-3	3,89E-3	0,51	0,64
7	"CRW53"	2,44E-3	3,7683E-3	0,50	0,58
9	"CRW63"	1,4E-3	1,64E-3	0,555	0,565
11	"CRW83"	0,94E-3	1,24E-3	0,55	0,63
13	"CRW11"	3,8622E-5	3,9178E-5	0,89	0,91
15	"CRW21"	5,334E-3	5,906E-3	0,73	0,83
17	"CRW24"	4,442E-5	4,998E-5	0,86	0,88
19	"CRW31"	3,8E-3	4,5E-3	0,58	0,60
21	"CRW42"	8,028E-4	8,472E-4	0,64	0,66
23	"CRW44"	1,56E-3	1,58E-3	0,50	0,52
25	"CRW51"	4,002E-3	4,358E-3	0,75	0,77
27	"CRW54"	1,74E-3	1,76E-3	0,63	0,65
29	"CRW61"	2,857E-4	4,023E-4	0,79	0,83
31	"CRW64"	4,78E-4	6,28E-4	0,63	0,75
33	"CRp1"	0,80E-2	0,85E-2		
34	"CRp2"	0,0160	0,0172		
35	"CRp3"	0,0239	0,0259		
36	"CRp4"	0,01975	0,02175		
37	"CRp5"	0,0239	0,0259		

No	Parameter	Minimum	Maximum	Unit
38	ΔP 1	Depend on external		Pa
39	ΔP 2	climate		"
40	ΔP 3	see Table A4.2.2		"
41	External temperature			$^{\circ}\text{C}$

Comparison of total air flow rates l are illustrated in Figure A4.2.5 to Figure 4.2.12. Measurements 1 are multi-tracer, while measurements 3 are made with SF_6 in several experiments. *JMF-simulations* are performed with COMVEN 1.3, while COMVEN 1.1 was used for *FA-simulations*. Differences between simulations and measurements themselves are generally small, but there are significant differences between measured and simulated air flow rates.

In the following figures, dark bars are uncertainty bands, defined by the standard deviation of results from the 100 runs.

Summer 1

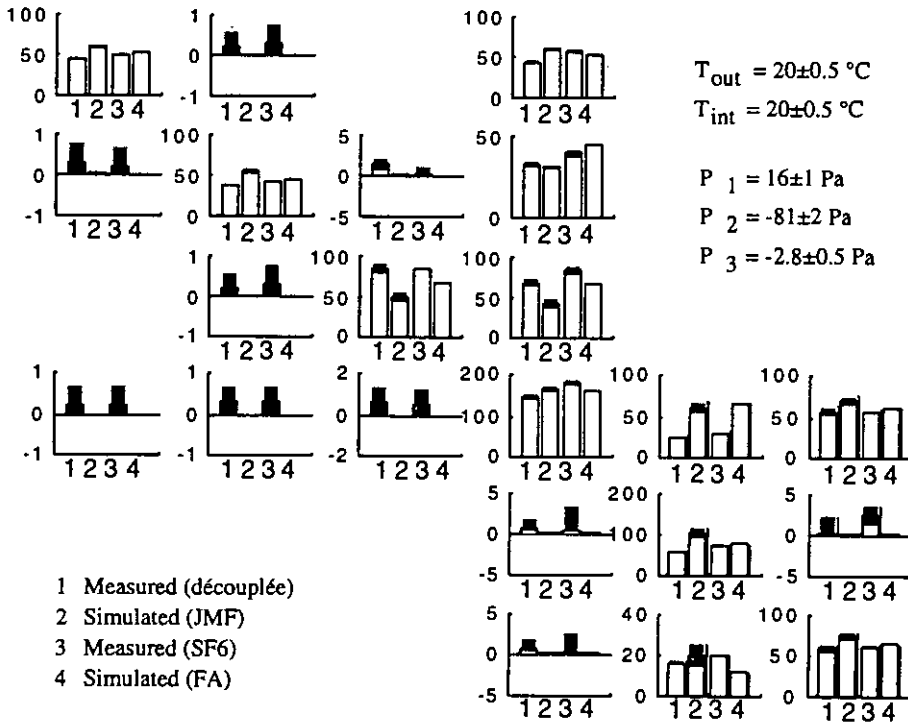


Figure A4.2.5: Comparison of two measurements and two simulations of air flow rates for Summer 1 scenario. Grey bars are uncertainty bands.

Summer 1

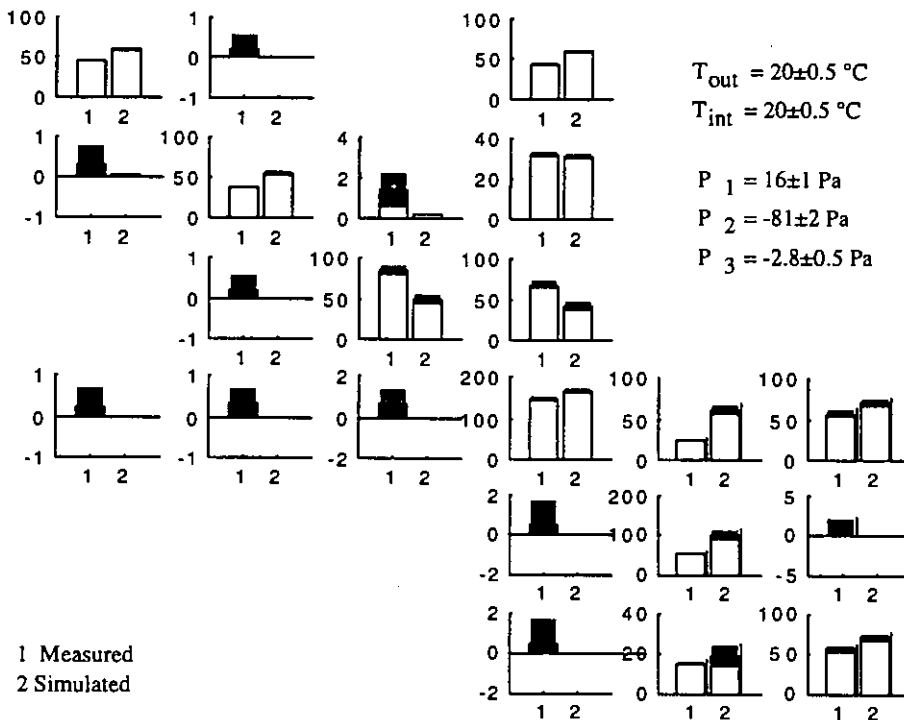


Figure A4.2.6: Comparison of multi-gas measurements and Comven 1.3 simulations of air flow rates for Summer 1 scenario.

Summer 2

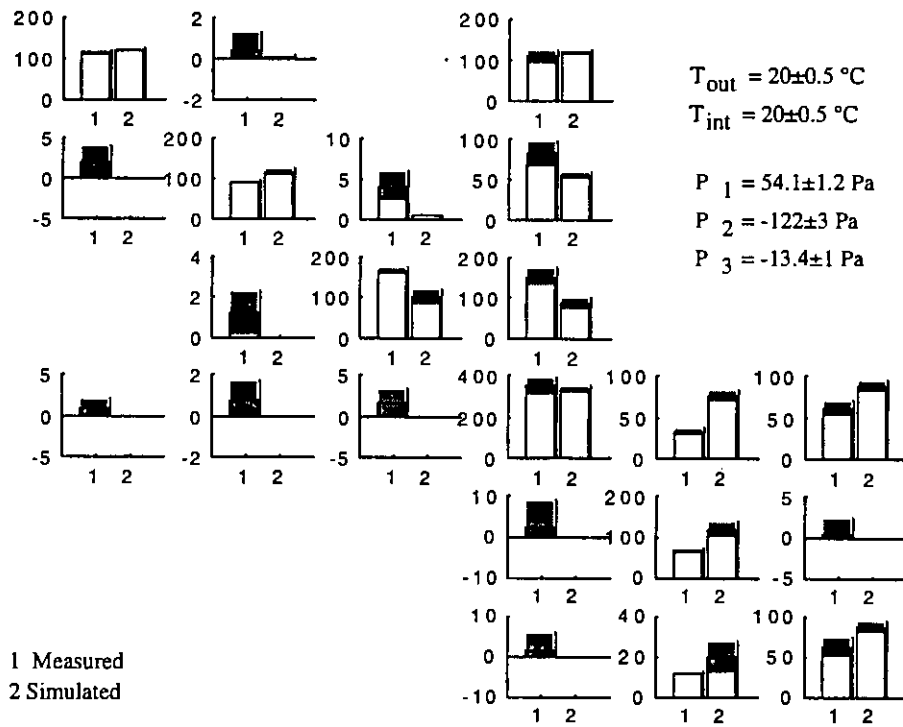


Figure A4.2.7: Comparisons of air flow rates for Summer 2 scenario.

Summer 3

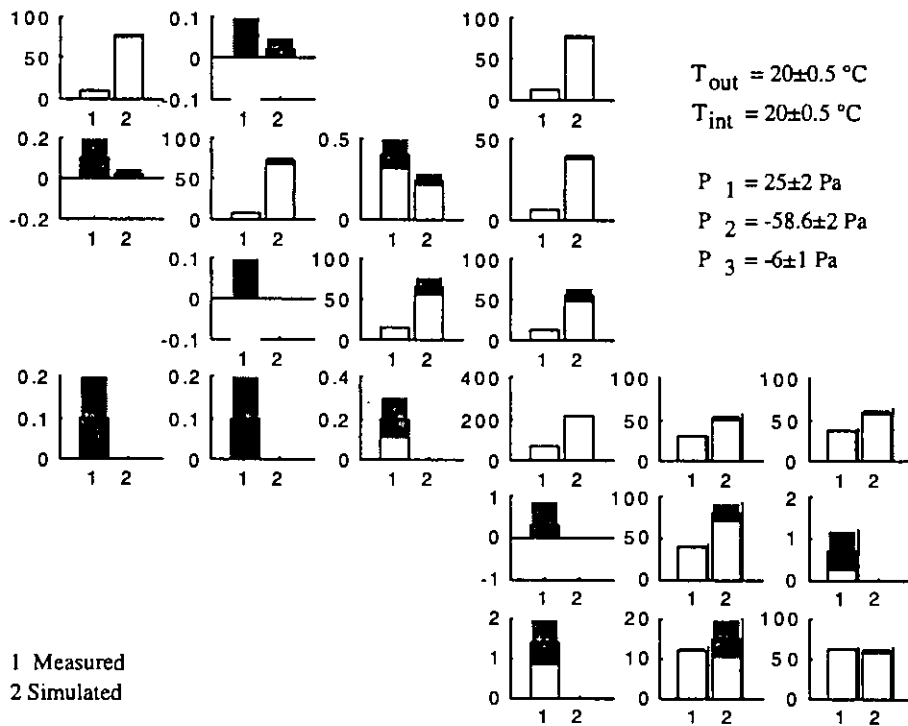


Figure A4.2.8: Comparisons of air flow rates for Summer 3 scenario.

Summer 4

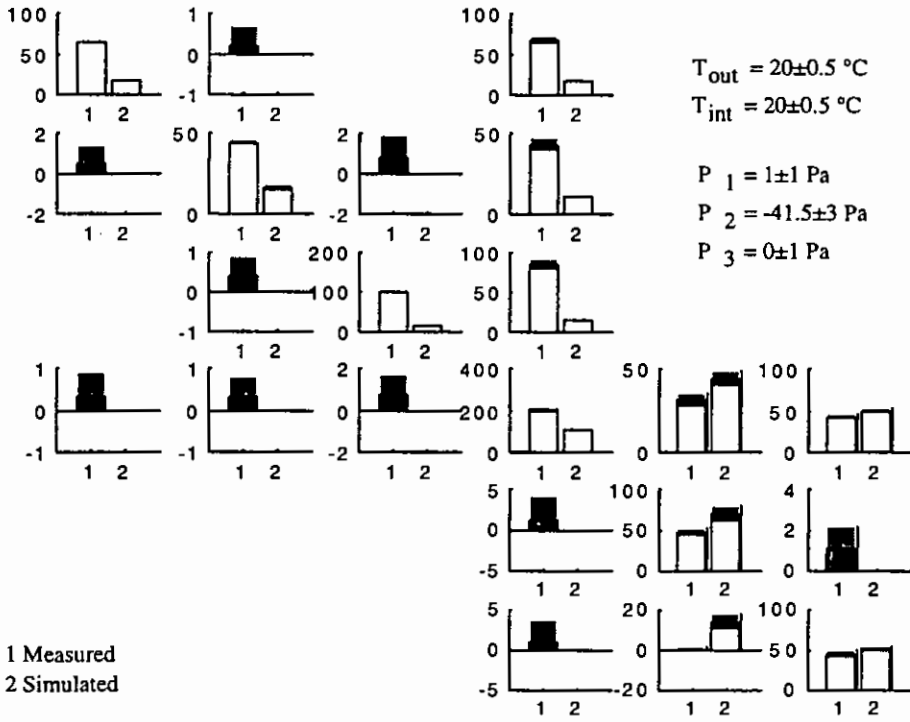


Figure A4.2.9: Comparisons of air flow rates for Summer 4 scenario.

Winter 1

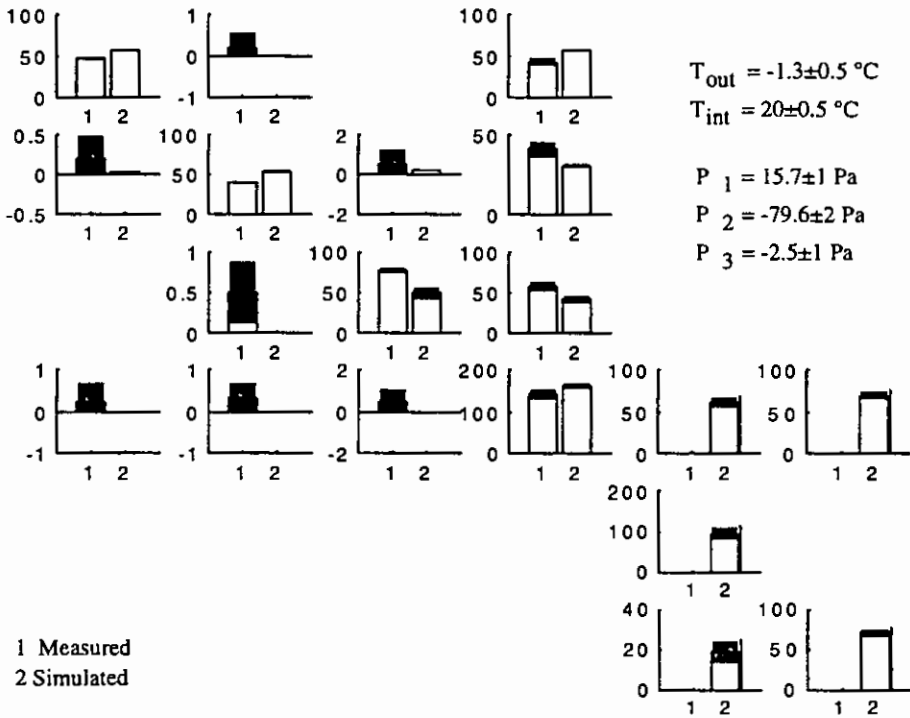


Figure A4.2.10: Comparisons of air flow rates for Winter 1 scenario.

Winter 2

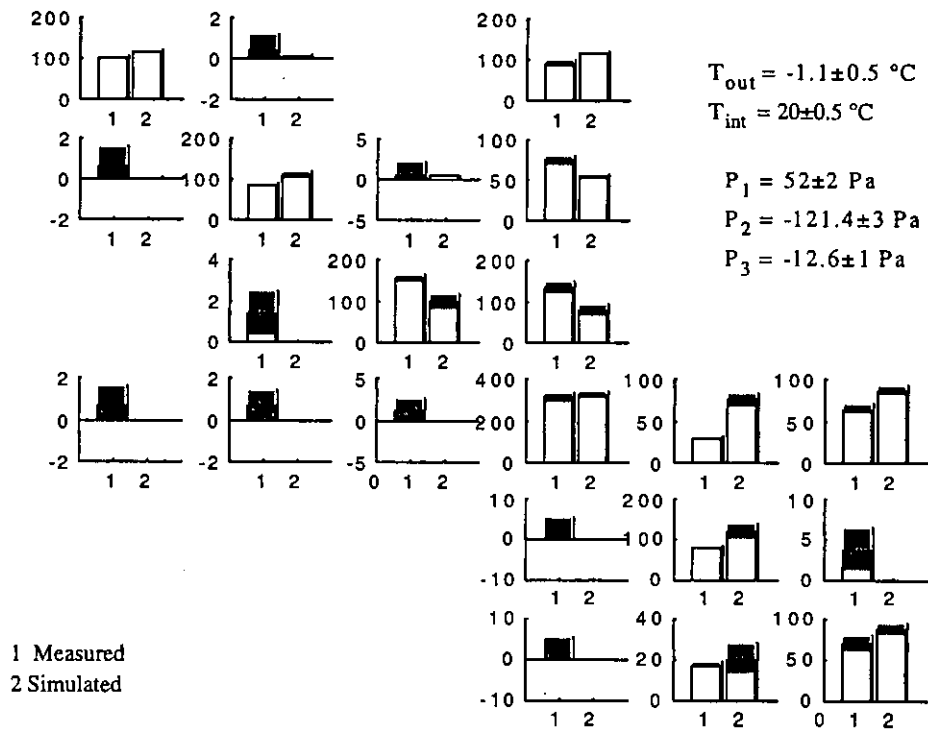


Figure A4.2.11: Comparisons of air flow rates for Winter 2 scenario.

Winter3

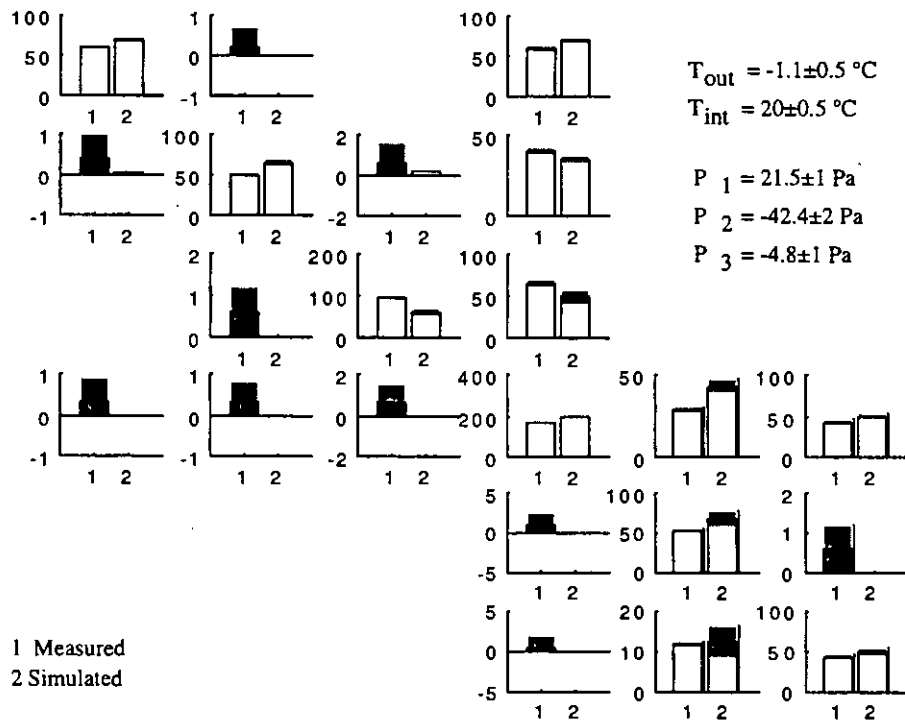


Figure 4.2.12: Comparisons of air flow rates for Winter 3 scenario.

A 4.2.5 Conclusions

In most cases, there are significant differences between calculated and measured air flow rates, even for total air flow rates in zones. There are several reasons for this:

- COMVEN has bugs: This does not seem to be the case since inter-model comparisons show results very close to those of other programs [Haghighat & Megri]. The alternative would be that all compared programs present the same bugs.
- The model does not correspond to the reality. This is possible, since two modellers have got slightly different results (see Figure A4.2.5)
- Confidence intervals on measurements are under estimated: This is possible, since two different measurement techniques sometimes produce significantly differing results.

It should be said that this comparison is the only one where most of the calculations were performed by the LESO team independently from the measuring team. Up to the time of drafting this report, no contact had been established between these teams to explain or reduce the discrepancies.

Several differences with climate 1 can be explained by the fact that pressure may not be homogeneous on facades, since the facade 1 fan is closer to zone 3 than to zones 1 and 2, and the facade 2 fan is closer to zone 5 than to zone 6. The value of facade pressure put into calculations were measured in front of zones 2 and 6. Therefore, pressure differentials between zones 3 and 5 and the exterior are underestimated.

A 4.2.6 References

- Amara, F.: Contribution a la caractérisation aéraulique des bâtiments. Étude des transferts aérauliques dans les locaux multizones. *Phd thesis at INSA de Lyon, April 1993.*
- Amara, F., Depecker, P., Allard, F.: Air flow patterns study in OPTIBAT cell - Inter zonal air flows. *Personal communication.*
- Haghighat, F., Megri A.: Inter-program and experimental validation of two air flow models: COMIS and CONTAM. *Personal communication.*
- Megri, A.: Modélisation des transferts aérauliques dans les bâtiments multizones équipés d'un système de ventilation; prise en compte de la qualité de l'air. *Phd thesis at INSA de Lyon, January 1993.*

A 4.3 Japan Solar House

A 4.3.1 Measured object

A Passive Solar House, originally constructed for research into passive solar system performance, at the campus of Tohoku University, Sendai, Japan, is used for measurement of air flows. The site plan and elevation are shown in Figure A4.3.1 (a) and (b), respectively. There are several laboratory buildings on the north and west sides of the house and a semi-underground test house on the south side. The house consists of two rooms of similar size with a corridor between them. The house plan and its section are shown in Figure A4.3.2. The rooms are 2.7 m wide, 5.5 m deep and 2.8 m high.

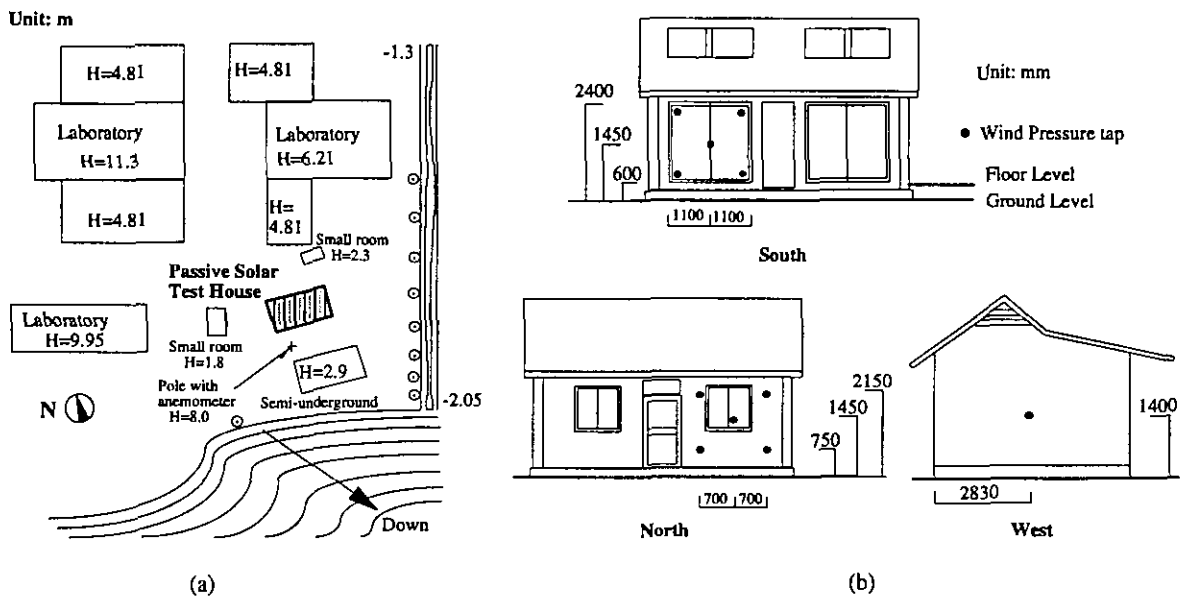


Figure A4.3.1: Site Plan and Elevation of Passive Solar Test House

For the measurement of air flow among three zones, the corridor and the west side room, which is divided into two zones, are used. The house plan of the three rooms is shown in Figure A4.3.2(b). The doors between two rooms and the corridor, and the partition wall between rooms 1 and 2 have a small vertical slit of 1 cm width. Also the doors between the east side room and the corridor are securely sealed to avoid any air exchange between them.

The 8 m long pole, which is located as shown in Figure A4.3.1(a), is equipped with a wind direction meter at the top and wind meters at different levels. The measuring heights are 8, 5, 2.7, 1.6 and 0.5 m above the ground level. Outdoor temperature is measured at a point close to the north window. Indoor temperatures are measured at the center of the rooms at a height of 1.4 m above the floor level. Measuring points of tracer gas concentrations are also located at the center of rooms and at the same level. Wind pressure taps on the outside walls are situated at the points shown as black circles in Figure A4.3.1(b). The point of reference pressure is assumed to be at the floor level of room 3. The accuracy of wind speed, temperature and pressure data in measurement is within the limit of $\pm 5\%$.

A 4.3.2 Measurements performed

Method and conditions

The concentration decay method with tracer gases, N_2O , SF_6 and $CHCl_2F$, is employed for measurement of air flows among the three rooms. The concentrations of these gases are measured every 6 minutes using the Bruel & Kjaer multi-gas monitoring system, which measures gas concentrations to within an uncertainty $\pm 3\%$.

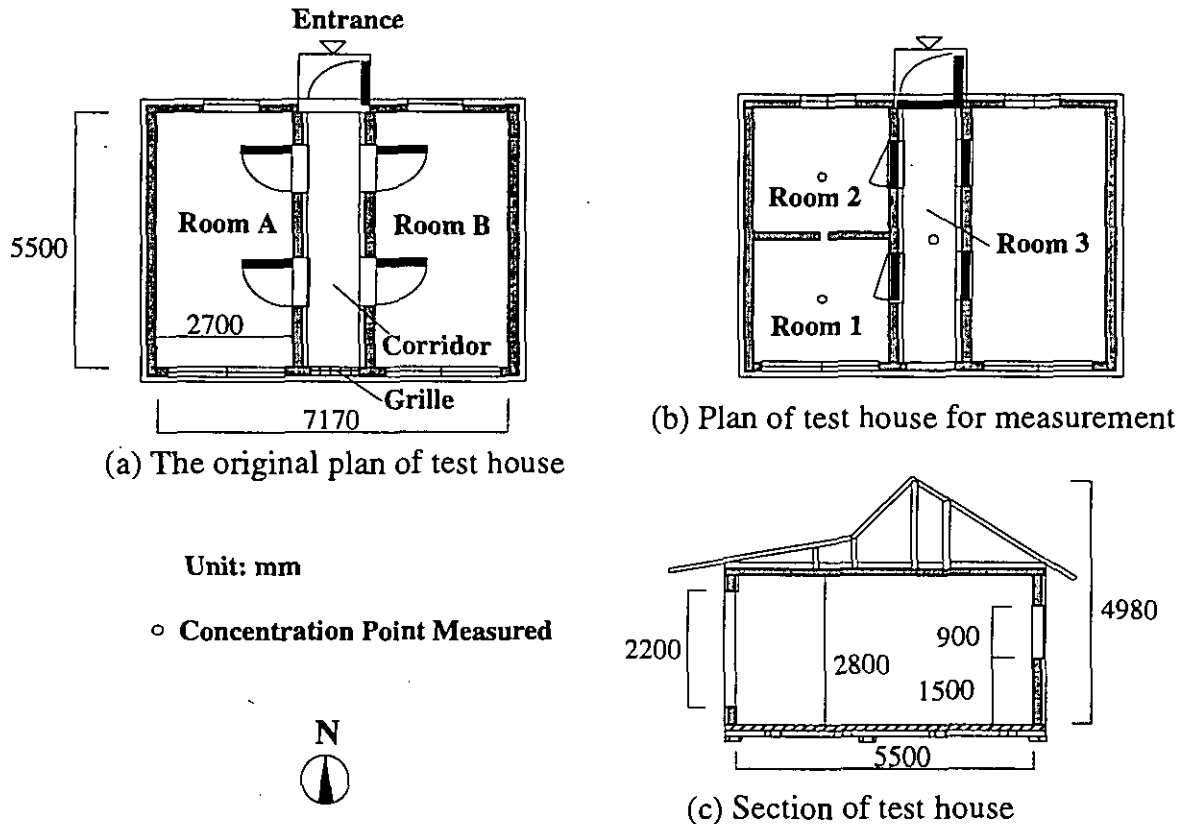


Figure A4.3.2: Plan and Section of Passive Solar Test House

Initially, the different tracer gases are injected into each room with the slits between rooms 1 and 2, 2 and 3 and 1 and 3 sealed during the injection. When the concentrations of each tracer gas reaches an appropriate level, the injection process is stopped. Indoor air is then mixed using a small electric fan for approximately 10 minutes. After the "perfect" mixing of indoor air is achieved, the seals of the slits are stripped off and the measurement of concentration decay is started. The duration of gas concentration sampling is 90 minutes. The experimental conditions are shown in Table A4.3.1.

Air leakage distribution

Equivalent leakage areas of the windows, walls, doors and other components are measured by the fan pressurisation method. The background leakage data in Table A.4.3.2 indicates the total leakage area of a defined zone and does not include the window, door and purpose made slits. Also, the distribution of the background leakage is calculated in proportion of the surface areas of the components. For example, the results of the undivided west side room (Room A in Figure A4.3.2(a)) indicate that the background leakage of room A, is 29 cm^2 ; then the leakage of interior partition between Room A and the corridor is about 6 cm^2 .

Table A4.3.1: Characterisation of the measurements for air flow comparison

Case No.	Case 1	Case 2	Case 3
Date	Aug. 6 1992	Aug. 6 1992	Aug. 8 1992
Measurement time	12:33 to 14:03	22:03 to 23:33	20:28 to 21:58
Time for simulation	12:51 to 13:03	22:21 to 22:33	20:55 to 21:07
Number of data points	15	15	15
Time step	6 minutes	6 minutes	6 minutes
Wind direction	SE	W	S
Average wind speed	1.06 m/s	0.46 m/s	1.18 m/s
Outdoor temperature	25.3 °C	23.2 °C	23.9 °C
Room 1 temperature	33.4 °C	26.0 °C	28.2 °C
Room 2 temperature	35.0 °C	26.2 °C	27.6 °C
Room 3 temperature	30.0 °C	44.0 °C	29.9 °C

In the case of 3 rooms, the equivalent leakage area of the slits between Rooms 1 and 3 (corridor), 2 and 3 and 1 and 2 are 248 cm², 301cm² and 172 cm² respectively, and for the entrance door it is 282 cm². The background leakage of the corridor, including the roof, interior partition between the corridor and Room A, and the exterior walls and floor, is 350 cm². The partition between Rooms 1 and 2, which is tightly sealed, does not have any leakage except through the slit.

$$Q = \frac{\alpha A}{10000} \sqrt{2g\rho} \left(\frac{\Delta P}{9.8}\right)^n \quad [\text{kg/sec}] \quad (\text{A4.3.1})$$

The air flow rate is calculated by Equation A 4.2.1 [Yoshino, 1995]. αA is the equivalent leakage area for the link pressure difference of 9.8 Pa, ΔP [Pa] is the pressure difference across the leakage and ρ [kg/m³] is the density of air within the link.

Table A4.3.2: Equivalent leakage area of Passive Solar Test House

	South window of room 1	North window of room 2	Door between room 1 & 3	Door between room 2 & 3	Door between room 3 & outside	Slit between room 1 & 2	Background leakage Room A	Background leakage Corridor
Equivalent leakage area αA [cm ²]	51.3	42.2	248	301	282	172	29	350
n : Air flow exponent [-]	0.625	0.625	0.588	0.588	0.625	0.588	0.625	0.625

Indoor gas concentrations

The example of gas concentration changes in Case 3, are shown in Figure A4.3.3. The concentration of tracer gas in an injected room decreases steadily. On the other hand, the gas concentration in the other two rooms increases initially as a result of continuous exchange of air, but ultimately decreases, as the concentration of the tracer gas in the injected room reduces over a period of time.

(CASE 3)

○ Room 1 ▲ Room 2 □ Room 3

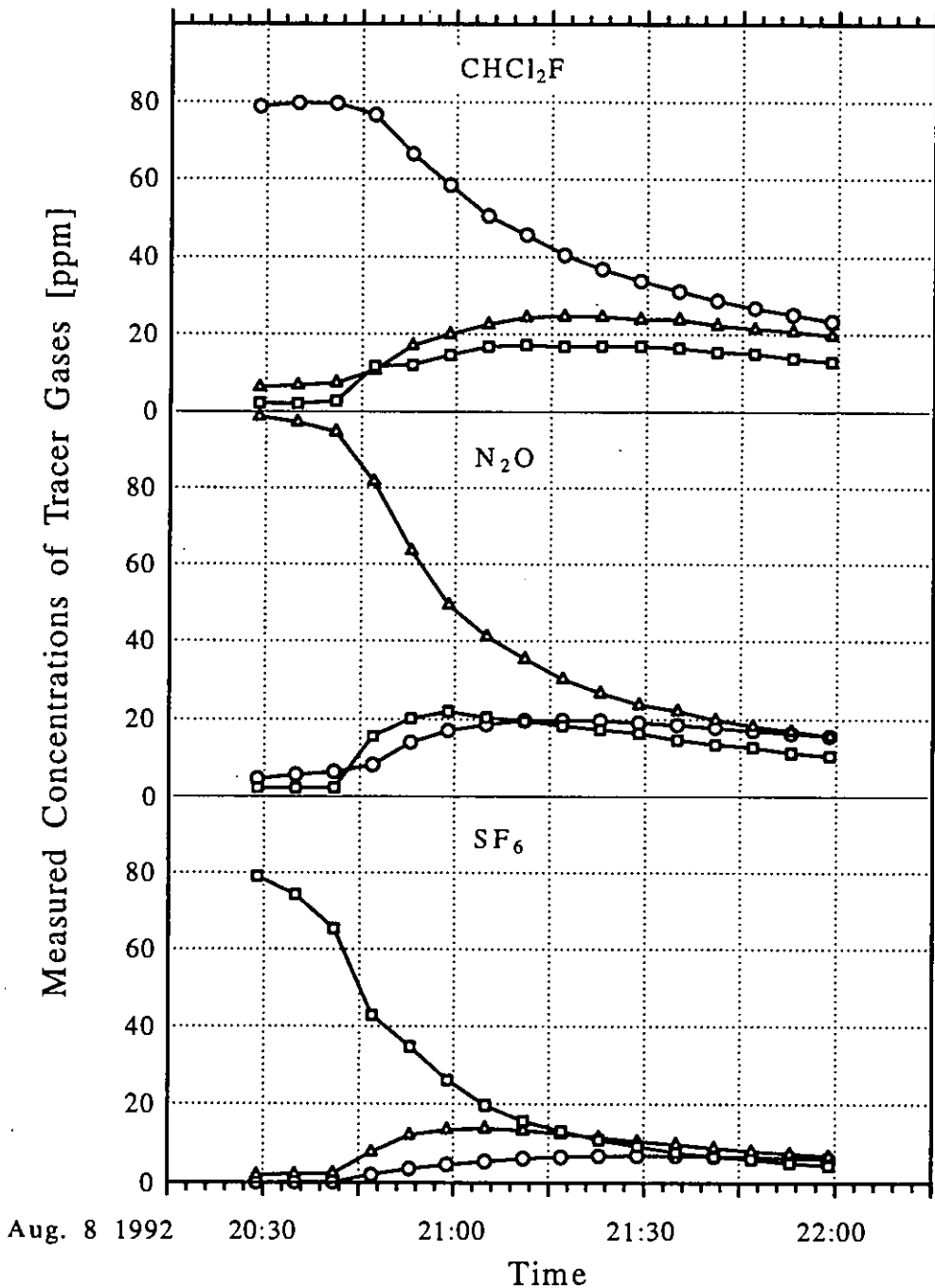


Figure A4.3.3: Profile of trace gases concentrations in Case 3

Air flows

The air flow rates through a room are evaluated using tracer gas method. In each case, it is assumed that the outside air does not contain any of the tracer gases. The air exchange rates between rooms may be calculated using three data sets of 12 minute decay profiles of tracer gas concentrations. The air flow pattern of 3 cases are shown in Figure A4.3.4(a). It can be seen that the air exchange rates between the various rooms exceeds those between each room and the outdoors. It is interesting that a small negative value of air exchange rate is included in

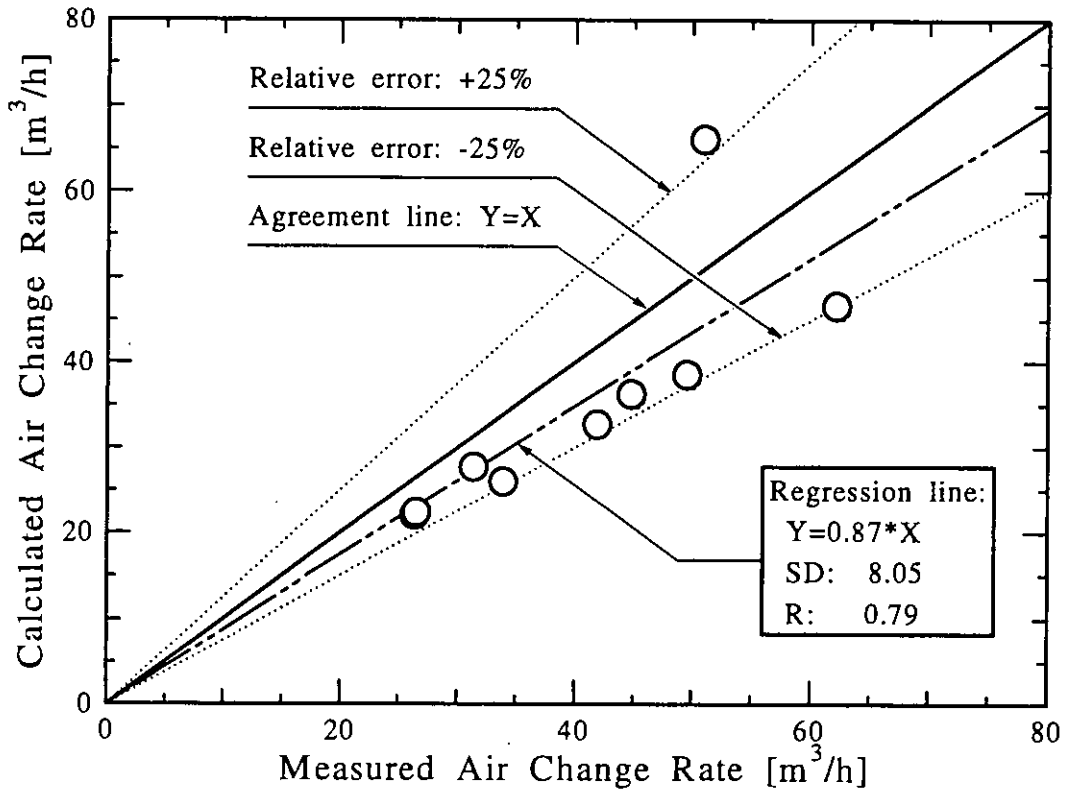


Figure A4.3.6: Comparison of measured and calculated air change rate

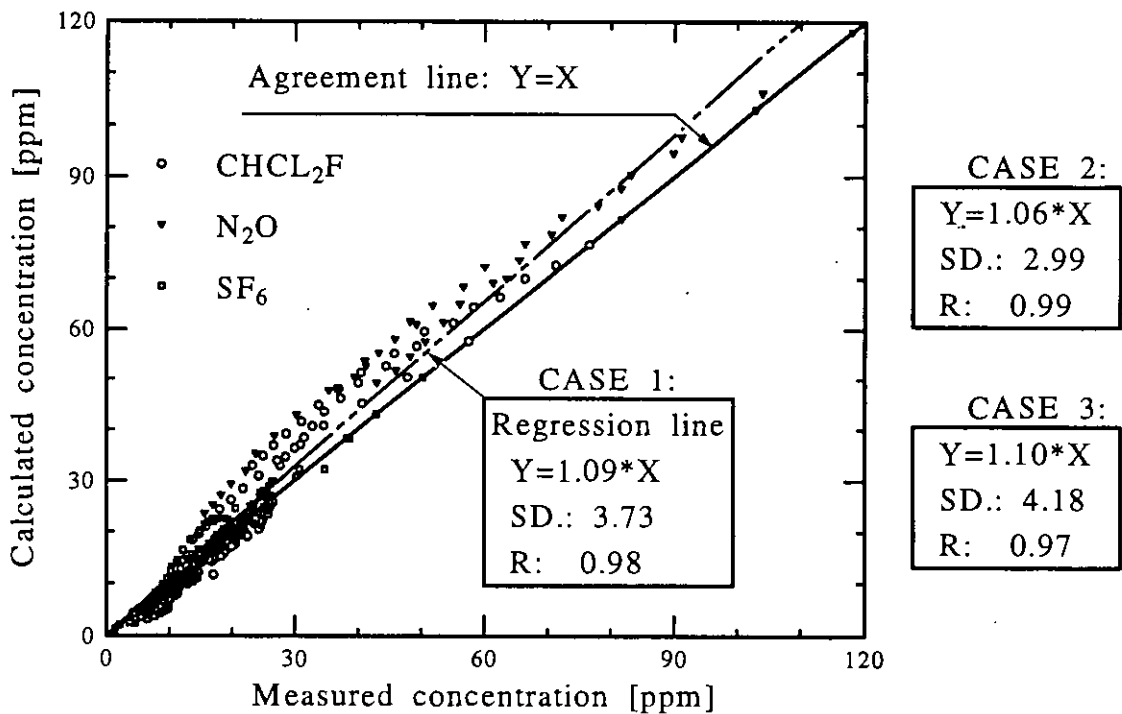


Figure A4.3.7: Comparison of indoor gas concentrations using regression analysis

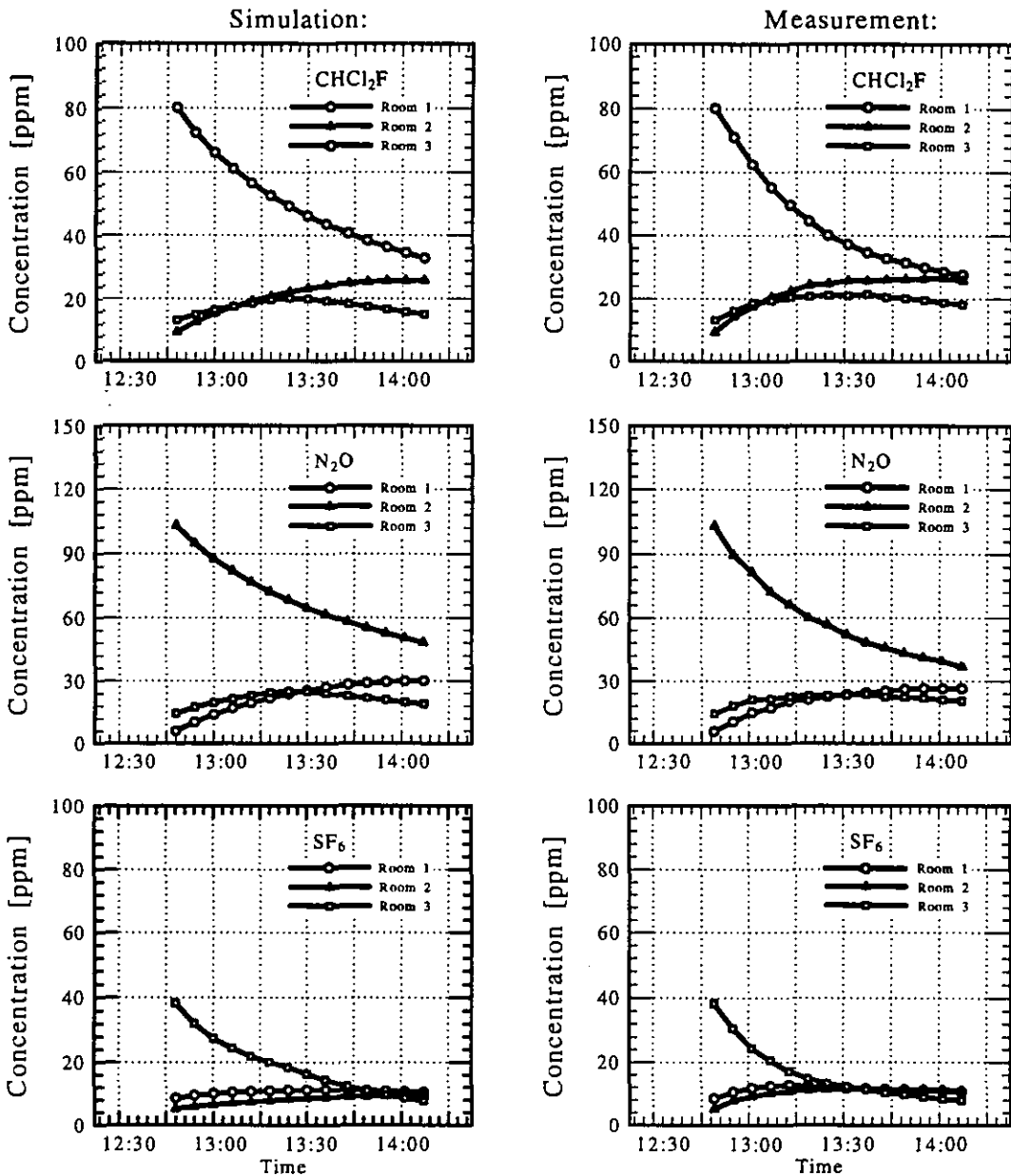


Figure A 4.3.8: Comparison of measured and calculated indoor gas concentrations

Indoor gas concentrations

Figure A 4.3.8 shows the simulation and the measurement results of three tracer gas concentration profiles versus time in Case 1. Figure A4.3.7 is a comparison of gas concentrations calculated with those from the measurement of three cases. The results of regression analyses indicate that the measured and calculated gas concentrations have a relatively good agreement, because the standard deviations, SD , and correlation coefficients, R , in three cases vary from 2.99 to 4.18 and from 0.97 to 0.99, respectively.

For these gas concentrations, the average factors calculated to measured values are from 1.06 to 1.10. The good agreement between measurement and simulation is achieved at certain time steps, but for the other time steps, the agreement is relatively poor. The reason may be due to the approximate average input data for simulation, especially wind pressure coefficients and the differences between measured and calculated air exchange rates. Also, it is possible that the "perfect mixing" assumption is not satisfied within every room.

A 4.3.4 Sensitivity analysis

A case study

Any measured data include confidence intervals corresponding to probable errors. Therefore, the comparison between measurement and calculation using sensitivity analysis is a necessary task for model evaluation. In the following section, Case 1 of the passive solar house is used to evaluate COMIS model using the sensitivity analysis method.

Input data uncertainty and output parameter

Table A4.3.4 shows the input parameters and their uncertainties for sensitivity analysis of Case 1 in the passive solar house. The first six parameters are related to air tightness measurement, the next eight are related to the climate data from measurement and the remaining two parameters are default data in simulation. These parameters play an important role in controlling the air flow rates of this building.

Table A4.3.4: Input parameters and uncertainties for sensitivity analysis of Case 1

No.	Parameter	Constant	Uncertainty
1	Flow coeff. of S window	0.0001475	5%
2	Flow exp. of S window	0.625	5%
3	Flow coeff. of outdoor N	0.003295	5%
4	Flow exp. of outdoor N	0.625	5%
5	Flow coeff. of slit	0.0022	5%
6	Flow exp. of slit	0.588	5%
7	Temperature of zone 1	33.4	1 °C
8	Temperature of zone 2	25.9	1 °C
9	Temperature of zone 3	28.2	1 °C
10	Wind pres. coeff. of 1	0.12	5%
11	Wind pres. coeff. of 2	0.22	5%
12	Wind pres. coeff. of 3	0.515	5%
13	Wind speed	1	10%
14	Outdoor temperature	25.15	1 °C
15	Humidity	10	10%
16	Barometer pressure	101.3	5%

On the other hand, a critical point of sensitivity analysis is to select the output parameters which are observed. The output parameters from COMIS model include air through flow link, air change rate of zone, pressure of each zone and etc. In this validation, air flows are selected as the output parameter expressed by air flow matrix [Roulet, 1991 and Z. Yun, 1995]. For Case 1 of the passive solar house, the volumetric air flow matrix is shown in Equation A4.3.2.

$$Q_v = \begin{bmatrix} q_{00} & -q_{01} & -q_{02} & -q_{03} \\ -q_{10} & q_{11} & -q_{12} & -q_{13} \\ -q_{20} & -q_{21} & q_{22} & -q_{23} \\ -q_{30} & -q_{31} & -q_{32} & q_{33} \end{bmatrix} = \begin{bmatrix} 22.8 & -3.9 & 0.0 & -19.1 \\ -4.41 & 27.4 & -11.3 & -11.8 \\ -3.35 & -13.3 & 22.3 & -5.41 \\ -15.0 & -10.2 & -11.0 & 36.2 \end{bmatrix} \quad (\text{A4.3.2})$$

Rewriting the matrix Q_v using the mass flow matrix Q [kg/h]:

$$Q = \begin{bmatrix} Q_{00} & -Q_{01} & -Q_{02} & -Q_{03} \\ -Q_{10} & Q_{11} & -Q_{12} & -Q_{13} \\ -Q_{20} & -Q_{21} & Q_{22} & -Q_{23} \\ -Q_{30} & -Q_{31} & -Q_{32} & Q_{33} \end{bmatrix} = \begin{bmatrix} 28.1 & -4.4 & 0.0 & -23.7 \\ -5.2 & 32.0 & -13.2 & -13.5 \\ -4.4 & -15.7 & 26.5 & -6.5 \\ -18.5 & -11.8 & -13.2 & 43.6 \end{bmatrix} \quad (A4.3.3)$$

Results of sensitivity analysis

The calculation procedure was implemented in a computer program. Using the sensitivity analysis data, each element Q in air flow matrix can be estimated by the following polynomial function (cf. § 1.3.1):

$$Q = \alpha_0 + \sum \alpha_i X_i + \sum \alpha_{ij} X_i X_j + \dots \quad (A 4.3.4)$$

Where α_0 , α_i/α_0 , and α_{ij}/α_0 are the constant, main effects and interactions effects of input parameters X , respectively. Table A4.3.5 shows the results of the sensitivity calculation in case 1. As shown in Table A4.3.4, the numbers of main effects and interactions are 16 and 31. It should be noted that the interaction coefficients are aliases.

Table A4.3.5: Main effect and some interaction effect coefficients

No.	1	2	3	4	5	6	7	8	9	10	11	12	13	14	15	16
coef.	α_1	α_2	α_3	α_4	α_5	α_6	α_7	α_8	α_9	α_{10}	α_{11}	α_{12}	α_{13}	α_{14}	α_{15}	α_{16}
No.	17	18	19	20	21	22	23	24	25	26	27	28	29	30	31	32
coef.	$\alpha_{1,2}$	$\alpha_{1,3}$	$\alpha_{1,4}$	$\alpha_{1,5}$	$\alpha_{1,6}$	$\alpha_{1,7}$	$\alpha_{1,8}$	$\alpha_{1,9}$	$\alpha_{1,1}$	$\alpha_{1,1}$	$\alpha_{1,1}$	$\alpha_{1,1}$	$\alpha_{1,1}$	$\alpha_{1,1}$	$\alpha_{1,16}$	$\alpha_{2,3}$
									0	1	2	3	4	5		
No.	33	34	35	36	37	38	39	40	41	42	43	44	45	46	47	
coef.	$\alpha_{2,4}$	$\alpha_{2,5}$	$\alpha_{2,6}$	$\alpha_{2,1}$	$\alpha_{2,1}$	$\alpha_{2,1}$	$\alpha_{2,1}$	$\alpha_{3,4}$	$\alpha_{3,5}$	$\alpha_{4,5}$	$\alpha_{6,1}$	$\alpha_{6,1}$	$\alpha_{6,1}$	$\alpha_{6,1}$	$\alpha_{10,15}$	
				3	4	5	6					3	4	5	6	

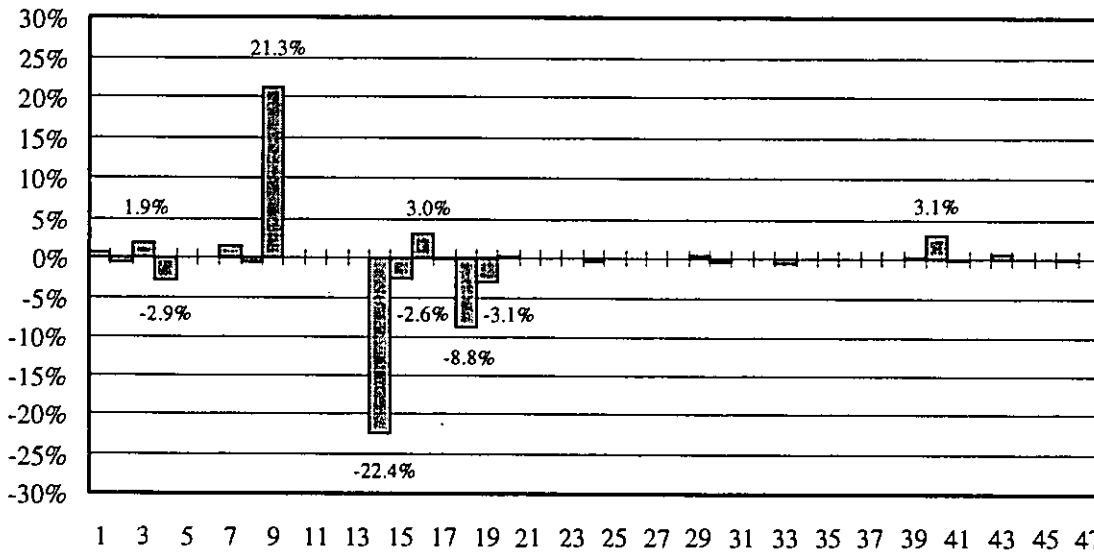


Figure A4.3.9: Effects of uncertainties on air flow rate of building(vertical axis) of 16 input parameters (horizontal axis).

Table A4.3.6: Sensitivity coefficients and related statistics of Case 1 of the passive solar house

Air flows	Q ₀₀	Q ₀₁	Q ₀₂	Q ₀₃	Q ₁	Q ₁₁	Q ₁₂	Q ₁₃	Q ₂₀	Q ₂₁	Q ₂₂	Q ₂₃	Q ₃₀	Q ₃₁	Q ₃₂	Q ₃₃
	0															
Const. α_0 [kg/h]	30.7	4.4	0.6	25.7	5.2	31.7	13.2	13.4	4.2	15.7	26.0	6.2	21.4	11.6	12.3	45.3
No. i	Effect α_i/α_0 [%]															
1	0.5	4.1	1.0	-0.1	3.9	0.6	0.0	0.0	-0.1	0.0	0.0	0.1	-0.1	0.1	0.0	-0.1
2	-0.6	-3.9	0.2	0.0	-3.5	-0.6	0.0	0.0	0.0	0.0	0.0	0.0	0.0	0.0	0.0	0.0
3	1.9	0.4	-0.4	2.2	-0.4	0.0	0.0	0.1	-1.0	0.0	-0.1	0.3	3.1	-0.2	-0.2	1.3
4	-2.9	-0.5	2.0	-3.5	0.5	0.0	0.0	-0.1	1.3	0.0	0.1	-0.3	-4.6	0.2	0.2	-2.1
5	0.0	-0.1	-0.9	0.0	0.1	2.3	5.2	0.2	-0.2	4.9	2.8	-0.5	0.0	-0.3	0.3	0.0
6	0.0	0.0	-0.1	0.0	0.0	-2.1	-4.9	-0.1	-0.1	-4.2	-2.5	0.2	0.0	0.1	-0.1	0.0
7	1.4	<u>12.7</u>	3.5	-0.6	6.3	<u>9.4</u>	<u>7.6</u>	<u>12.3</u>	0.0	<u>7.8</u>	4.4	-1.2	0.5	<u>10.3</u>	1.0	3.1
8	-0.7	-0.1	-2.3	-0.8	0.1	-3.7	<u>-8.7</u>	-0.4	-10.1	<u>-7.8</u>	<u>-15.7</u>	<u>-39.6</u>	0.9	0.3	<u>-23.9</u>	-6.0
9	<u>21.3</u>	<u>-18.9</u>	<u>-82.1</u>	<u>30.5</u>	<u>16.7</u>	<u>-4.5</u>	0.1	<u>-17.2</u>	<u>41.4</u>	-0.1	<u>13.1</u>	<u>27.2</u>	<u>18.4</u>	-4.9	<u>31.2</u>	<u>15.9</u>
10	0.0	0.0	-0.3	0.0	0.0	0.0	0.0	0.0	0.1	0.0	0.1	0.2	0.0	0.0	0.1	0.0
11	0.0	0.0	-0.2	0.0	0.0	0.0	0.0	0.0	0.0	0.0	0.0	0.0	0.0	0.0	0.0	0.0
12	0.1	0.0	0.5	0.1	0.0	0.0	0.0	0.0	0.0	0.0	0.0	0.0	0.1	0.0	0.0	0.1
13	-0.1	0.2	-1.4	0.2	0.0	0.0	-0.1	0.2	1.9	0.0	0.2	-0.5	-0.5	0.0	1.2	0.1
14	<u>-22.4</u>	5.5	<u>98.9</u>	<u>-29.9</u>	<u>-23.5</u>	-1.6	0.5	4.8	<u>-33.8</u>	-0.3	-2.3	14.1	<u>-19.9</u>	<u>-6.0</u>	-9.8	<u>-13.6</u>
15	-2.6	1.1	1.6	-3.6	-4.1	-0.2	0.1	0.9	-4.9	-0.1	-0.3	2.2	-1.8	-0.9	-1.5	-1.5
16	3.0	3.0	3.0	3.0	3.0	2.9	2.8	2.9	3.0	2.8	2.9	2.8	3.0	2.9	2.9	3.0
Main effects [%]	31.4	24.3	<u>130.6</u>	43.2	30.4	12.0	13.9	21.9	54.8	13.1	21.6	50.2	27.9	13.3	40.7	22.4
Interactions [%]	9.9	2.8	85.0	9.7	2.6	0.6	1.0	1.8	6.1	0.8	2.4	8.3	14.9	1.2	6.3	6.2
All effects [%]	32.9	24.5	<u>155.8</u>	44.3	30.5	12.0	13.9	22.0	55.1	13.1	21.7	50.9	31.7	13.3	41.2	23.2
Standard Deviation	10.1	1.1	0.9	11.4	1.6	3.8	1.8	2.9	2.3	2.0	5.7	3.1	6.8	1.5	5.1	10.5

Figure A4.3.9 shows the effects of uncertainties of input parameters on the air flow rate of a building (ventilation rate). It can be found that the parameters of outdoor temperature (No. 14) and temperature of room 3 (No. 9) has greater effect on the building ventilation rate than other parameters. On the other hand, the error combination of two parameters (No. 18) including the leakage area of the south and north windows also affects the result of ventilation rates in a wider range.

Comparison of air flow range

Estimated air flow results using the tracer gas method also include a series of errors. In this study, we assess these errors considering that the accuracy of the tracer gas concentrations and temperatures are 3% and 1°C. Figure A4.3.10 shows the comparison of measured and calculated air flow rates using results of sensitivity analysis. Taking the standard deviations into account, it can be seen that the majority of measured and calculated results are in agreement. Table A4.3.6 illustrates the same type of comparison but at the level of the flow matrix.

From this case study, the multizone air flow model is coherent with measurement results and gives a reasonable numerical prediction. The measurement errors of input parameters have an important effect on output estimated by tracer gas method and simulated by a multizone air flow model. The errors cause the average values of simulation and measurement air flows to

have a difference. The sensitivity analysis of multizone model and tracer method show that the two series of air flow mostly have an agreement range, if the errors of measured input parameters are taken into account.

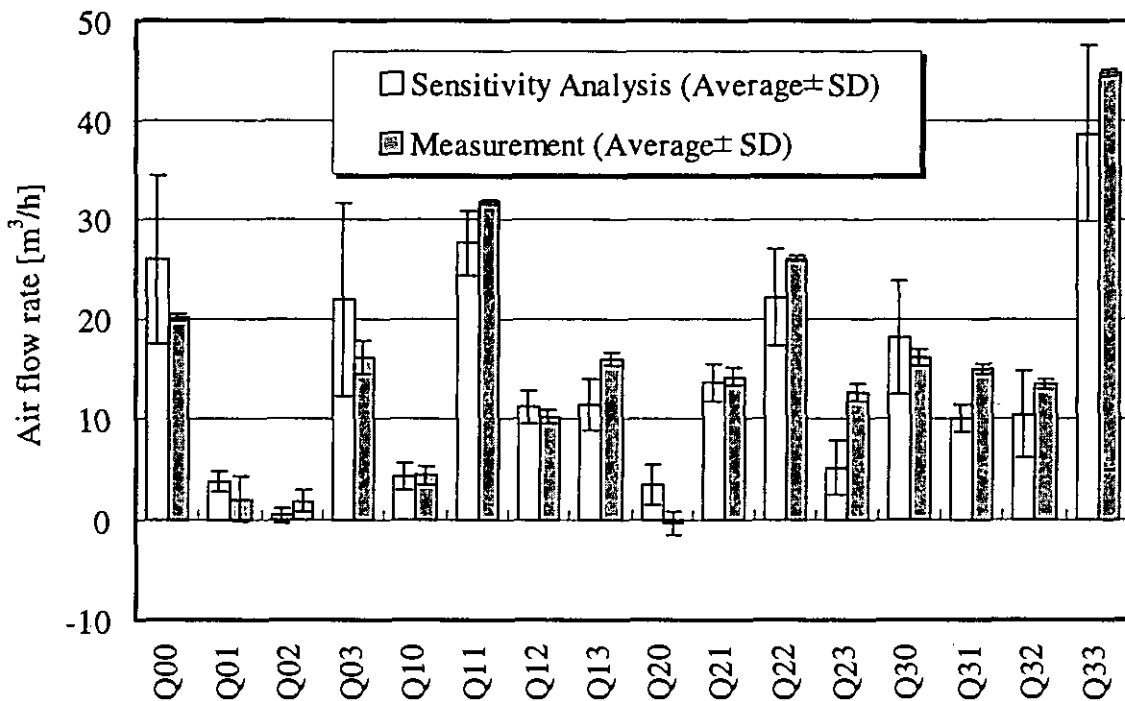


Figure A4.3.10: Comparison of measured air flow rates with calculated rates using results of sensitivity analysis

A 4.3.5 Conclusions

In order to evaluate the COMIS model, a passive solar house which is not equipped with any mechanical ventilation system is used. The natural ventilation in the house is controlled by wind and indoor- outdoor temperature differences. For measurement of the multi-room air flow, 3 rooms and 3 tracer gases are used. The results of air flow rates under three different conditions are assessed with decay method of multi-tracer gas.

Using the COMIS model, the three cases of multizone air flow and pollutant transport pattern are simulated utilising the data measured in situ. By comparing the average air flows between measurement and simulation, the relative error of air change rates is mostly within $\pm 25\%$. These results are both encouraging and reasonable because the drive of natural ventilation is unsteady and is treated by average data. For comparison of tracer gas concentrations, the average factors calculated to measured values are from 1.06 to 1.10 for three cases. It can be concluded that indoor air pollutant concentrations tend to be overestimated under natural ventilation, so the simulation of multizone air flow and pollutant transport leads to a safe design of indoor air quality using the COMIS model.

Furthermore, experimental evaluation of the COMIS model is conducted using the sensitivity analysis method in order to assess the effect of uncertainty or error of parameters from measurement. By comparing air flow range between measurement and simulation, it is found that there are common ranges between the two series of data. Therefore, it can also be concluded that the COMIS model is practicable for such case.

A 4.3.6 References

- Fürbringer J. M.: Evaluation procedure using sensitivity analysis of model and measurement, *International symposium on air flow in multizone structure, Sept., 9, 1992 in Budapest.*
- Roulet C. -A., Vandaele L.: Air flow pattern within buildings measurement techniques, *AIVC TN 34, 1991.*
- Yoshino H. et al: Measurement of multizone ventilation using a passive solar test house, *International symposium on air flow in multizone structure, Sept., 9, 1992 in Budapest.*
- Yoshino H. et al: Simulation and measurement of air infiltration and pollutant transport using an passive solar test house, *American Society of Heating, Refrigerating and Air-Conditioning Engineers Symposium, 1995.1.28-2.1 in Chicago.*
- Zhao Y. et al: Measurement of multizone airflow rates of a passive solar test house, *Collective abstracts of academic research symposium, Tohoku branch of Architectural Institute of Japan, June, 19, 1993. (in Japanese).*
- Zhao Y. et al: Measurement of multizone infiltration rate using a test house and comparison with calculation of a multizone infiltration model, *Proceeding of academic research symposium of the Society of Heating, Air-Conditioning and Sanitary Engineerings of Japan, Oct. 22, 1993. (in Japanese).*
- Zhao Y. et al: Validation of multizone air flow model and its application, *Phd Thesis of Tohoku University, Sendai, 980-77, Japan, Jan. 20, 1995.*

Japanese Family House

A 4.3.7 Measured object

The measurements were conducted using a two-story Japanese family house in Sukagawa city, Fukushima prefecture, Japan. Figures A4.4.1 and 4.4.2 show the elevation and the floor plan of the house. The first and second floors are 0.6 and 3.4 m above the ground level floor, respectively. The width from the east to the west of the house is 10 meters and the depth from the north to the south is 8 meters. The total floor area of this house is 133 m² with an air volume of 350 m³. The building is 7.5 m high. The interior of the test house is considered to have 9 rooms. The hall on the first and second floors are connected by a void and stairs, and are considered as two zones. The number of zones are shown in Figure A4.4.2. Zone No. 10 indicates outdoor.

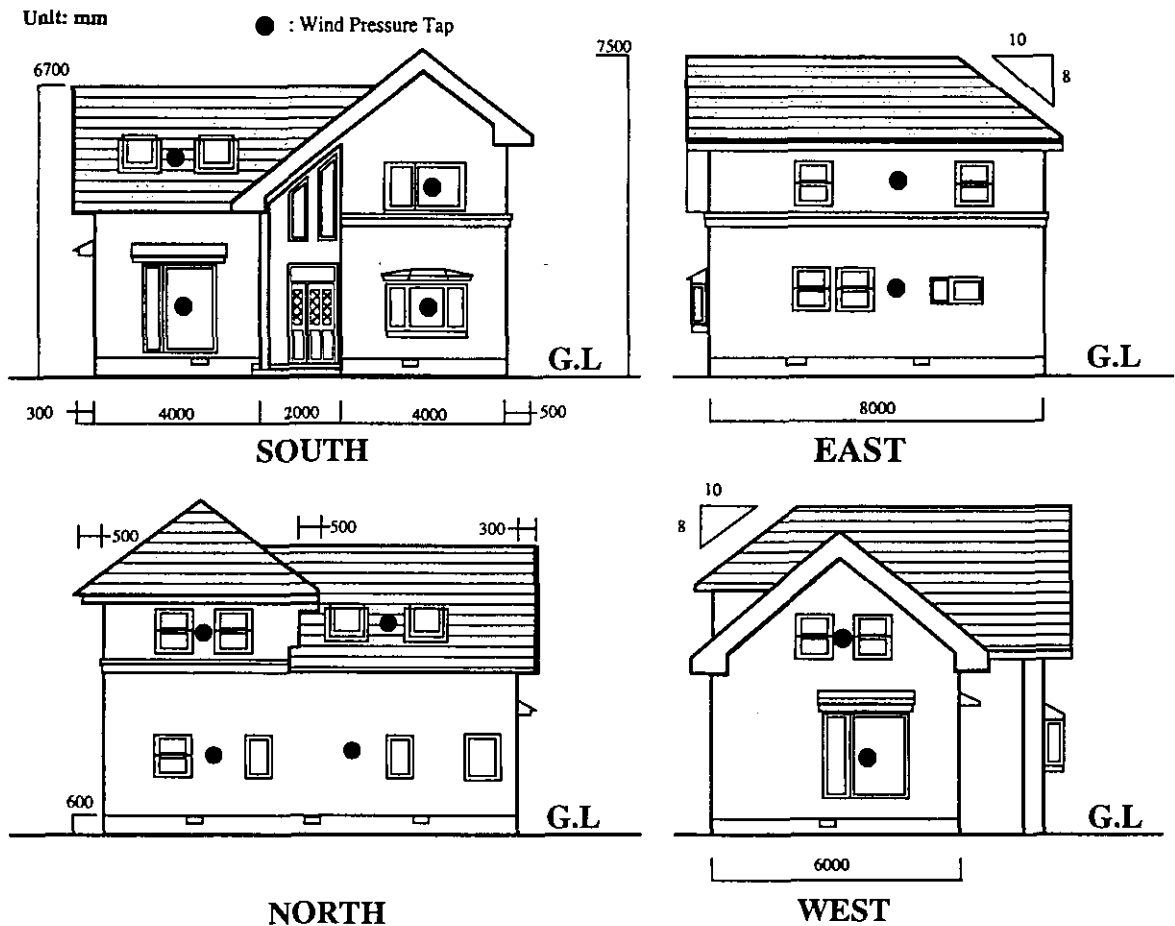


Figure A4.3.1: Elevation of Japanese family House

An 8 m long pole which is located at the south west of the house, is equipped with a wind direction meter at the top and five wind meters at different levels. The measuring heights are 8, 5, 2.7, 1.6 and 0.5 meters above ground level. Outdoor temperature is measured at the four points around the external walls. Indoor temperatures are measured at the centers of the rooms at a height of 1.1 m above floor level. Measuring points for tracer gas concentration are also similarly positioned. Wind pressure taps on the outside walls are located at the points shown as black circles in Figure A4.4.1. The point of reference pressure is assumed to be at the ground level below the first floor.

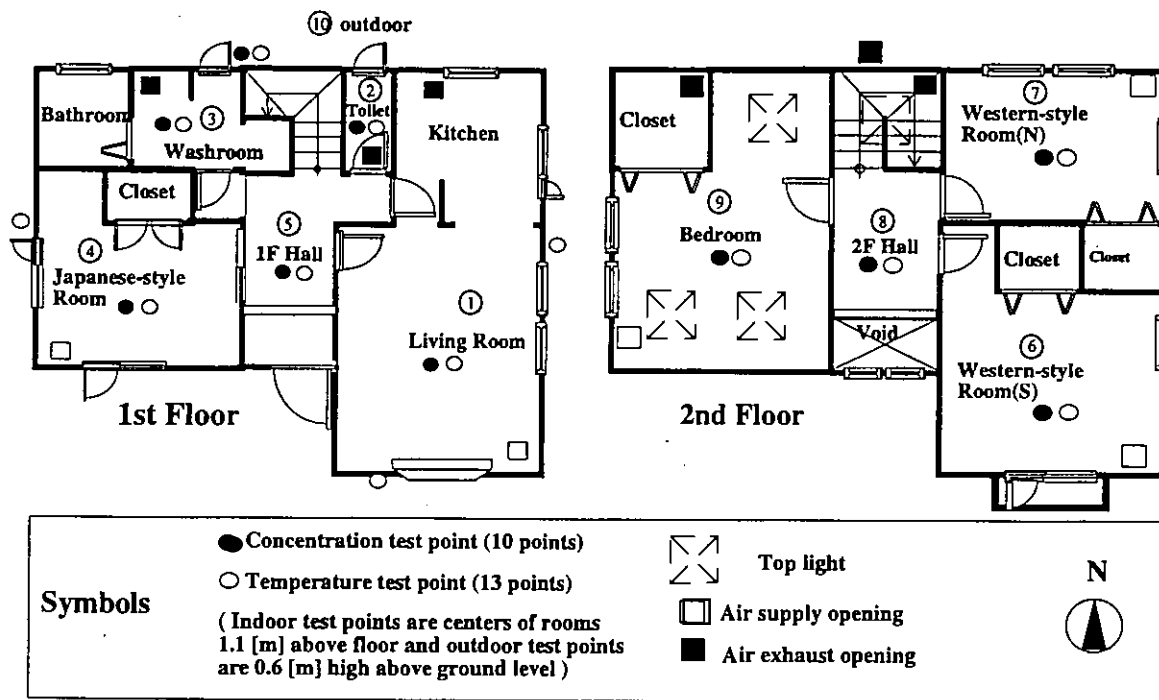


Figure A4.3.2: Floor plan of Detached Test House

A 4.3.8 Measurements performed

Conditions and method

In order to measure the air flows and indoor gas concentrations, the living room is heated with six heaters of equal power and the ventilation system is not operating. All internal doors are closed. The average values of wind and outdoor and indoor temperatures during the measurements are shown in Table A4.4.1. It is found that the two measurement data sets for air flow and indoor gas concentrations are almost the same.

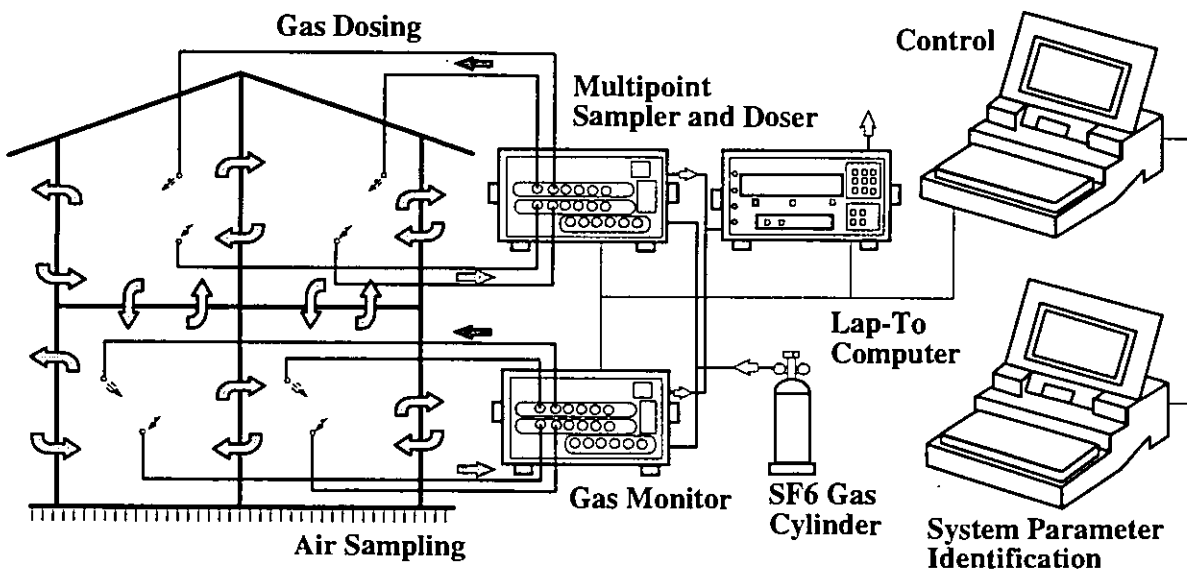


Figure A4.3.3: Diagram of multizone air flows measurement system

Table A4.3.1: Characterization of the measurement periods selected for comparison

Measurement	Air flows	Indoor gas concentrations
Date	30 to 31 Jan. 1994	31 Jan. to 1 Feb. 1994
Measurement time	10 hours	16 hours
Time for simulation	3 hours	15 hours
Number of tracer gas concentration data points	180	900
Time step	10 minutes	10 minutes
Average wind direction	East	East
Average wind speed	2.32 m/s	1.42 m/sec
Outdoor mean temperature	-6.86 °C	-4.30 °C
Zone 1 to 9 mean temperature [°C]	33.89, 19.57, 14.63, 11.81, 16.04, 13.60, 13.03, 16.16, 11.24.	33.35, 18.26, 12.54, 15.64, 15.62, 15.94, 13.21, 15.71, 13.20.

Method of air flows measurement

The measurement of air flow is carried out using a method of system parameter identification developed by H. Okuyama [1992]. Figure A4.4.3 is a diagram of multizone air flow measurement system. Rectangular pulses of SF₆ tracer gas are injected in each room for identification. The changes of concentration which occur in each zone result from the response to the injection and dilution from incoming air. The gas injection schedule is shown in Figure A4.4.4. The indoor gas concentration of each room is sampled every ten minutes. Based on these data, every one-minute data are calculated by linear interpolation approximation. In each room, fans are used for mixing indoor air with tracer gas.

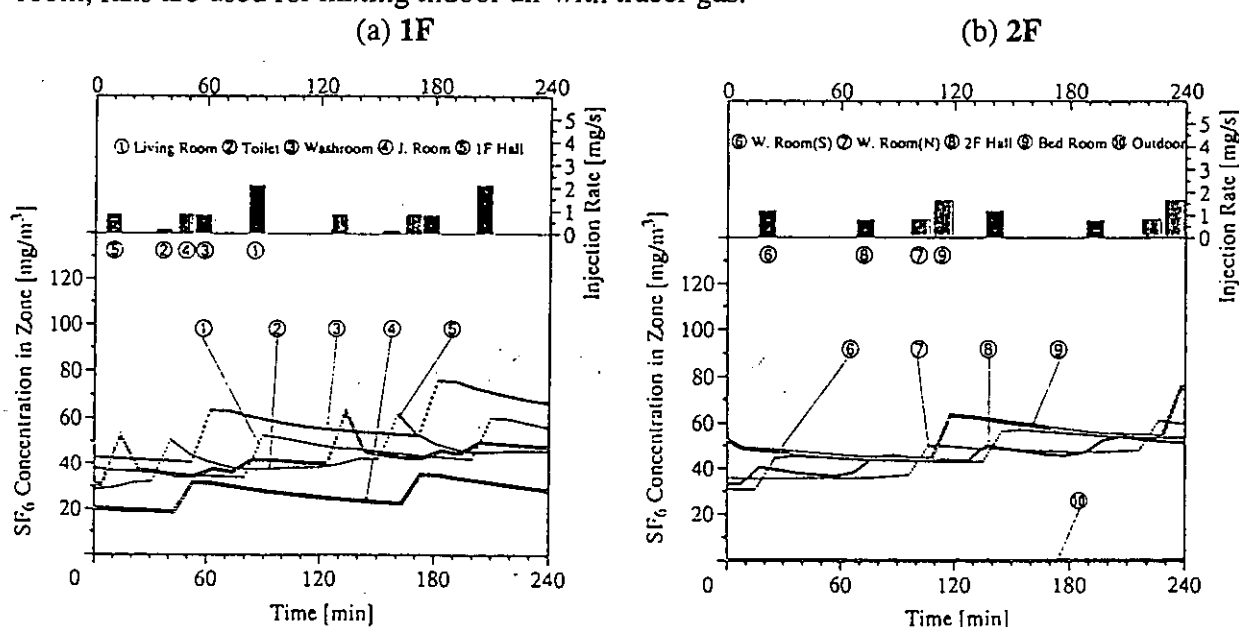


Figure A4.3.4: Profiles of tracer gas concentrations and injection for air flows measurement

Measurement of the indoor gas concentration

For the evaluation of the multizone indoor pollutant transport model, the measurement of indoor gas concentrations is carried out. The system for measuring air contaminant (i.e. tracer

gas) concentration is the same as that for air flow. Tracer gas injection is shown in Figure A4.4.5. The gas is only injected into the living room for one hour from the beginning of the measurement. The indoor gas concentration of each room is sampled every ten minutes.

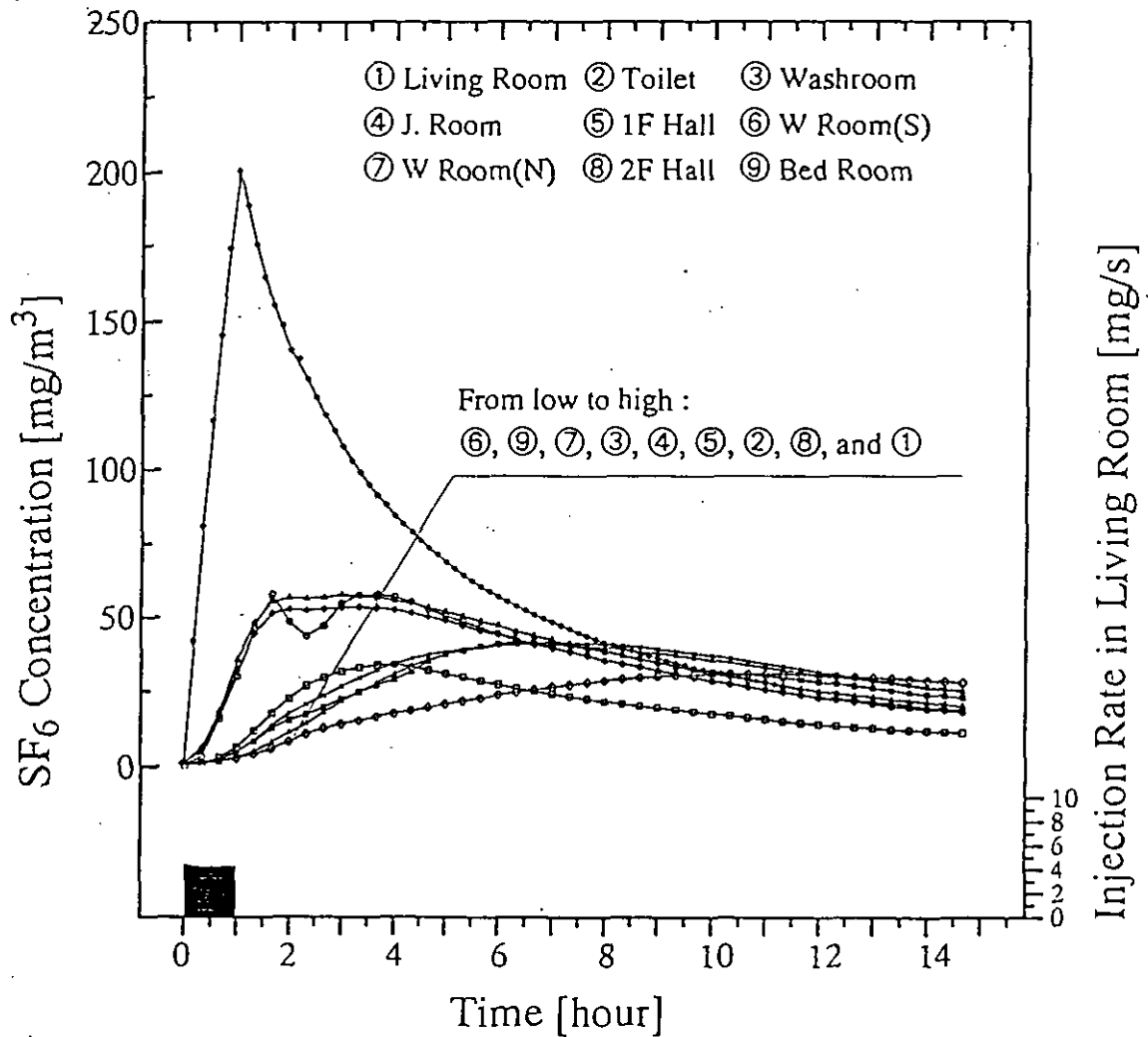


Figure A4.3.5: Profiles of tracer gas concentrations and injection for indoor gas concentrations measurement

Air leakage distribution

Effective leakage areas of the windows, walls, doors and other components are measured by the fan pressurisation method. The results of the leakage distribution is shown in Table A4.4.2. The equivalent leakage area for the link pressure difference of 9.8 Pa, *ELA*, of external wall and windows is 33.5 cm² and 67.0 cm², respectively. The total of the *ELA* of internal door is 910 cm². The equivalent leakage area per floor area of the building envelope is 0.8 cm²/m².

Air flow estimation

The concentration profiles of tracer gas in 9 rooms are shown in Figure A4.4.5. The concentration in each room increases sharply during the injection of the tracer gas. After the injection is finished, the concentrations decrease slowly. The concentrations of other rooms are affected due to inter-zonal air flows. The 180-minute average of air flow rates between rooms is estimated using the system parameter identification method. For this measurement, it is assumed

that the gas concentration in a room is mixed instantly and uniformly. The results of air flows and air change rates are shown in Figure A4.4.6.

The air flow rates between the living room, which is heated, and the hall, on the first floor, are higher than those between other rooms. The inter zonal air flow rates exceed the infiltration rates between indoor and outside. For this building, the outdoor air infiltration rate is only 0.05 volumes per hour.

Indoor gas concentrations

For the measurement of indoor concentrations, the tracer gas is injected into the living room for 1 hour. As shown in Figure A4.4.5, the concentration in the living room reaches 200 mg/m³. After the injection stops, the concentration in living room goes down fast. The concentrations in other zones increase slowly until they reach a maximum After that they decrease gradually over a period of time. In the toilet, the concentration does not change smoothly. The reason for this may be that the volume of the toilet is too small to be easily influenced by wind turbulence.

Table A4.3.2: Equivalent leakage areas of Japanese family house

Element/Component	ELA	1/n
Building envelope	33.50	1.25
Living Room South Window	3.44	1.27
Living Room East Window	0.00	1.25
Windows of Toilet, Washroom and Bathroom	17.49	1.50
Windows of Japanese-style Room	19.66	1.53
South Window of Western-style Room(S)	6.06	1.50
Windows of Western-style Room(S), (N) and Bedroom	9.28	1.42
Top Light Windows(Ventilating Opening CLOSED)	11.29	1.56
Vestibule Door	0.00	1.50
Air Conditioner Outlet	0.00	1.20
Air Supply Opening(CLOSED)	0.00	1.21
Air Supply Opening(OPEN)	51.26	1.62
Air Exhaust Opening(OPEN)	20.86	1.55
Kitchen Door	103.47	1.78
Living Door	106.51	1.69
Toilet Door	113.82	1.60
Washroom Door	120.31	1.76
Door of Japanese-style Room	106.18	1.80
Door of Western-style Room(S)	119.24	1.81
Door of Western-style Room(N)	135.23	1.77
Bedroom Door	106.18	1.80
<i>ELA : Equivalent Leakage Area</i> <i>n : Flow Exponent of leakage</i>		

Air change rate in each zone [1/hour]

zone	1	2	3	4	5	6	7	8	9	10
ach	0.38	0.17	0.13	0.55	4.07	0.17	0.44	5.2	1.52	0.05

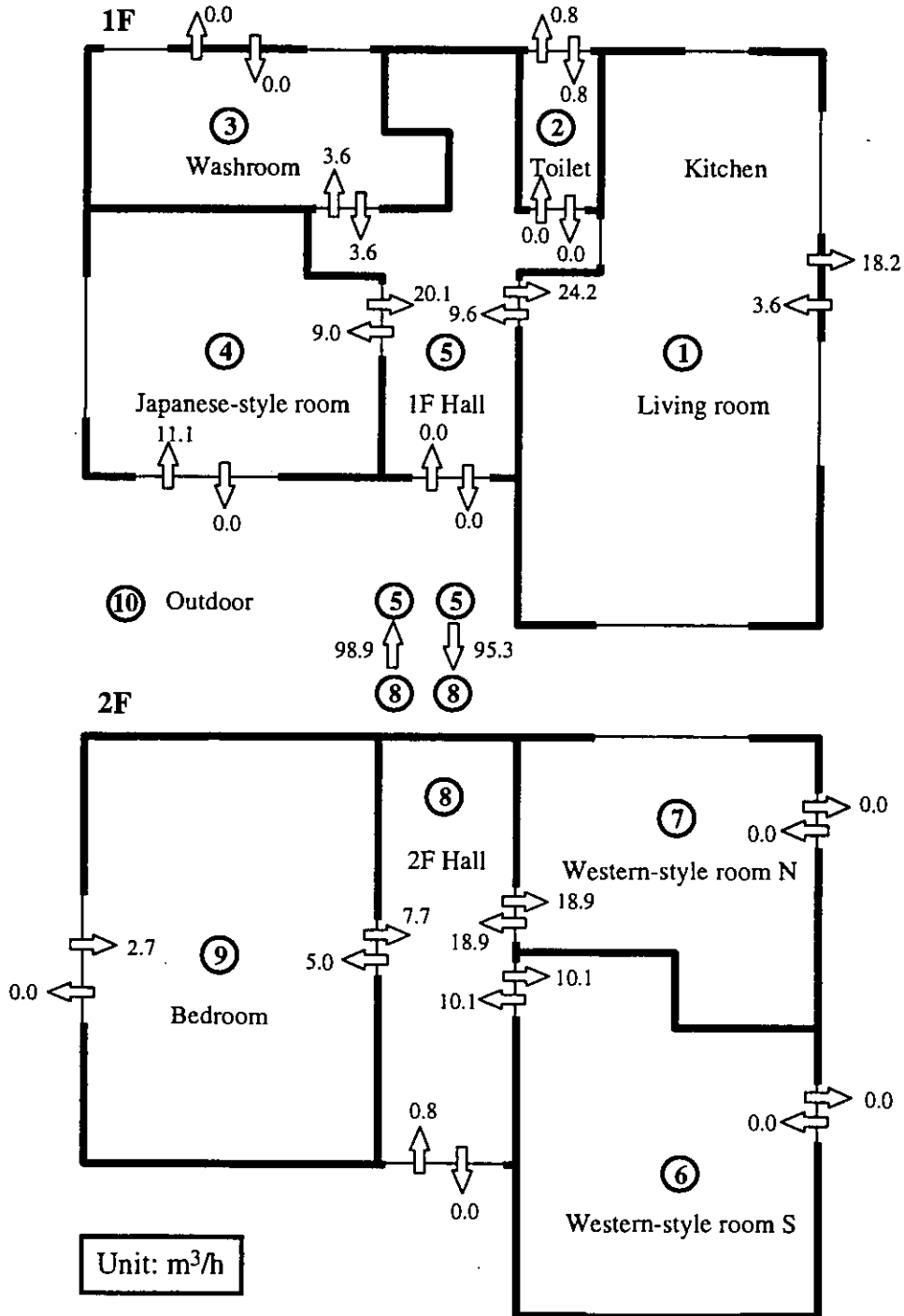


Figure A4.3.6: Measured air flow rates and air change rates

Air change rate in each zone [1/hour]

zone	1	2	3	4	5	6	7	8	9	10
ach	0.42	0.97	0.22	0.44	1.32	0.14	0.17	1.32	0.18	0.11

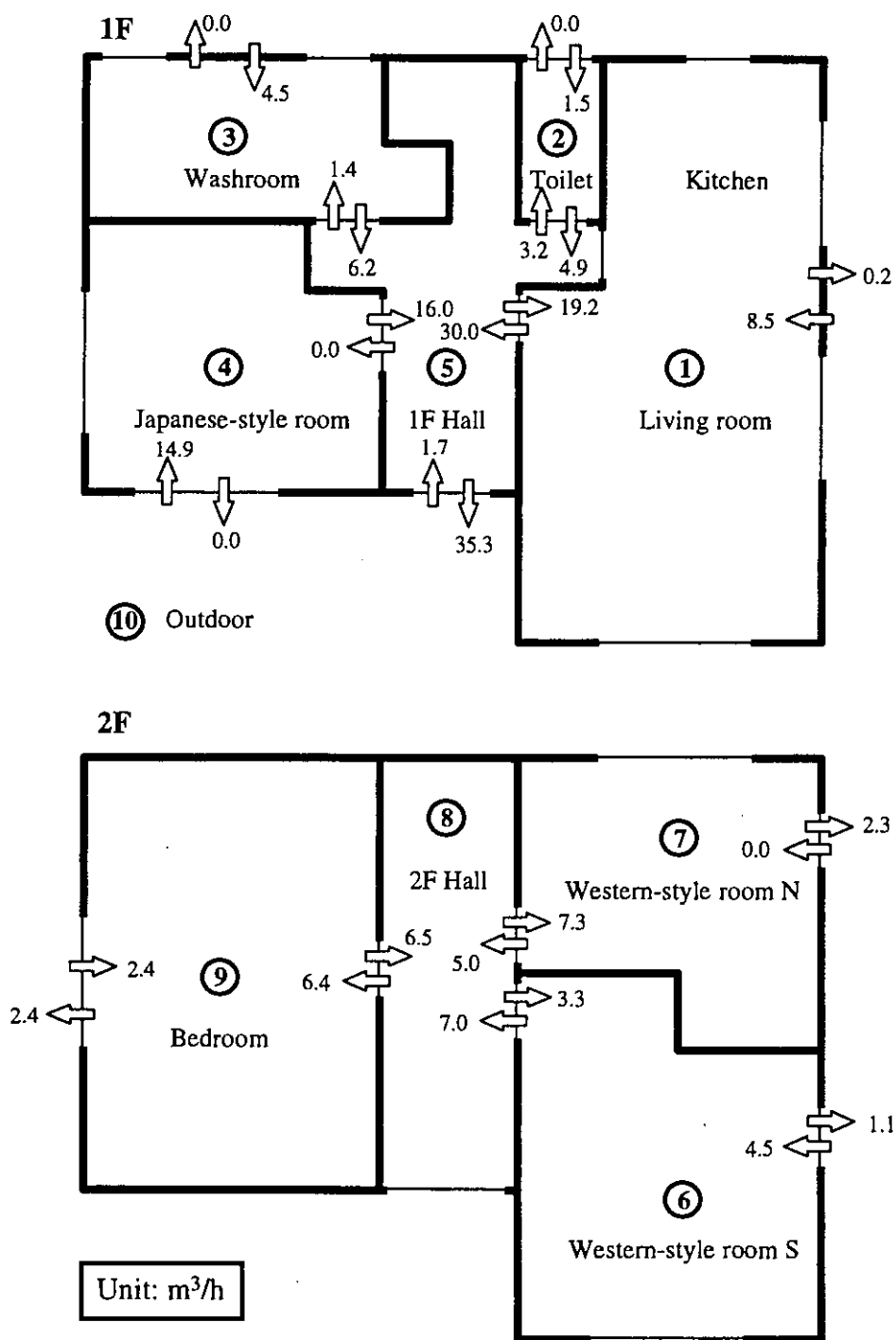


Figure A4.3.7: Simulated air flow rates and air change rates

A 4.3.9 Comparison of measured and calculated data

Input data of simulation

For simulation of air flows, the input data of wind and temperature are 180-minute average values as shown in Table A4.4.1. The input leakage data of the test house is the same as shown in Table A4.4.2. For the simulation of indoor gas concentrations, the characteristics of the wind direction, wind velocity and temperature is illustrated in Figure A4.4.8. Input data of temperature is averaged for ten minutes. The wind velocity is averaged for thirty minutes.

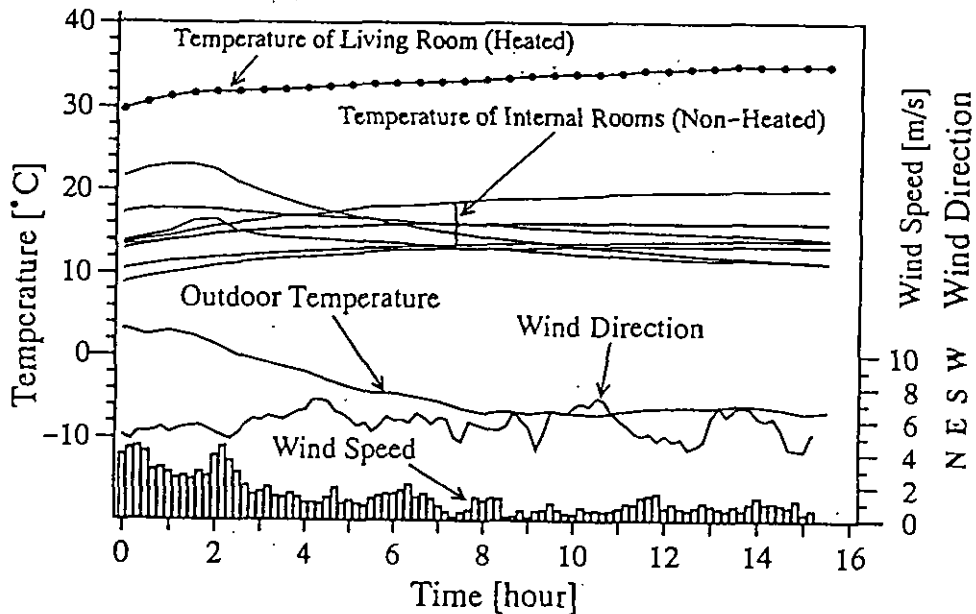


Figure A4.3.8: Wind and temperature in measurement of indoor gas concentrations

Comparison method

The relationship between measured and calculated data and the influence of the respective errors are shown in Figure A4.4.9. Error analysis is not carried out, so the comparisons are conducted by using the average data and the linear regression analysis.

Air flow measurement is done with an airtight test house and the zone layout of this building is shown in Figure A4.4.2. Though the hall is treated as two zones for measurement purposes, it is considered as one zone for the simulation because of the existence of a large opening between halls 1F and 2F. Therefore, comparison between measurement and simulation does not include air flow between these two halls. Even though zones 5 and 8 are kept in the air flow figures, this does not mean two zones. The results of air flow simulation are shown in Figure A4.4.7. For simulation, since the hall is not divided into two zones, the two air flow paths between halls 1F and 2F do not exist and therefore the four air flow paths between these halls and outdoors are assumed to be two paths.

Air flows

The network used for simulation is shown in Figure A4.4.10. The calculated air flow rates are illustrated in Figure A4.4.7. It can be seen that a good agreement between simulation and measurement is achieved for some rooms. For other rooms, the agreement is poor.

Figure A4.4.11(a) presents a comparison between the measured and the calculated air change rates. It is clarified that both air change rates are close for some rooms, except for the toilet,

which has a smaller air volume and therefore shows a difference between the measurement and calculation result. The regression coefficient between the two sets of air change rates is 0.95 (i.e. : 1/1.05). The correlation coefficient between measurement and calculation is 0.70.

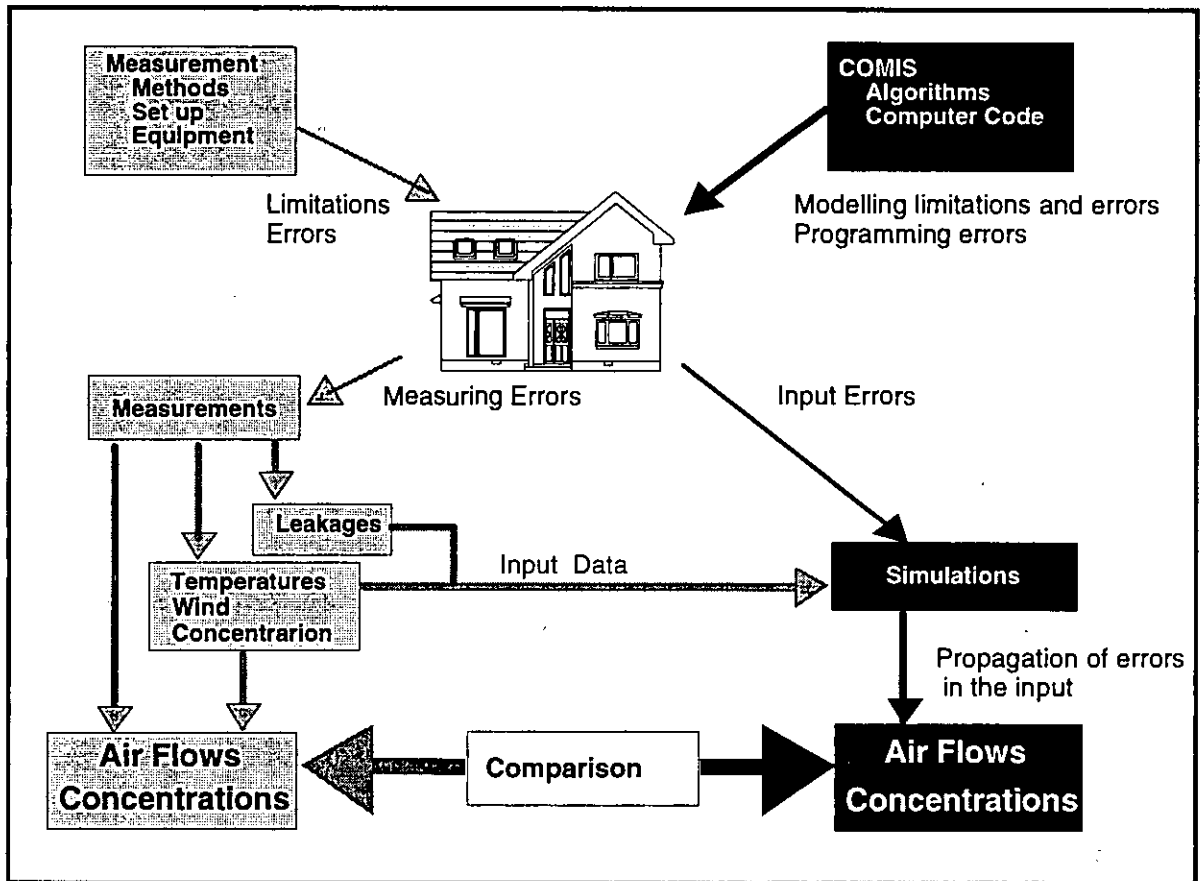


Figure A4.3.9: Comparison method of measured and calculated results

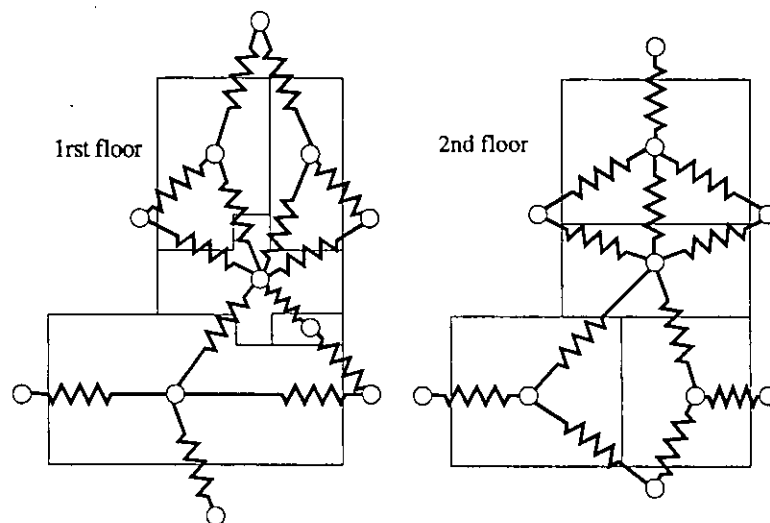


Figure A4.3.10 Flow network of the Japanese family house

On the other hand, Figure A4.4.11(b) presents a comparison between the measured air flow rates and the calculated results. It can be found that both air change rates are different for many of flow paths and the regression coefficient between the two sets of air change rates is 1.54 (i.e. : 1/0.65). The reason for these differences could be due to the fact that the full meas-

urement error, including error propagation through the identification method may exceed $\pm 20\%$, depending on the measurement conditions [Roulet, 1991].

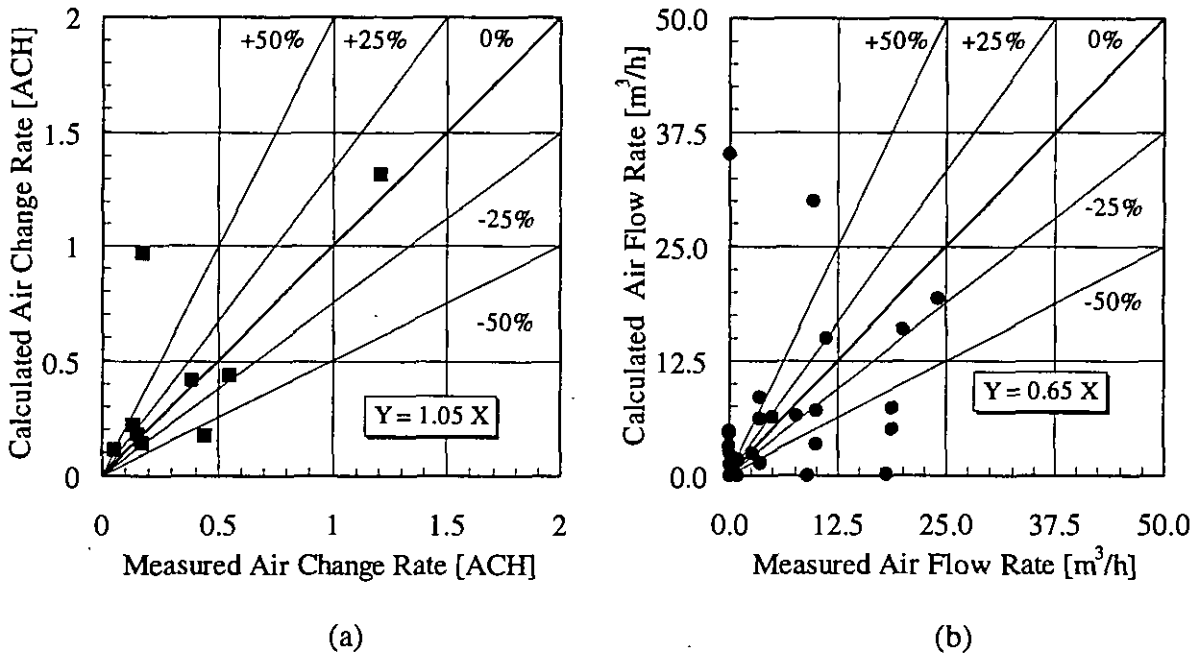


Figure A4.3.11: Comparison of measured and calculated air flows

An other reason could be that the measured results are average values of air flow taken over a period of three hours during which time the climatic conditions may have changed and air change rates are not always stable. However, simulated air flows are based on stable condition where the climate data are average values from measurements. Moreover, well-mixing is difficult to achieve because a large fan affects the air flow of zone and it can not be used for mixing. Overall, the simulation results are considered reasonable because their accuracy is based on the accuracy of the average input data and the measurement technique.

Indoor gas concentrations

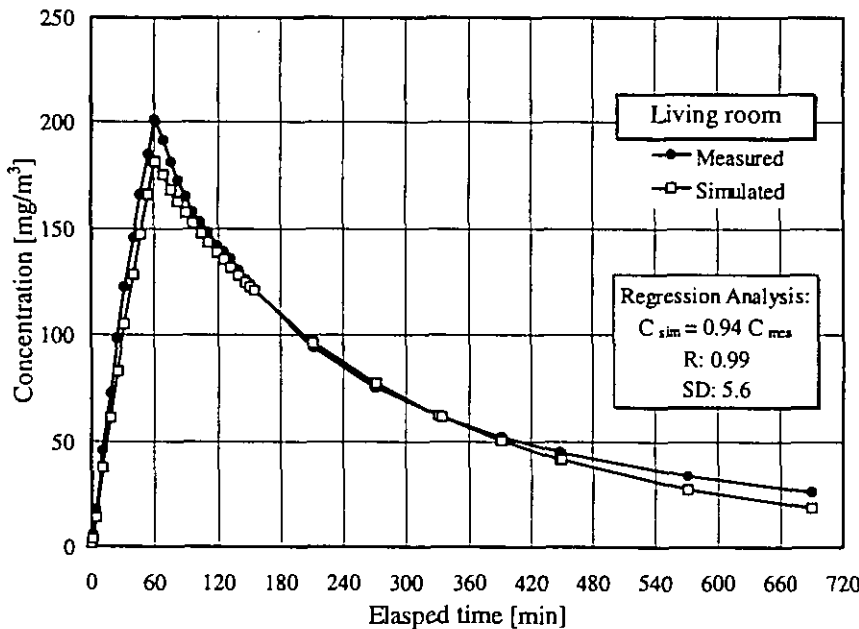


Figure A4.3.12: Comparison of measured and simulated gas concentrations of living room

The simulation of indoor concentration change was conducted using the concentrations measured when tracer gas injection started, as initial gas concentrations. Figure A4.4.12 shows a measured and simulated indoor gas concentration profile of the living room where tracer gas has been injected. It reveals that two sets of results agree well. Figure A4.4.13 shows comparison of indoor concentrations measured and simulated in all zones of building.

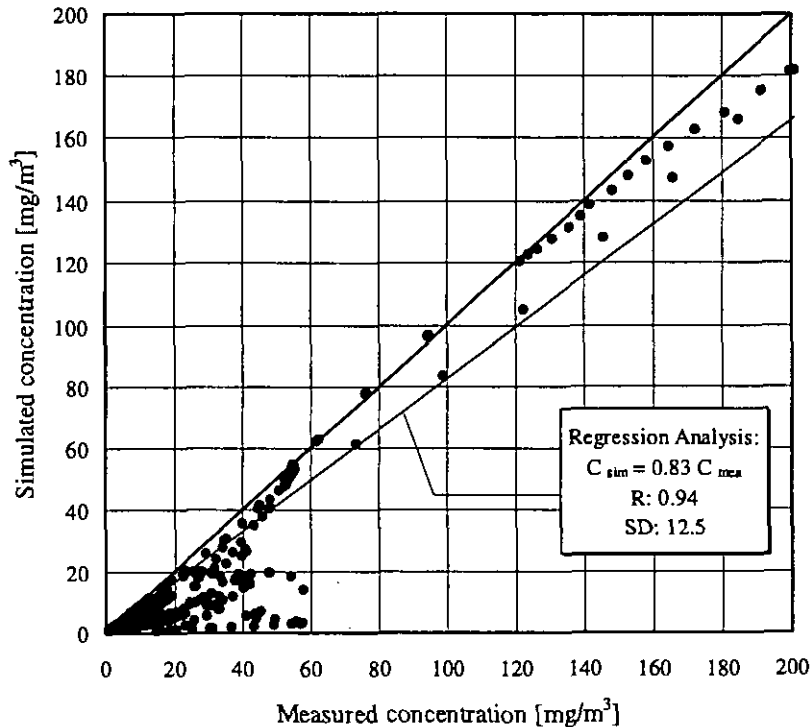


Figure A4.3.13: Comparison of measured and simulated indoor gas concentrations

The results indicate that, while the measured and calculated gas concentrations are not same, neither are they not remarkably different. The regression coefficient and correlation coefficient between calculated and measured concentration is 0.83 and 0.94 by linear regression analysis. The good agreement between measurement and simulation is achieved for some rooms, but for the other rooms it is not quite so good. The reason may be that air flow rates used for the pollutant transport calculation differ from the actual rates. In addition, it may also be caused by the approximated average input data for simulation, especially the wind pressure coefficients and distribution of leakage areas.

A 4.3.10 Conclusions

For measurement of the multizone air flow and indoor pollutant transport, nine zones and SF₆ tracer gas are utilised in an airtight Japanese family house. A system identification method is used for the evaluation of air flows. The multizone air flows and pollutant transport pattern are simulated by the COMIS model, using the data measured in situ as input.

For air change rates, the regression coefficient and the correlation coefficient between the two sets of air change rates are 0.95 and 0.70. The differences between the two sets of air change rates is not significant, because of uncertainties resulting from measurement error and error propagation through the simulations. But for air flow rates, large differences between measurement and simulation remain.

For indoor gas concentrations only, measured and simulated profiles of tracer gas concentrations in the living room, where gas is injected, have a good agreement. In all zones of the building, the regression coefficient and correlation coefficient between the two sets of results are 0.83 and 0.94, respectively. The good agreement between measurement and simulation is achieved for some rooms, but for the other rooms it is a little worse. The reason may be that air flow rates for pollutant transport calculation have some differences compared with the real rates.

Overall, the simulation results are considered to be reasonable because their accuracy is based on the accuracy of the average input data and the measurement technique. From the results of the case presented here, the conclusion can be drawn that the COMIS model is useful for simulation of multizone air flow and pollutant transport. Experimental validation should be continued to certify the accuracy of this model especially considering the error accompanying the measured values.

A 4.3.11 References

- Roulet C. -A. et al: Air flow pattern within buildings measurement techniques, *AIVC TN 34*, 1991.
- Okuyama H.: Recent Progress on the Multi-Chamber Airflow Measurement System, *International Symposium on Room Air Convection and Ventilation Effectiveness*, 22-24 July, 1992 in Tokyo, Japan.
- Zhao Y. et al: Measurement of multi-zone ventilation rates using an airtight house, *Collective Abstract, Academic Research Symposium, Architectural Institute of Japan*, 9 Sept., 1994, (in Japanese)
- Zhao Y. et al: Simulation and measurement of air flow and pollutant transport using an airtight house, *Proceeding of academic research symposium of the Society of Heating, Air Conditioning and Sanitary Engineering of Japan*, 8 Oct., 1994.
- Zhao Y. et al: Validation of multizone air flow model and its application, *PhD Thesis of Tohoku University, Sendai*, 980-77, Japan, Jan. 20, 1995.

A 4.4 LESO three storey office building

A 4.4.1 Measured object

The LESO building is a three storey, medium sized office building on the campus of the Swiss Institute of Technology in Lausanne. It consists of nine south oriented cells with passive solar facades, a few differently orientated rooms, and a staircase. To the north, the building is attached to another laboratory building, the LEA building. The left hand side diagram in Figure 4.5.1 shows the building and its room numbers, whilst the right hand picture details the surrounding area which clearly illustrate the rather heavily shielded exposition of the LESO building.

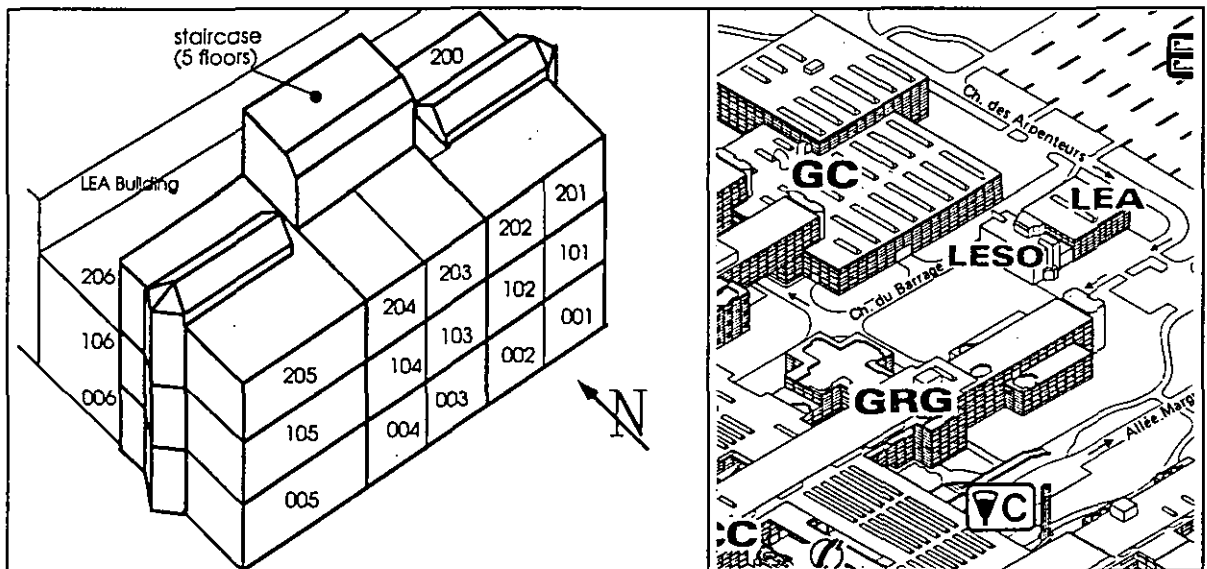


Figure 4.5.1: The LESO building (with the attached LEA building, left) and its surroundings (right)

A 4.4.2 Measurements

In this particular building component leakages have been carefully determined by extensive measurements using the guarded zone pressurisation technique [Roulet *et al*, 1991; Fürbringer *et al*, 1991]. Boundary conditions (meteorological data, pressure differential at facades) were recorded continuously. Air flows rate were measured during several periods of time with single and multiple tracer gas constant concentration technique [Compagnon *et al*, 1991].

Building related measurements, including aerualic data, have been measured for many years. The data concerning the leakage characteristics and the air flows have been compiled in a set referred to as the "LESO data set" [Fürbringer *et al*, 1990].

From this data set, three periods have been selected for the comparison, the characteristics of which are summarised in Table A4.5.1:

Table A 4.5.1 Characterization of the measurement periods selected for comparison

Period	Series 1-88	Series 2-88	Series 3-88
Date	24/25 Dec 1988	27 Dec 1988	27 Dec 1988
Time	22h30 to 07h00	03h00 to 06h00	15h00 to 19h00
Number of data points	18	7	9
Time step	0.5 h	0.5	0.5
Wind sector	N	E and W	S
Mean wind speed	1.5 m/s	≈ 0 m/sec	decreasing from ≈1.4 to ≈0.2 m/sec
Outdoor temperature	3 °C	4.5 °C	6 °C
Indoor temperature	19 to 22 °C	19 to 22 °C	20 to 23 °C
Wind situation	Steady wind speed and direction from north	Almost no wind	Decreasing wind from approx. south
Archimedes Number $\frac{\Delta\theta_{in-outside} g H_{Staircase}}{\theta_{in} V_{Wind}^2}$	48.3	large	253

Measured and calculated air flows have also been compared for other time periods, especially in winter 1987. For the results of this comparison, see [Dorer, 1992] and [Dorer, 1993].

Climatic data were measured as both instantaneous and average values over 15 minutes. From these values, an average wind speed value for a 30 min period has been derived, the direction being the instantaneous value.

Air leakage data have been measured using a guarding zone technique with two fans [Fürbringer, 1991].

Air flows have been determined by constant concentration multi tracer gas technique and by interpreting the measurements using mass conservation equations [Compagnon, 1991]. For each zone i the global incoming air flow Q_{ai} was determined as the weighted sum of the individual air flows coming from outside (Q_{oi}) or from adjacent zones j (Q_{ji}):

$$Q_{ai} = Q_{oi} + \sum_{j=1,N} \eta_{ji} Q_{ji} \quad (N = \text{total number of zones}) \quad (\text{A4.5.1})$$

The weighting coefficients η_{ji} are functions of the tracer gas concentration levels in each zone and are determined from the tracer gas concentrations during the measurements.

From the per zone values Q_{ai} , a global value for the whole building is formed as given below, weighting the Q_{ai} - values per zone with the respective zone volume V_i :

$$Q_{a-Building} = \frac{1}{\sum_{i=1,N} V_i} \sum_{i=1,N} Q_{ai} V_i \quad (\text{A4.5.2})$$

In fact, this value does not differ significantly from the simple sum of all Q_{ai} - values.

A 4.4.3 Modelling and simulations

For the sensitivity analysis as well as for the simulation of the measured periods, the building is represented by a network which consists of 11 zones and a total of 28 air flow links. These air flow links represent the measured leakages and are modelled by the well-known power law model for crack flow. In order to bring proper input to the simulations, some coefficients,

which were measured globally, have been split up between two or more conductance elements, especially in the staircase zone. The effect of the regrouped conductances has been evaluated and the consequences of the applied partition has been investigated in [Fürbringer et al, 1993].

A typical section of such a network is given in Figure A4.5.2 for the second floor of the building. More detailed information on the modelling of the building may be found in [Dorer, 1992]

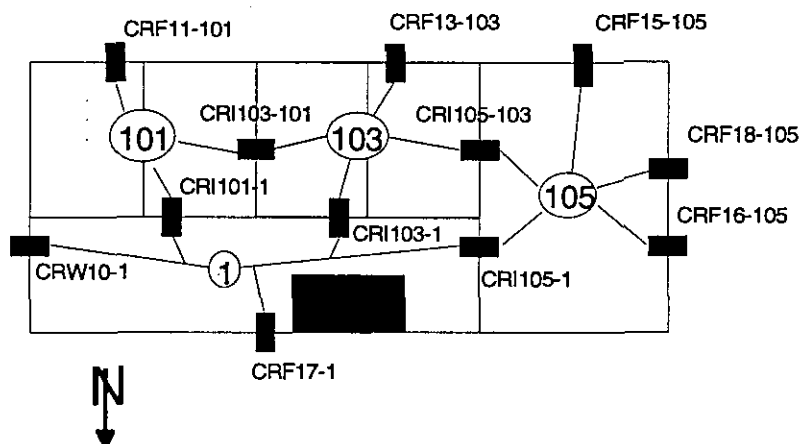


Figure A4.5.2: Typical section of the flow network (Floor 2).

A 4.4.4 Sensitivity analysis

The sensitivity (to input uncertainties) of the LESO Building simulated with COMIS has been studied using factorial design and Monte-Carlo method [Dorer, Fürbringer et al, 1992].

The Monte-Carlo design was used to calculate the confidence intervals of the simulated data to be compared with experimental data. The method, presented in § 1.3.1, consists in choosing input parameters at random. The method is easy to use, especially the analysis which is very simple. The counterpart is that the resulting information is smaller than that provided by more complex methods. But it is the proper method to calculate confidence intervals.

In that study, uniform distribution $U(-1,1)$ has been used to create the design matrix for MISA (cf. A.2). For each time step, 100 simulations were performed which determined a confidence interval of $\pm 10\%$ on the estimated means and standard deviations (eq. 1.6 and 1.9 in §1.3.1). The description of the varied parameters and their range of variation, corresponding to the experimental uncertainties, is given in Table A4.5.2 and results are reported in the graphics of experiment vs. simulation comparison (A4.5.8-10).

Table A4.5.2: parameters varied in the sensitivity analysis

Number	Parameters	Range
45	air tightness coefficients	50%
45	air tightness exponents	25%
9	volumes	10%
1	wind angle	$\pm 15^\circ$
4	temperature gradient	10%

An additional study was made using the Monte-Carlo design to analyse the effect of the pressure coefficient uncertainty which was not included in the confidence interval estimation shown above. For that analysis, an arbitrary uncertainty of 50% has been considered. The be-

haviour of the mean age of air is presented in Figures 4.5.3-6 for some zones presenting typical behaviour. The average of the mean age of air τ in each zone and the corresponding relative standard deviation σ_{τ}/τ are shown for the 4 main wind directions θ and wind speed v between 0 m/s to 6 m/s.

Figure A4.5.3 presents the behaviour of the mean age of air $\tau(v, \theta)$ in the hall. This zone corresponds to the entrance hall which has a very untight door, a stair case through 5 floors (from the basement to the attic) and some additional zones at each floor. The evolution of the mean air age is more or less inversely proportional to the wind speed. Note the stronger ventilation when the wind blows from the south. The behaviour of the standard deviation σ_{τ}/τ (due to the uncertainty of pressure coefficient's) is more complex. When the wind blows from the south or north: At low wind speed, σ_{τ}/τ decreases with the increase of wind since the inverse behaviour is observed at high wind speed. In the situation without wind no error can come from *pressure coefficient* uncertainty.

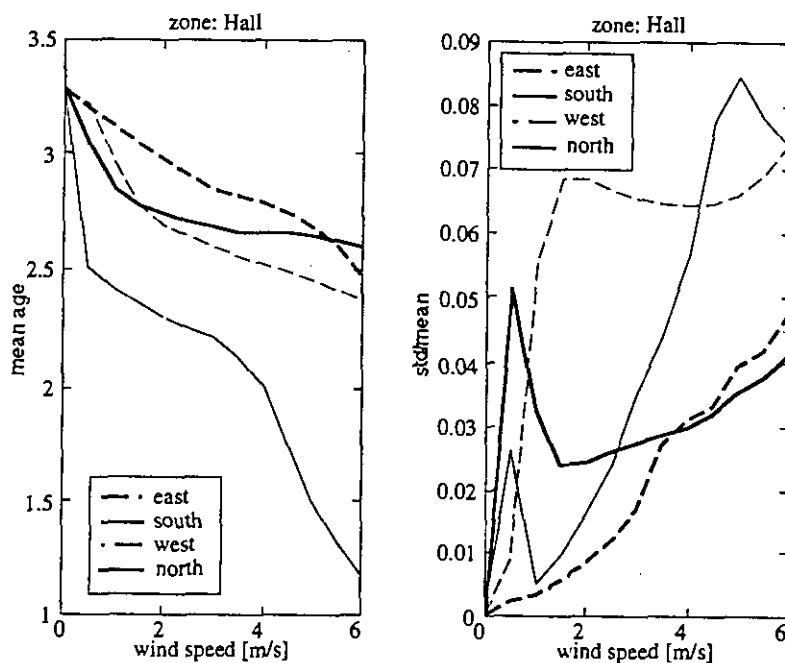


Figure A4.5.3:
Mean age of air
and its standard
deviation calcu-
lated by the Monte-
Carlo method for
the hall of the LESO
Building.

When the wind blows from the west, which corresponds to the most airtight side of this zone, the inaccuracy of the simulation is proportional to the wind speed. When the wind blows from the east, the behaviour is still different, showing a quick increase at low wind speed, followed by a cup form.

The next zone (005) is situated at the west side of the first floor. When the wind speed increases from 0 m/s to 6.5 m/s the age of air decreases if the wind blows from the west since it increases if the wind blows from the north or east. If the wind blows from the south, a maximum can be observed near 5 m/s indicating some equilibrium between driving forces. Passing this point some flows change direction. The relative standard deviation σ_{τ}/τ increases with wind speed. For low wind speeds, smaller than 2 m/s the σ_{τ}/τ does not pass 3% since it get 20% for high wind speeds and even 40% for the equilibrium situation when the wind comes from the south. The values of the mean age of air, between 2 and 6 hours is satisfactory.

Zone 103 is situated on the second floor, at the centre of the south facade. If the wind blows from the north or west, the mean age of air decreases exponentially with the wind speed. The same behaviour occurs when the wind blows from the south or east except that the age of air begins to increase till it reaches a maximum. The values are very high, getting to a satisfactory

level at high wind speeds only. The standard deviation is also high, approaching 100% of the mean when the wind blows from the east. The behaviour changes from one wind direction to another indicating a different pattern of flows.

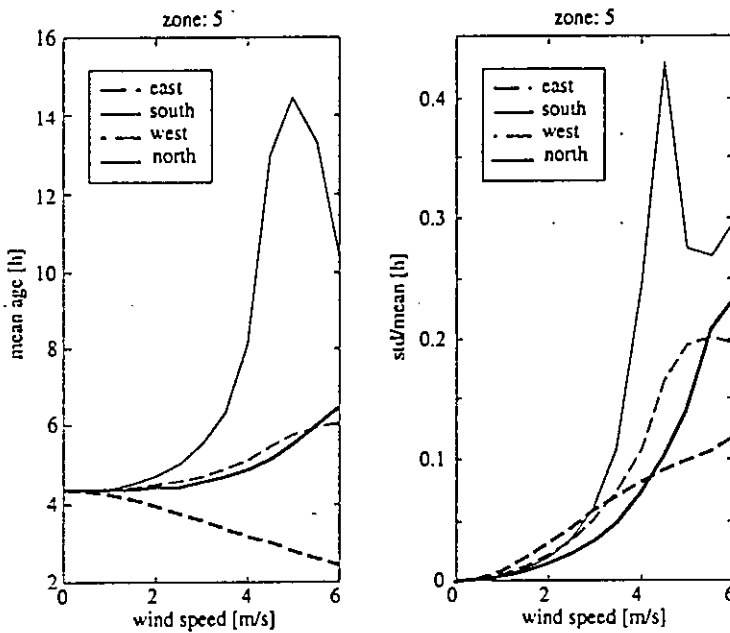


Figure A4.5.4: Mean age of air and its standard deviation calculated by the Monte-Carlo method for Zone 005 of the LESO building

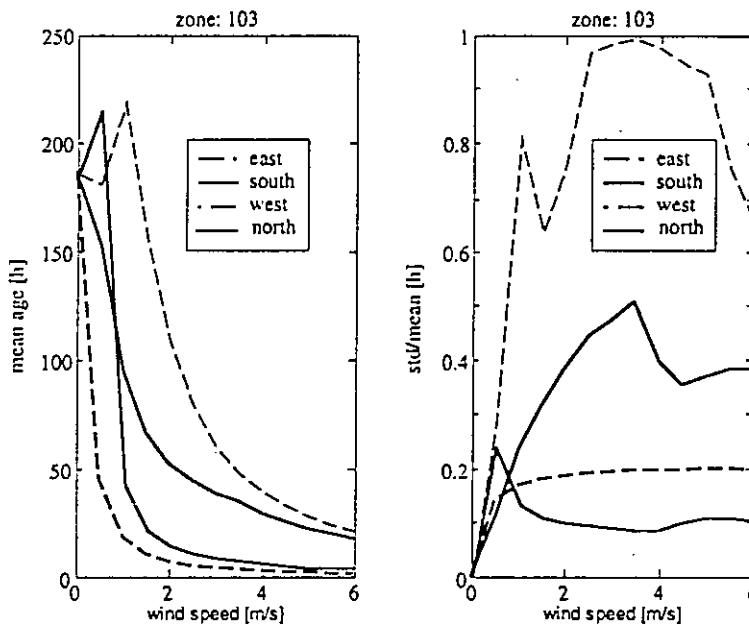


Figure A4.5.5: Mean age of air and its standard deviation calculated by the Monte-Carlo method for zone 103 of the LESO Building.

The behaviour of a zone on the third floor is also shown in Figure A4.5.6. The evolution of the age of air when the wind velocity increases is still different. For two wind directions (north and west) the ventilation has equilibrium points around 3 m/s and 5 m/s. For the other directions there is a monotonic decrease. The value of the air age is between 2 hours and 7 hours which is acceptable. The standard deviation shows an irregular behaviour for both wind direction producing a maximum.

The sensitivity to the pressure coefficient uncertainty depends on wind direction and also wind speed. This short study again shows the necessity of having tools (easy to use) to perform on line sensitivity analysis and parametric study when simulating.

This study shows also that pressure coefficient still is a critical parameter.

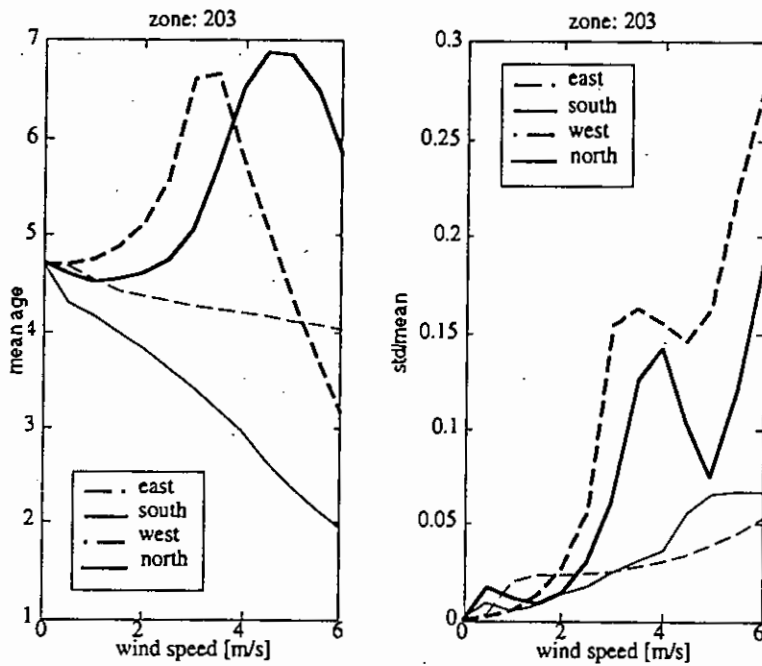


Figure A4.5.6: Mean age of air and its standard deviation calculated by the Monte-Carlo method for zone 205 of the LESO Building.

A 4.4.5 Relation between measurements and simulation

Similarly to a good empirical evaluation, as many input parameters as possible should be taken from the measured data set for the simulation. On the other hand, the observed output should be determined independently from the measurements. In this study, most of the input parameters are taken from the LESO data set. Nevertheless the resulting air flows Q_{ai} are determined according to Equation. A4.5.1 from the calculated individual Q_{oi} and Q_{ji} flows, but with the η_{ij} based on the measurements. Thus the calculated Q_{ai} values are not pure simulation results.

The relation between measured and calculated data and the influence of the respective errors are shown in Figure A4.5.7.

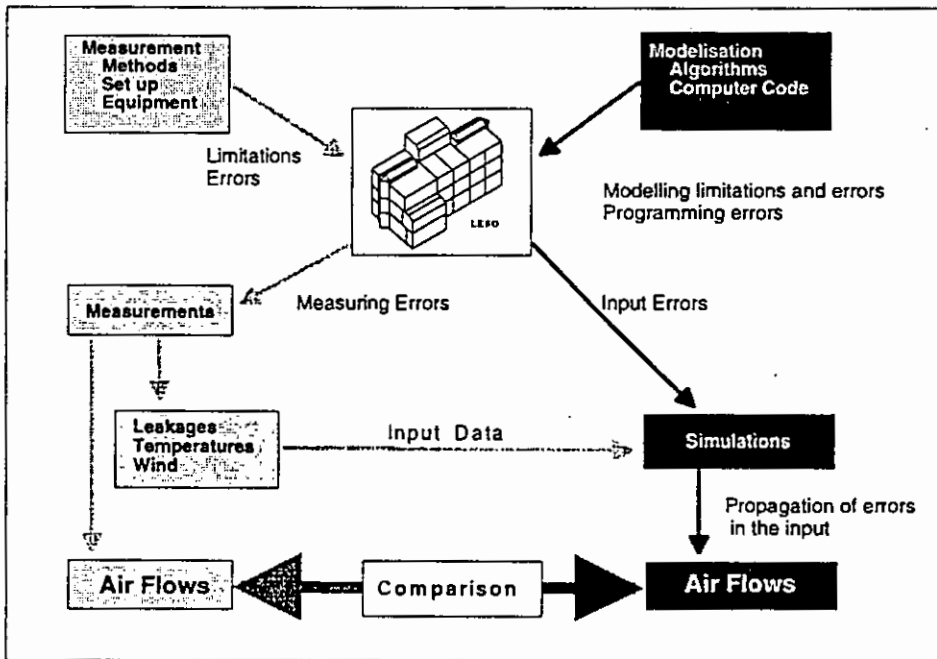


Figure A4.5.7 Comparison of measured and calculated air flows for the LESO building

A 4.4.6 Comparison of measured and calculated results

The results of the comparison are shown in Figures A4.5.8 to A 4.5.13. The values for $Q_{a-Building}$ from both measurements and simulations are plotted against the time, together with the respective confidence intervals.

Period 1 (Series 1-88)

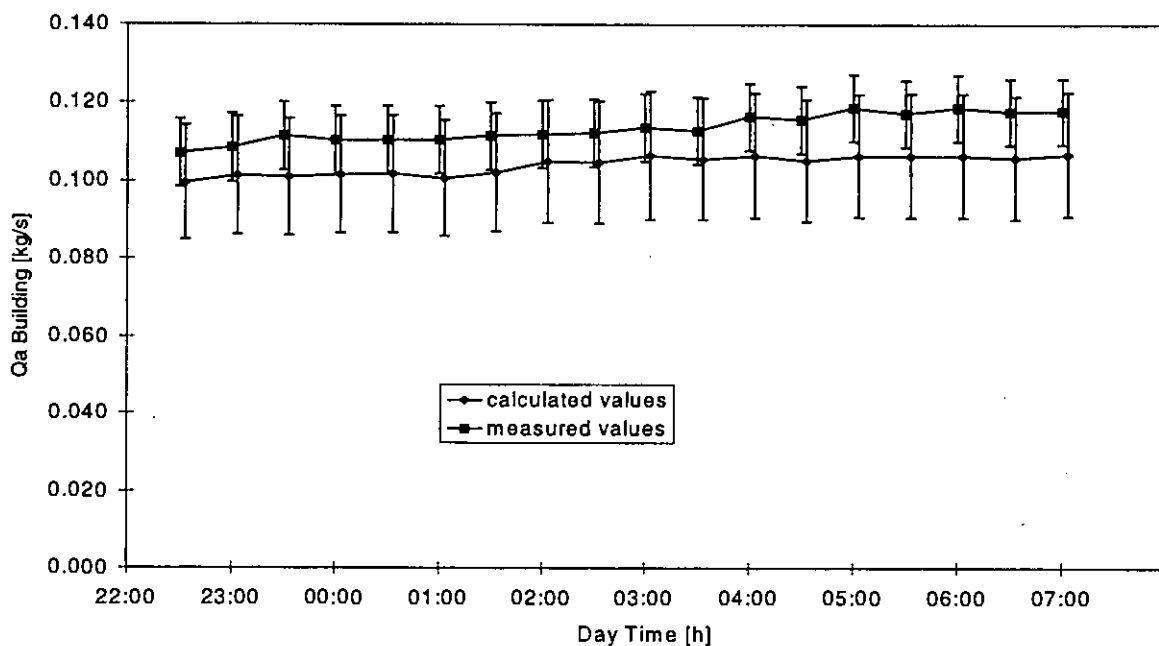


Figure A4.5.8 Comparison of measured and calculated results, Period 1

Period 2 (Series 2-88)

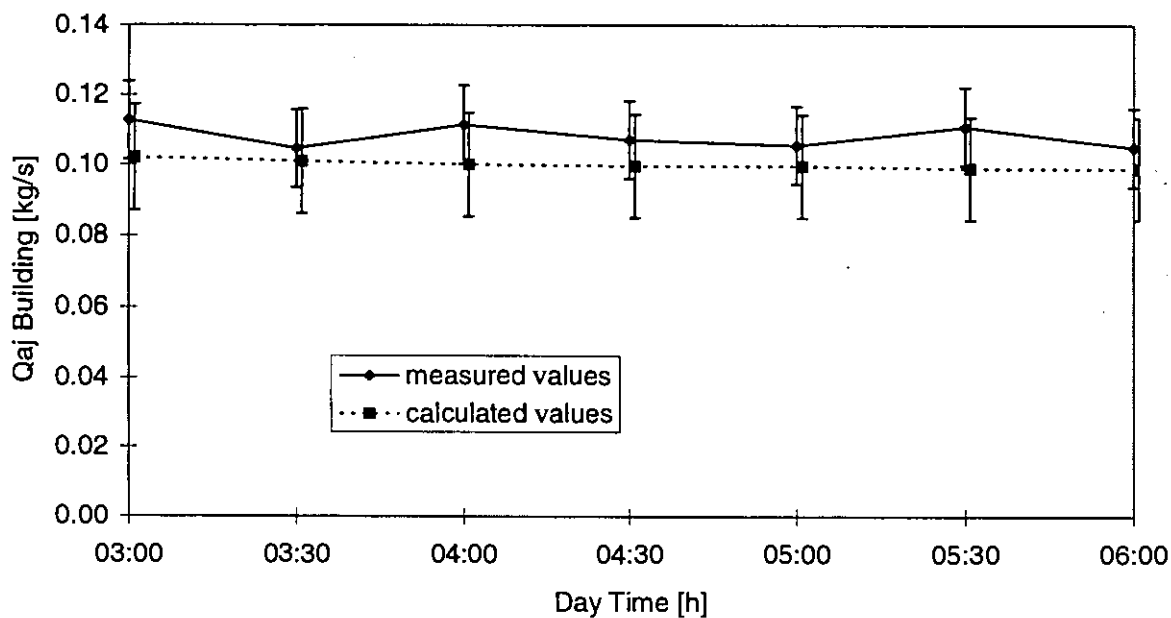


Figure A4.5.9 Comparison of measured and calculated results, Period 2

Period 3 (Series 3-88)

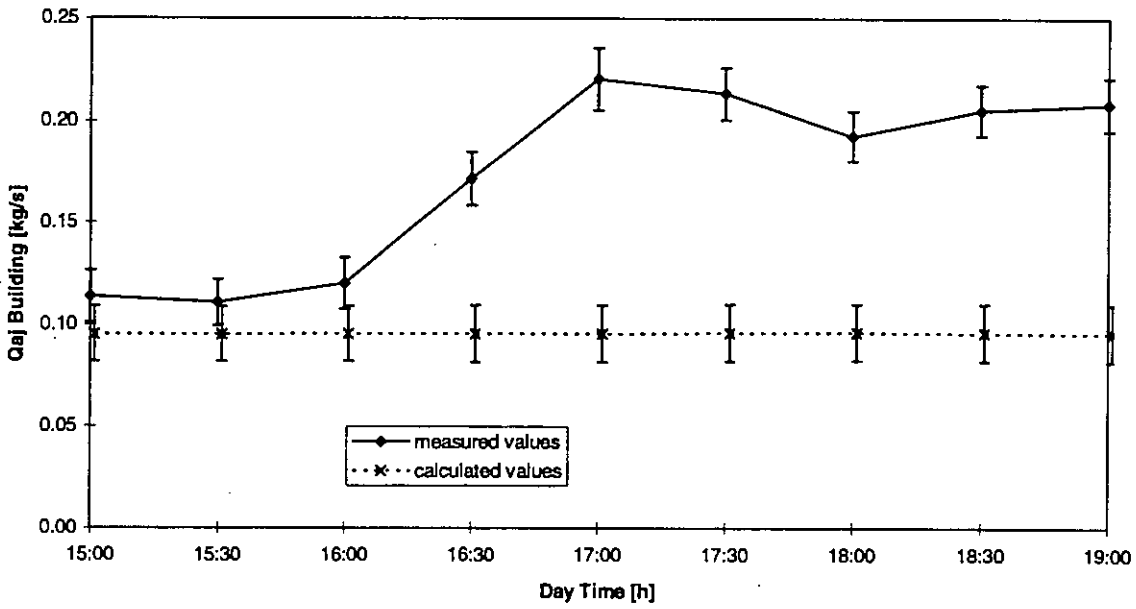


Figure A4.5.10 Comparison of measured and calculated results, Period 3

Since for this period, the agreement between measured and calculated data is quite poor, this case has been investigated in more detail. For this reason, some additional figures are included in this subsection.

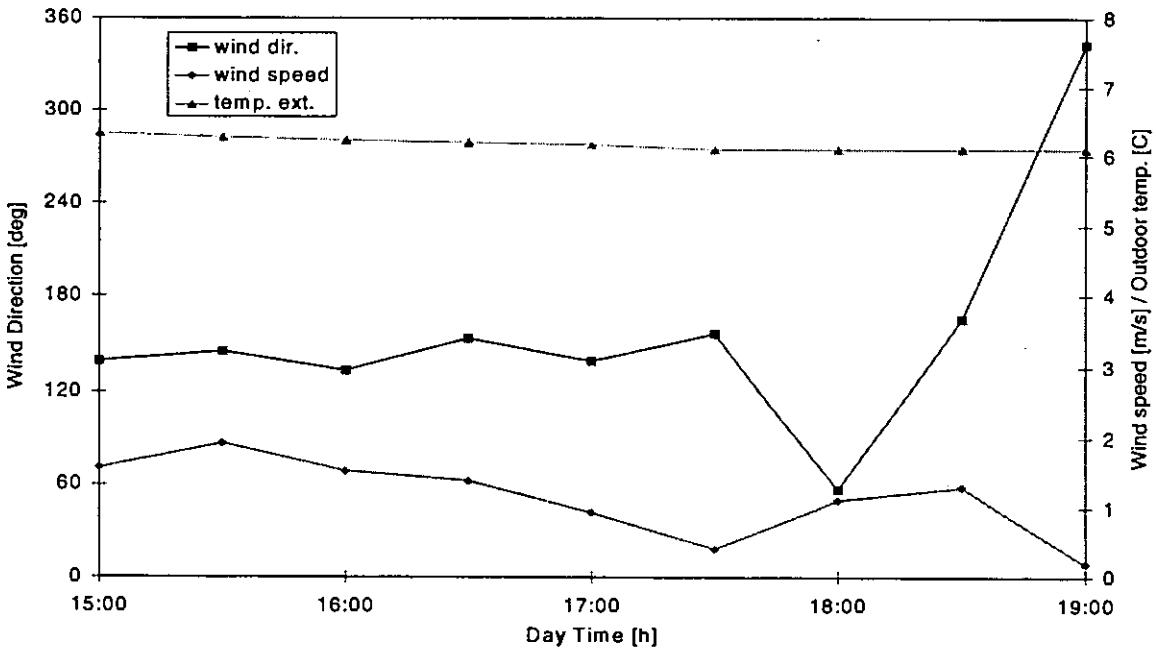


Figure A4.5.11 Wind speed and direction and external temperature for Period 3

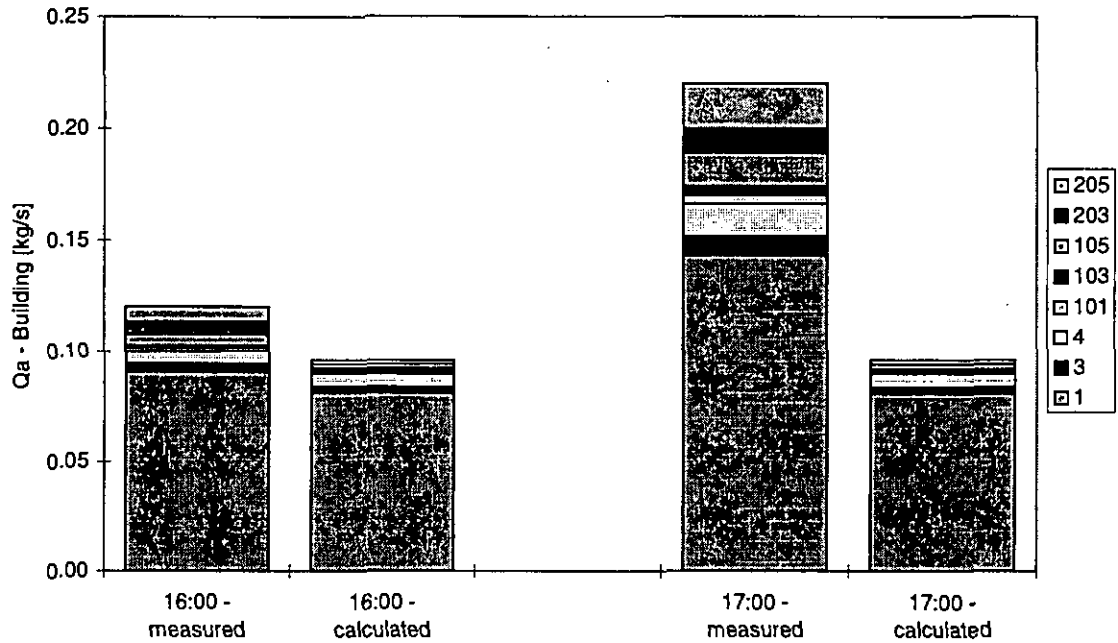


Figure A4.5.12 The Q_a -values for the individual zones for two time steps in Period 3

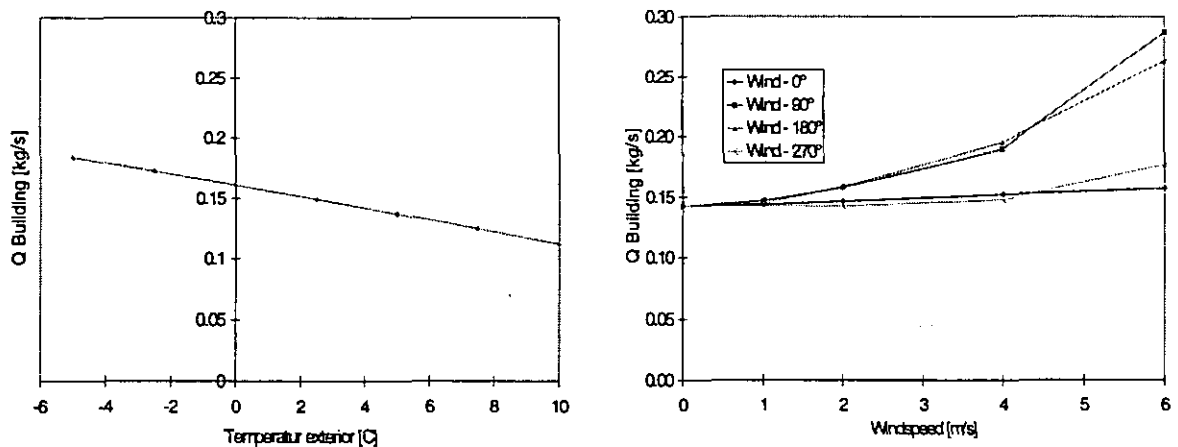


Figure A4.5.13 The influence of stack and wind effect on the total building flow Q . Internal air temperature $20\text{ }^{\circ}\text{C}$. Stack effect and no wind (left), Wind effect at $T_{ext} = 4\text{ }^{\circ}\text{C}$ (right).

A 4.4.7 Summary and Conclusions

For the calm (no wind) situation (period 2-88), the measurements and simulations are in good agreement, which means the respective error bars do overlap. From this we conclude that the modelling is representing the real building well, especially in respect to the leakage distribution. There is no explanation for the general small underestimation of the air flow.

In period 3 (3-1988) the wind speed decreases from approx. 1m/sec to 0.2 m/sec at steady wind direction. Surprisingly, the big difference between measured and calculated values appears during the end of the period, where the wind speed is low and one could expect that the agreement should be in the same range as in period 2.

As shown in Figure 4.5.14, an increase in the flow rate due to lower wind is not unrealistic when in range A. This can be explained by an adverse effect of stack and wind pressures, resulting in a decrease of the overall driving pressure.

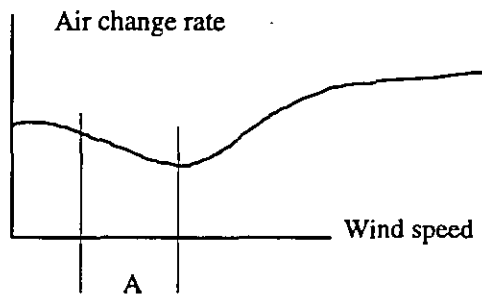


Figure A4.5.14 Interaction of stack and wind induced air change (qualitative only)

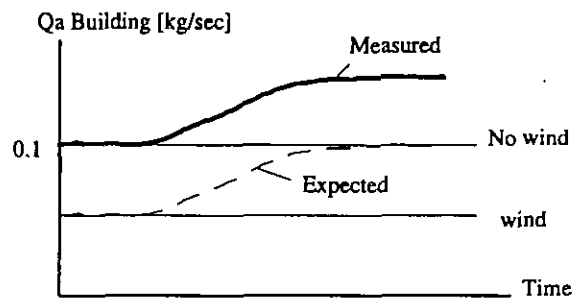


Figure A4.5.15 Measured and expected Q_a -Building values (qualitative only).

One could also expect that the values for Q_a would coincide rather at the end of the period when the wind is low and that a deviation would more likely occur at the beginning of the period (see Figure A4.5.15). Since there was good agreement for Periods 1 and 2, one would expect that also in this case, at least for the low wind time, the agreement should be good, which obviously is not the case.

Nevertheless, as shown in Figure A4.5.13, for the specific building and climatic periods analysed, the wind effects become important only above 1.5 to 2m/sec approximately.

From this one can conclude that the reason for the large difference between measured and calculated values is most probably not related to the modelling itself, but rather to effects of parameters which are not well reflected in the input data. A list of such factors is given below, with factors of higher probability listed first:

- Sudden change in the building leakage characteristic (door could be opened)
- Wind fluctuations, which have a big effect on ventilation rate, but which are not well represented by the average wind speed input data.
- Measurement problems in this specific time interval
- Effects of solar radiation changes (quite unlikely because 16:00 is quite a late daytime in December)

A 4.4.8 References

- Compagnon R.; Fürbringer J.-M. and Jakob M.: *Mesure d'échange d'air entre les locaux et avec l'extérieur. Final report NEFF 339.2, EPFL-LESO, Lausanne, Switzerland 1991.*
- Dorer V.; Fürbringer J.-M.; Huck F. and Roulet C.-A.: *Evaluation of COMERL with the LESO Dataset. Final Report ERL, EMPA 175, CH-8600 Dübendorf, Switzerland, 1992.*
- Dorer V.; Fürbringer J.M.: *Comparison of Multizone Air Flow Measurements and Simulations of the LESO Building Including Sensitivity Analysis, 14th AIVC Conference, 1993.*
- Fürbringer J.-M.; Compagnon R. and Roulet C.-A.: *Validation de programmes de calcul des échanges d'air à l'aide de mesures expérimentales. Final report NEFF 339.1 LESO-PB, EPFL, Lausanne, Switzerland, 1990.*
- Fürbringer J.-M. and Roulet C.-A.: *Study of Errors Occurring in Measurement of Leakage Distribution in Buildings by Multifan Pressurisation. Building and Environment, 26, 1991.*
- Roulet C. -A. et al: *Air flow pattern within buildings -Measurement techniques, AIVC TN 34, 1991.*

A 4.5 Single sided ventilation in a 2-zone test cell

A 4.5.1 Measured object

General description

This experiment was performed in an outdoor PASSYS test cell. These cells are designed to evaluate performances of passive solar components. They consist of a very well insulated test room with an exchangeable wall orientated to the South and a service room for technical equipment. The latter is connected to the test room by an insulated door. The cell is represented on Figure A4.5.1.

Table A4.5.1: Inside dimensions of the two rooms in the test cell.

Feature	TEST ROOM	SERVICE ROOM
Height (m)	2.50	3.29
Length (m)	4.86	2.40
Width (m)	2.50	3.58
Volume (m ³)	30.4	28.3

For the single sided ventilation experiment, the so-called "reference wall" was employed as South component. It is made up of three layers: wood (12 mm), PS30 (100 mm) and wood (12 mm) and had a vertical opening of about 0.25 m² (=0.5 x 0.5) in a first experiment and an opening of about 0.37 m² (=0.75 x 0.5) in a second experiment. The internal door was kept open and its opening was reduced to 1 m². This results in a 2-zone building with single sided ventilation taking place in only one of the zones.

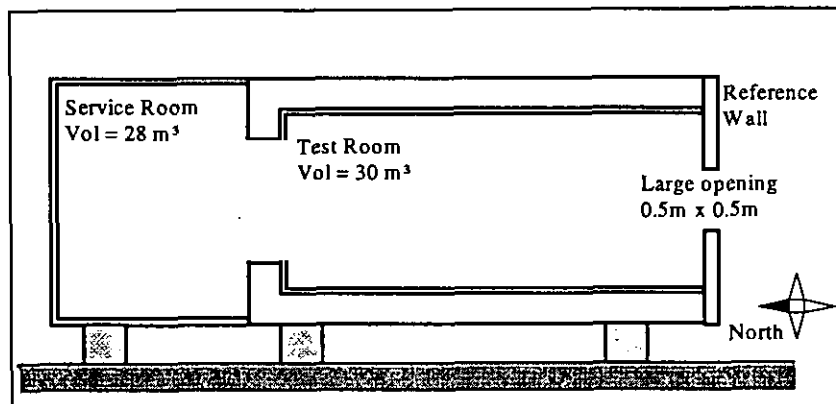


Figure A4.5.1: The PASSYS test cell - sectional view

A detailed description of the PASSYS test cell can be found in [Wouters P., Vandaele L, 1994]

Objectives of the experiment

The aims of the experiment and the analysis performed are:

- to see to what extent COMIS is able to simulate air flow rates through large openings,
- to evaluate the influence of the wind (not simulated by COMIS) on the single sided ventilation air flows in the external opening,
- to check whether the wind has an effect on the air flows through the internal large opening between the 2 zones.

Heating and cooling sequences

In order to get large variations of the temperature differences through both openings, both heating and cooling systems of the PASSYS cell were used. The sequence is as follows:

- from 0h00 to 6h00: heating in the service room full power (± 1000 W),
- from 6h00 to 12h00: heating in the service room half power (± 500 W),
- from 12h00 to 18h00: cooling in the test room full power (± 600 W),
- from 18h00 to 0h00: cooling in the test room half power (± 300 W).

Figure A4.5.2 shows variations of temperature differences through both openings.

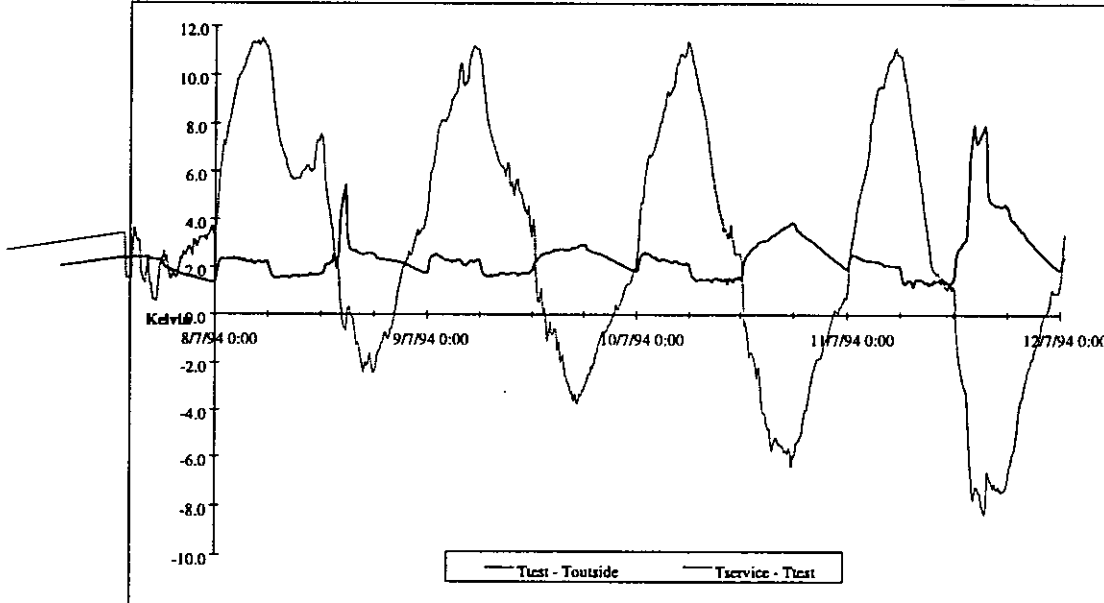


Figure A4.5.2 : Temperatures differences through internal and external openings

Note: Figure A4.5.2 to Figure A4.5.5 are values measured for the case of an opening of 0.5m. x 0.5m. The parameters of the second measurement period (opening = 0.75m. x 0.5m.) are not given as figures in this text.

A 4.5.2 Measurements performed

The measurements performed can be categorised in 2 groups:

- 1) measurements which are input parameters for COMIS
 - temperatures,
 - temperature gradients: for each room 2 temperature gradients are calculated from the temperatures measured on 3 different heights (near the floor, in the middle and near the ceiling); in Figure A4.5.4 one can see that these temperature gradients are often very important. On the other hand, the temperatures seem to be rather constant in a horizontal plane as one can see in Figure A4.5.4, where the 5 temperatures measured on different places in the middle of the room are nearly always the same.
 - heights and widths of the openings,
 - wind velocity and direction,
- 2) measurements of the air flow rates through both openings (tracer gas technique) which are compared with the output of COMIS. Results are given later in the text.

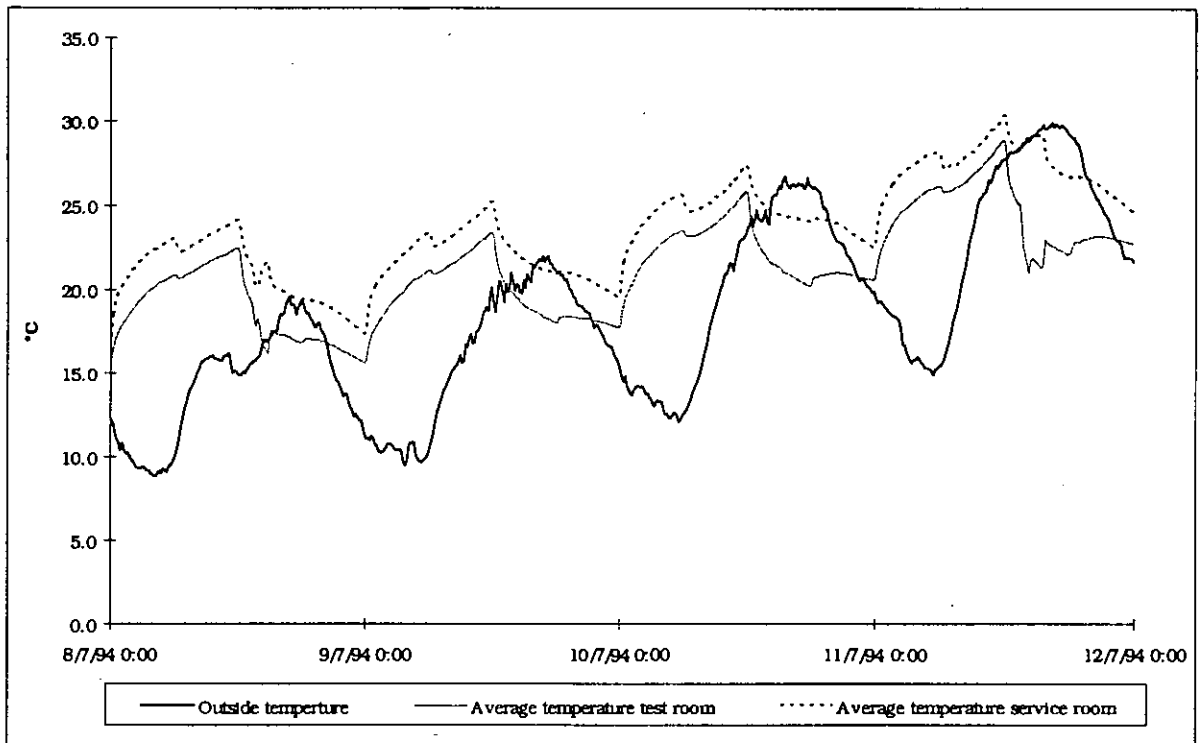


Figure A4.5.3: Results of the temperature measurements

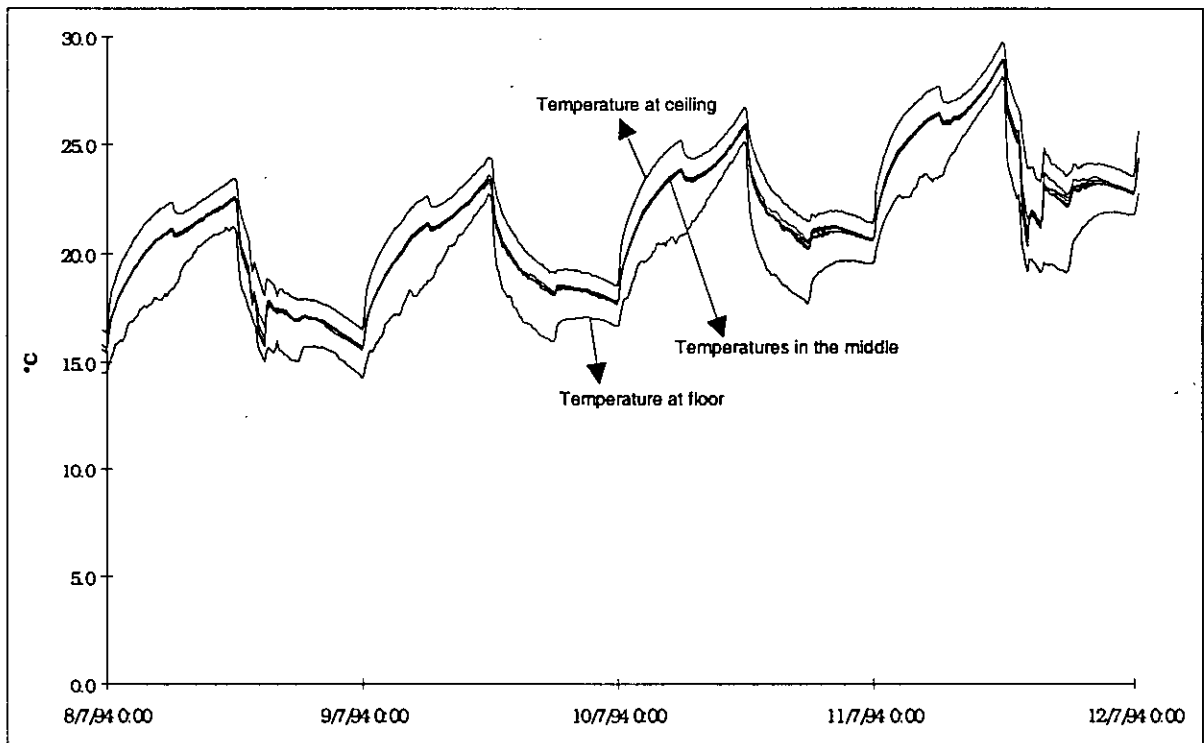


Figure A4.5.4: Temperatures on different places in the test room.

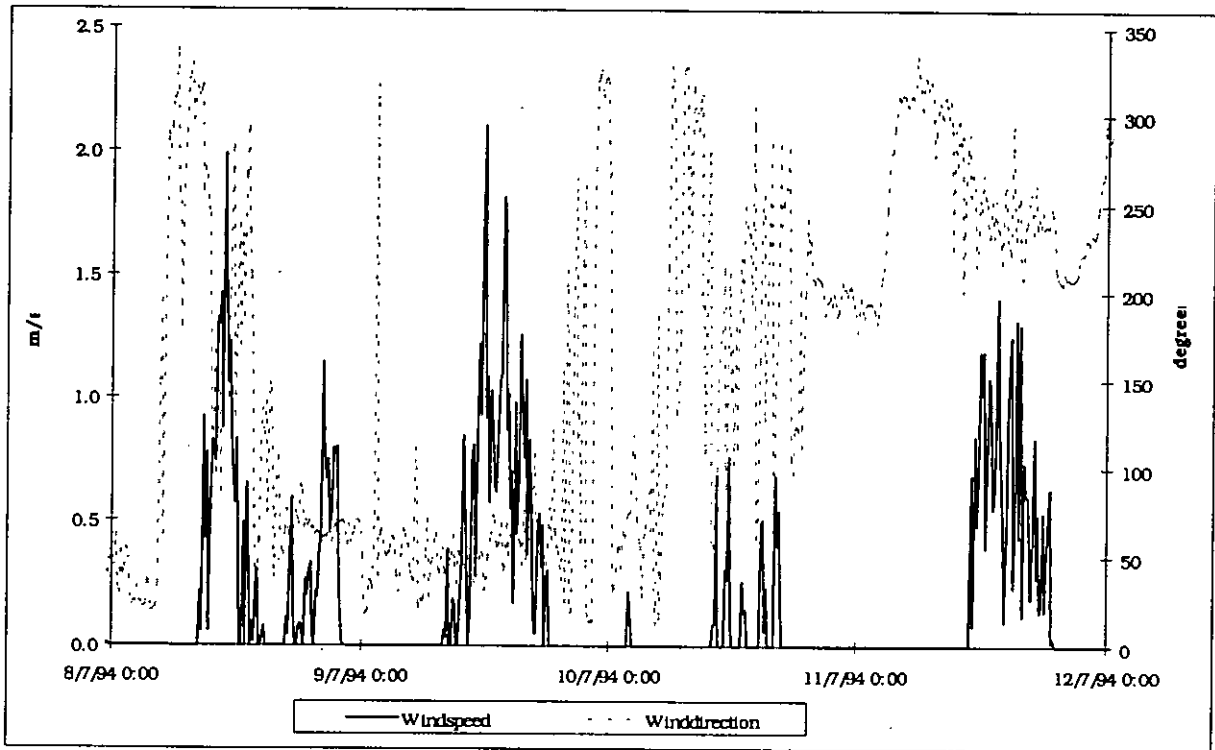


Figure A4.5.5: wind velocity and wind direction

Input parameters for COMIS

Temperatures: The air temperatures in the rooms are measured with double-shielded, type T thermo-couples. It is known from experience that their total accuracy is about 0.2 K. Positions of the sensors are given in Figure A4.5.6. In total there are 7 measurements of the air temperature in the test room and 3 in the service room.

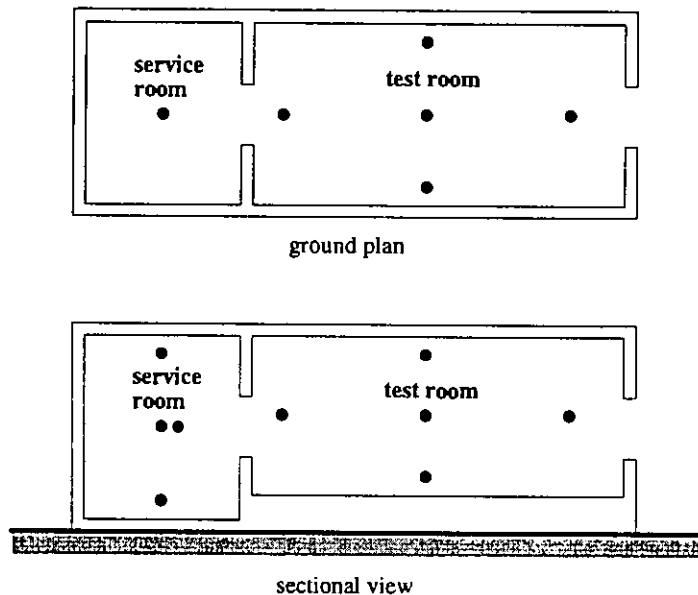


Figure A4.5.6 - Position of the air temperature measurement points

Temperature gradients are derived from the air temperature measurements. Two temperature gradients are calculated for each room:

- from floor to centre,

- from centre to ceiling.

The accuracy of the gradients is assumed to be 0.2 K/m.

Wind velocity and direction are measured at 10m height. The accuracy's are 5% for the velocity and 10 degrees for the direction.

Outside temperature is measured with a ventilated thermocouple to avoid the effect of the solar and sky radiation. Its total accuracy is assumed to be 0.5 K. An accuracy of 0.2 K was assumed in the COMIS simulations, which a bit optimistic.

Heights and widths: The error on these values is assumed to be 2 cm, which is usual in buildings.

Air flow rates through large openings

The measurement of single sided ventilation air flow with tracer gas technique must be performed with care. Indeed, when the ventilation is due to the temperature difference through the large opening, a clear air flow pattern appears in the room. The cold air runs down on the floor whereas the hot air goes up. This makes it impossible to keep the tracer gas concentration homogenous in the measured space and therefore, classical tracer gas technique is difficult to apply. It must be noticed that, on the contrary, when the wind is the main "motor" of the ventilation, no clear air flow pattern appears in the room and the tracer gas concentration is more homogeneous (cf. chapters A4.8 - and A4.9).

Technique used: The intention was to measure the air flow rates through the internal door and through the external window. Two tracer gases were used. R22 was continuously injected in the service room on 8 different places (to increase homogeneity) and SF6 in the test room in a diffuse way through air distribution hoses.

Tracer gas techniques are based on the mass balance equation for tracer gas in the measured space. For example, for the test room of the cell this equation is:

$$\frac{dm_{SF6}}{dt} = S_{SF6} - Q \cdot C_{leaving} \quad (\text{kg/s}) \quad (\text{A4.6.1})$$

Where:

- m_{SF6} = mass of SF6 contained in the room (kg),
- S_{SF6} = injection rate of SF6 in the test room (kg/s),
- Q = air flow rate through the large opening (m^3/s),
- $C_{leaving}$ = SF6 concentration of the air leaving the room (kg/m^3).

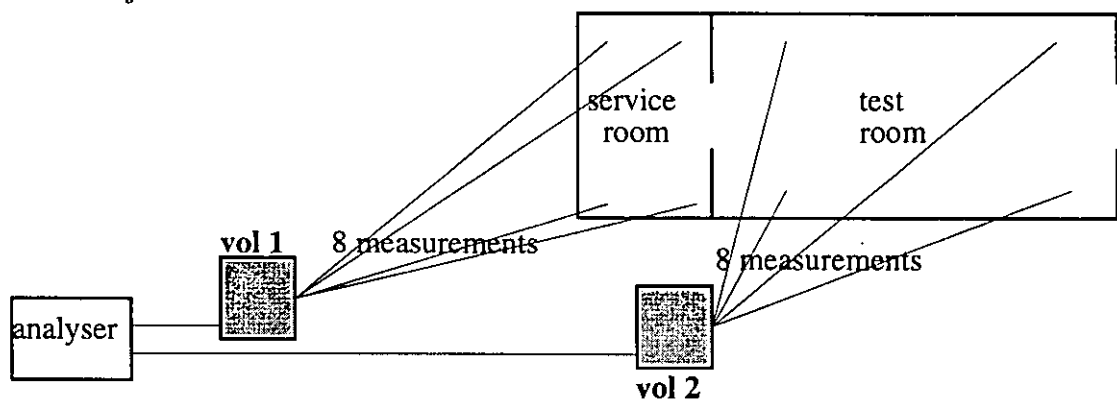


Figure A4.5.7: Principle of the use of mixing volumes.

Several sampling points for concentration measurements were placed: 8 distributed in each room and 2 in each large opening. The 8 points distributed in each room are connected to a "mixing volume". The air is continuously drawn from the 8 points and then mixed in the volume. The concentration in the volume is then measured. This is an easy way of making an average in the time (time constant of the volume is about 5 min [$\tau = V/Q$]) and in the space (8 points) of the SF₆ concentration with only one measurement.

The main difficulty is to estimate the concentration of the air leaving the room since it is not homogenous in the room. The points placed in the opening itself can help but when the wind blows in the opening the concentrations measured at these places fluctuate heavily due to turbulence, and are no longer representative for the concentration of the air leaving the room. Therefore the average concentration in the room was chosen to approximate the gas concentration in the air leaving the room.

The total mass of tracer gas in the room is estimated as the volume of the room multiplied by the average concentration in the room. Knowing the mass of gas contained in the room and the concentration of the air leaving the room, the mass balance equation provides the air flow rates through the large opening.

Accuracy of the measurements: The error on the air flow measurement is difficult to be estimated because, besides the measurement error on concentrations and injection rates, one must take into account the representativity error, i.e. the fact that the concentration of the air leaving the cell is not exactly the average concentration in the cell.

Assumptions: Error on the injection rate = 5%
 Error on the measurement of the concentration leaving the room (= measurement error and representativity error) = 10%

The error on the air flows through the external opening and through the internal opening are not the same. For the internal opening the air flow is calculated with the concentration difference between both rooms. The error on the concentration difference is twice the error on the concentration.

Total error on air flow rate through the external opening = 15%
 Total error on air flow rate through the internal opening = 25%

A 4.5.3 Modelling and simulations performed

Modelling of the problem

The Figure A 4.6.8 shows the model used to simulate the PASSYS test cell with COMIS 1.2.

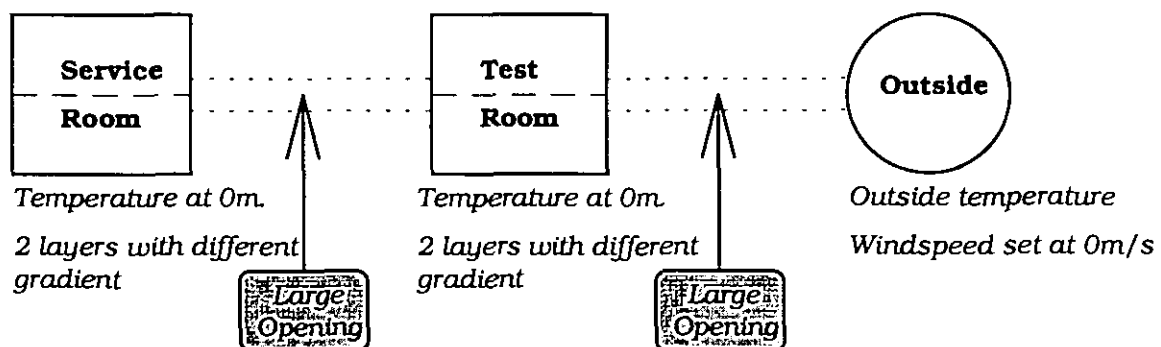


Figure A4.5.8 : Principle of modelling

The algorithm for large openings, used in COMIS 1.2 can be found in the COMIS-fundamentals [COMIS, 1990].

If we assume a large opening, the pressure difference at any level z is:

$$P_1(z) - P_2(z) = (P_{01} - P_{02}) - g \cdot \left[\left(\rho_{01} \cdot z + b_1 \cdot \frac{z^2}{2} \right) - \left(\rho_{02} \cdot z + b_2 \cdot \frac{z^2}{2} \right) \right] \quad (\text{A4.6.2})$$

The velocity at any level z is then:

$$v(z) = \left[2 \cdot \left(\frac{P_1(z) - P_2(z)}{\rho} \right) \right]^{1/2} \quad (\text{A4.6.3})$$

The neutral planes in the large opening are found by setting

$$P_1(z) - P_2(z) = 0 \quad (\text{A4.6.4})$$

Once the neutral planes are found the air flows through the opening can be found by integrating between these neutral planes:

$$Q_{0,z_1} = C_d \cdot \theta \cdot W \cdot \int_0^{z_1} v(z) \cdot dz \quad (\text{A4.6.5})$$

$$Q_{z_1,z_2} = C_d \cdot \theta \cdot W \cdot \int_{z_1}^{z_2} v(z) \cdot dz \quad (\text{A4.6.6})$$

$$Q_{z_2,h} = C_d \cdot \theta \cdot W \cdot \int_{z_2}^h v(z) \cdot dz \quad (\text{A4.6.7})$$

Where: C_d = Discharge coefficient (takes into account the contraction of the flow).

θ = Reduction factor (defines the effective opening of a large opening).

W = Width of the opening.

Simulations performed

Two different ways to perform the sensitivity analysis

1) Monte Carlo analysis

A high number of simulation runs is performed (in our case 100). For each run the input parameters are changed in a random way, following a normal distribution determined by the measured value and its accuracy (= 95%-interval of the measured value). In that way, the standard deviation of the 100 obtained results will be the standard error on the final result.

2) Fractional Factorial Analysis

This is an analysis where for each run the parameters are changed in such a specific way that it is possible to separate the effect of each parameter (main effect) and also the effect of the interaction of 2 parameters (effect of the first order), without having to perform too many simulation runs.

To perform these sensitivity analyses MISA [Fürbringer, 1992] was used.

For more explanation about how to perform Fractional Factorial Analysis and Monte-Carlo analysis with the use of MISA see [Fürbringer, 1994].

Monte Carlo analysis: Three temperature measurements are performed at different heights in each room. As a consequence, two gradients can be determined for each room. The measurement results show that these gradients vary heavily during the measurement time. Those variations are due to the change of the cooling/heating powers. Unfortunately, a schedule for the temperature gradient is not enclosed in COMIS 1.2.

Since the time step between two measurements is 10 minutes, which yields 144 measurement points for each day, it is impossible to use MISA for each point of time to determine the error by a Monte-Carlo analysis. Indeed, it would imply the need to prepare 144 range files for each day we want to simulate.

To take into account the variation of the gradients, without having to perform too many simulations, 2 different approaches are examined:

- 1) A first simulation is performed using MISA, but without doing a sensitivity analysis. In this case MISA is used as a schedule for the temperatures and the gradients. In the design file the real values (for the temperatures and the gradients) are given for each run and in the range file the values are 1 and -1, so the value taken to perform the simulation is the value from the design file. A run is performed for each 10 minutes.

This kind of simulation is performed for two different periods:

- 1) A first simulation is done for the period from July 8, 17h25 to July 11, 12h15. In this case the dimensions of the external window are 0.5m x 0.5m.
 - 2) A second simulation is done for the period from July 19, 17h00 to July 25, 00h00. The dimensions of the external window are 0.5m x 0.75m.
- 2) Monte-Carlo analyses for 8 successive periods of each 6 hours. Most of the gradients have rather constant values during periods of 6 hours. These periods are mainly determined by the levels of the heating or cooling powers, which change every 6 hours. Schedules are used for the temperatures, the gradients are given fixed values for each period. This means that for each period a different range file is used. The temperatures are averaged over periods of thirty minutes to perform the simulation in COMIS in order to limit the calculation time. The total simulation covers a period of 2 days, namely July 9 and 10.

By performing these two kinds of simulations it is possible on the one hand to determine the 95%-confidence interval (approach 2) and on the other hand to know the influence of averaging the gradients over periods of 6 hours on the air flows (by comparing approach 1 with approach 2). If only approach 2 would be performed one would not have an idea of the error made by taking average values for the gradients.

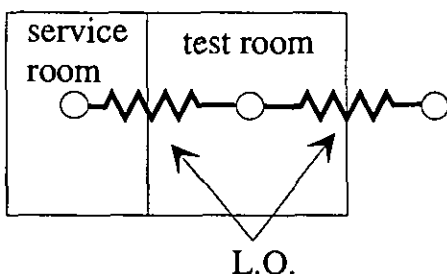


Figure A4.5.9: Network used for the simulation of the PASSYS cell

A **Fractional Factorial analysis** is performed for 2 specific moments, 1 during heating in the service room and 1 during cooling in the test room. For these 2 analyses a $2_{IV}^{(12-6)}$ -design is used.

Results of the simulations with COMIS 1.2 and comparisons with the measurements

Approach 1: For these simulations the 95%-interval of the results can not be determined, because a Monte-Carlo analysis was not performed. This has been done in the second approach. The discharge coefficient has been given a value of 0.6. For the first period; the external opening is 0.5m x 0.5m.

The average values for the measured and simulated air flows through both openings over the whole period (=from July 8, 17h25 to July 11, 12h15) are:

Table A 4.5.2: Comparison of the average values of measured and simulated air flow rates.

Situation	COMIS -simulation	Measurement
External opening	47 m ³ /h	64 m ³ /h
Internal opening	208 m ³ /h	202 m ³ /h

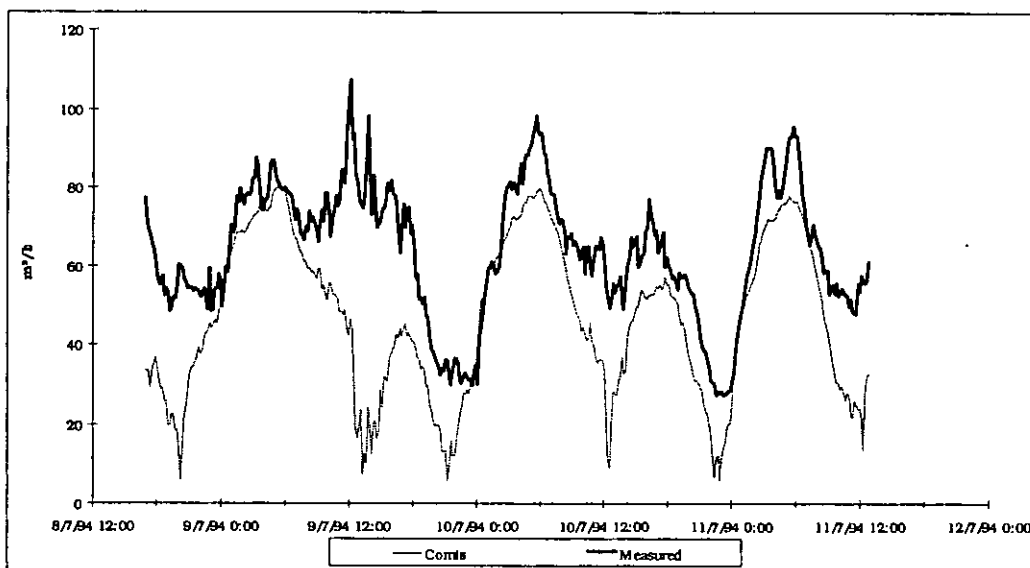


Figure A4.5.10 : Air flow through external opening; comparison between measurement and simulation. First period.

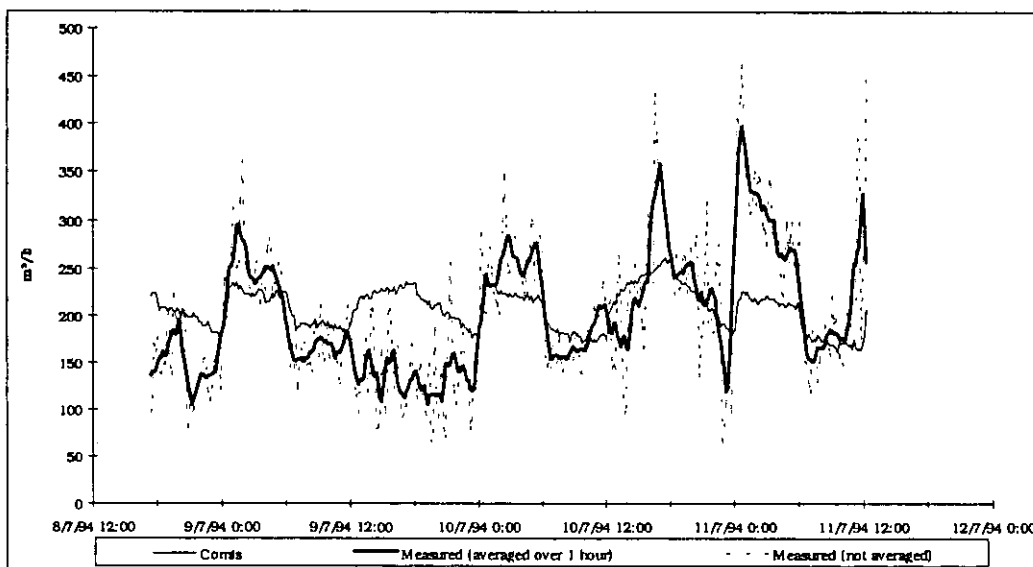


Figure A4.5.11 : Air flow through internal opening; comparison between measurement(averaged and not averaged) and simulation. First period.

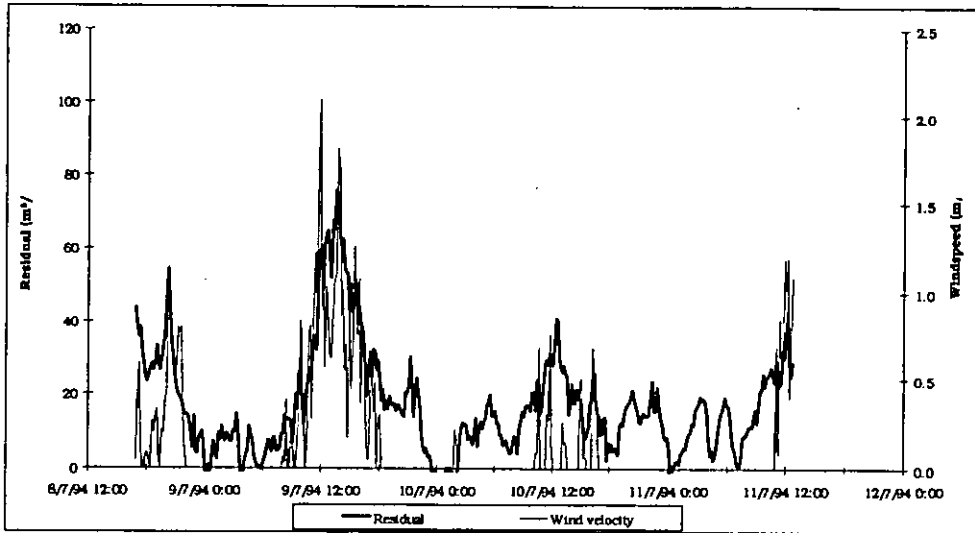


Figure A4.5.12 : Residual (meas. - sim.) and wind speed; external opening. First period.

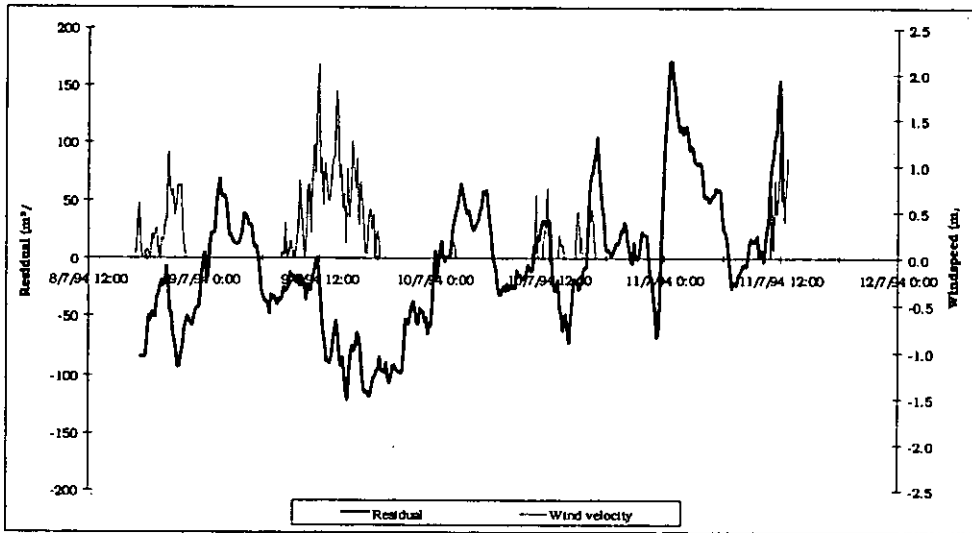


Figure A4.5.13 : Residual (meas.t - sim.) and wind speed; internal opening. First period.

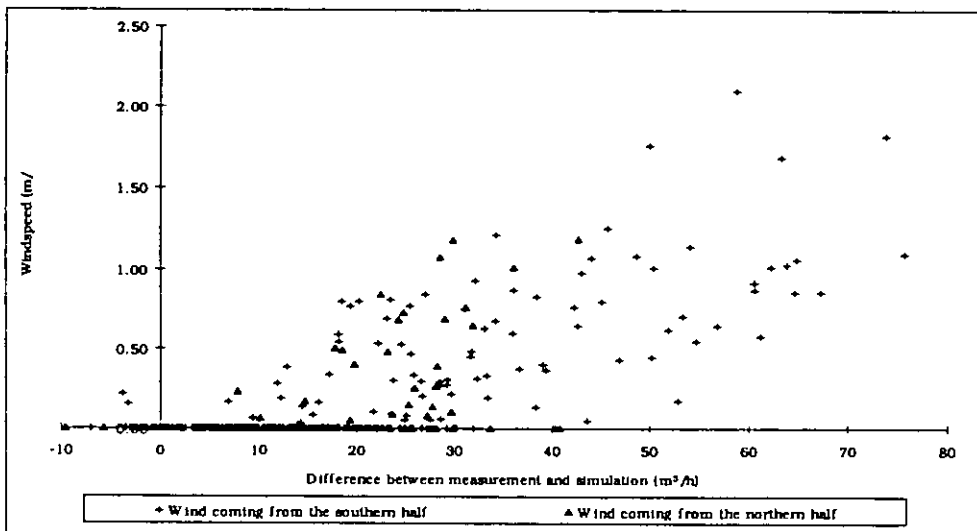


Figure A4.5.14 : Correlation between residual and wind speed for external opening. First period.

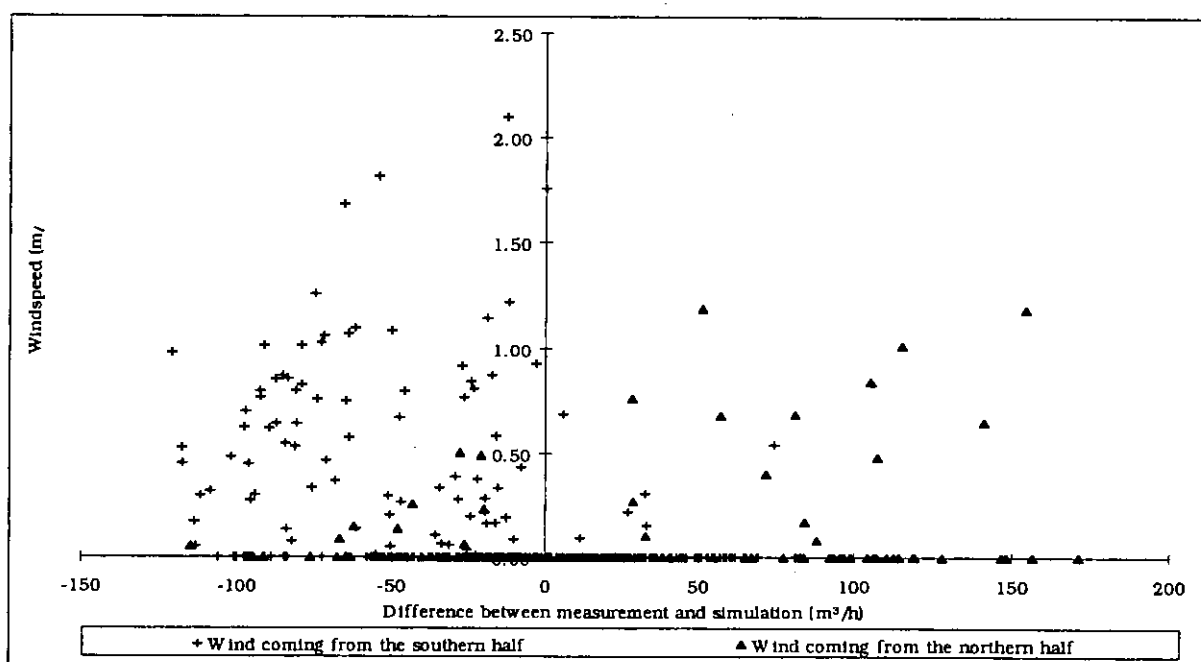


Figure A4.5.15 : Correlation between residual and wind speed for internal opening. First period.

The average values of measurement and simulation are nearly the same for the internal opening (see Table A 4.5.2). For the external opening the difference between the averages of measurement and simulation is much higher. This is mainly caused by the fact that COMIS does not take into account the effect of the wind on the air flow rate through the opening, because there is no algorithm enclosed to calculate this.

Comparing Figure A4.5.10 with Figure A4.5.11 one can see that in spite of the fact that the average values are almost equal for the internal opening, the simulation is not very precise. In fact, the evolution of the simulated air flow rate during time is better for the external opening (when one takes only the moments without wind into account).

The first reason is that the air flows through the internal opening are much more difficult to measure than the air flows through the external opening, because the difference in concentration between both rooms is not so high. Moreover, there is also a problem of very unstable air movements due to the heating convectors in the service room. As one can see the measurements were averaged over 1 hour in Figure A4.5.11.

In Figure A4.5.12 and Figure A4.5.14 one can see that there is a quite good correlation between the wind speed and the residual of measurement and simulation. This means that the higher differences are caused by the wind. The slope of the correlation seems even to depend on the wind direction (see Figure A4.5.14).

On the other hand, for the internal opening no clear correlation is found between the residuals and the wind speed (see Figure A4.5.13 and Figure A4.5.15)

In a second period; the external opening: was open to 0.75m (= height) x 0.5m.

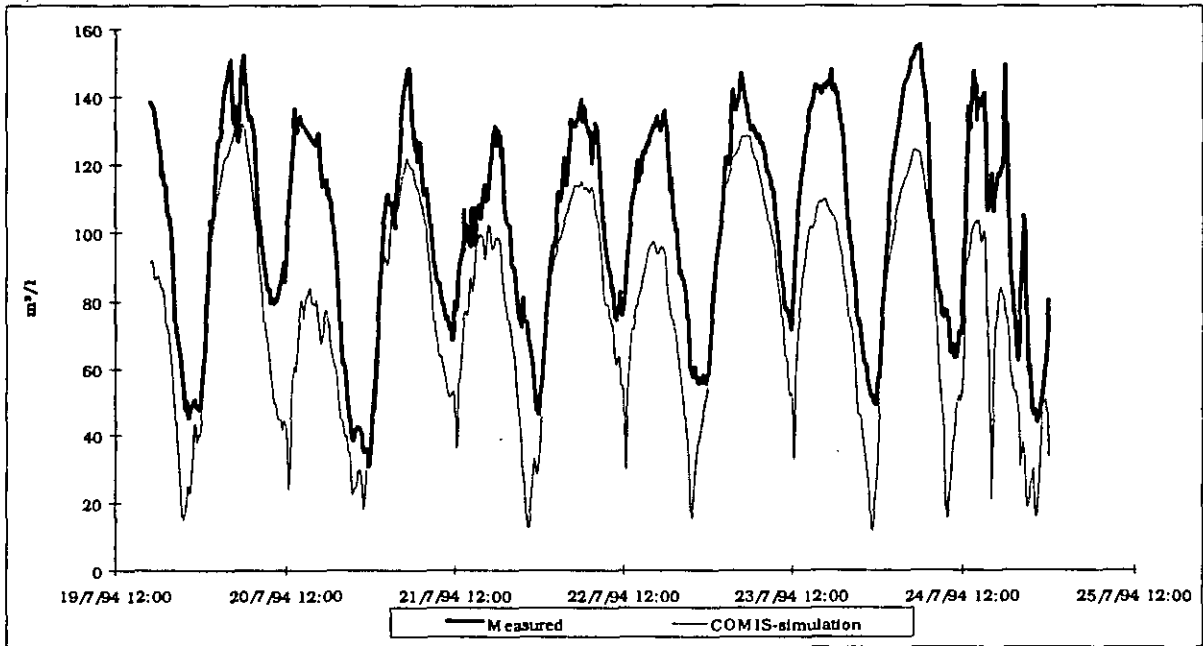


Figure A4.5.16: Air flow through external opening; comparison between measurement and simulation. Second period.

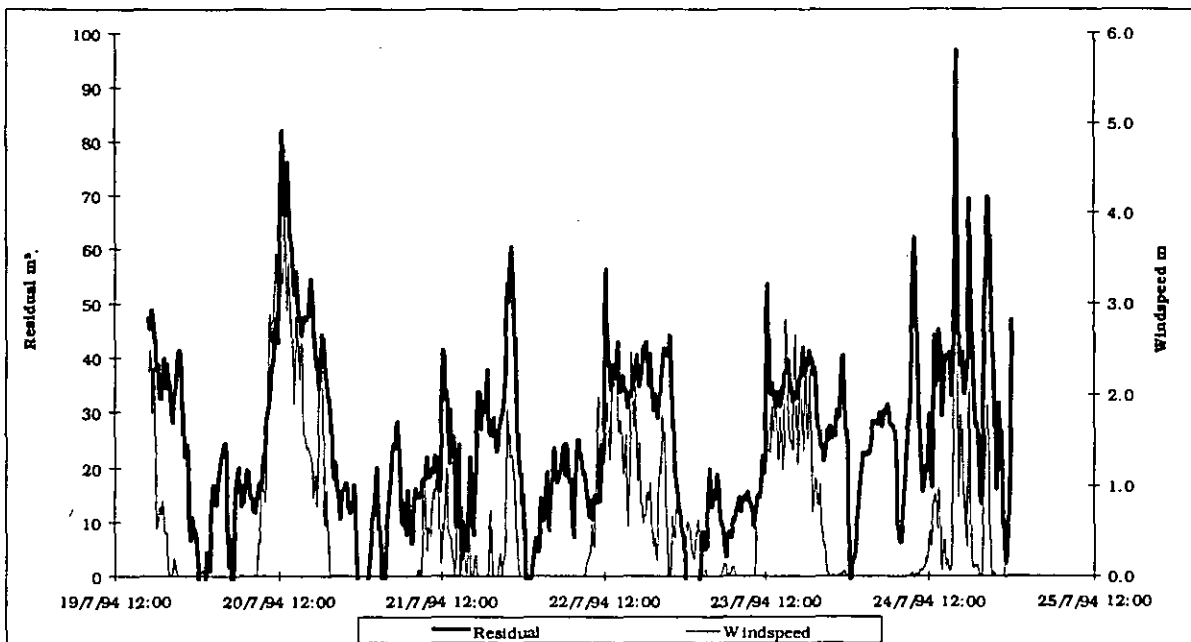


Figure A4.5.17: Residual (measurement - simulation) and wind speed; external opening. Second period.

Approach 2: These simulations were done over 8 periods of 6 hours each. Normally, the average of these simulations is not as good as the values found with the previous simulation because the gradient-values were averaged over 6 hours. The advantage of this method is that a Monte-Carlo is performed and thus we know the value of the 95%-interval.

The value of the C_d is also varying for the different runs. The 95%-interval for the C_d is between 0.55 and 0.65.

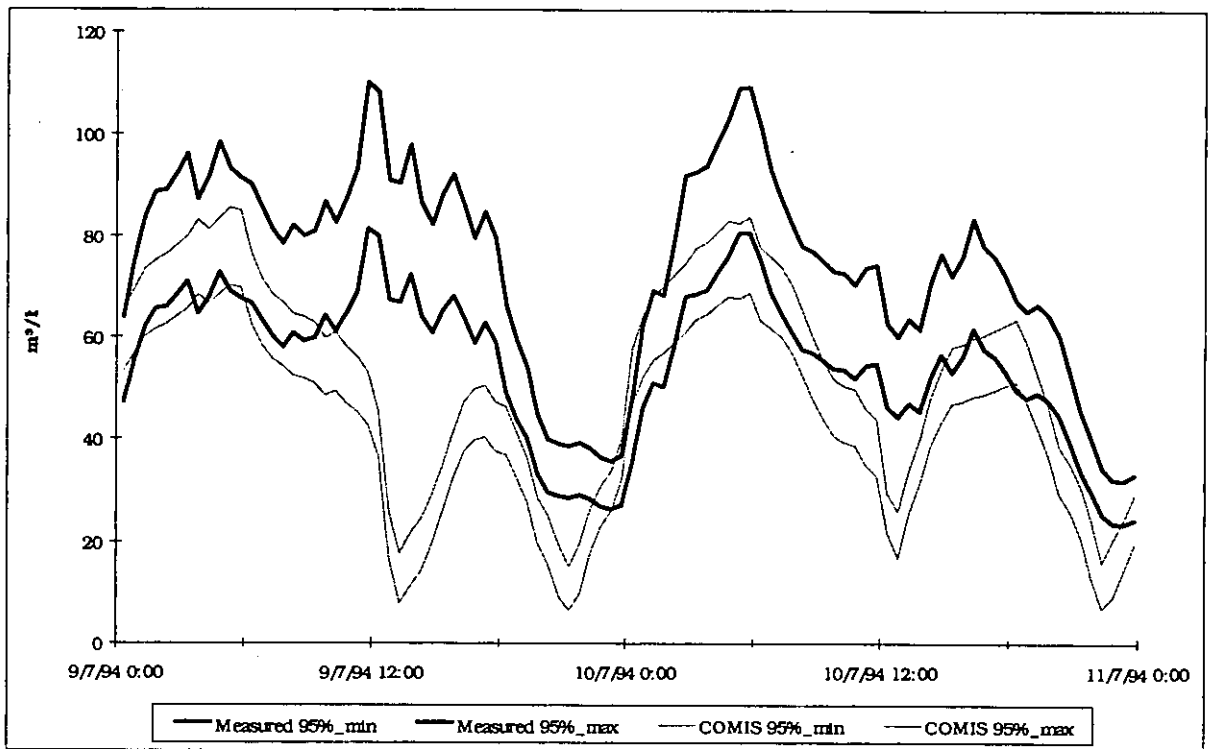


Figure A4.5.18: 95%-intervals of measurement and simulation for the external opening. First period.

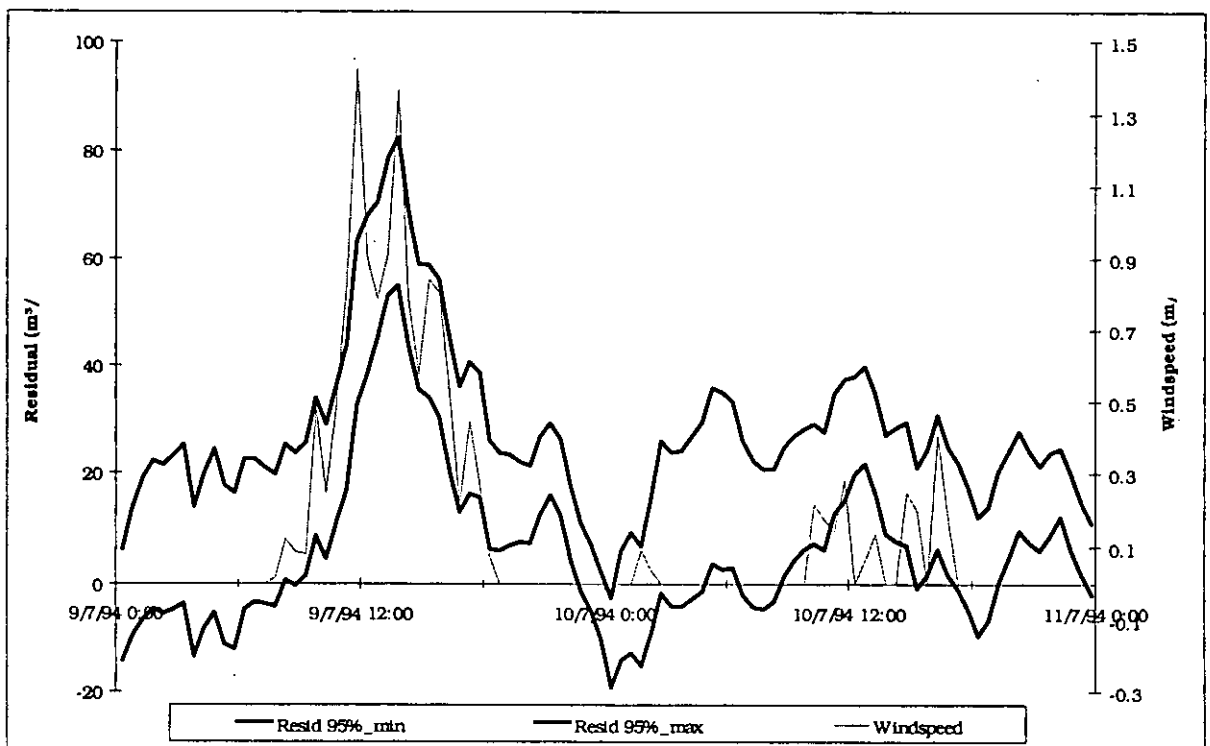


Figure A4.5.19: Wind speed and 95%-interval of residual (= measurement - simulation) for air flow rate through external opening. First period.

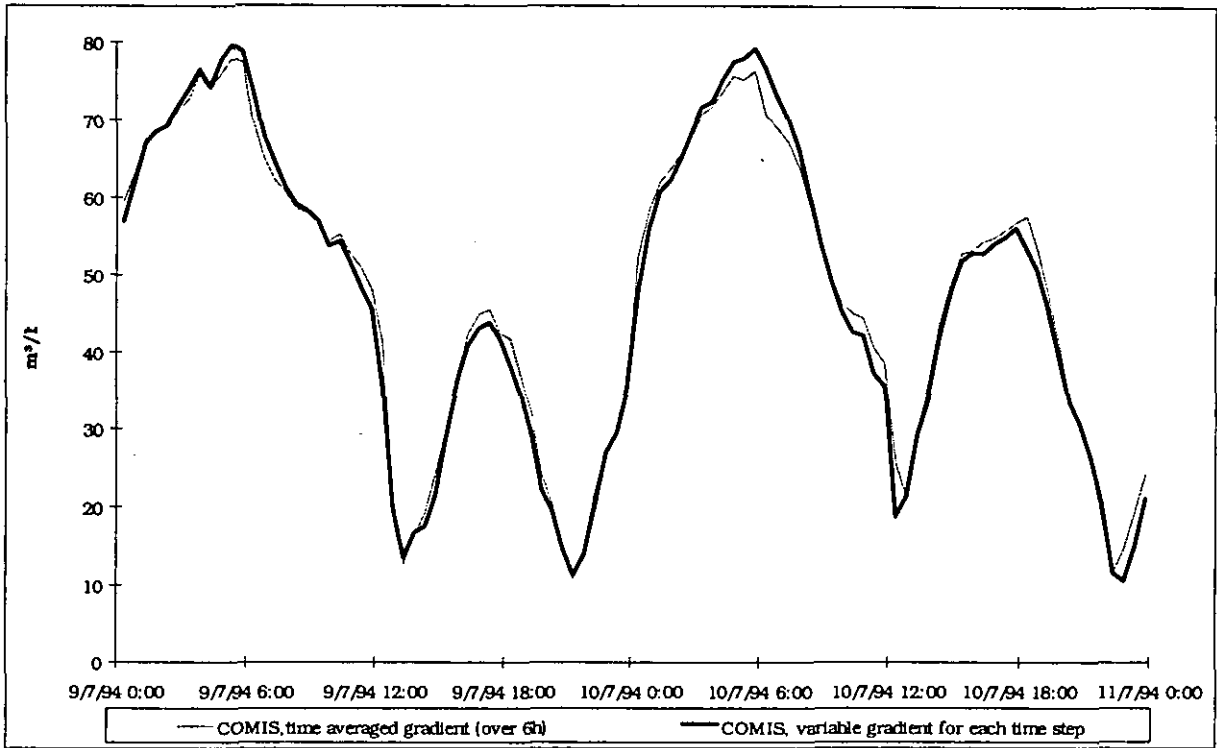


Figure A4.5.20: Comparison between the simulation results obtained with the 2 different approaches for the air flow through the external opening. First period.

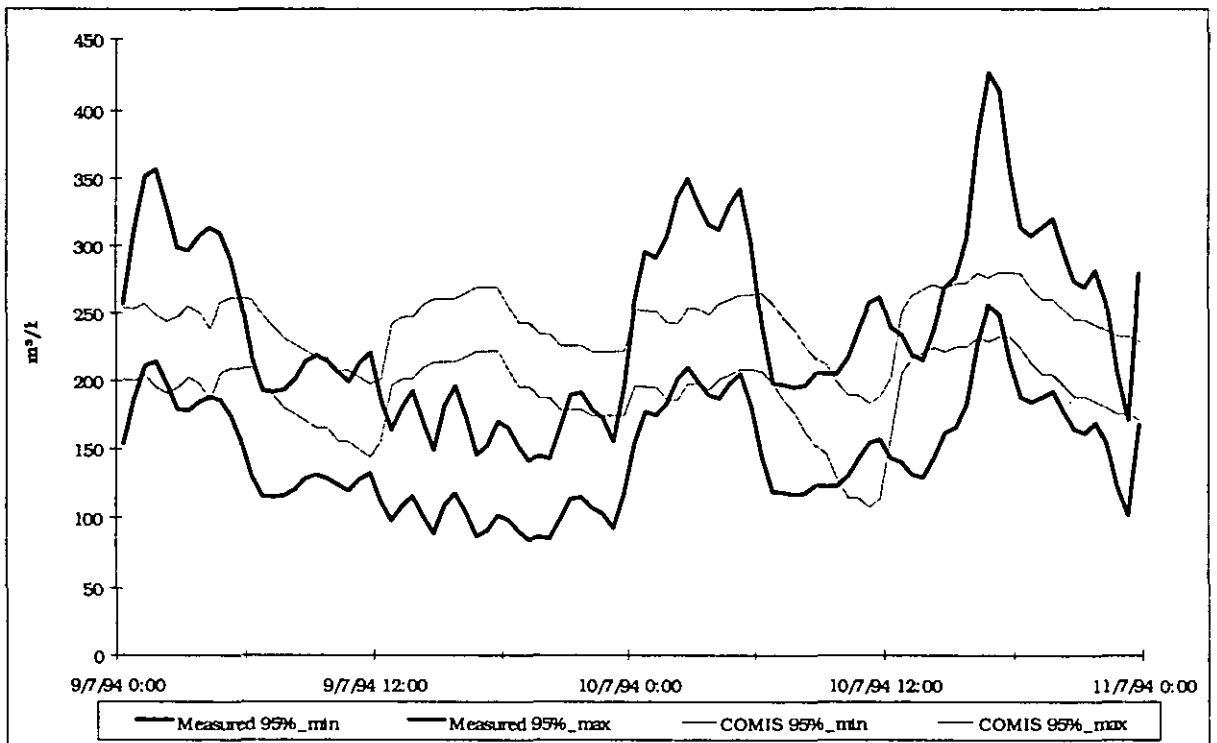


Figure A4.5.21: 95%-intervals of measurement and simulation for the internal opening. First period.

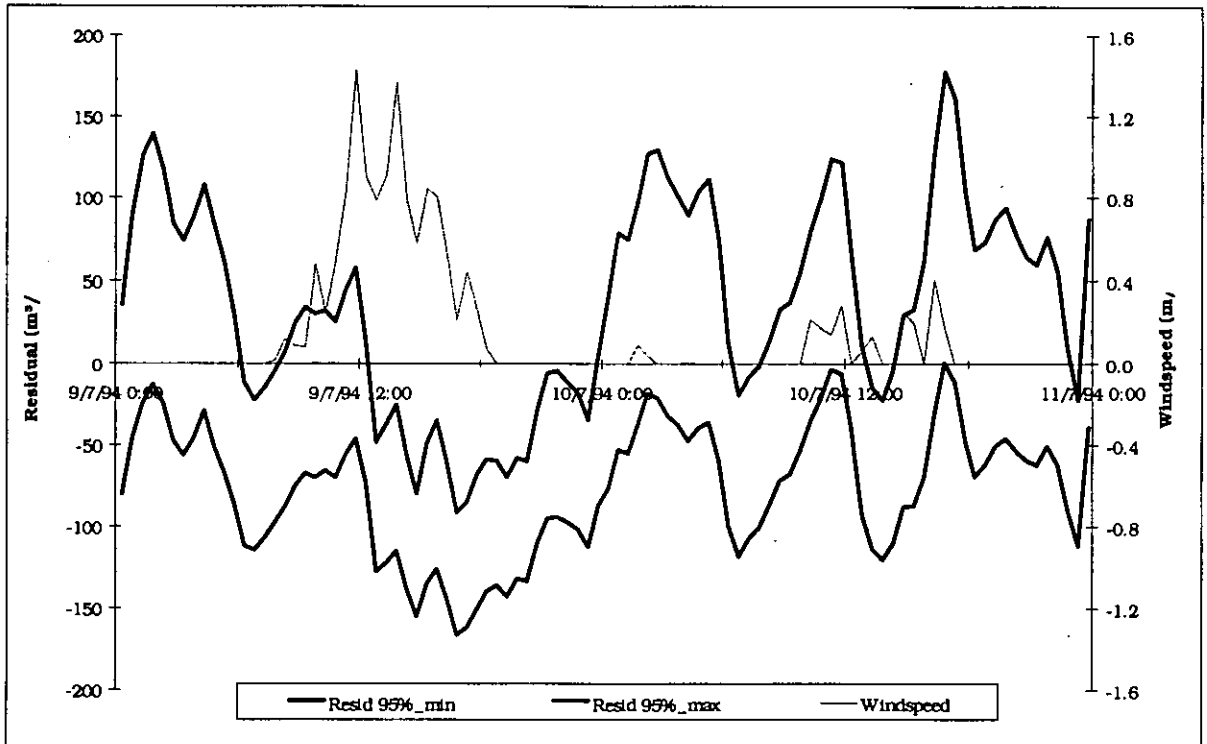


Figure A4.5.22: Wind speed and 95%-interval of residual (= measurement - simulation) for air flow rate through internal opening. First period.

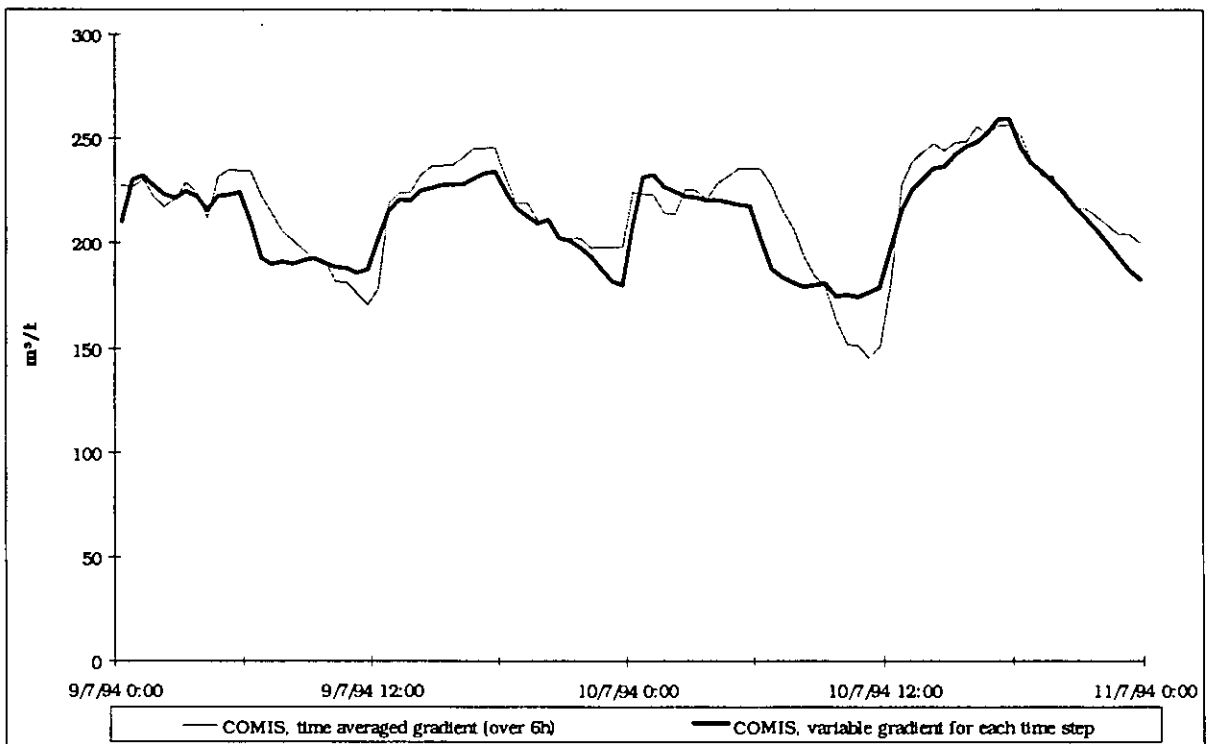


Figure A4.5.23: Comparison between the simulation results obtained with the 2 different approaches for the air flow through the internal opening. First period.

As one can see in Figure A4.5.20 the averaging of the temperature gradient over a period of 6 hours, has practically no influence on the air flow rate through the external opening. The influence on the air flow rate through the internal opening is already more important (largest difference between the two approaches approx. 15%) as shown by Figure A4.5.23.

In Figure A4.5.18 (external opening) one can see that the 95%-intervals of measurement and simulation are not overlapping during certain periods. Figure A4.5.19 shows that this is mainly caused by the influence of the wind. Indeed, the X-axis is nearly always enclosed by the 95%-interval of the residual, except for the periods with wind. The 95%-interval of the residual is found in the following way:

$$Error_{residual} = \sqrt{Error_{measurement}^2 + Error_{simulation}^2} \quad (A4.6.8)$$

For the internal opening, one can see in Figure A4.5.21 and Figure A4.5.22 that the 95% intervals again do not overlap during the whole period. The relation between air flow rate and wind speed is not so clear as for the external opening.

It has to be mentioned again that the error on the measurement of the air flow through the external opening is about 15%, whereas for the internal opening the error is 25%. As a result the 95%-interval of the residual is larger for the internal opening than for the external opening.

In Figure A4.5.18 one can see clearly that even for the periods without wind the simulation is still nearly always smaller than the measurement. The same remark can be made for the second period (see also Figure A4.5.10 for the first period and Figure A4.5.16 for the second period). How can this be explained ?

One could think that this is caused by a wrong value of the discharge coefficient C_d . Indeed, a higher C_d gives a higher air flow rate. But the C_d doesn't seem to be the main cause. As one can see in Figure A4.5.16 (for example) the lowest air flow rates simulated with COMIS would have to be multiplied with a factor 2 or even 3. This means actually that a new C_d would have to be applied which is 2 or 3 times higher than the current one (= 0.6). This is impossible. Probably the main cause of the difference between measurement and simulation is that COMIS 1.2 doesn't take a certain turbulence effect into account. This turbulence effect is a constant value which is the minimal air flow through a certain opening. Indeed, one can intuit that even without any wind and temperature difference there will still be an air flow through a large opening, at least by thermal diffusion.

Fractional Factorial analysis

A fractional factorial analysis was performed for two specific moments:

- 1) July 9, 3h20: heating in the service room. Figure A4.5.24 and Figure A4.5.25.
- 2) July 9, 15h20: cooling in the test room. Figure A4.5.26 and Figure A4.5.27.

Table A4.5.3: Values of the parameters for the two fractional factorial analyses.

Parameter Number	Parameter Name	Value at 3h20	Value at 15h20
1	width of internal opening	1 m	1 m
2	height of internal opening	1 m	1 m
3	Cd for both openings	0.6	0.6
4	width of external opening	0.5 m	0.5 m
5	height of external opening	0.5 m	0.5 m
6	temperature in test room	16.9 °C	16.6 °C
7	temperature in service room	18.3 °C	18.9 °C
8	gradient in test room down	2.4 °C/m	1.9 °C/m
9	gradient in test room up	1.3 °C/m	1.0 °C/m
10	gradient in service room down	2.9 °C/m	1.8 °C/m
11	gradient in service room up	0.9 °C/m	1.7 °C/m
12	outside temperature	10.2 °C	20.5 °C

In Table A 4.6.4 the errors on the different input parameters are repeated, to ease the evaluation of the following figures.

Table A4.5.4: Overview of the errors applied on the different parameters.

Parameter	Parameter name	Standard error
1	width internal opening	± 0.02 m
2	height internal opening	± 0.02 m
3	Cd internal and external opening	± 0.05
4	width external opening	± 0.02 m
5	height external opening	± 0.02 m
6	temperature test room	± 0.2 °C
7	temperature service room	± 0.2 °C
8	gradient test room down	± 0.2 °C/m
9	gradient test room up	± 0.2 °C/m
10	gradient service room down	± 0.2 °C/m
11	gradient service room up	± 0.2 °C/m
12	temperature outside	± 0.2 °C

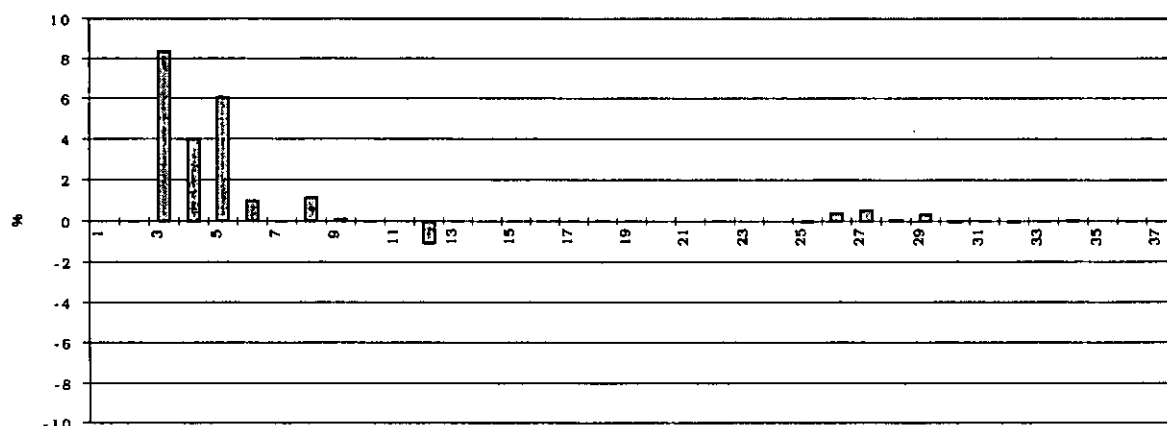


Figure A4.5.24: Main effects and effects of the first order for the air flow through the external opening: July 9, 3h20.

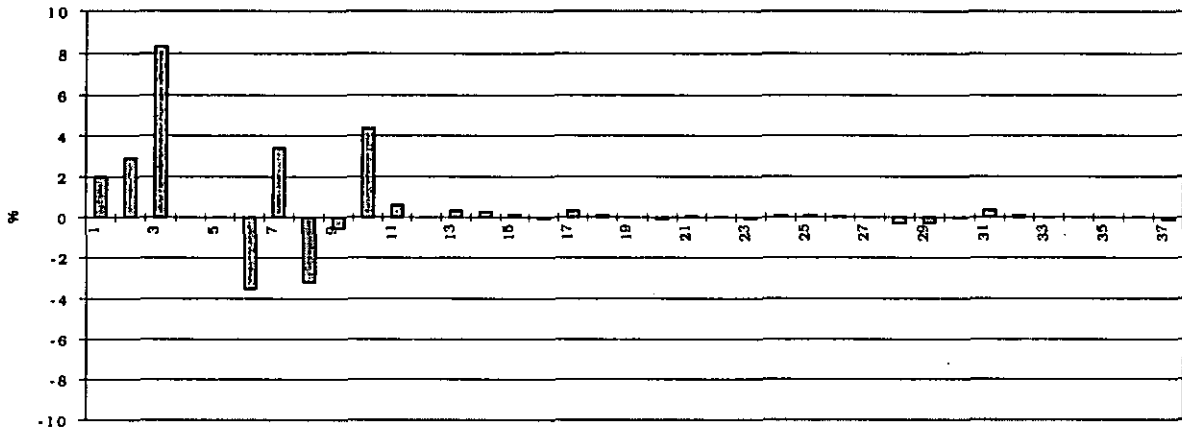


Figure A4.5.25: Main effects and effects of the first order for the air flow through the internal opening: July 9, 3h20.

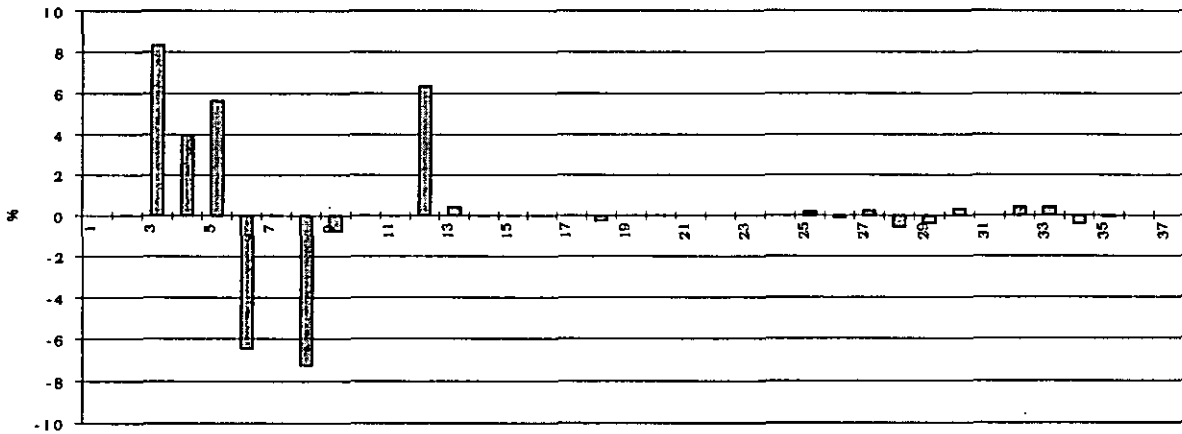


Figure A4.5.26: Main effects and effects of the first order for the air flow through the external opening. July 9, 15h20.

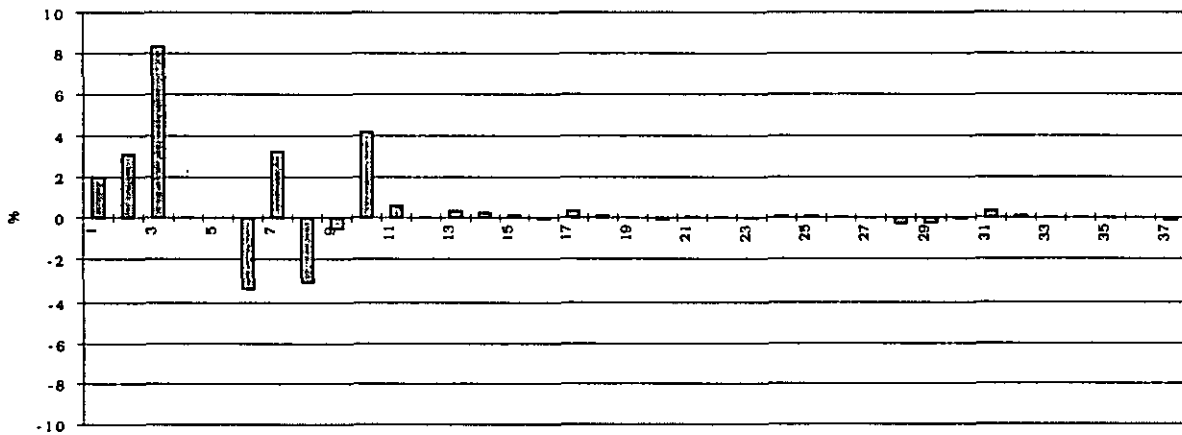


Figure A4.5.27: Main effects and effects of the first order for the air flow through the internal opening. July 9, 15h20.

Parameters 1 to 12 are main effects (the Numbers 1-12 in the figures correspond with the same parameter numbers as in Table A4.5.4). Parameters 13 to 37 are effects of the first order

(= 2-factor interactions), these are the additional effects caused by the variation of 2 parameters in the same time.

One can see in Figures A 4.6.24 to 27 that only the main effects are important.

The discharge coefficient seems to be a very important parameter. A change of 8% (= 0.05/0.6) in the discharge coefficient leads to a change of 8% in air flow rates. This is logical since the air flow is proportional to the discharge coefficient. A good choice of this parameter will be very important but, on the other hand, it is not easy to know its exact value.

Comparing Figure A4.5.25 with Figure A4.5.27 one can see that the main effects are nearly the same for every parameter although in Figure A4.5.25 the service room is warmed up and in Figure A4.5.27 the test room is cooled down.

Comparing Figure A4.5.24 with Figure A4.5.26 one can notice that the effect of the temperature and the gradient-down in the test room and the effect of the outside temperature are much higher when cooling in the test room, because at that moment the difference in temperature between test room and outside is very small (see Table A4.5.5), and thus a relatively small change for one of these values will have an important effect.

These temperature differences can be calculated from Table A4.5.3:

Table A4.5.5: Temperature difference between outside and test room for two specific moments.

Time	T_{out}	T_{test} at 1.25 m ⁽¹⁾	ΔT
at 3h20	10.2 °C	19.9 °C	9.7 °C
at 15h20	20.5 °C	19.0 °C	1.5 °C

Comparison between the results obtained with COMIS 1.2 and those obtained with a simple model

In the Technical report of annex 20 a simple model is given to calculate the air flow rate through large openings [van der Maas, 1992].

$$m' = 0.04 \cdot W \cdot H^{3/2} \cdot \sqrt{\Delta T} \quad (\text{kg/s}) \quad (\text{A4.6.9})$$

In Figures A 4.6.28 and 29, the results obtained with the simple model are compared with the air flows obtained with COMIS 1.2. This has only been done for the first period.

One can see very clearly in Figures A 4.6.28 and 29 that the results obtained with the simplified model do not differ very much from those obtained with COMIS 1.2. The differences are probably mainly caused by the temperature gradients: COMIS 1.2 takes them into account, the simple model does not.

¹1.25 m is the middle of the opening. The temperature in the test room at that height is calculated with the value of gradient-down.

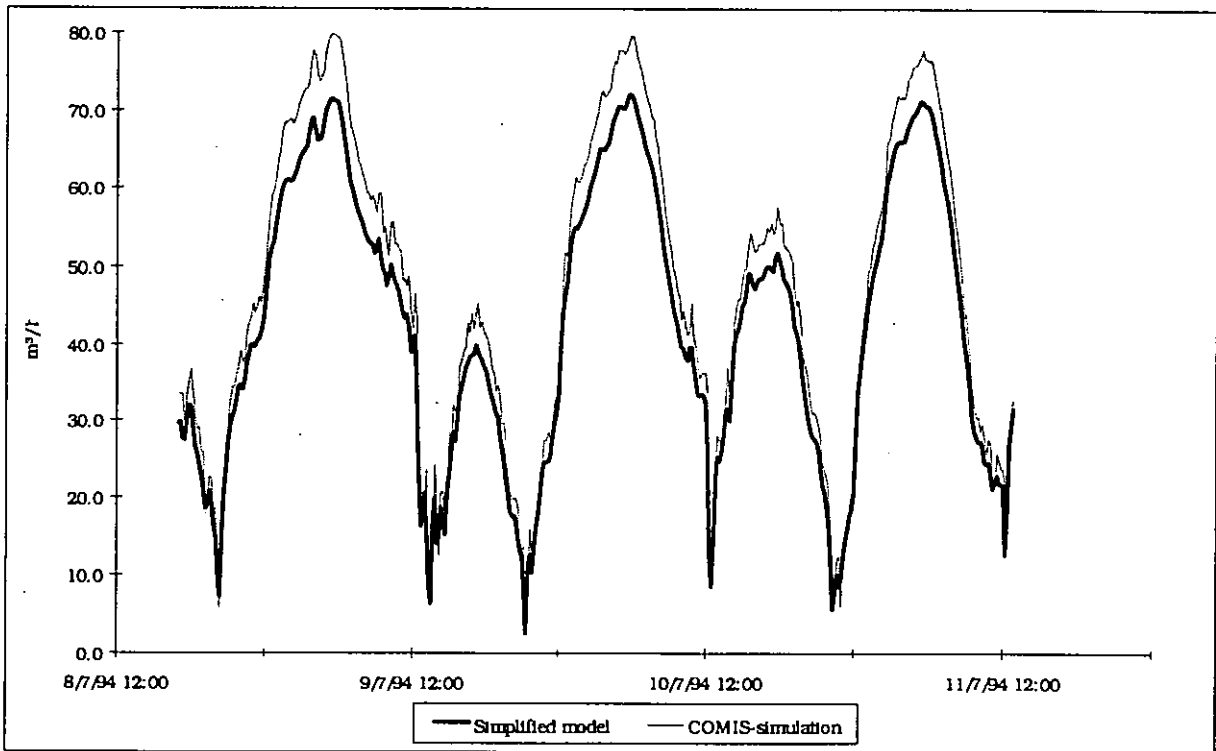


Figure A4.5.28: Comparison of the air flows obtained with COMIS 1.2 and with a simple model. External opening.

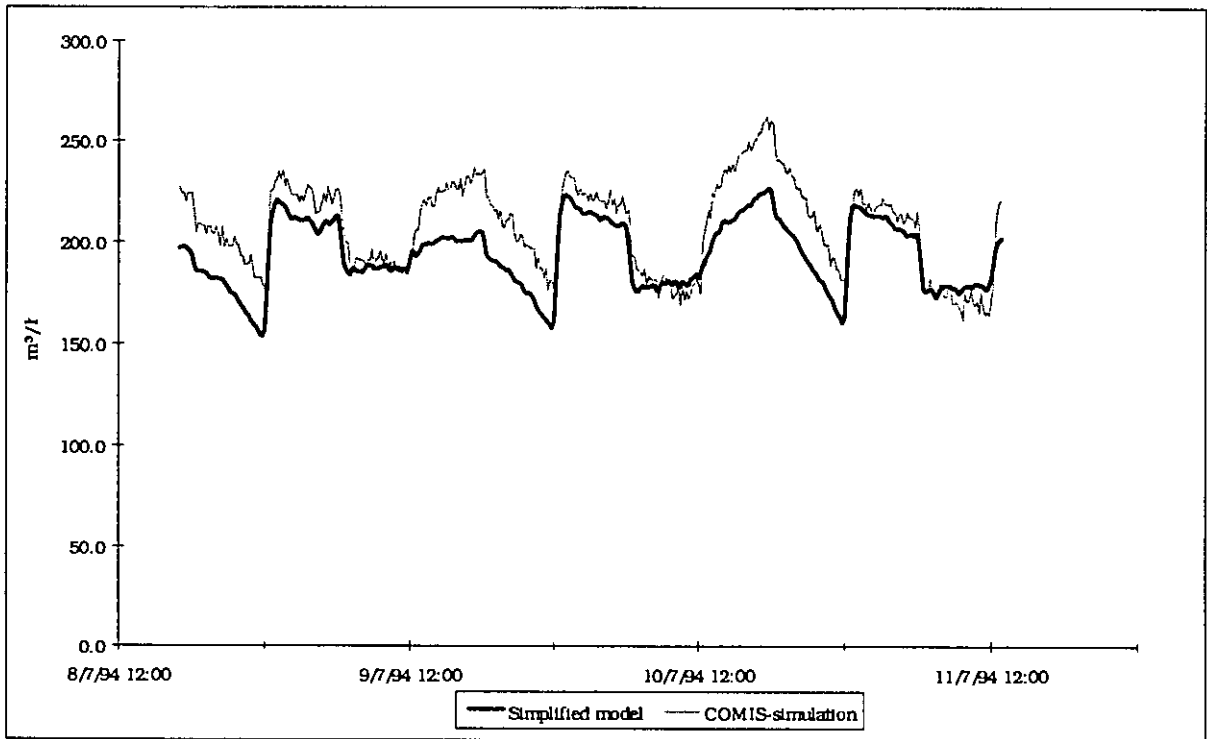


Figure A4.5.29: Comparison of the air flows obtained with COMIS 1.2 and with a simple model. Internal opening.

A 4.5.4 Conclusions

In COMIS 1.2 no algorithm is enclosed which can calculate the effect of the wind on the air flow rate through large openings. Nevertheless, the wind has an important influence on the air flows through the large external opening. As a consequence, the importance of such an algorithm is rather great.

The influence of the wind on the air flow through the large internal opening did not appear in such a clear way from the performed measurements. Probably the effect is quite small.

Not only the wind caused differences between measurement and simulation. Since the differences were rather high in cases with little wind and small temperature differences, one can presume the existence of another effect which indicates that, even without wind and temperature difference, ventilation through a large external opening occurs, due to turbulences.

Finally, it is important to mention that the similarity between the results of COMIS 1.2 and the simple model is rather good. This will change if an algorithm for the wind effect on large openings is incorporated in COMIS.

A 4.5.5 Acknowledgements

The participation of the Belgian Building Research Institute (WTCB/CSTC) to Annex 23 'Air Flow Modelling' of the Implement Agreement on Energy Conservation and Community Systems, is made possible with the financial support of the Ministry of the Flemish Community.

A 4.5.6 References

- Fürbringer J.M.: Evaluation Procedure using Sensitivity Analysis of Model and Measurement. LESO. *Proc. International Symposium on Air Flow in Multizone Structures, Budapest, September 1992.*
- Fürbringer J.M.: Sensibilité de modèles et de mesures en aéraulique du bâtiment à l'aide de plans d' expériences. *PhD thesis. Lausanne EPFL, 1994.*
- International Energy Agency: Fundamentals of the Multizone Air Flow Model- COMIS, *AIVC Technical Note 29. May 1990.*
- Van Der Maas J.: Annex 20, Air Flow Patterns within Buildings. Air Flow through Large Openings in Buildings. *Technical Report (Subtask 2). LESO-PB, EPFL, Lausanne Switzerland. June 1992.*
- Wouters P., Vandaele L.: The PASSYS Services, *Summary Report. BBRI and EC DG XII. Brussels 1994 EUR 15113 EN*

A 4.6 Namur Flat: Contaminant Spreading

A 4.6.1 Measured Object

General description

The building is situated in a suburban area near Namur in Belgium. The building has 9 storeys, with 4 apartments on each floor. The measurements have been done in an unoccupied flat on the ground floor. The apartment contains 7 rooms: living room, kitchen, hall, toilet, bathroom and 2 bedrooms. Overall dimension are a total surface of 76 m² and a total volume of 206 m³ (ceiling height = 2.7 m). See Figure A4.6.2 for a sketch of the apartment (which is enclosed by two other ones) and Table A4.6.1 for the room volumes.

Table A4.6.1: Volumes of the different rooms in the apartment.

Room	volumes
Living room	53 m ³
Kitchen	15 m ³
Bedroom 1	34 m ³
Hall	17 m ³
Bedroom 2	21 m ³
Bathroom	8 m ³
Toilet	4 m ³

The inside air is extracted by natural ventilation from bathroom, kitchen and toilet through vertical ventilation ducts. These ducts are connected to the common ventilation ducts by a so-called shunt-type connection. There are also air inlets in the living room and in the 2 bedrooms (in the upper part of the windows).

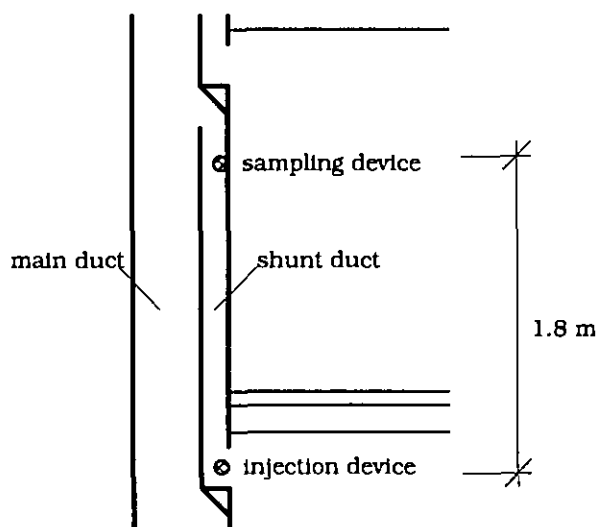


Figure A4.6.1: Shunt-type connection for the ducts for natural ventilation & measurement "duct-flow".

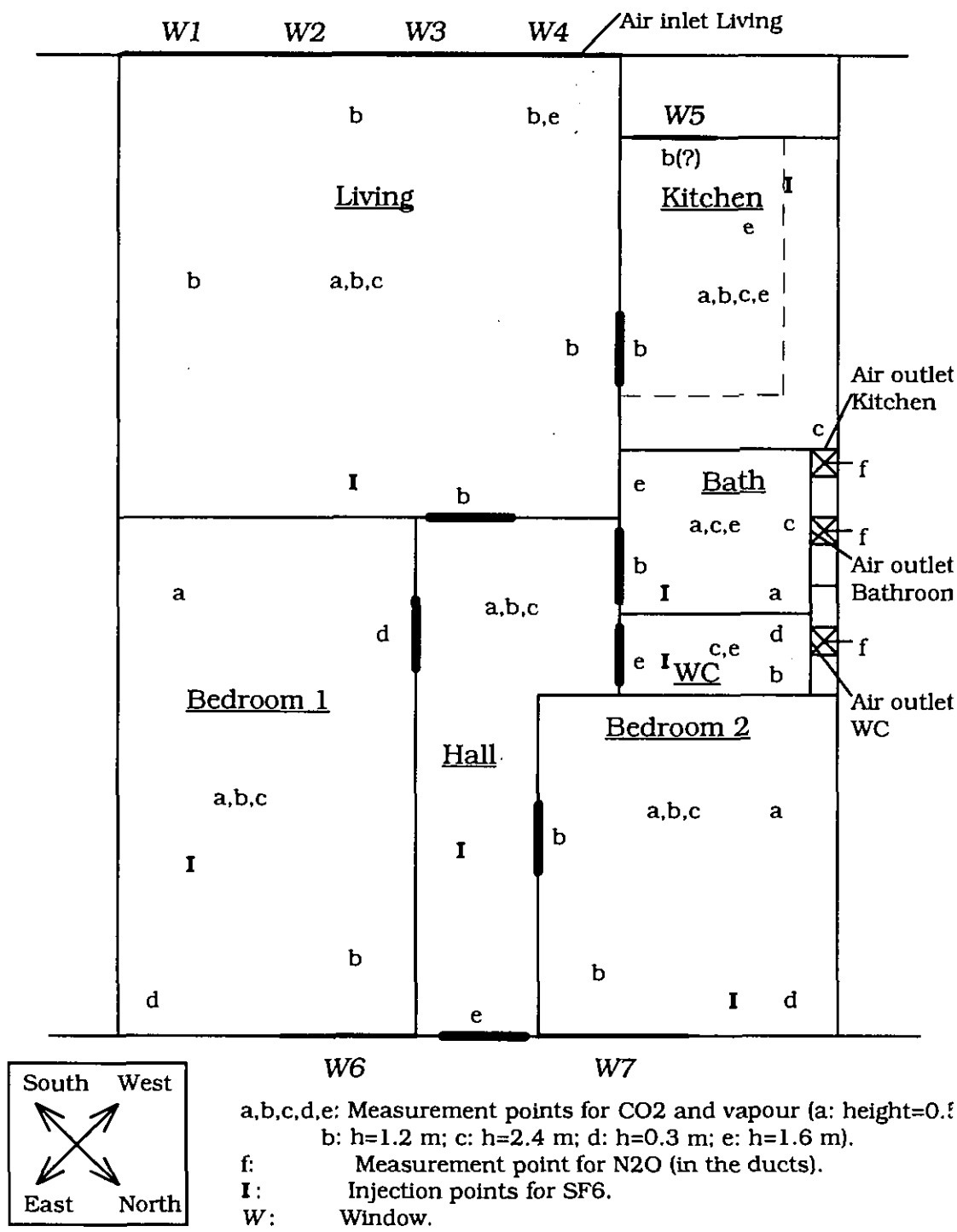


Figure A4.6.2: Sketch of the apartment where the measurements were done.

Leakage characteristics

Before starting the measurement of the air flows and the pollutant spreading, a whole range of pressurisation measurements were performed in the flat in order to have an idea of the building's air tightness.

The total envelope leakage is characterised as follows:

$$Q = 28.3 \cdot (\Delta p)^{0.64} \quad [\text{m}^3/\text{h}] \quad (\text{A4.7.1})$$

To determine the leakage distribution, the flowfinder (=compensating flow meter) was used. The following results were found:

- kitchen: 12 %
- bedroom 1: 6 %
- bedroom 2: 10 %
- bathroom: 11 %
- toilet: 4 %
- living room: 35 %
- entrance door: 22 %

A 4.6.2 Measurements performed

Airflow through the ducts

To determine the airflow through the ducts, N₂O tracer gas is injected at a constant rate behind the outlet grilles for natural ventilation. The concentration is measured in the shunt ducts, near the place where it is coming out in the main duct. This is shown clearly in Figure A4.6.1. The air flow rate can be calculated as follows:

$$Q = 3600 \cdot \frac{S}{C} \quad (\text{A4.7.2})$$

With: Q = air flow rate. [m³/h]
 S = injection rate of the tracer gas [ml/s]
 C = concentration of the tracer gas [ppm]

Fresh air flow into each room

The fresh air supply into each room is determined by the constant concentration technique. SF₆ is injected as tracer gas at a the target concentration of 30 ppm. Every room has one injection point and one measurement point (see Figure A4.6.2). Each time step, the concentration is measured in each room, the amount of SF₆ required to reach 30 ppm is automatically calculated and injected. The outdoor air flow rate is calculated from the quantity of tracer gas injected. Small fans are used to improve the homogeneity of tracer concentration in the rooms.

Contaminant spreading

During specific periods CO₂ and water vapour are injected to simulate the presence of persons in the flat. The injections are done in one room, the measurements in all the rooms; in total there are 50 measurement points situated in different places in the dwelling. In Figure A4.6.2 the position of these measurement points is given. The injection of water vapour is done with a humidifier placed on an electronic balance.

External and inside conditions

The outside temperature is measured at ground floor level, and the wind speed and wind direction on the building's roof. Also the reference levels for the concentration of CO₂ and N₂O are measured outside. Finally, the pressure difference across the building (SW and NE facade) is measured at the 5th floor.

Inside the flat the temperature is measured at the 50 places where the relative humidity and the concentration of CO₂ are measured.

Overview table*Table A4.6.2: Overview table of the different injections and measurements.*

type	injection points	measurement points
CO ₂	1	50
H ₂ O	1	50
N ₂ O	3	3
SF ₆	7	7
Inside temperature	-----	50

A 4.6.3 Sensitivity Analysis (Generality)***Purpose of the simulations***

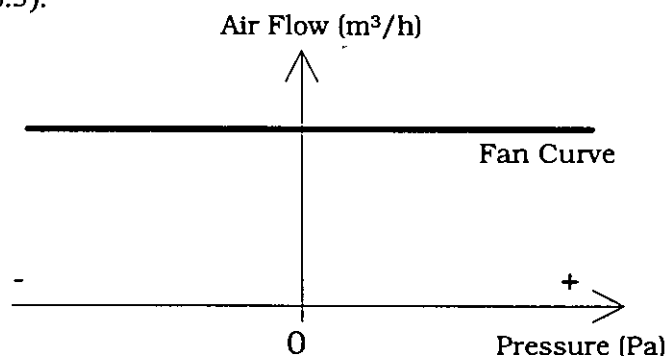
We will especially focus on the simulation of the contaminant spreading in the apartment, starting from the given fresh air supply. The purpose is to compare the simulation results with the measured concentrations, in order to examine the validity of COMIS 1.2 concerning pollutant spreading. The sensitivity analysis performed with MISA makes it possible to evaluate the effect of the different parameters on the final result (cf. §1.3).

The reason why, for example, the fresh air supply will not be simulated is that some important parameters haven't been measured, because these measurements were part of another research project and the dataset was initially not supposed to be used for later simulation. Some of the parameters that are short are for example:

- The Pressure coefficients: the pressure difference between the inside and the outside of the outer walls hasn't been measured, and it is difficult to find suitable pressure coefficients in the literature.
- The air flow rates through the ducts do not only depend on the duct characteristics but also on the ventilation patterns in the other apartments, which are connected to the same main duct for natural ventilation.

Approach of the problem

The fresh air supply in each room is not supposed to be simulated. This means that it has to be entered as a given parameter for each room and for each time step. This is simulated in COMIS by putting a fan in each external wall. Each fan is characterised by a linear and horizontal fan curve, which means that the air flow through the fan is not depending on the pressure difference (see Figure A4.6.3).

*Figure A4.6.3: Input of the fresh air supply using the fan algorithm.*

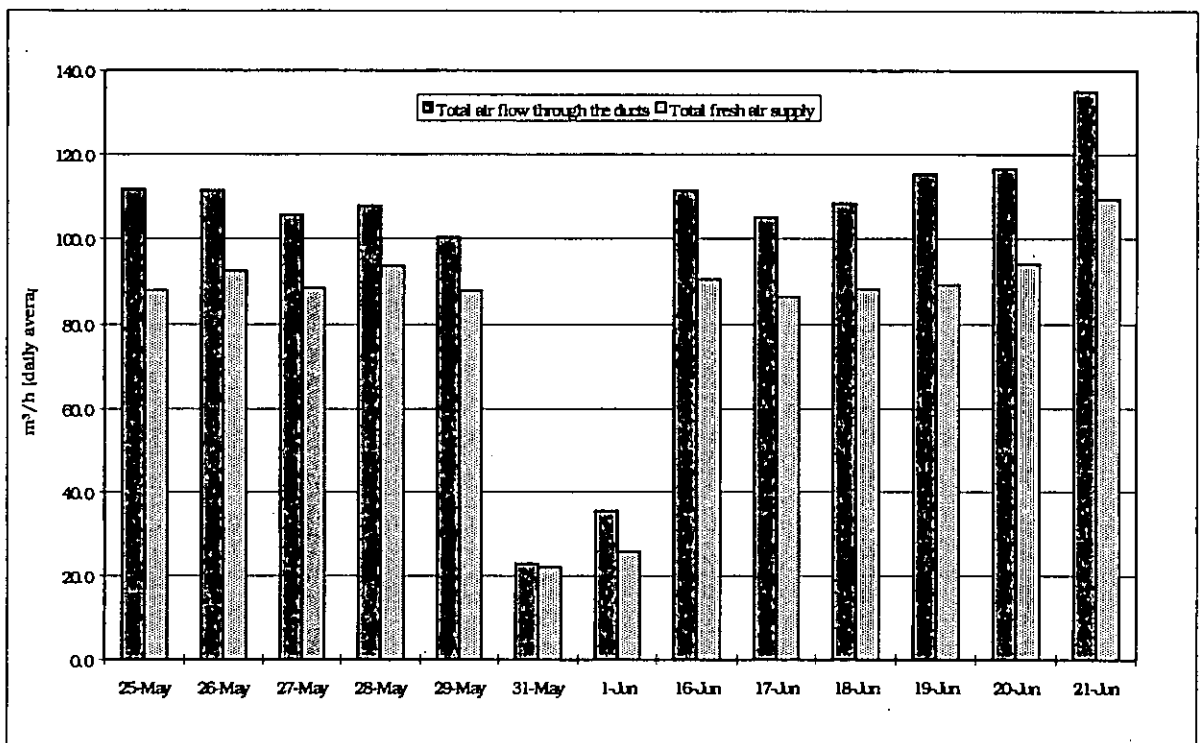


Figure A4.6.4: Comparison between the daily averages of the total fresh air supply and the total ductflow

The fresh air supply is changing in time. From our measurements we know the amount of fresh supplied each hour, so the fan schedules were used in the input file to simulate this.

The air flows through the ducts can't be entered as fan flows because the measured total duct flow is larger than the measured total fresh air supply. This is shown in Figure A4.6.4.

Normally we would expect the opposite, because:

$$\text{Fresh Air Supply} = \text{Cross Ventilation} + \text{Duct flow}$$

The cross ventilation may be zero which means that:

$$\text{Fresh Air Supply} \geq \text{Duct flow}$$

Possible causes are:

- Error made in the measurement of the N_2O concentration in the ducts. There are only 2 meters between injection and measurement of the tracer gas; probably, this is not enough to guarantee homogeneity.
- Error made in the measurement of the SF_6 concentration in the rooms, due to an insufficient homogeneity. In Figures A 4.7.5 and A 4.7.6, some examples are given to show to what extent the CO_2 concentration (SF_6 is only measured on 1 place for each room) can differ for different places in the same room.

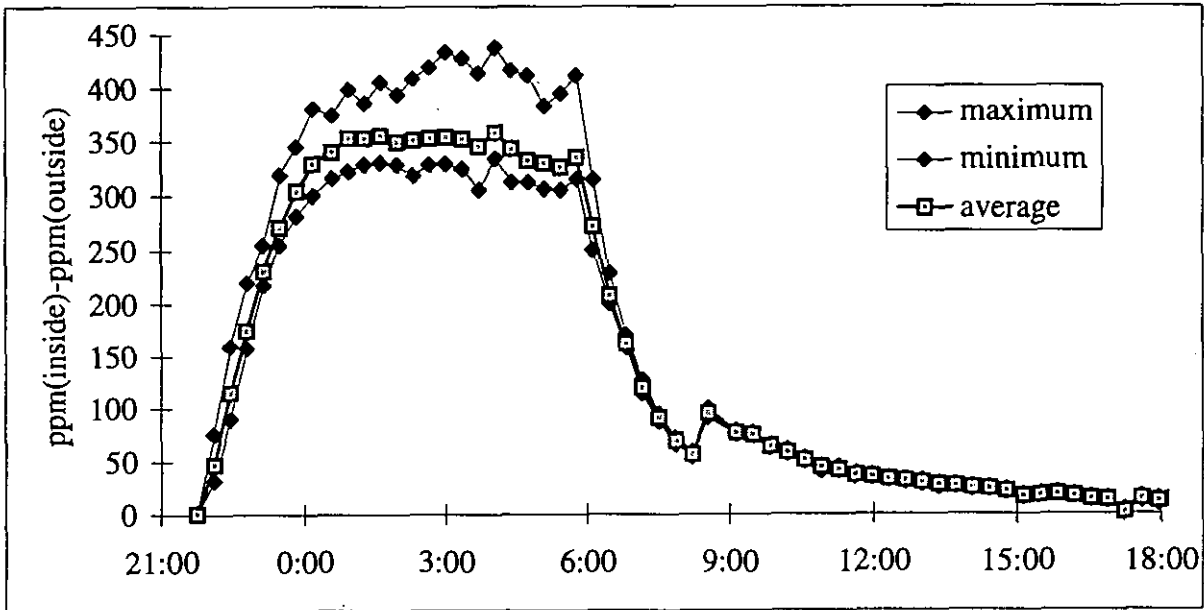


Figure A4.6.5: Concentration of CO₂ on different places in the living.

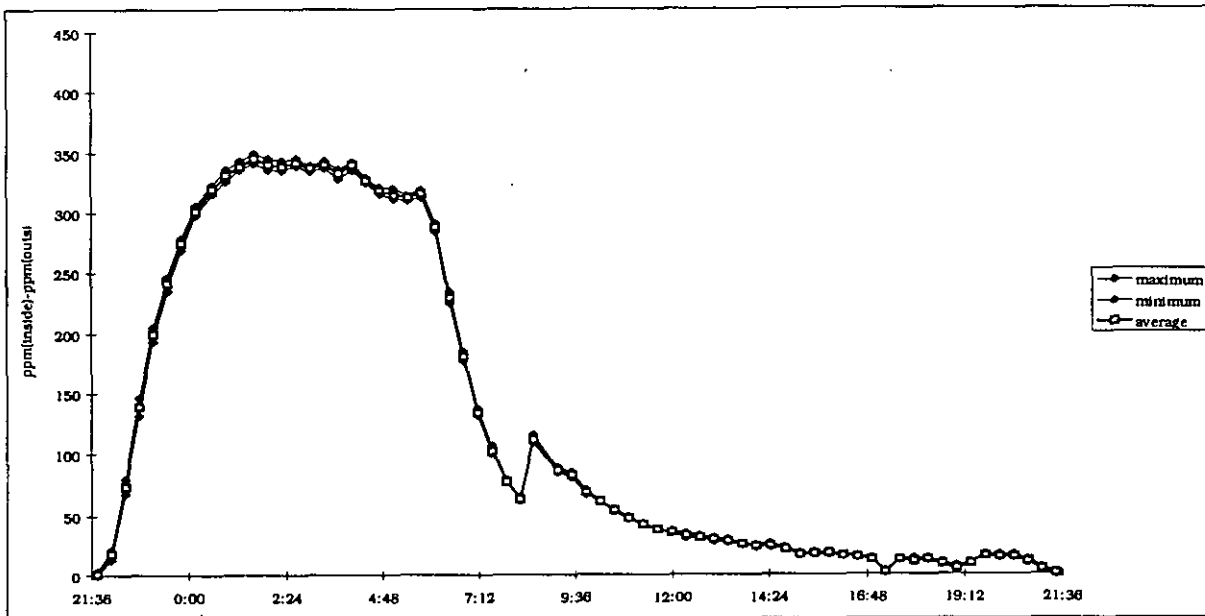


Figure A4.6.6: Concentration of CO₂ on different places in the kitchen.

It is clear that the homogeneity of a tracer gas is not always guaranteed in certain rooms, which will decrease the accuracy of fresh air supply measurements.

Nevertheless, we will work with the fresh air change rates as given parameters instead of the duct flows. The ducts will be simulated as cracks, because we don't know the real characteristics of the ducts. The only error that is made by doing this is an error on the pressure in the flat.

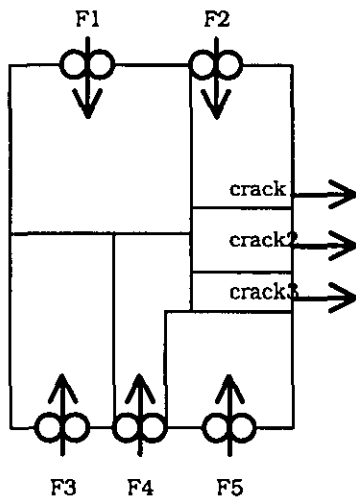


Figure A4.6.7: Use of fans and cracks to simulate the air flows in the apartment

The characteristics of the cracks are chosen in such a way that the proportion of the flows through the cracks is equal to the proportion of the real flows through the ducts.

Due to the fact that the fresh air supplies are entered as known parameters (simulated by fans), the external conditions should not have an influence on the air flows in the apartment, because the purpose of these fans is just to eliminate the influence of external conditions. This is realised in the following way:

- Wind speed = 0 m/s.
- Temperature difference between outside and the bathroom, the toilet and the kitchen = 0°C (the other rooms can not be influenced by a temperature difference with outside, because the fans are regulating the air flows entering these rooms from outside). This is impossible because the temperatures in bathroom, toilet and kitchen are not equal. For this purpose the outside temperature is taken the same as the average temperature of these 3 rooms because in this case the influence of the external temperature will be minimal and the flows through the ducts (which are simulated by cracks) will be mainly determined by the fan-flows and the internal conditions.

Two different ways to perform the sensitivity analysis.

To run MISA, the only difference between the 2 methods is the design-file, this is the matrix file in MISA that determines which value has to be given to the different parameters, starting from the ranges of the parameters in the range file [Fürbringer, 1994]. Nevertheless the objective of the 2 methods is totally different:

- *Fractional Factorial Design:* In this case the design file is built up by values 1 or -1 (1 means that we take the upper value in the range file to do the simulation, -1 means the lower value) in such a specific way that it is possible to find the main effect of each parameter on the final result. Moreover, the two-factor interactions are found (these are the additional effects caused by the variation of two parameters in the same time). These effects are confounded in a certain way, depending on the resolution of the design (this means that they are not found separately but in groups, for more explanation, see [Fürbringer, 1994]). For the following simulations a $2_{IV}^{(32-26)}$ design was used. This is a design of resolution IV which means that the main effects are not confounded with one another nor with the two-factor interactions, but the two-factor interactions are confounded with one another. The number of simulation runs is determined by the design-type. In our case ($2_{IV}^{(32-26)}$) the number of runs is 64. For more theory: see [Fürbringer, 1994].

- **Monte Carlo Design:** In this case the design file is built up by random values with a normal distribution with mean value 0 and standard deviation 1 (1= upper value in the range file, -1= lower value in the range file). In this design file the values were limited between -2 and 2, to avoid illogical input. By taking random values for the parameters, a whole series of combinations is examined. In our case a 100 runs were performed. It is shown in [Fürbringer, 1994] that the average and the standard deviation of the final result of the simulations stay nearly constant when the number of runs is higher than 60.

Performed simulations

1. Situation 1: In this case the *inside doors are open*, the outlet ducts also, and the inlet grilles are closed; the injection of water vapour and CO₂ is done in bedroom 2, from 22h00 to 00h00 on 26/5/90.
2. Situation 2: In this case the *inside doors are closed*, the outlet ducts for natural ventilation are open and the inlet grilles are closed; the contaminants are injected in bedroom 2, from 22h00 to 00h00 on 25/5/90.

A 4.6.4 Sensitivity Analysis of Situation 1: inside doors open.

Standard deviation of the input parameters:

The parameters in Table A4.7.3 are supposed to be constant in time. For the temperature the average value was taken for each room, in space as well in time: this is a good approximation because the temperature-difference is important and this is almost unvarying.

Table A4.6.3: Range of varied parameters, determined by their standard deviations, in Situation 1 (doors open). The interval determined by the standard deviation is the half of the confidence interval (95 %).

No	Parameter	Minimum	Maximum
1	Door width	0.8 m.	0.9 m.
2	Door height	1.95 m.	2.05 m.
3	Discharge coefficient	0.55	0.65
4	Temperature in Living	26.3 °C	27.3 °C
5	Volume of Living	50.35 m ³	55.65 m ³
6	Temperature in Kitchen	25.2 °C	26.2 °C
7	Volume of Kitchen	14.25 m ³	15.75 m ³
8	Temp. in Bedroom1	23.6 °C	24.6 °C
9	Volume of Bedroom1	32.3 m ³	35.7 m ³
10	Temperature in Hall	25.3 °C	26.3 °C
11	Volume of Hall	16.15 m ³	17.85 m ³
12	Temp. in Bedroom2	23.5 °C	24.5 °C
13	Volume of Bedroom2	19.95 m ³	22.05 m ³
14	Temp. in Bathroom	25.4 °C	26.4 °C
15	Volume of Bathroom	7.6 m ³	8.4 m ³
16	Temperature in Toilet	24.7 °C	25.7 °C
17	Volume of Toilet	3.8 m ³	4.2 m ³
18	T-gradient in Living	0.8 °C/m	1.0 °C/m
19	T-gradient in Kitchen	0.5 °C/m	0.7 °C/m
20	CO ₂ injection rate	0.0000234 kg/s	0.0000286 kg/s

The following parameters are variable:

The fresh air supply: each hour another fan speed is given in a fan schedule. The standard deviation is supposed to be $\pm 10\%$ of the measured value. Parameter 21-25.

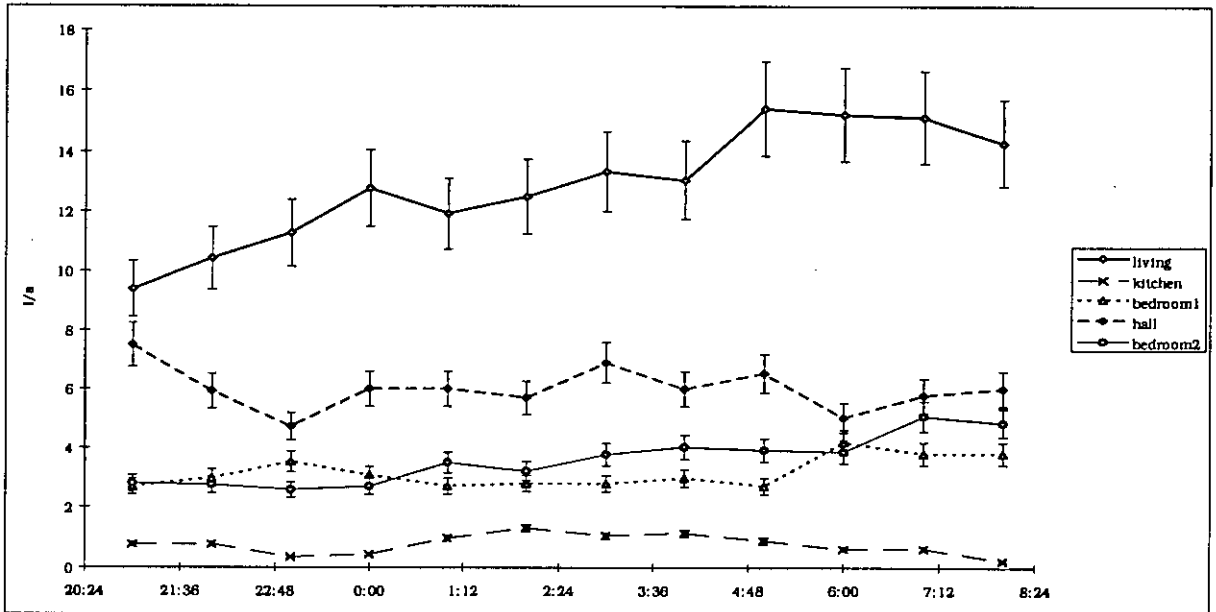


Figure A4.6.8: Variation of the fresh air supplies in each room with their estimated errors. DOORS OPEN.

The absolute humidity: The absolute humidity is not constant during the simulation period due to the injection of water vapour in Bedroom 2. The injection of water vapour will not be simulated because the sink strength is not known and the absorption of water vapour is not negligible. Therefore the humidity will be entered as a known parameter by using a schedule. The standard deviation is supposed to be a constant value (± 0.1 g/kg). At first view this error seems to be very small; and for the explanation see further in the text, where the values of the standard deviations are explained. In the Figure A 4.7.9, the humidity levels in bedroom 2 and in the hall are shown.

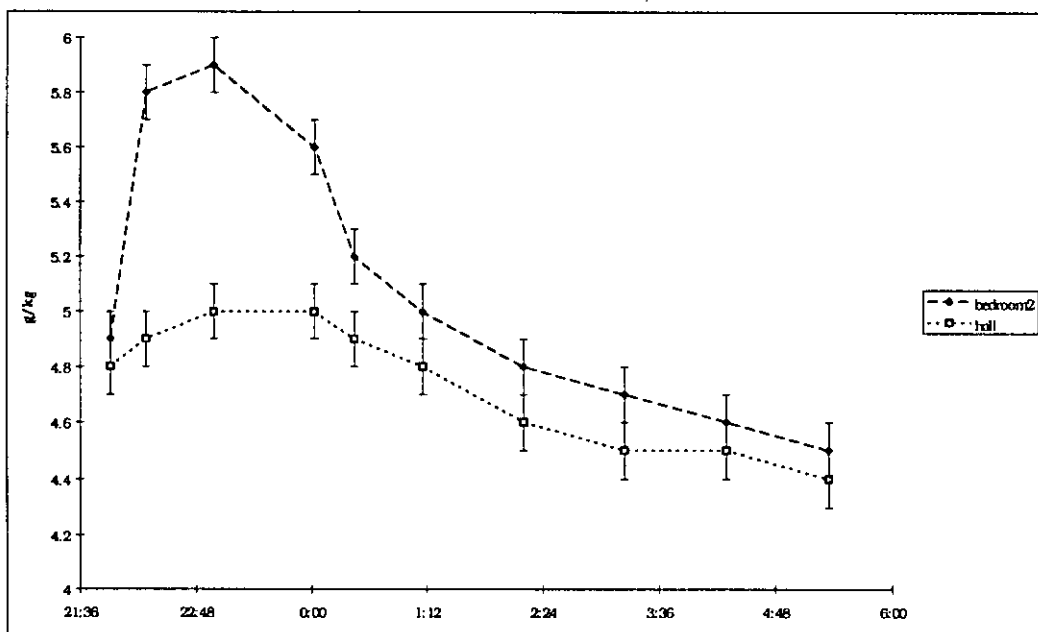


Figure A4.6.9: Variation of the absolute humidity in bedroom 2 and in the hall.

Due to the fact that a schedule is used to describe the change in humidity on one hand and that we want to know the effect of the value of the humidity over the whole period of simulation on the other hand, we introduced more than 32 parameters in the range file. In total there are 95 parameters with which to do the sensitivity analysis. For that purpose the design file (= matrix-file) for 32 parameters is taken, where Parameters 26-32 are the humidity's in the different rooms at the first time step, and the columns 33 to 95 are added, which are copies of one of the columns 26-32. E.g., in the range file used for this analysis Parameter 26 is the humidity in the living room at the first time step, and Parameters 33-41 are the humidity's in this room for the following time steps. In the design file the columns 33 to 41 are copies of column 26.

An explanation is given below for the range chosen for the different parameters:

- *Height and width of the doors:* ± 5 cm. (parameter 1 and 2).

Such a high standard deviation is chosen, because it is difficult to know the effective dimensions, which determine the flow through the large opening.

- *Temperatures:* $\pm 0.5^\circ\text{C}$. (parameters 4, 6, 8, 10, 12, 14 and 16).

The temperature was measured on different places in each room. The value used for simulation is the average of these measurements for each room, but in the following figures one can see that the temperature can vary in an important way from one place to another in the same room. As we do not know for sure that the average temperature is representative to describe the phenomenon, the range is taken large enough.

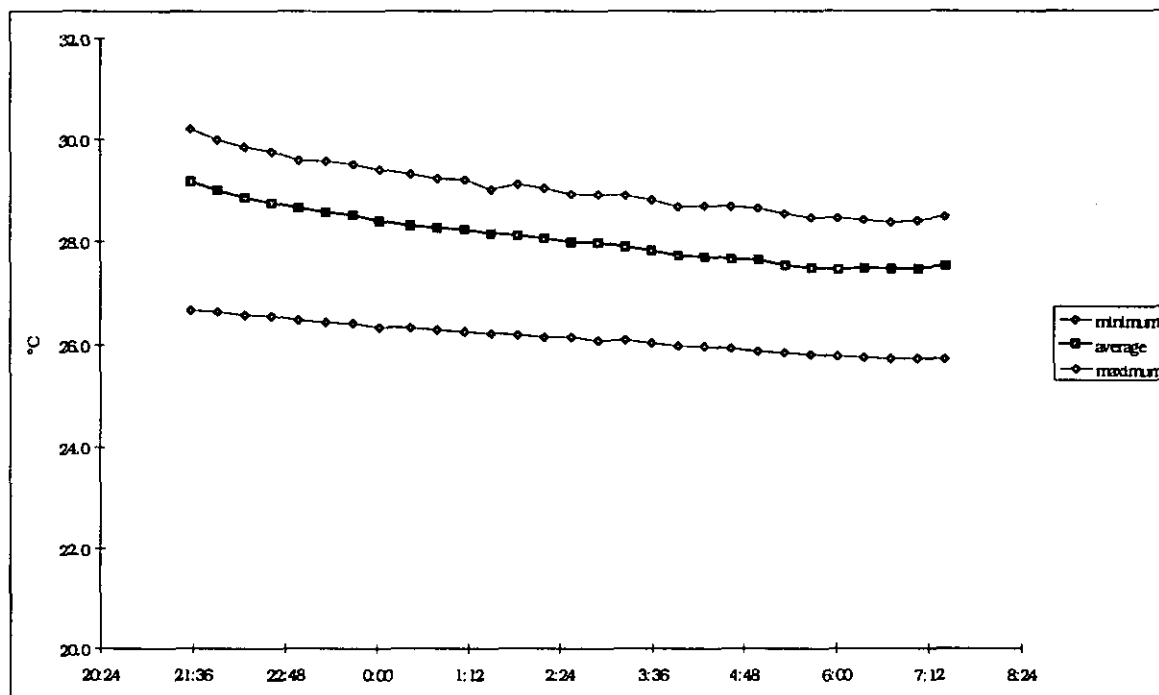


Figure A4.6.10: Range of temperatures measured in the living room (= room with largest spread).

One can see that the spread of the temperatures in the Living room is very high. This is caused by the sunshine. The sun is shining more upon the wall at the kitchen-side than upon the opposite wall. For the other rooms the homogeneity is a lot better as one can see in Figure A4.6.11. It is possible that the range used for the temperatures will not be large enough for the Living room.

- *Temperature gradient:* $\pm 0.1^\circ\text{C}$. (Parameters 18 and 19).

The standard deviation of the start temperature (at level 0m.) is taken rather high (0.5 °C) to take into account the lack of homogeneity. As a result the standard deviation of the gradient can be taken much smaller.

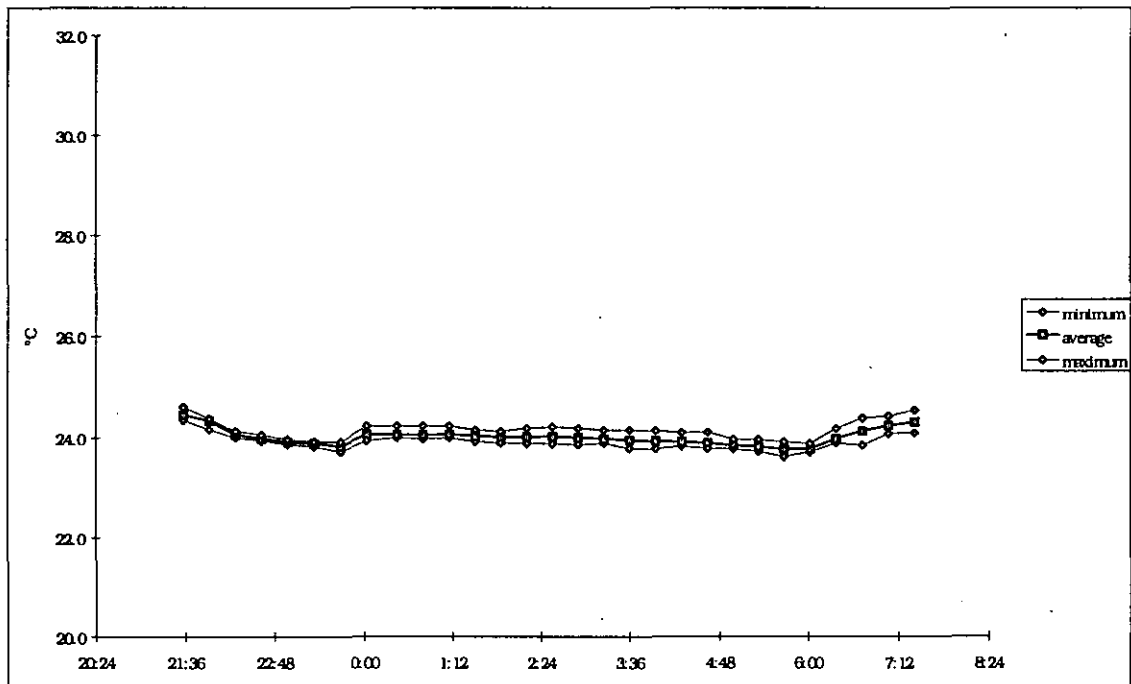


Figure A4.6.11: Range of temperatures measured in bedroom 2

- **Volumes:** $\pm 5\%$. (Parameters 5, 7, 9, 11, 13, 15, 17).

The apartment was not occupied. As a result the error caused by the furniture when calculating the volume was not very high: only the kitchen contained furniture. Nevertheless we took a standard deviation of $\pm 5\%$ for **each** room for the following reasons:

- * At the windows important errors can be made due to the recess (caused by the position of the window in the external wall).
- * The measurement equipment, the bath, the toilet... have a certain volume.

- **Discharge coefficient:** ± 0.05 . (Parameter 3).

This value was chosen to know the importance of a good knowledge of the discharge coefficient.

- **Injection rate of CO₂:** $\pm 10\%$. (Parameter 20).

The reason why such a high standard deviation is assumed for the injection rate is the fact that this value could not have been verified in detail. The value used for simulation has been calculated in 2 different ways and we found a value of about 14 ml/s. The problem is that we used other measurements to do this calculation, like the air flow through the ducts, the concentration in these ducts. The error on these measurements will enlarge the error on the injection rate.

- **Fresh air flow rate (= flow through fans):** $\pm 10\%$. (Parameters 21 to 25).

These values are determined by using the constant concentration method (with SF₆ as tracer gas). When one looks at the Figure A4.6.5 and Figure A4.6.6 (CO₂-concentration), it is clear that a good homogeneity cannot always be guaranteed. This has an important influence on the value of the fresh air supply.

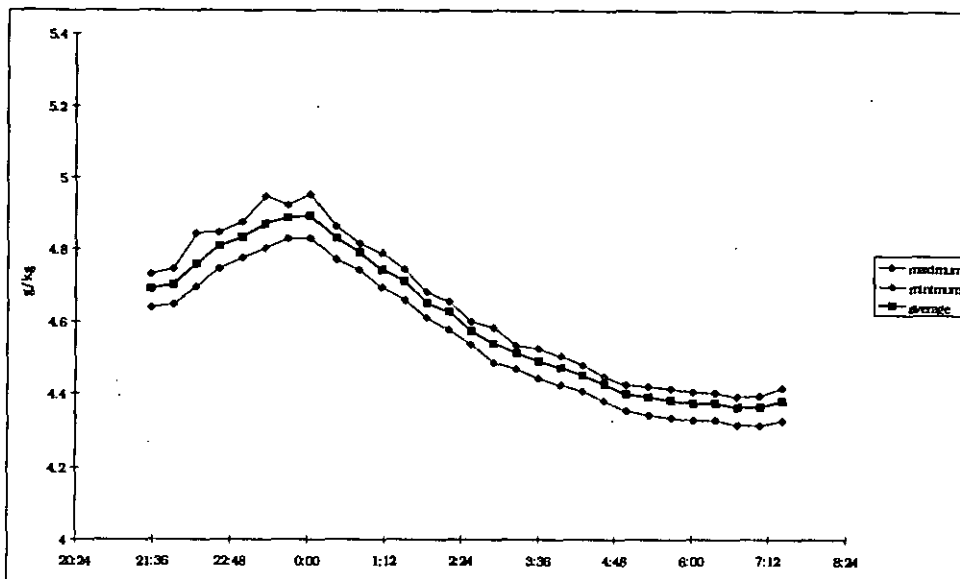


Figure A4.6.12: Range of absolute humidity measured in the living room.

● Humidity: ± 0.1 g/kg. (parameters 26 to 95).

At first impression this standard deviation seems to be too small. Nevertheless, when one looks at the absolute humidity in the different rooms before injection, it turns out that the differences between the rooms are smaller than 0.1 g/kg (except for bedroom 2 (0.2 g/kg), but the water to be injected is situated in that room). What is more, the homogeneity of the water vapour is a lot better than the homogeneity of the CO₂. In Figure A4.6.12 one can see that also the differences due to homogeneity are smaller than ± 0.1 g/kg. Due to the fact that only the difference in humidity between the rooms is important, this standard deviation is high enough. In other words, a systematic error on the measurement of the humidity will have no influence on the final result, since the measurement in each point is done by the same analyser.

Results of the Fractional Factorial Analysis.

There are 44 simulation points (time steps at which a simulation is done) and 7 different rooms. That means 308 (= 44 x 7) different relative effects are found for each of the 32 parameters. Some of the results are shown on the Figures A4.7.13 to A4.7.18:

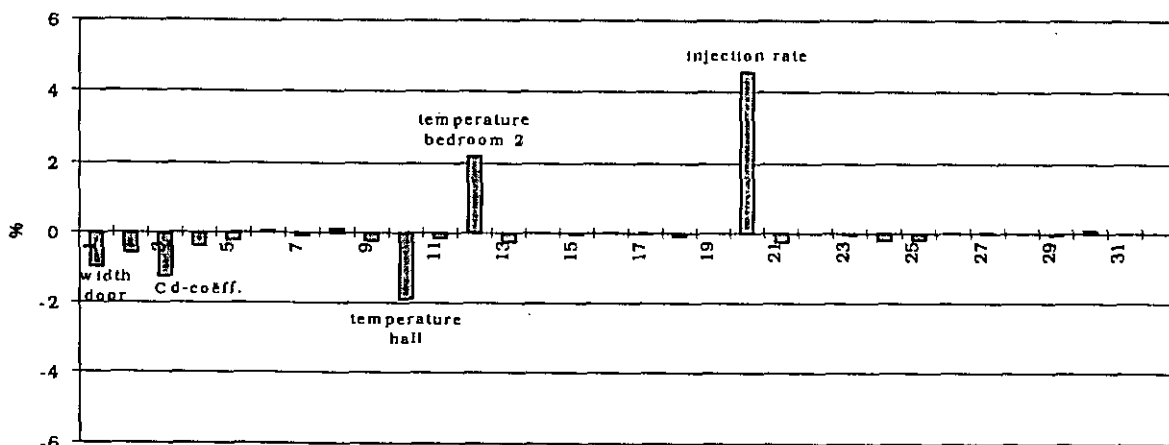


Figure A4.6.13: Main effects for the CO₂-concentration in bedroom 2 at 23h00. DOORS OPEN.

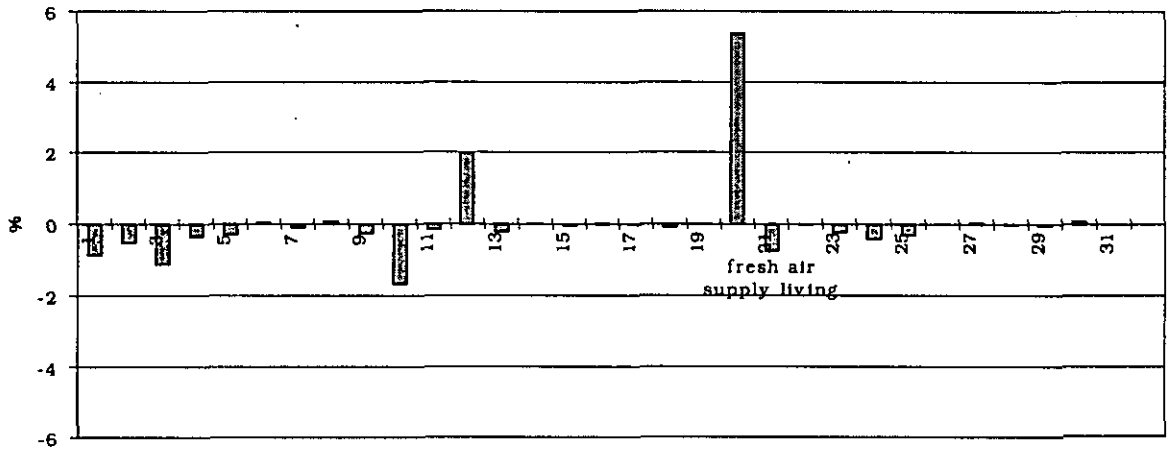


Figure A4.6.14: Main effects for the CO₂-concentration in bedroom 2 at 0h00. DOORS OPEN.

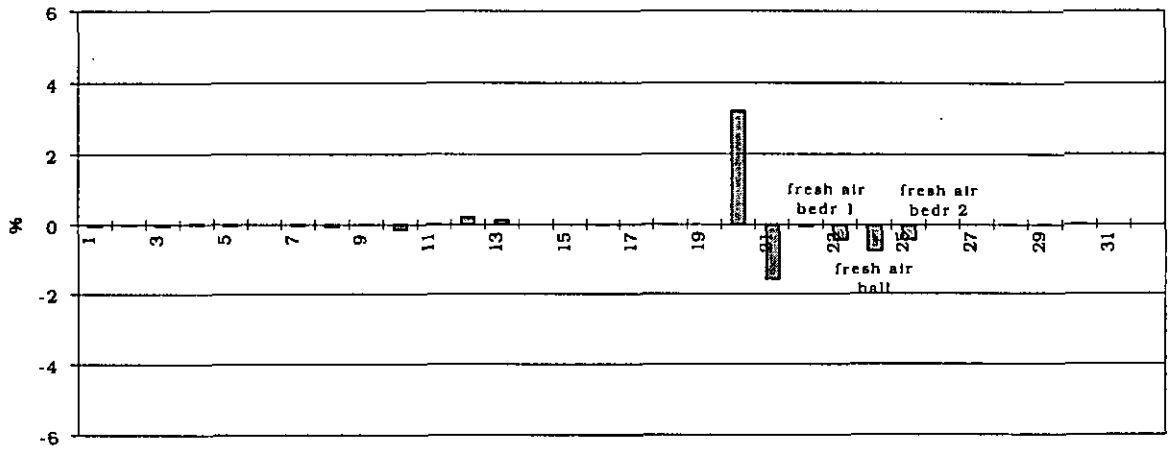


Figure A4.6.15: Main effects for the CO₂-concentration in bedroom 2 at 01h00. DOORS OPEN.

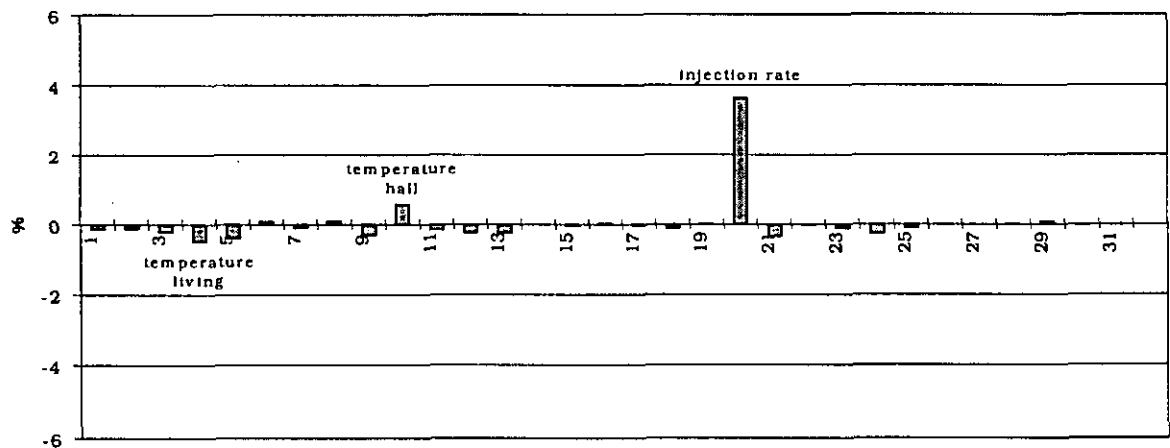


Figure A4.6.16: Main effects for the CO₂-concentration in the hall at 23h00. DOORS OPEN.

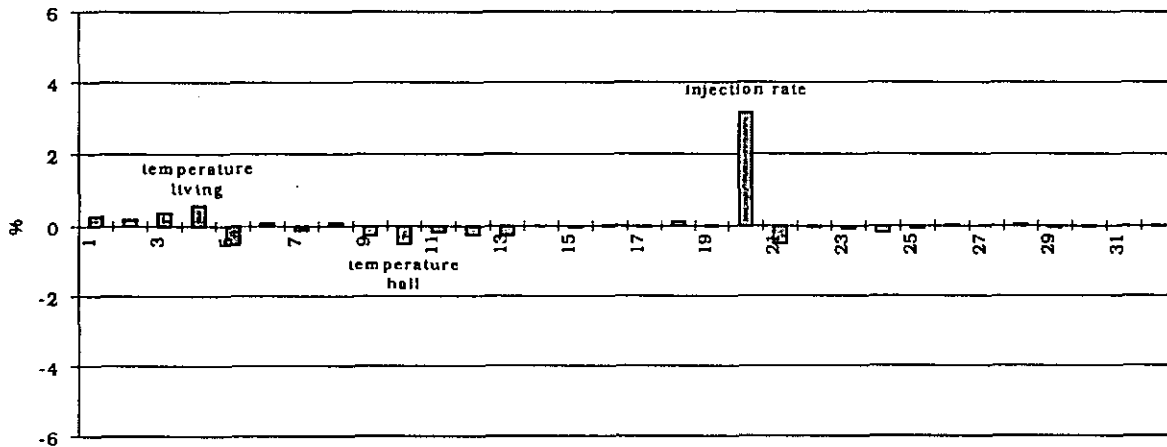


Figure A4.6.17: Main effects for the CO_2 -concentration in the living room at 23h00. DOORS OPEN.

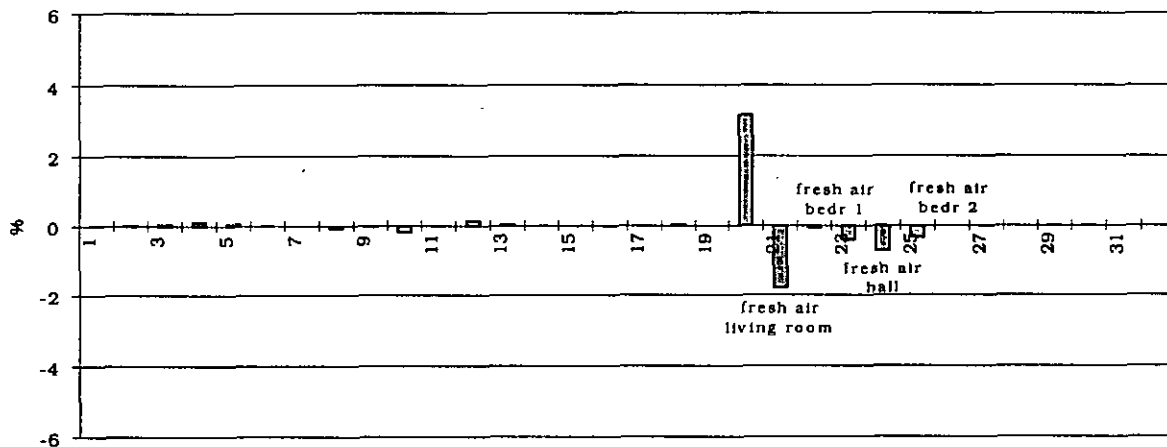


Figure A4.6.18: Main effects for the CO_2 -concentration in the living room at 01h00. DOORS OPEN.

Which conclusions can be drawn out of these figures ?

1. The concentration in the injection room during injection (from 22h00 to 00h00) is mainly determined by the injection rate, the temperature difference between bedroom 2 and the hall and the characteristics of the door between both rooms (width, height, C_d -coeff.). When injection of the CO_2 stops (at 0h00), the impact of the fan speed in each room (=fresh air supply) on the final result is increasing, while the effect of the door dimensions and the temperature difference is becoming negligible.

Explanation of the bar-charts: e.g. in Figure A4.6.13:

- For the injection rate one can see an effect of approx. +4.5 % at 23h00. The confidence interval for this injection rate is ± 10 %. So, one can say that **overestimating** the injection rate by 10 % has as an effect that the concentration in the room at 23h00 will be 4.5 % **higher**.
- The temperature in the hall has an effect of approx. -2 % at 23h00. This means that taking the **upper** value for this temperature in the range file will give a **decrease** of the concentration in bedroom 2 with 2 % at 23h00. The minus-sign means that a high input value will give a lower result. This is logical in this case because a higher temperature in the hall

means a higher temperature difference between the rooms and thus a higher double-flow (= a better mixing) and as a result a lower concentration in the injection room.

2. The concentrations in the other rooms are mainly determined by the injection rate and after injection also by the fresh air supplies.
3. The effects vary a lot in function of the time: e.g. the effect of parameter 12 (=temperature in bedroom 2), see Figure A4.6.19. The temperature difference between the 2 rooms has mainly an effect on the concentration in bedroom 2 when there is a concentration difference between the 2 rooms. This difference in concentration is fluctuating in time (see Figure A4.6.20) and as a result the effect of the temperature in bedroom 2 will vary in nearly the same way (Figure A4.6.19)
- 4) It has to be mentioned that the effects 1, 2 and 3 are combined effects of changing these value

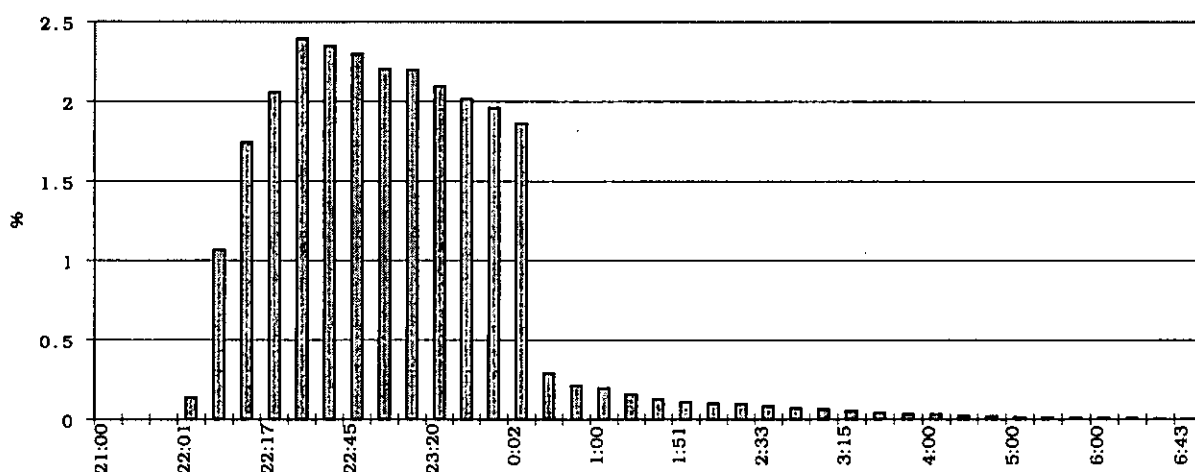


Figure A4.6.19: Variation of the effect of the temperature in bedroom 2 on the CO₂-concentration. DOORS OPEN.

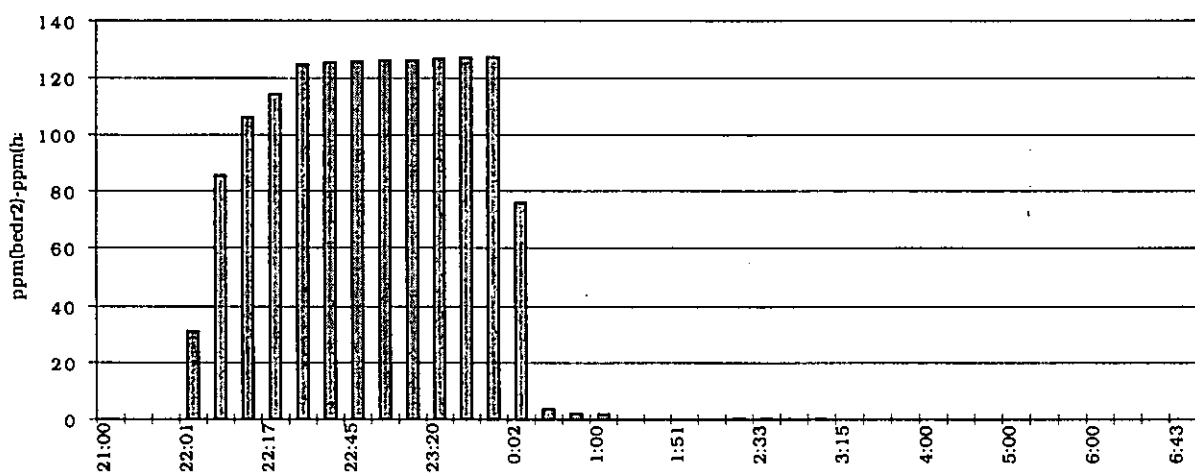


Figure A4.6.20: Difference in CO₂-concentration between bedroom 2 and the hall, simulation.

Results of the Monte Carlo Analysis.

A Monte Carlo Analysis was performed with 100 runs. The average and the 95%-interval of the 100 obtained results were calculated for each room. In the Figure A.4.7.21, the result of the simulation is shown for the injection room, this is bedroom 2. The 95% interval is presented by the error bars. The error on the measurement of the concentration is supposed to be 5%, due to incomplete homogeneity. All CO₂-concentrations, even the external value, were measured with the same analyser.

It is important to mention that the average line of Figure A4.6.22 and the simulation line of Figure A4.6.21 are exactly the same. The reason why it doesn't seem to be so is that in Figure A4.6.21 only the simulation results are given for the moments on which there are also measurement results, thus making the comparison between measurement and simulation possible. By doing this the simulation value at 0.00h is missing in Figure A4.6.21, and is only given at 0.02h. This explains the different shapes between Figure A4.6.21 and Figure A4.6.22.

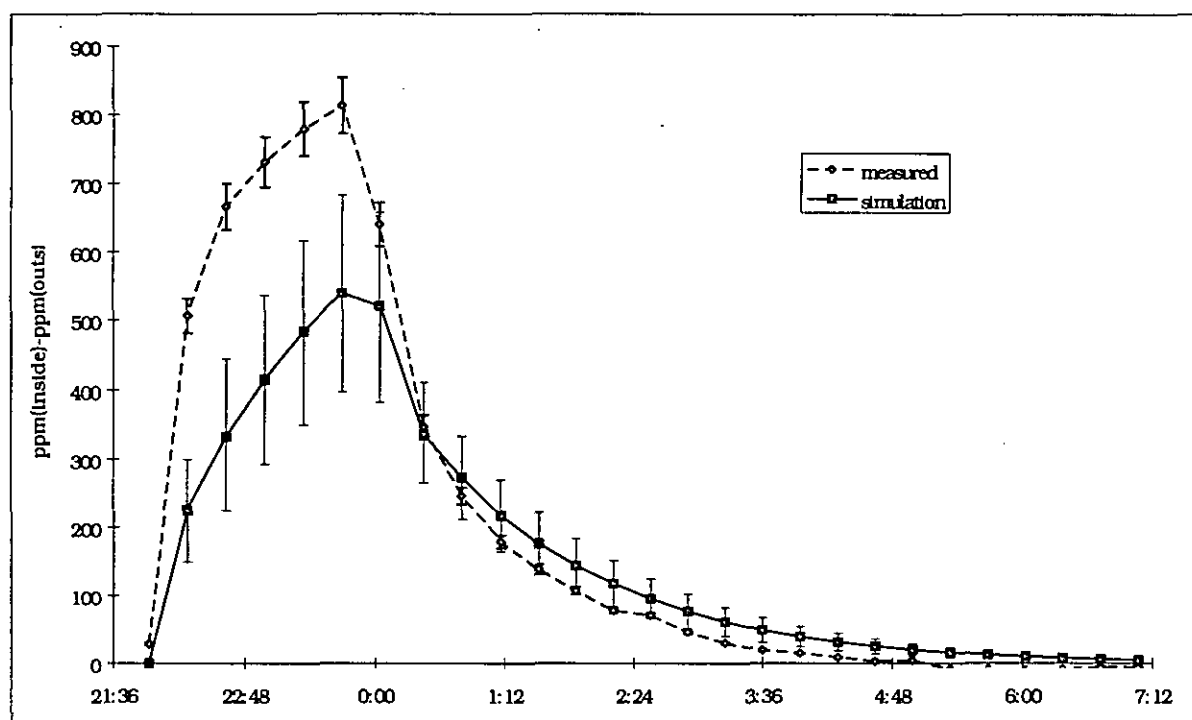


Figure A4.6.21: CO₂ concentration in bedroom 2: simulated and measured. DOORS OPEN.

One can see that during the injection the simulated concentration is a lot smaller than the measured concentration. The explanation for this is given in what follows.

When one compares the position of the 95% interval with the position of the minimum and maximum values, it is clear that the distribution of the final result is not normal. But it is just the line of the maximum values that has a good agreement with the measurements.

There must be a parameter with a wrong value. Which one ?

Due to the fact that there is only a big difference during the injection, the most logical possibilities are the injection rate and the temperature difference (indeed, looking at Figure A4.6.13 up to Figure A4.6.18, one can see that only these parameters have an important influence during injection).

For the other rooms (Figure A4.6.23 to Figure A4.6.26) the level of agreement is much better. In Figure A4.6.13 up to Figure A4.6.18 one can see that the injection rate has a high effect on

the concentration in all the rooms, on the other hand the temperature difference has only an important influence on the result for bedroom 2. Indeed, by changing the injection rate the similarity should become better for the injection room, but worse for the other rooms. One can conclude that the difference is mainly caused by a wrong value for the temperature difference between hall and bedroom 2.

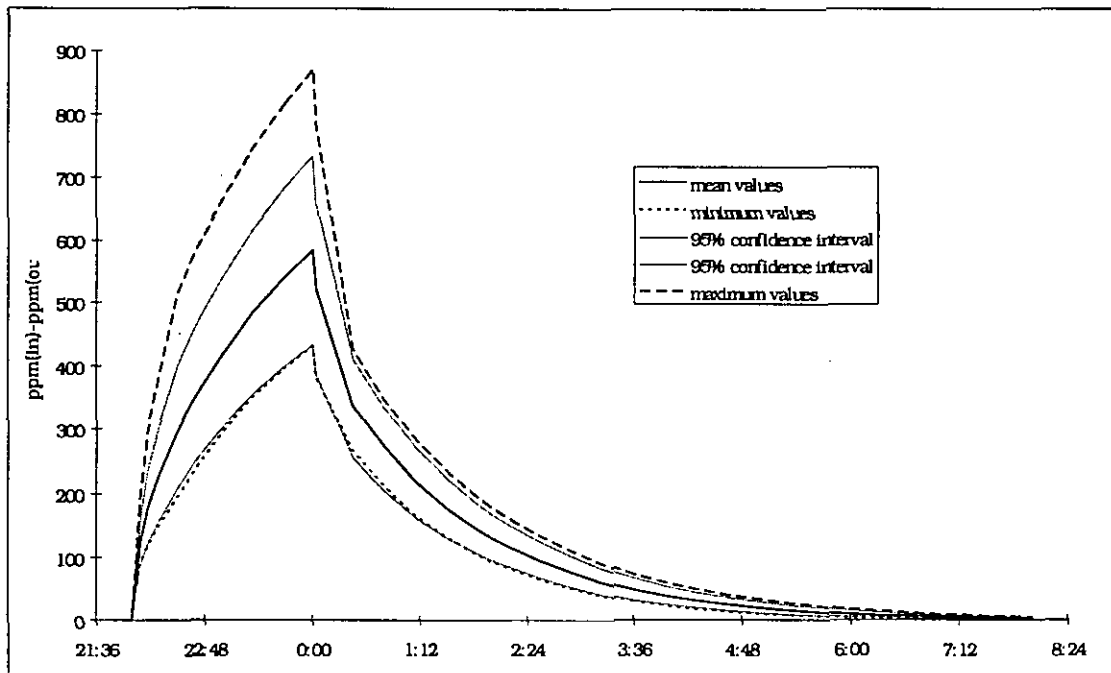


Figure A4.6.22: CO₂-concentrations in bedroom 2, significant values of the Monte Carlo Analysis. DOORS OPEN.

This can be illustrated by looking at the temperatures for the runs which give high concentrations (at 0.00h):

Table A4.6.4: Some of the simulation runs examined more in detail.

Number of runs	Concentration difference between bedroom 2 and outside	Multiplication factor temperature hall	Multiplication factor temperature bedroom 2	Temperature difference
40	750 ppm	-0.76	2.00	0.42 °C
53	783 ppm	-1.76	1.17	0.30 °C
82	868 ppm	-1.48	1.44	0.34 °C

The average temperature difference between hall and bedroom 2 is 1.8 °C.

- Temperature hall: 25.8 °C ± 0.5 °C
- Average temperature bedroom 2: 24.0 °C ± 0.5 °C

The multiplication factor is the value in the design file with which the standard deviation of a parameter is multiplied. In this case the standard deviation is 0.5°C.

The three concentrations in the table are all higher than the upper border of the confidence interval (95 %) of the simulation result (= 733 ppm), and in the three cases the temperature difference between the hall and bedroom 2 is very small. From the literature, [van der Maas, 1992], one can see that the mass flow through a large opening is nearly proportional with the square root of the temperature difference. A low difference will cause a low two-way flow through the door and as a result the injected CO₂ won't leave the injection room so easily.

The fact that the concentration is very high for run 82 has to do with the combination of small temperature difference and high injection rate (multiplication factor for the injection = 1.56).

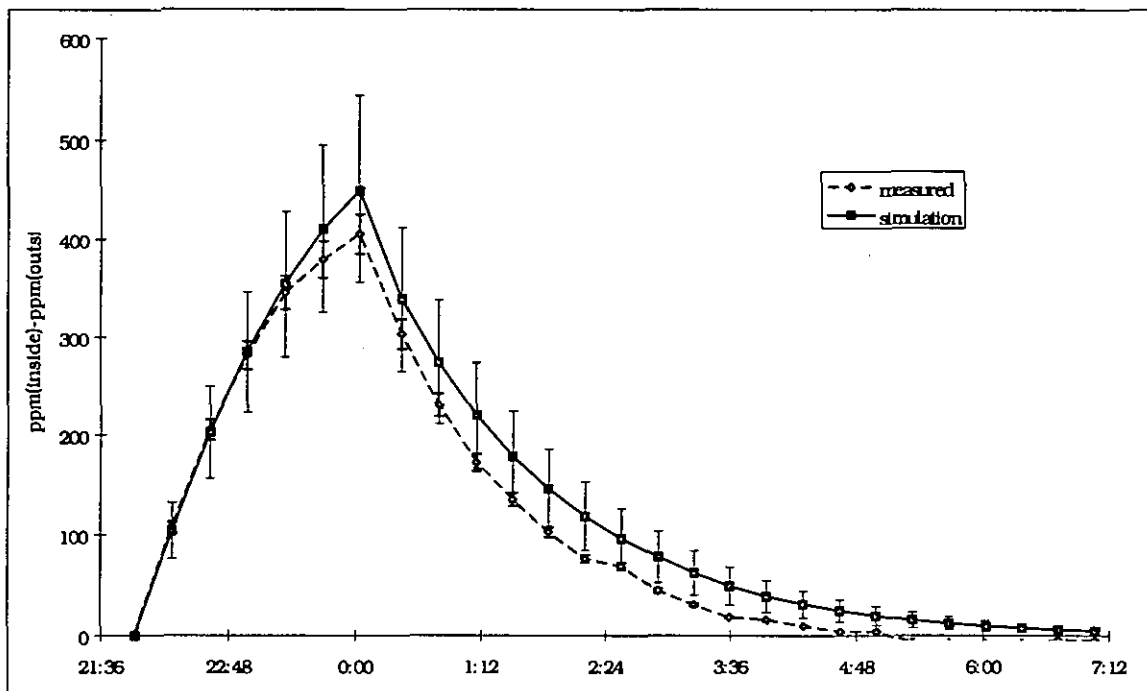


Figure A4.6.23: CO₂-concentration in toilet, simulated and measured. DOORS OPEN.

These findings confront us with the difficulty of choosing a good room temperature. In other words, is the average room temperature a representative value to describe the flows through large openings? A lot depends on where the different temperatures are measured. One can wonder if it wouldn't be better to measure the temperatures in the lower and the upper part of the opening and use these values as 'room' temperatures. Unfortunately, these temperatures were not measured in this case, so this proposition can't be tested.

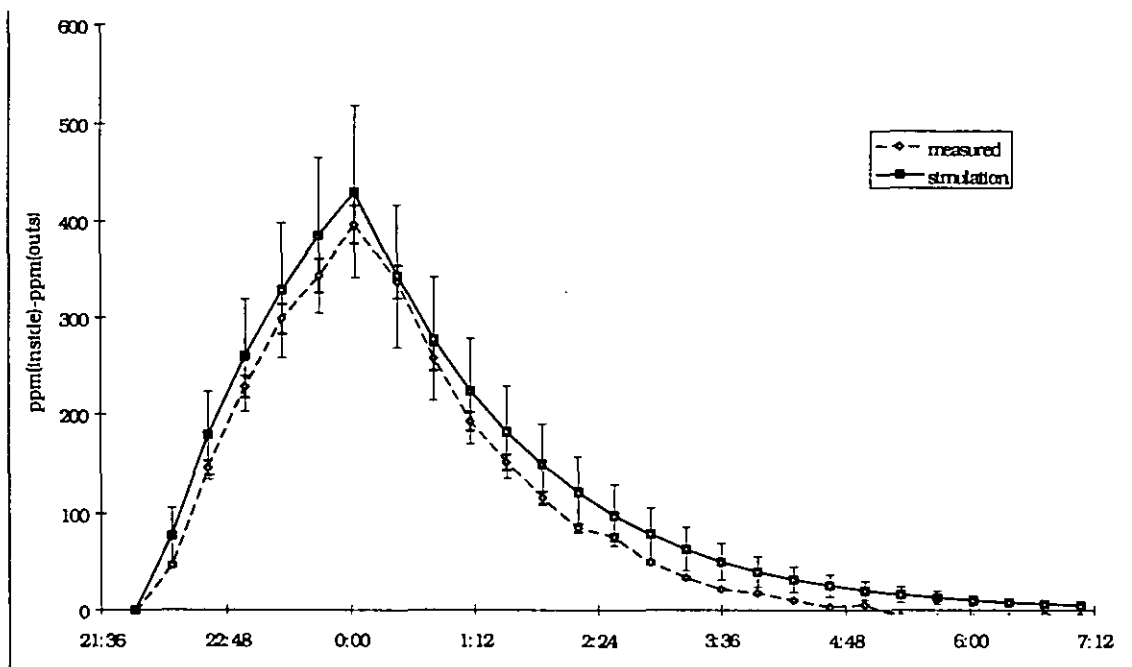


Figure A4.6.24: CO₂-concentration in bedroom 1, simulated and measured. DOORS OPEN.

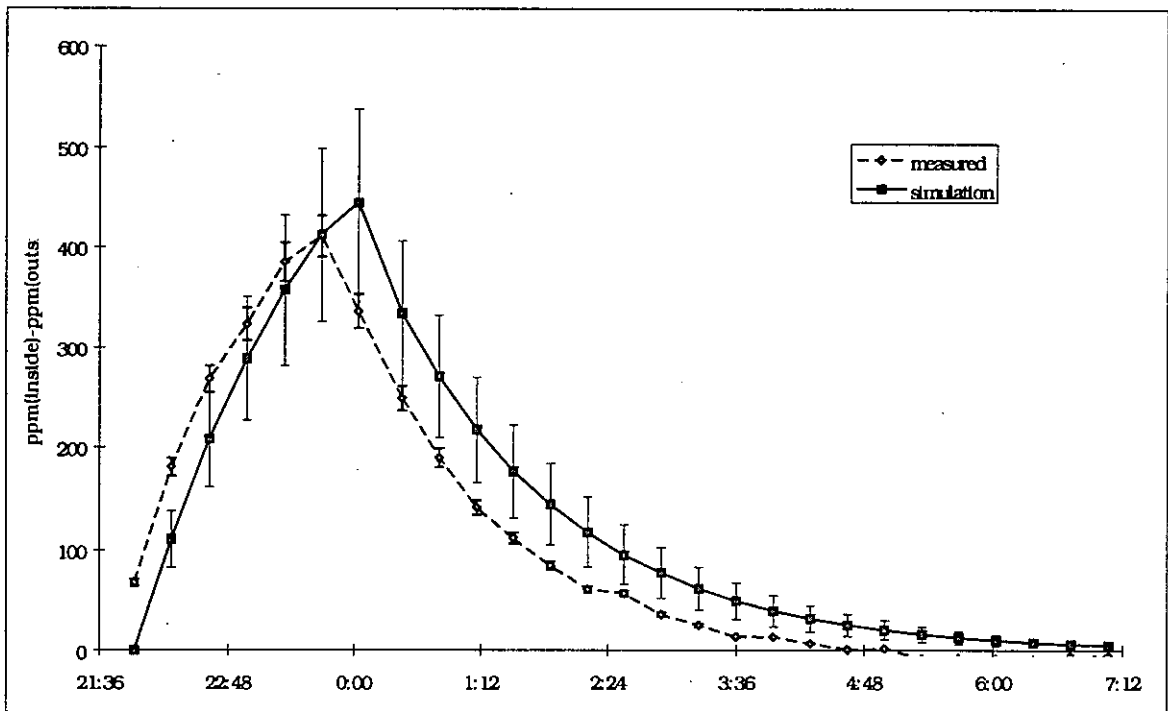


Figure A4.6.25: CO₂-concentration in the hall, simulated and measured. DOORS OPEN.

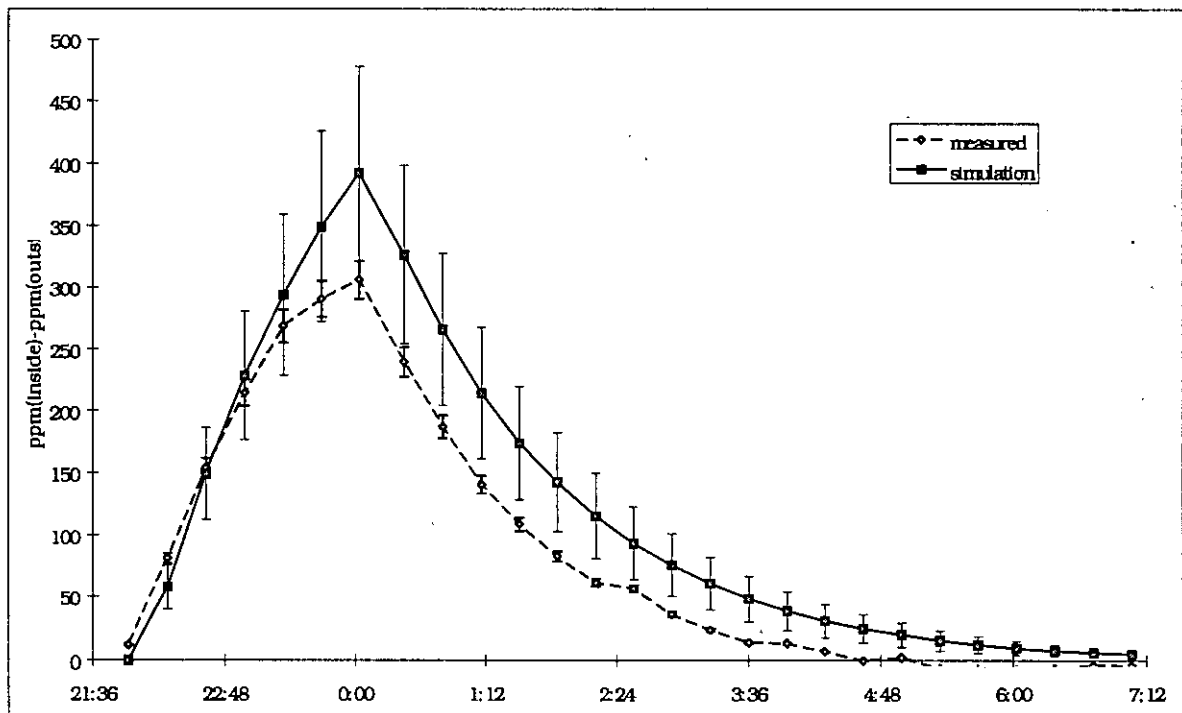


Figure A4.6.26: CO₂-concentration in the living room, simulated and measured. DOORS OPEN.

Results of a second Fractional Factorial analysis with inside doors open.

When the temperature difference becomes smaller, the effect of the temperatures on the final result will be much higher than these found in Figure A4.6.13 to Figure A4.6.15. This can be shown by doing a new sensitivity analysis with slightly modified ranges for the temperatures in hall and bedroom 2. Other (more representative ?) values were chosen for the hall and bed-

room 2, namely the temperatures measured nearest to the door in the middle of the total height.

The values are: - temperature hall: 25.5 °C
 - temperature bedroom 2: 24.1 °C

Instead of a standard deviation of 0.5 °C, a value of 0.7 °C is taken for these 2 rooms and also for bedroom 1. In this way the case of nearly equal temperatures will be included more frequently in the Monte Carlo analysis and the effect of this phenomenon will be visual in one of the effects of the first order, found with the Fractional Factorial analysis (see Figure A4.6.34). A summary of the differences between the two simulations is shown in Table A4.6.5. In the following Figures some results of the performed sensitivity analysis in case 2 are shown.

Table A4.6.5: Differences between the two simulations.

Type	CASE 1	CASE 2
Temperature hall	25.8 °C ± 0.5 °C	25.5 °C ± 0.7 °C
Temperature bedroom 2	24.0 °C ± 0.5 °C	24.1 °C ± 0.7 °C
Temperature bedroom 1	24.1 °C ± 0.5 °C	24.1 °C ± 0.7 °C

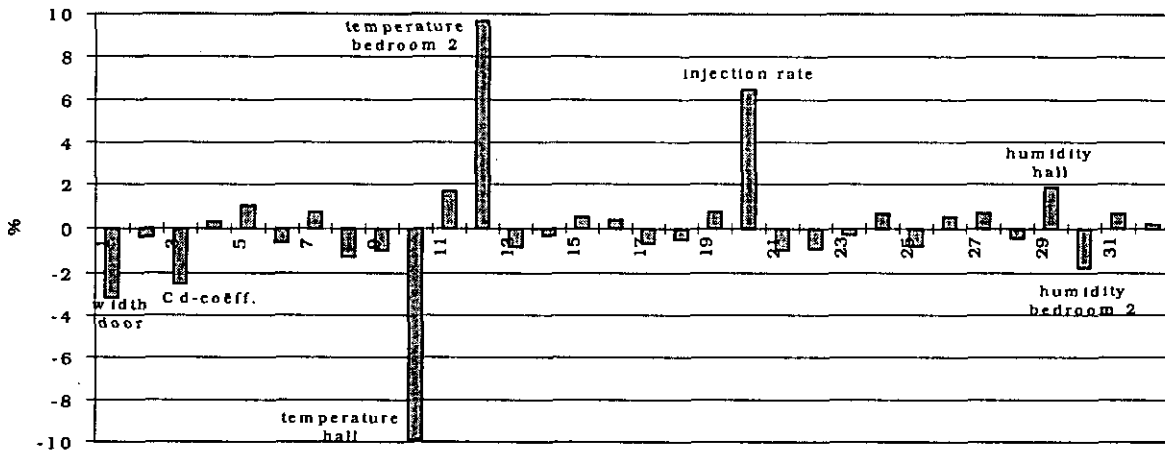


Figure A4.6.27: Main effects for the CO₂-concentration in bedroom 2 at 23h00. DOORS OPEN, CASE 2.

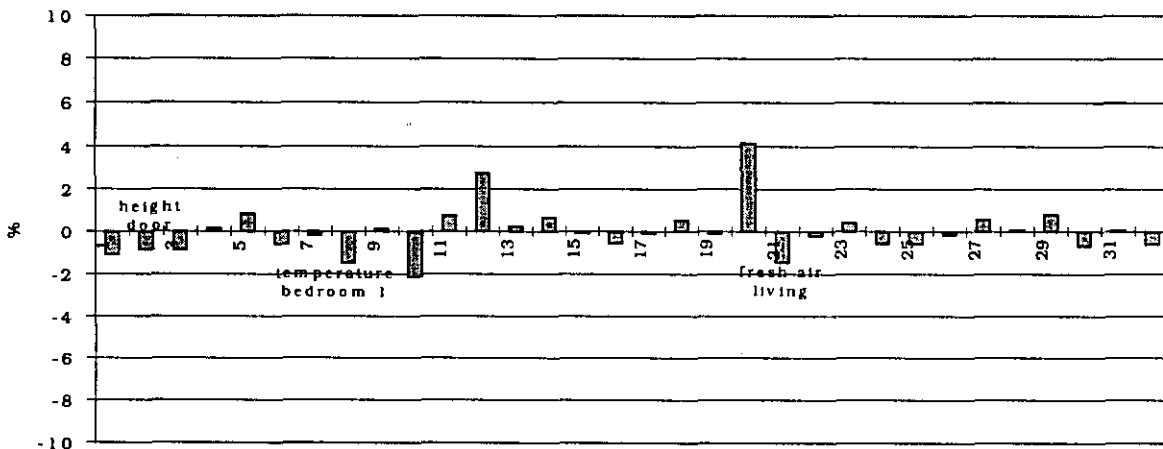


Figure A4.6.28: Main effects for the CO₂-concentration in bedroom 2 at 01h00. DOORS OPEN, CASE 2.

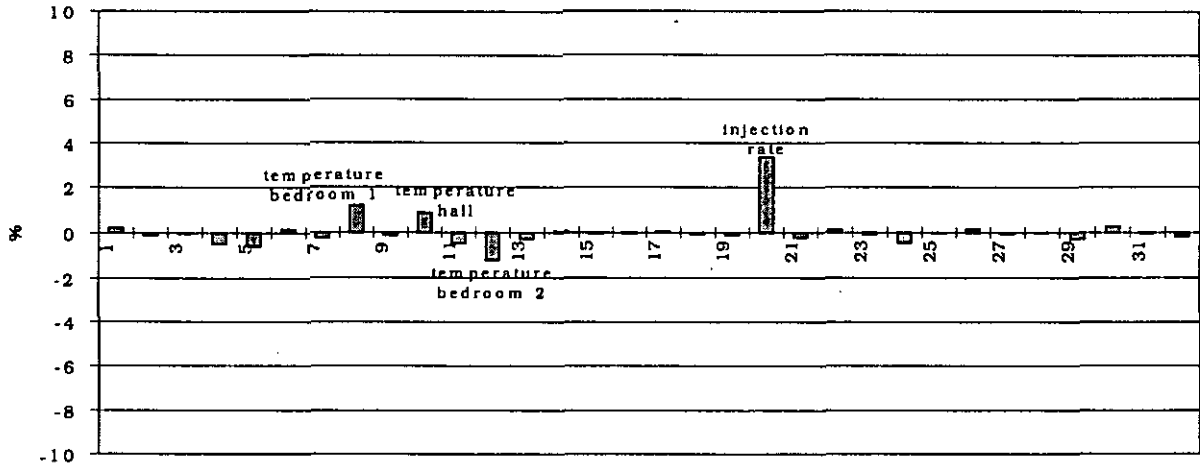


Figure A4.6.29: Main effects for the CO₂-concentration in the hall at 23h00. DOORS OPEN, CASE 2.

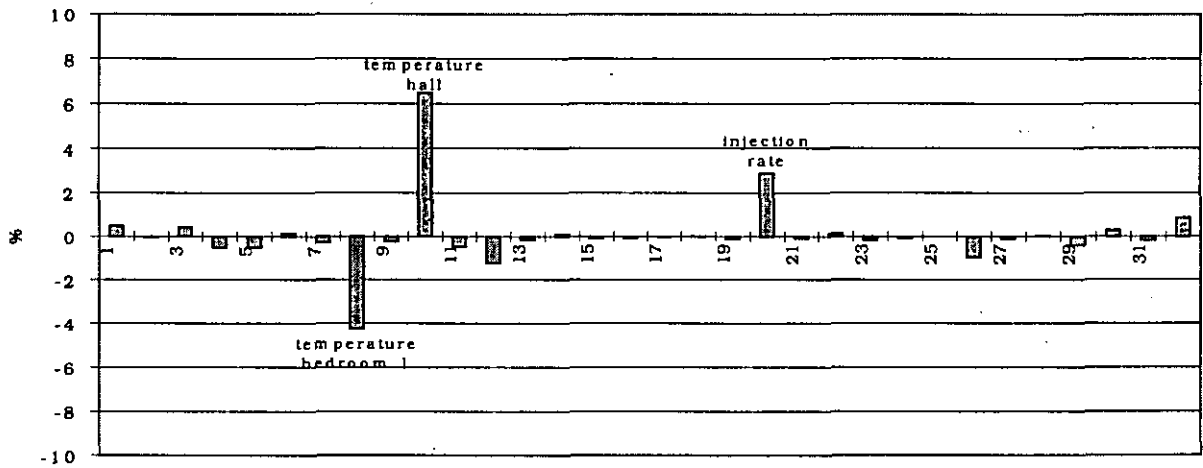


Figure A4.6.30: Main effects for the CO₂-concentration in bedroom 1 at 23h00. DOORS OPEN, CASE 2.

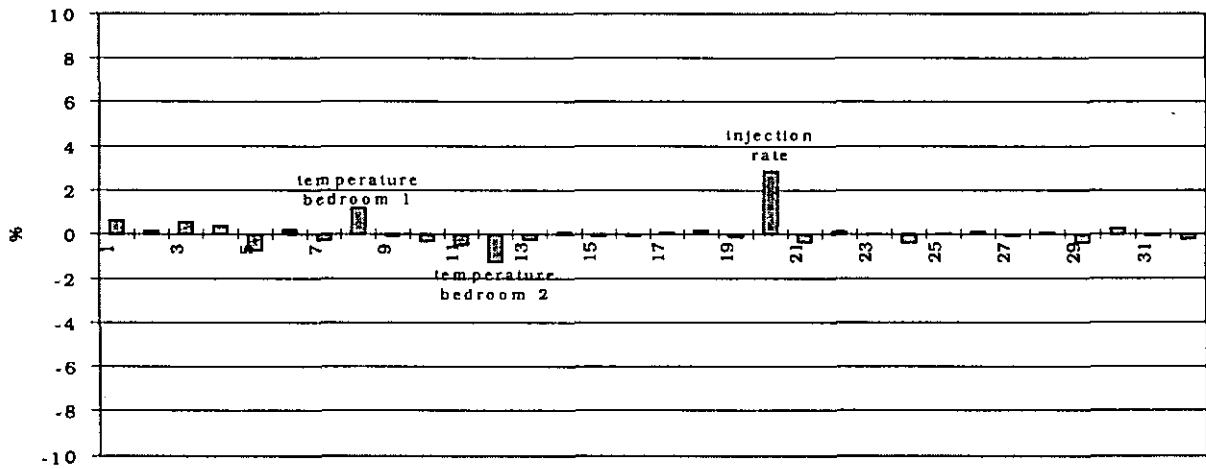


Figure A4.6.31: Main effects for the CO₂-concentration in living room at 23h00. DOORS OPEN, CASE 2.

Remarks for the different figures:

As one can see, the effect of the temperature difference between hall and bedroom 2 has become very important for the concentration in bedroom 2 during the injection period. From $\pm 2\%$ using the first range (Figure A4.6.13) to $\pm 10\%$ using the second range (Figure A4.6.27). In range 1 the smallest temperature difference to calculate the main effects is $1.3\text{ }^{\circ}\text{C}$ (maximum temperature in bedroom 2 and average in the hall, average temperature in bedroom 2 and minimum in hall), in range 2 it comes to $0.7\text{ }^{\circ}\text{C}$.

It is clear that, when the temperature difference has a value nearby $0\text{ }^{\circ}\text{C}$, a small error on this value has an important influence on the final result. The larger the temperature difference, the smaller the influence of an error on the result.

It is important to mention that the sensitivity analysis performed here, gives rather extreme results. Nevertheless, these results are important to clarify the problems with which one has to deal during measurements and sensitivity analysis.

The effect of the temperature difference is also important in bedroom 2. But, where in bedroom 2 the concentration the effects were the same for the two temperatures, in bedroom 1 this is not the case (see Figure A4.6.30). The effect of the temperature in the hall is higher because the concentration in bedroom 1 is dependent upon the concentration in the hall which is determined by the double flow (and thus the temperature difference) through each of the 5 hall-doors. Taking another temperature for bedroom 1 will not have such an important effect because only the double flow through the door of bedroom 1 will change significantly, and thus the concentration in the hall will change less.

Furthermore one notices in Figure A4.6.27 that the humidity in both rooms also has an effect on the final result. What's more, this effect is important taking into account that the standard deviation has been taken $\pm 2\%$ and that the effect on the concentration is also about 2% (comparatively speaking the effect is even more important than the effect of the injection rate, for which an uncertainty of 10% gives an effect of 'only' 6%).

It is very important to take into account the flow caused by the difference in humidity, especially when the temperature differences are small !

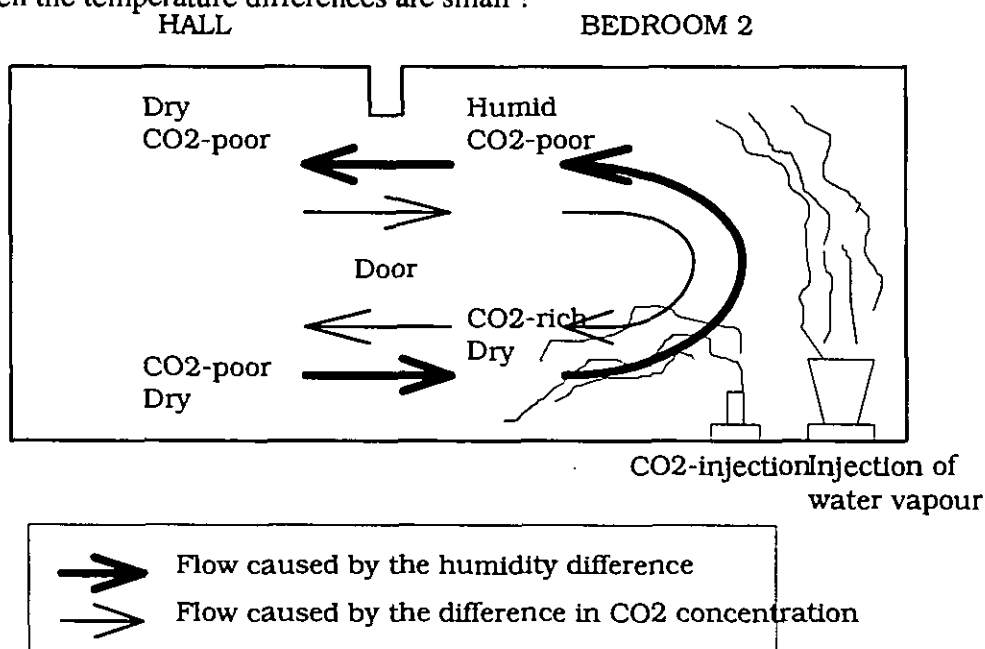


Figure A4.6.32: Representation of the air flows caused by concentration differences.

When the temperature difference is very small or equal to 0, the air flow through the door is mainly caused by the concentration difference of CO₂ and water vapour between the two rooms. Due to the fact that humid air is lighter than dry air, and CO₂-rich air is heavier than CO₂-poor air, the two double flows will oppose each other.

What is the size of these flows ?

- *The flow caused by the water vapour:* As one can see in Figure A4.6.9 the difference in humidity at 23h00 is about 1 g/kg. The difference in density is thus 0.0007 kg/m³. 1 °C temperature difference corresponds to a difference in density of about 0.0033 kg/m³ (at about 0 °C). Accordingly, the effect of the difference in water vapour is the same as a temperature difference of about 0.20 °C.
- *The flow caused by the CO₂:* The difference in CO₂-concentration at 23h00 is about 125 ppm (= 0.2 g/kg). This corresponds to a temperature difference of 0.05 °C.

Together the flows, due to concentration differences, correspond to the flow by a temperature difference of 0.15 °C.

It is also clear that some of the effects of the first order will be important for this second case.

These first order effects are confounded with other effects of the first order. Each bar in the figure is a combination of 16 effects of the first order. Nevertheless, when one reasons logically it is possible to determine which effects of the first order are important and which are not important.

In Figure A4.6.34 one can see that some of the effects of the first order are very important. The list giving which effects of the first order are confounded with each other can be found in [Fürbringer, 1994].

- α_{41} : Here the most important effects of the first order are probably the combined effect of α_1 (= width of the door) and α_{10} (= temperature of the hall) and the combined effect of α_{12} (= temperature in bedroom 2) and α_{20} (=injection rate).
- α_{43} : α_1 (= width of the door) and α_{12} (= temperature in bedroom 2);
 α_{10} (= temperature of the hall) and α_{20} (=injection rate).
- α_{51} : It is almost certain that the most important part of this value is caused by the effect of the first order which is the combination of α_{10} (temperature hall) and α_{12} (temperature bedroom 2) and also by the effect of the first order which is the combination of α_1 (width of the door) and α_{20} (injection rate).
- α_{50} , α_{52} , α_{53} and α_{55} are mainly the effects of the first order caused by a combination of a temperature and a humidity.

In Figure A4.6.33 one can see that the effects of the first order are almost all negligible for the Fractional Factorial Analysis performed with the first range. Nevertheless the only differences between the two ranges are the values of 3 temperatures (hall and two bedrooms). It is clear that a good knowledge of the temperatures means everything.



Figure A4.6.33: Effects of the first order for the CO_2 -concentration in bedroom 2 at 23h00. DOORS OPEN, CASE 1.

From this, one can deduce for range 2 that α_{51} is mainly a combined effect of the two temperatures, because for range 1 α_{51} is very small and the combined effect of α_1 (width of the door) and α_{20} (injection rate) is the same for the two ranges since the injection rate or the width of the door were not changed. The high value for this effect of the first order confirms what was already said before, namely that the influence of an identical error on the temperatures becomes more important as the temperature difference reduces.

In the first sensitivity analysis the minimal temperature difference between the two rooms was $0.8\text{ }^\circ\text{C}$, in this case it is $0\text{ }^\circ\text{C}$. The maximal temperature difference is $2.8\text{ }^\circ\text{C}$ in both cases.

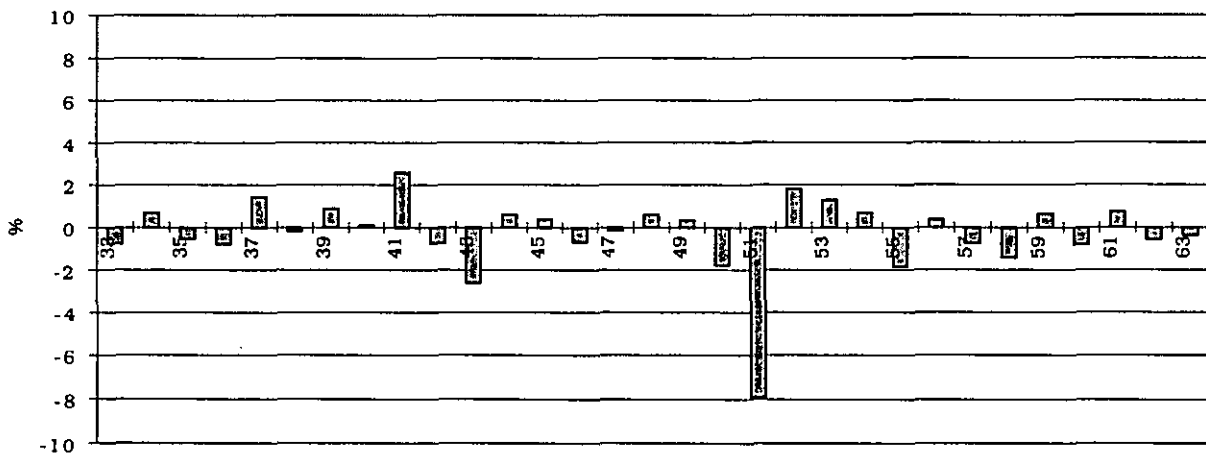


Figure A4.6.34: Effects of the first order for the CO_2 -concentration in bedroom 2 at 23h00. DOORS OPEN, CASE 2.

Results of a second Monte Carlo Analysis for the situation with the inside doors open.

This Monte Carlo Analysis is performed with the same range file as the second Fractional Factorial Analysis. In other words, the only differences from the first Monte Carlo Analysis are three temperatures in the range file (see table in 4.6.4).

In the following figures some results are shown of the Monte Carlo Analysis with this second range file (= case 2).

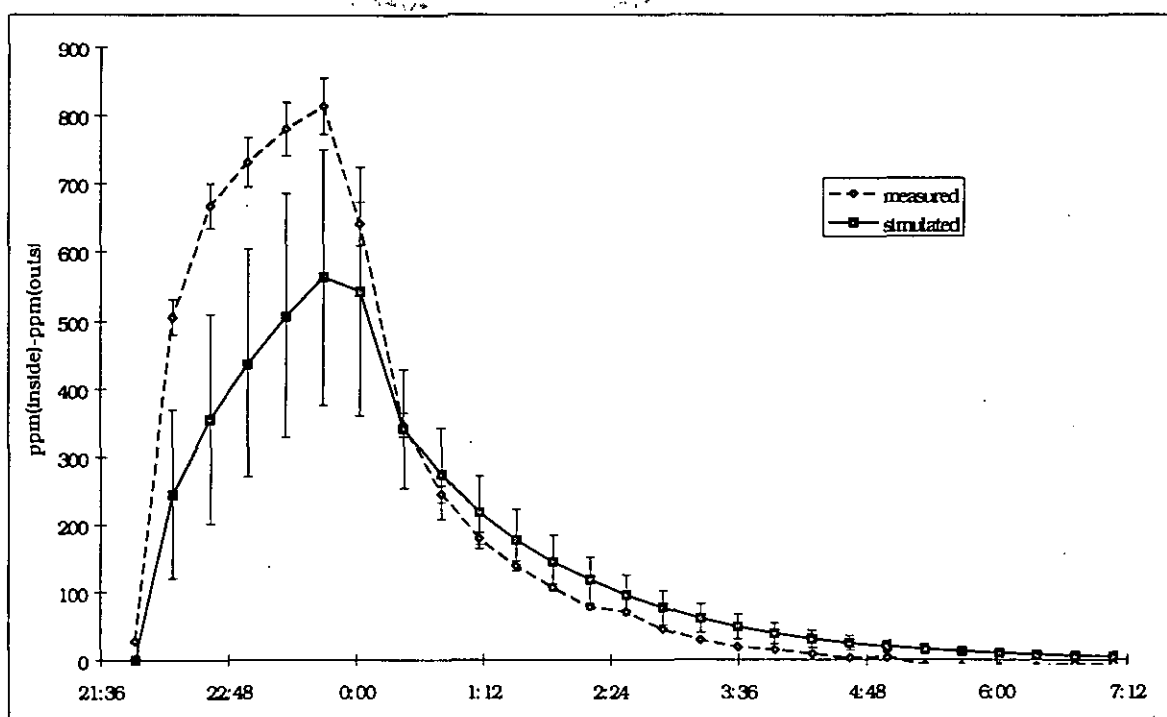


Figure A4.6.35: CO₂-concentration in bedroom 2: simulated and measured. DOORS OPEN, CASE 2.

The measured results are still much higher than the simulated ones. Nevertheless, if one compares this figure with Figure A4.6.21 (= same figure for range 1), one notices that the error bars (95%-interval) became bigger for the last case. And in comparison with Figure A4.6.22 the maximum values on Figure A4.6.36 are much higher.

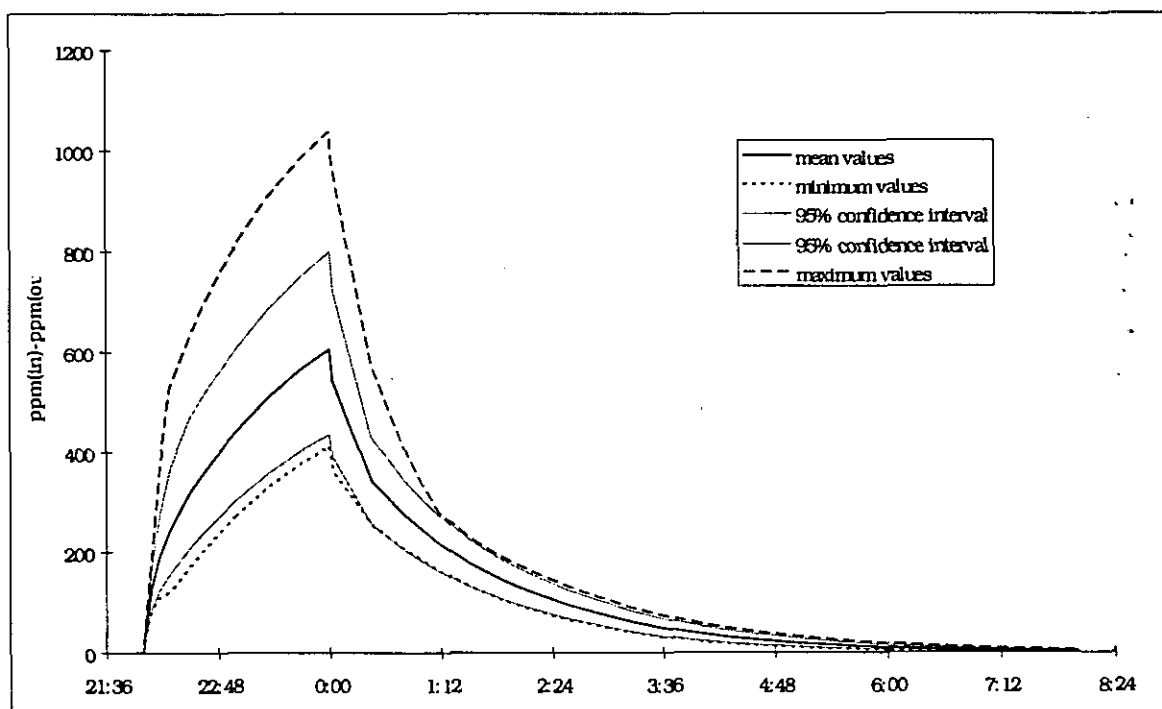


Figure A4.6.36: CO₂-concentration in bedroom 2: significant values of the Monte Carlo Analysis. DOORS OPEN, CASE 2.

However, the problem remains the same: the measured results are not situated between the 95%-borders of the simulation. In other words, probably we will have to change the average values of the temperatures instead of the ranges of uncertainty to find simulation results that satisfy. This is caused by the fact that the distribution is not normal.

One could think that the origin of the problem is the uncertainty on the measurement of the concentrations.

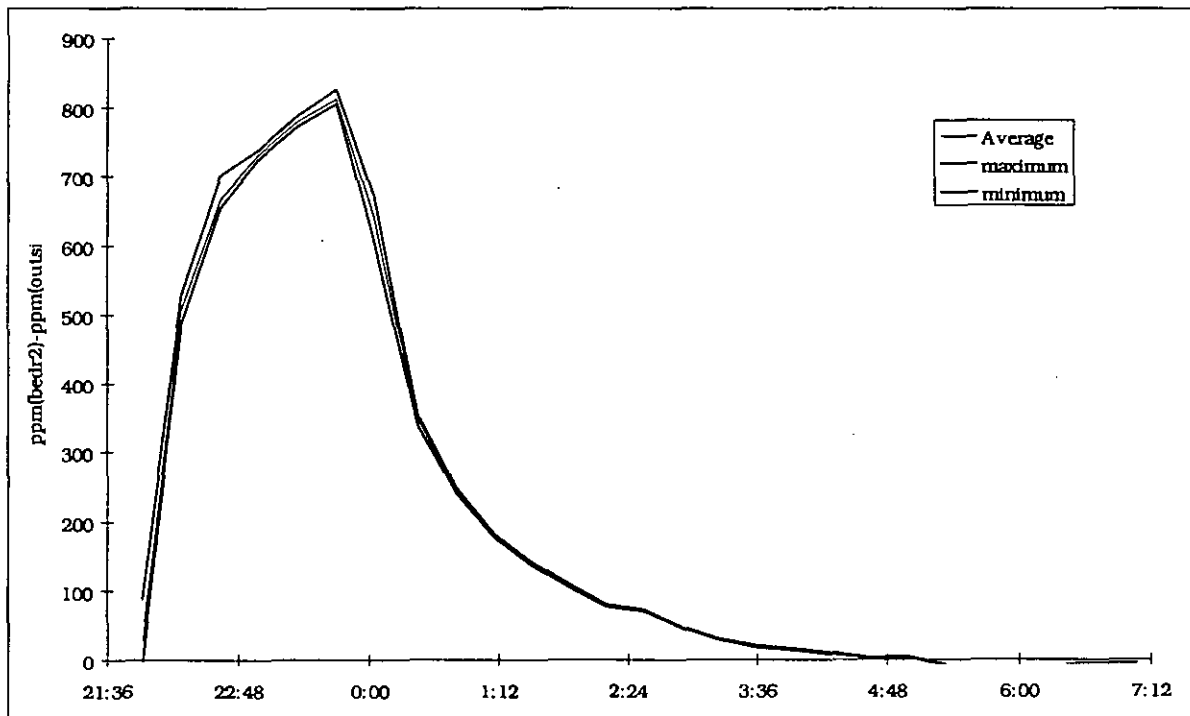


Figure A4.6.37: CO₂-concentration in bedroom 2: range of measured values.

It is clear that there is nearly no problem of homogeneity (see Figure A4.6.37) and as a result the error bars for the measurements (= error of 5%) are more than large enough.

The results for the other rooms are shown in Figures 4.7.38 and 4.7.39. Comparing Figure A4.6.38 with Figure A4.6.25, one can see that there is almost no difference between both figures. If there is no difference for the concentration in the hall, there will certainly be no difference for the other rooms, except maybe for bedroom 1, where the range of the temperature was taken a bit larger.

Finally, the importance of a good choice (or in other words, a good knowledge) of the different 'room'-temperatures in the apartment to perform the simulation, is shown once more in Figure A4.6.39. It is shown in this Figure that a simulation with real temperature difference gives a much smaller CO₂ concentration than a simulation with a very small temperature difference of 0.05 °C between the rooms. It is clear that it is not relevant to simplify the simulation by taking a uniform temperature for the whole apartment, if there are temperature differences between the rooms, even when these differences are not very high.

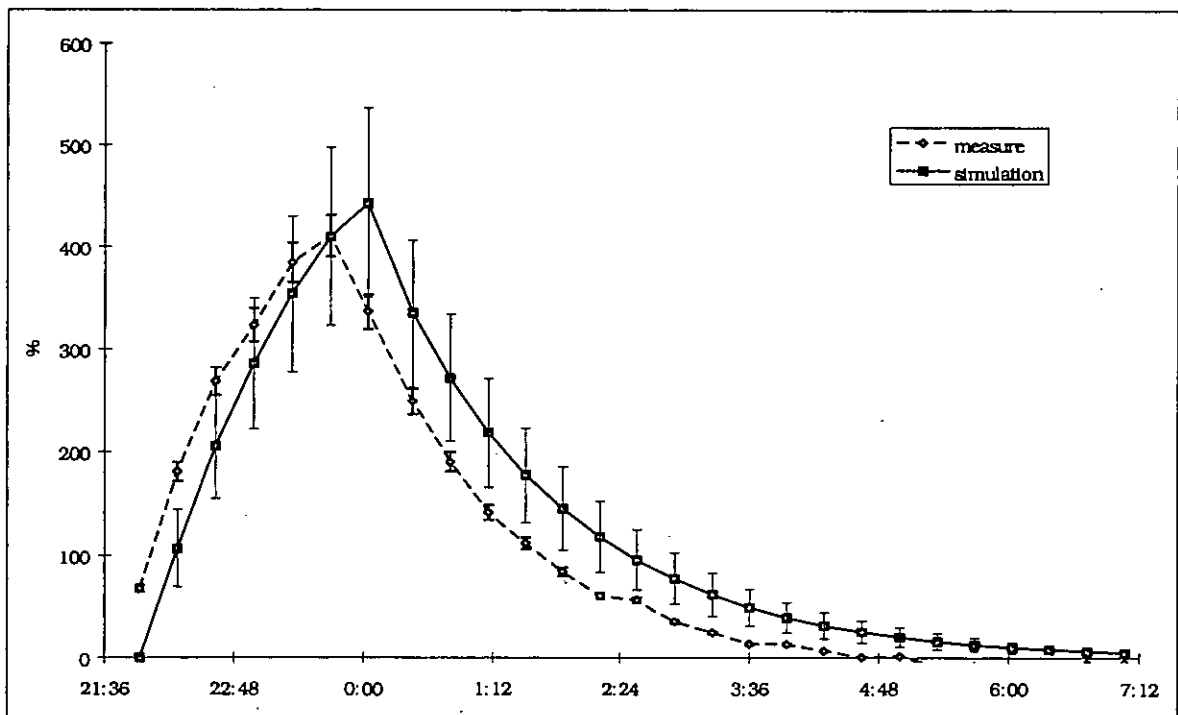


Figure A4.6.38: CO₂-concentration in the hall: simulated and measured. DOORS OPEN, CASE 2.

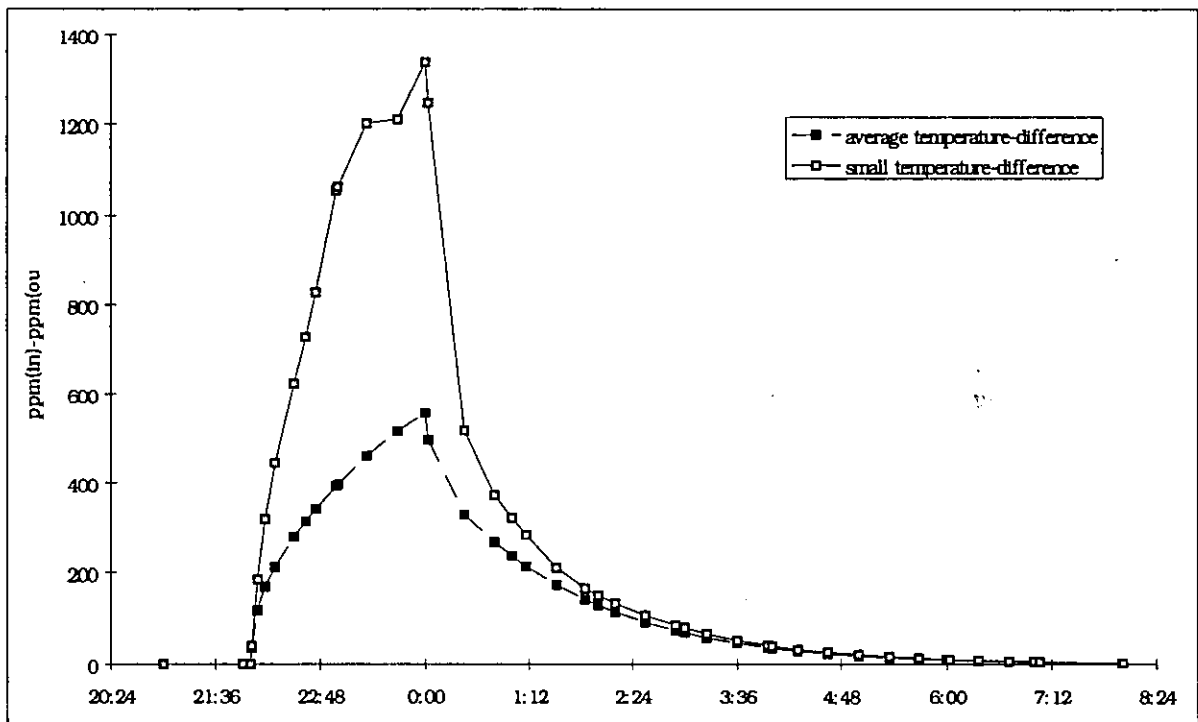


Figure A4.6.39: CO₂-concentration in bedroom 2: two COMIS-simulations with different temperature inputs. DOORS OPEN.

A 4.6.5 Sensitivity Analysis of Situation 2: inside doors closed.**Standard deviation of the input parameters:****Table A4.6-6: Range of certain parameters, determined by their standard deviations. DOORS CLOSED.**

No	Parameter	Minimum	Maximum
1	Leakage of Bedroom 2 door(up)	0.0018 kg/s@1Pa	0.0048 kg/s@1Pa
2	Leakage of Bedroom 2 door(down)	0.0018 kg/s@1Pa	0.0048 kg/s@1Pa
3	Leakage of Bedroom 1 door	0.0018 kg/s@1Pa	0.0048 kg/s@1Pa
4	Leakage of Living room door	0.0018 kg/s@1Pa	0.0048 kg/s@1Pa
5	Leakage of Kitchen door	0.0018 kg/s@1Pa	0.0048 kg/s@1Pa
6	Leakage of Bathroom door	0.0018 kg/s@1Pa	0.0048 kg/s@1Pa
7	Leakage of Toilet door	0.0018 kg/s@1Pa	0.0048 kg/s@1Pa
8	Exponent Bedroom 2 door	0.55	0.65
9	Temperature in Living	28.6 °C	29.6 °C
10	Volume of Living	50.35 m ³	55.65 m ³
11	Temperature in Kitchen	25.0 °C	26.0 °C
12	Volume of Kitchen	14.25 m ³	15.75 m ³
13	Temp. in Bedroom1	23.5 °C	24.5 °C
14	Volume of Bedroom1	32.3 m ³	35.7 m ³
15	Temperature in Hall	24.2 °C	25.2 °C
16	Volume of Hall	16.15 m ³	17.85 m ³
17	Temp. in Bedroom2	23.2 °C	24.2 °C
18	Volume of Bedroom2	19.95 m ³	22.05 m ³
19	Temp. in Bathroom	25.2 °C	26.2 °C
20	Volume of Bathroom	7.6 m ³	8.4 m ³
21	Temperature in Toilet	24.5 °C/m	25.5 °C/m
22	Volume of Toilet	3.8 m ³	4.2 m ³
23	Injection rate of CO ₂	0.0000234 kg/s	0.0000286 kg/s
32	Temperature gradient in Living	0.8 °C/m	1.0 °C/m

The parameters in the table are supposed to be constant. Again the value for the temperatures is an average value both in time and place for each room. Parameters 33 to 38 are the exponents of the other doors. Copies in the design file of column 8.

The following parameters are variable in time:

1. The fresh air supply:

These are the Parameters 24 to 28. The standard deviation is supposed to be $\pm 10\%$.

2. The absolute humidity:

Parameters 29 to 31 humidity in bedroom 2, hall and living room.

Parameters 39 to 59 humidity in bedroom 2 (variable in time), in kitchen, in bedroom 1 (variable), in bathroom (variable) and in toilet (variable). These parameters have columns in the design file which are copies of the columns 29, 30 or 31.

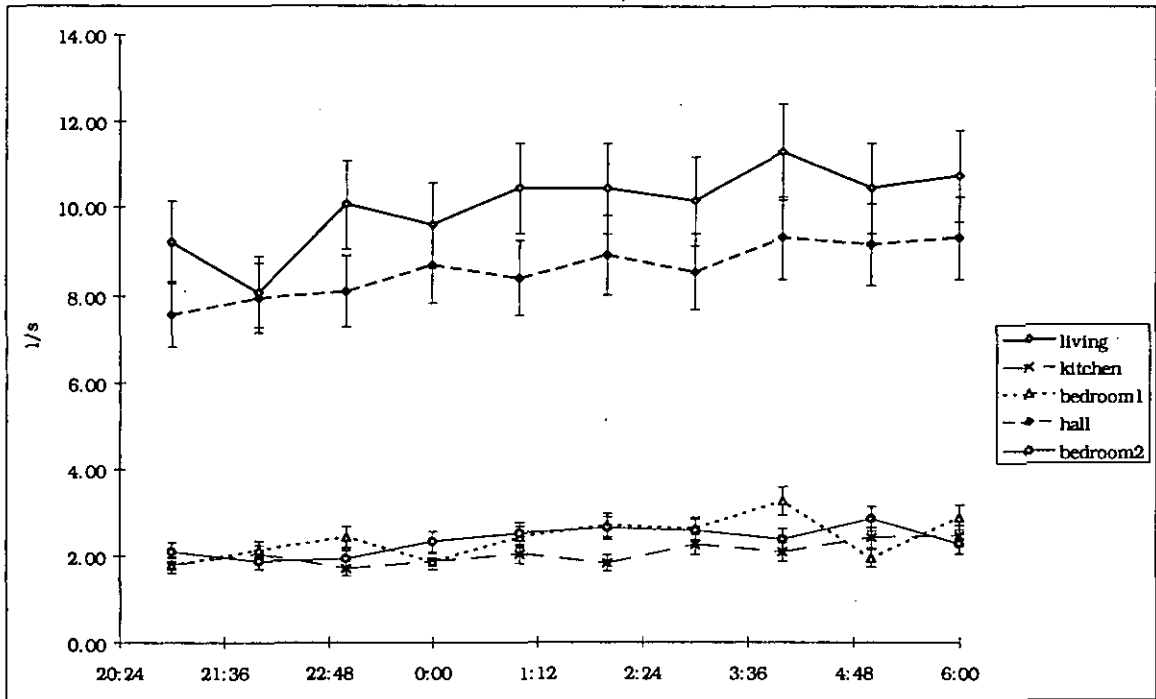


Figure A4.6.40: Variable value of the fresh air supplies in each room with their estimated errors. DOORS CLOSED.

Explanation of the range chosen for the parameters:

Air flow coefficient of the cracks of the doors:

No measurements were performed to determine the leakage characteristics of the doors. The estimation was made of a crack of 0.6 cm. at the bottom of the door and a crack of 0.6 cm at the top of the door (these are realistic values).

$$C = C_d \cdot A \cdot \sqrt{\frac{2}{\rho}} \tag{A4.7.3}$$

With: C_d = discharge coefficient (0.61)
 A = leakage surface (0.85m x 0.005m)
 ρ = density of the air (1.2 kg/m³)

The result is: $C = 0.0033 \text{ kg/s at 1 Pa}$

Due to the fact that the real value is not known at all, the standard deviation is taken very high: $\pm 50\%$. So, the case of a very airtight door will also be examined in the Monte Carlo Analysis, namely when the multiplication factor in the design file is nearby -2.

For the first door the separate effect of the upper crack and the lower crack is examined by taking two parameters in the range file with a different column in the design matrix. For the other doors the two cracks (upper and lower) are getting the same value in the range file.

- The other parameters: See the case with the inside doors open for the explanation of the range which is chosen for the different parameters.

Results of the Monte Carlo Analysis.

A Monte Carlo Analysis was performed with 100 runs. The results are given in Figures 4.7.41 to 4.7.43.

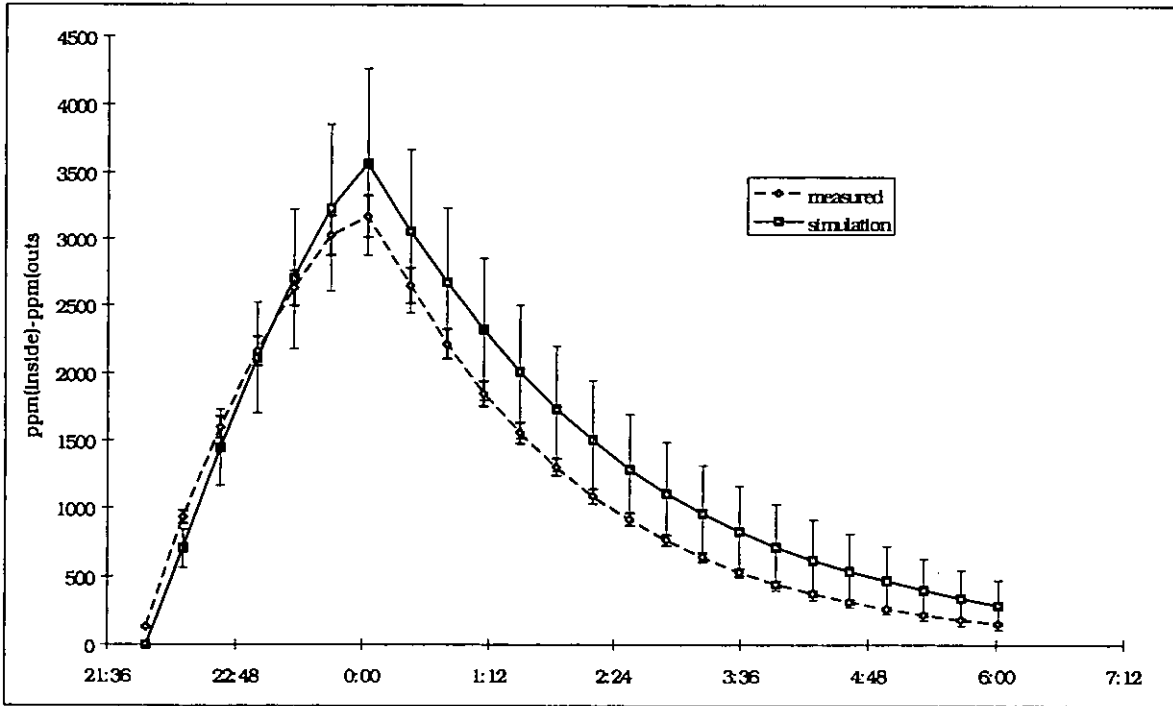


Figure A4.6.41: CO₂-concentration in bedroom 2: simulated and measured. DOORS CLOSED.

The figure for the toilet is about the same as the one for the bathroom (Figure A4.6.43).

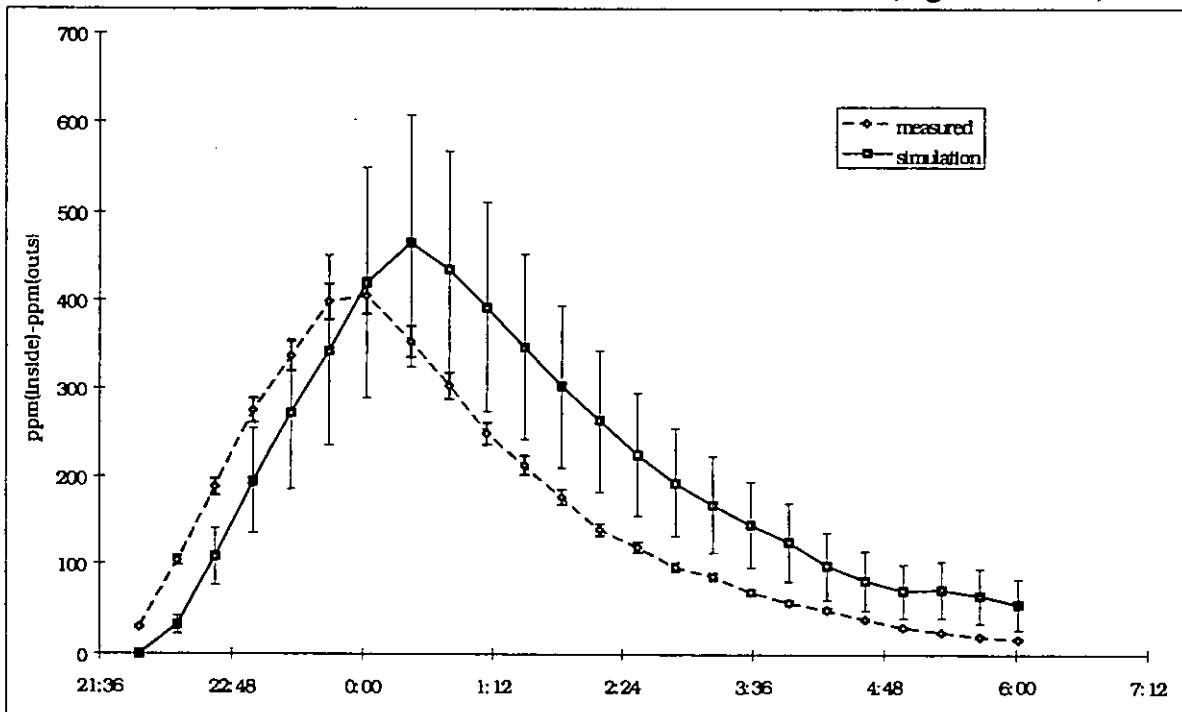


Figure A4.6.42: CO₂-concentration in the hall: simulated and measured. DOORS CLOSED.

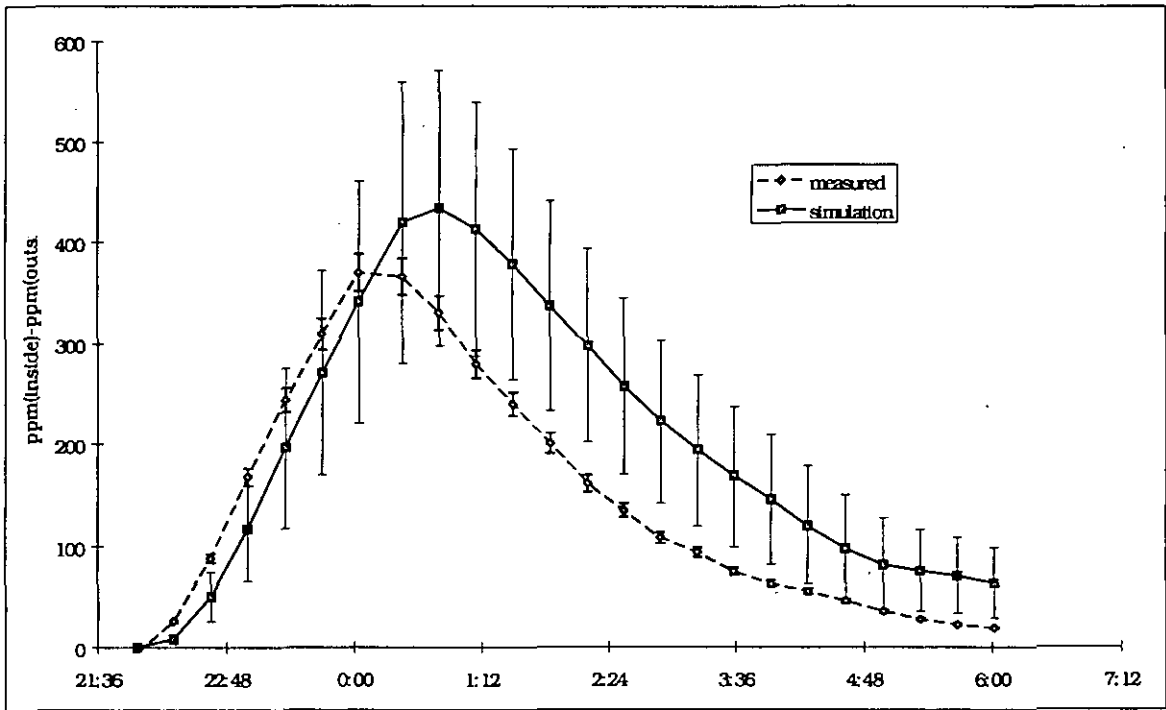


Figure A4.6.43: CO₂-concentration in the bathroom: simulated and measured. DOORS CLOSED.

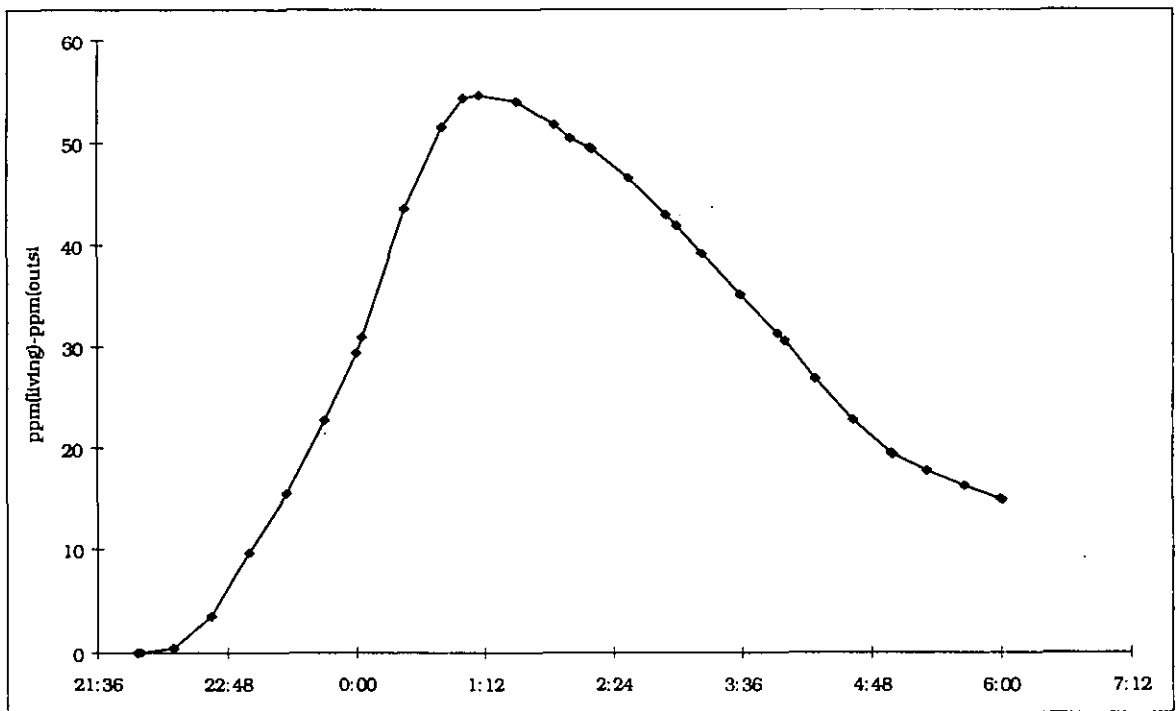


Figure A4.6.44: Maximum of the simulated CO₂-concentrations in the living room. DOORS CLOSED.

One can notice that there is a good similarity between measurement and simulation for the injection room (Figure A4.6.41). For the other rooms it can be seen that there is a shift in the time. The measured concentration stops increasing when the injection ceases in bedroom 2, whereas the simulated concentration continues to increase for a while. The fact that the concentrations are still increasing in the other rooms after the injection stopped in bedroom 2 is

logical because the concentration difference between the bedroom and the other rooms is very high. In this respect it is strange that this is not the case for the measured concentrations although the concentration difference is nearly the same as for the simulated results. This could be caused by the fact that, due to the closed doors, the airflow through the ducts of natural ventilation is not so high. In other words the measured fresh air supply is higher than the flow through the ducts. The difference between the two is the cross ventilation. This means that a part of the air entering the room through the outside wall is leaving through the same wall (back to the outside).

The measured concentrations in bedroom 1, living room and kitchen are nearly zero (with the outside concentration as reference) during the whole period. Nevertheless, for about 1/3 of the simulation runs the concentration is not zero for the living room (and kitchen), as one can see in the following figure.

Whether the concentration increases in the living room and kitchen depends on the values of the air flow coefficients of the doors between the different rooms and on the fresh air flow rates. In other words, it is a case of following 'the line of least resistance' for the air to the ducts of natural ventilation. The comparison in Table A4.6.7 illustrates this.

Table A4.6.7: Two simulation runs examined more in detail.

Features	Run 7	Run 79
Concentration (above outside) in the Living room at 1:09 h. (time of maximum)	55	0
Multiplication factor for door living room	0.72	-2.00
Multiplication factor for door kitchen	1.38	-0.26
Multiplication factor for door bathroom	-2.00	-0.20
Multiplication factor for door toilet	-0.33	1.48

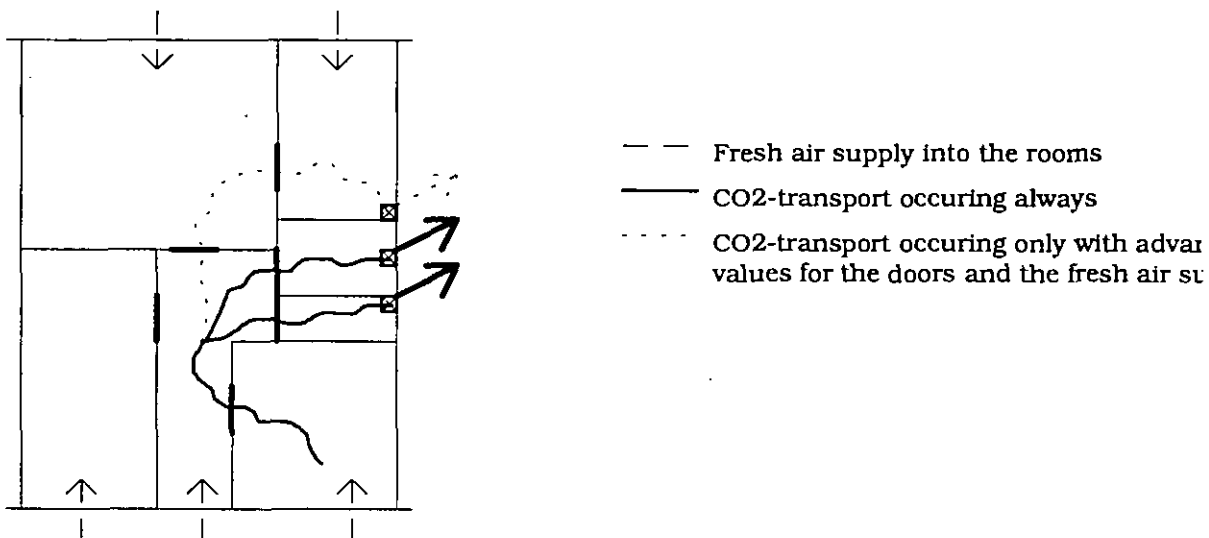


Figure A4.6.45: Sketch to clarify the influence of door characteristics and fresh air supplies on the concentration of CO₂ in the living room.

Run 7: large cracks for living room and kitchen, small cracks for bathroom and toilet. In this case it is possible for the air of the hall to leave the flat partly through the duct in the kitchen

Run 79: small cracks for living room, large cracks for toilet. In this case the air in the hall will only leave through the ducts in the bathroom and toilet.

If all the doors have about the same resistance (expected in this flat), there will be no increase of the concentration in the living room and the kitchen.

Use of a simple model if no double flow.

One can wonder if it is really necessary to use COMIS to perform these simulations, since a much simpler model can be used. For the injection room the following equation is valid:

$$V \cdot \frac{dC}{dt} = S - Q \cdot C \tag{A4.7.4}$$

where: $V =$ volume (m³)
 $C =$ concentration (ppm)
 $S =$ injection rate (m³/s)
 $Q =$ fresh air supply (m³/h)

The result of this equation is:

1. During injection: $C = \frac{S}{Q} \cdot \left(1 - e^{-\frac{Q \cdot t}{V}}\right)$ (A4.7.5)

2. After injection: $C = C_{\max} \cdot e^{-\frac{Q \cdot t}{V}}$ (A4.7.6)

Since Q is neither constant nor a known function of time, there has to be worked in time steps:

1. During injection: $C_i = \frac{S}{Q} - \left(\frac{S}{Q} - C_{i-\Delta t}\right) \cdot e^{-\frac{Q \cdot \Delta t}{V}}$ (A4.7.7)

2. After injection: $C_i = C_{i-\Delta t} \cdot e^{-\frac{Q \cdot \Delta t}{V}}$ (A4.7.8)

For the other rooms equation (A4.7.7) can be used, where the injection rate S is then the sum of the multiplication of the air flows to the specific room with the CO₂-concentrations of these air flows.

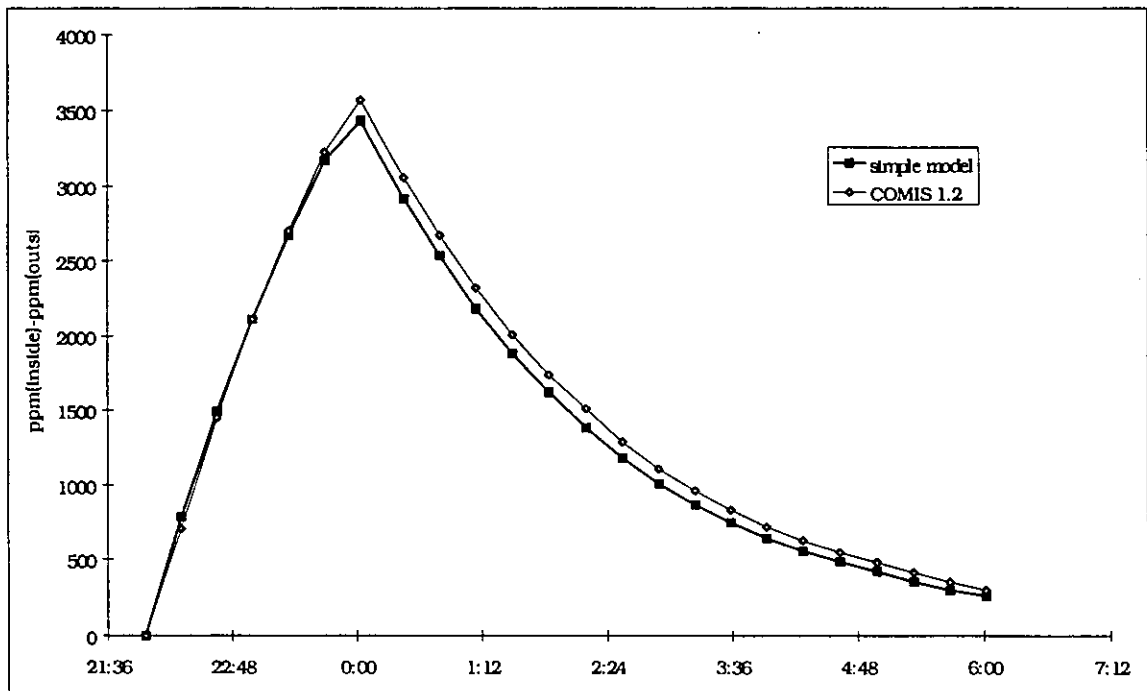


Figure A4.6.46: Comparison between two simulation models for CO₂-concentration in bedroom 2. DOORS CLOSED.

For example for the Hall:

- *Injection rate = Fresh air supply Bedroom 2 x Concentration Bedroom 2*
- *Air supply = Fresh air supply Bedroom 1 + Fresh air supply Bedroom 2 + Fresh air supply Hall + (Airflow through duct Kitchen - Fresh air supply Living room - Fresh air supply Kitchen).*

The last term (between brackets) is supposed to be zero in our case. As a result the air supply to the hall is equal to the sum of the air flows through the ducts of bathroom and toilet (with a small correction due to the problem shown in Figure A4.6.4).

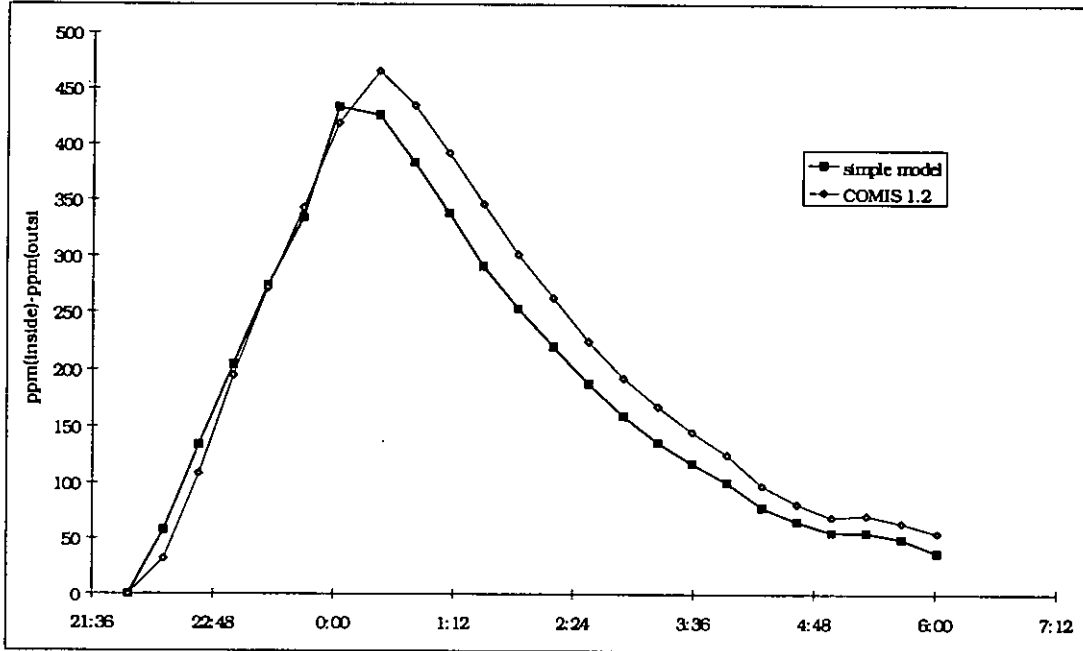


Figure A4.6.47: Comparison between two simulation models for CO₂-concentration in the hall. DOORS CLOSED.

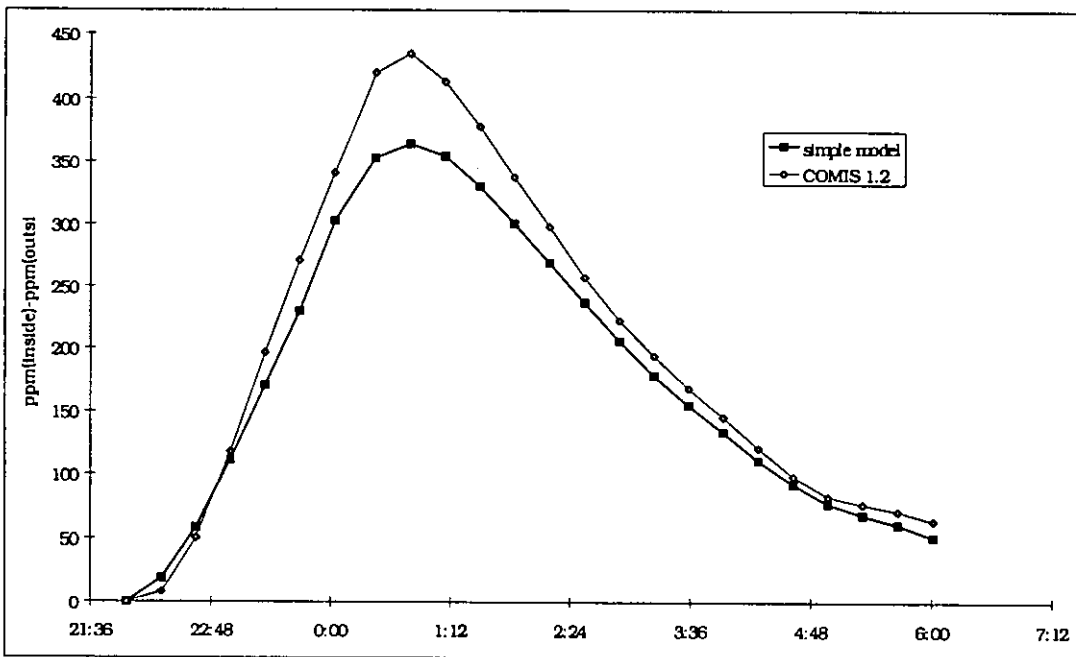


Figure A4.6.48: Comparison between two simulation models for CO₂-concentration in the bathroom. DOORS CLOSED.

Some of the results of these simulations are given in Figures 4.7.46 to 4.7.48, in comparison with the results with the COMIS -simulations. The similarity between the two results seems to be good.

Considering this, it is important to mention that one has to be prudent in the use of complicated simulation models. In this case it took much more time to perform a simulation with COMIS than with the simplified model. Besides, an additional disadvantage of complicated simulation models is that one risks loosing a clear view of the problem and its results. This does not mean at all that COMIS 1.2 is superfluous; for the previous case (with the inside doors open) a simple way to solve the problem does not really exist. Also when the fresh air supply is not given, it can be very interesting to use COMIS to do the calculations out of the weather conditions.

Results of the Fractional Factorial Analysis.

Some of the results are shown in Figures 4.7.49 to 4.7.56:

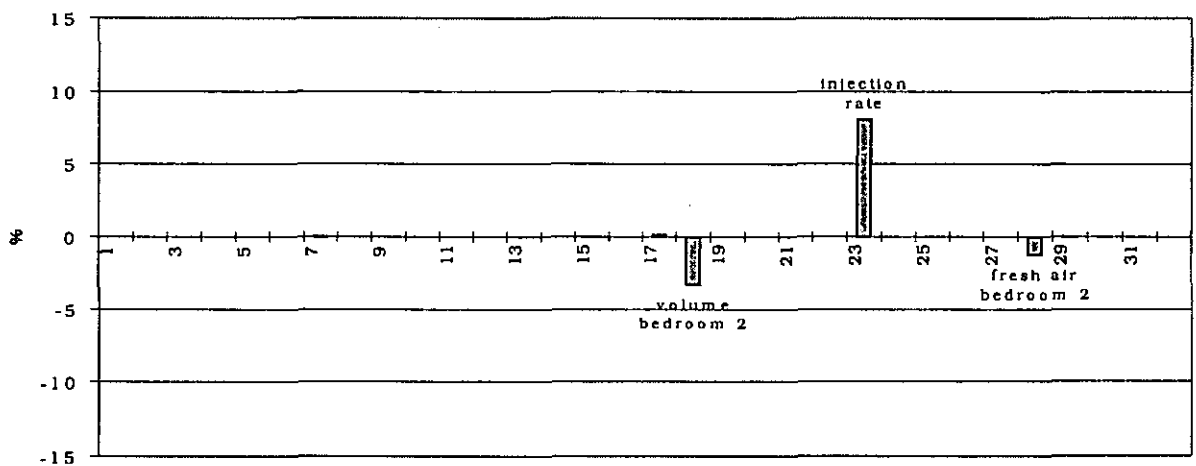


Figure A4.6.49: Main effects for the CO₂-concentration in bedroom 2 at 23h00. DOORS CLOSED.

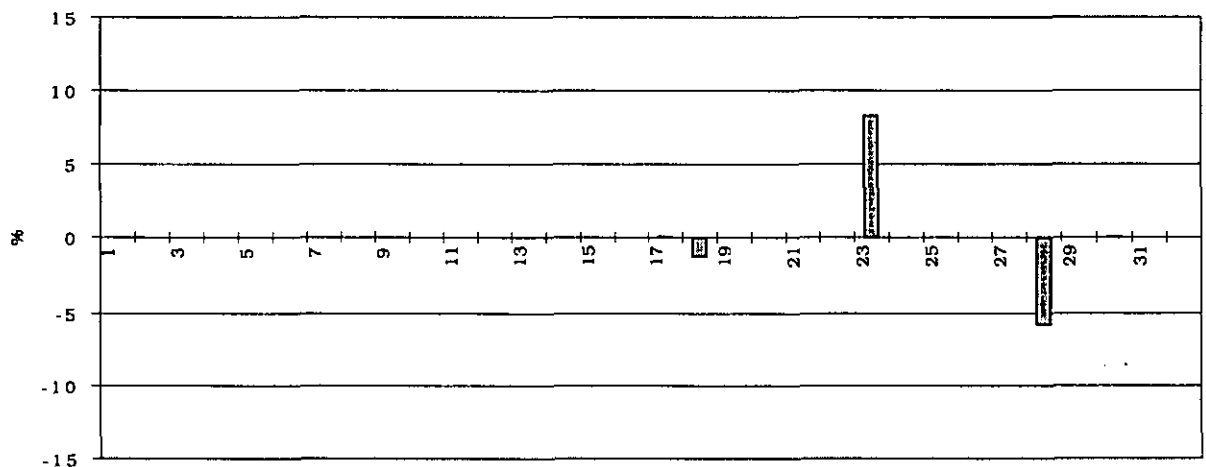


Figure A4.6.50: Main effects for the CO₂-concentration in bedroom 2 at 01h00. DOORS CLOSED.

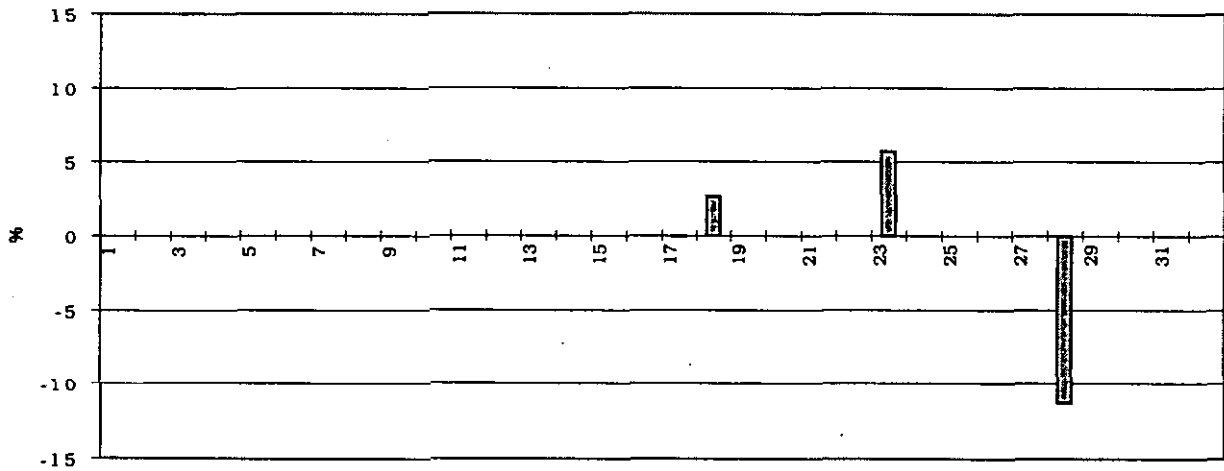


Figure A4.6.51: Main effects for the CO₂-concentration in bedroom 2 at 04h00. DOORS CLOSED.

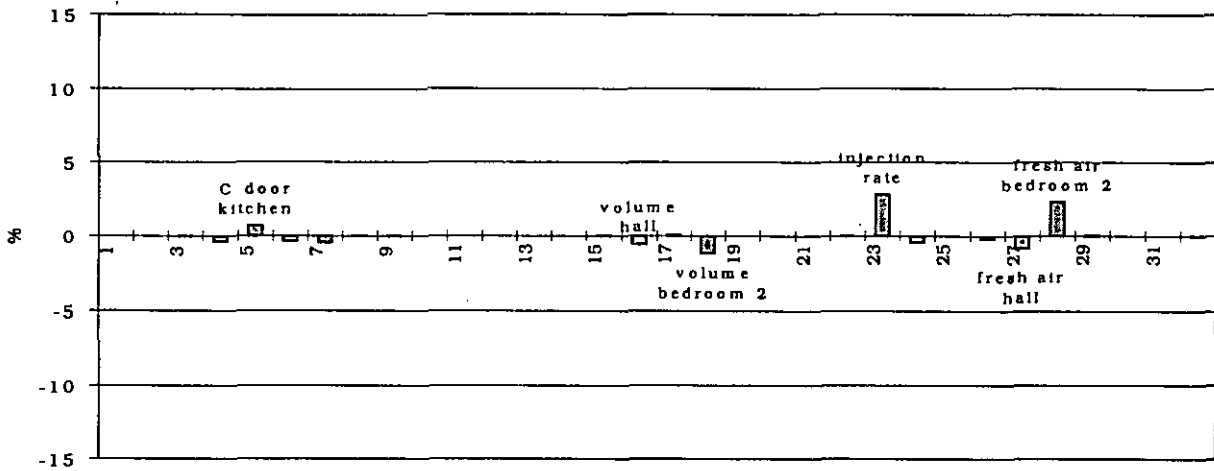


Figure A4.6.52: Main effects for the CO₂-concentration in the hall at 23h00. DOORS CLOSED.

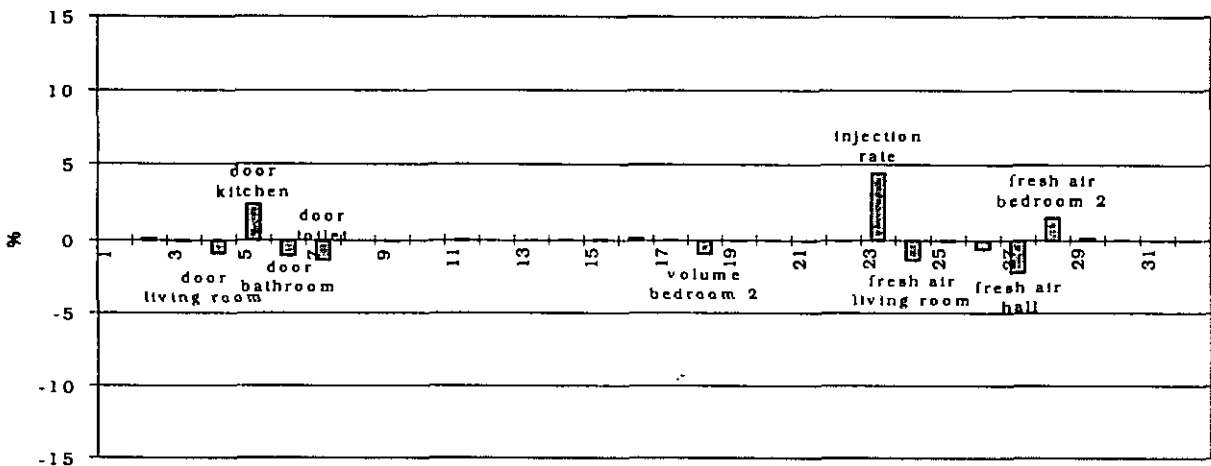


Figure A4.6.53: Main effects for the CO₂-concentration in the hall at 01h00. DOORS CLOSED.

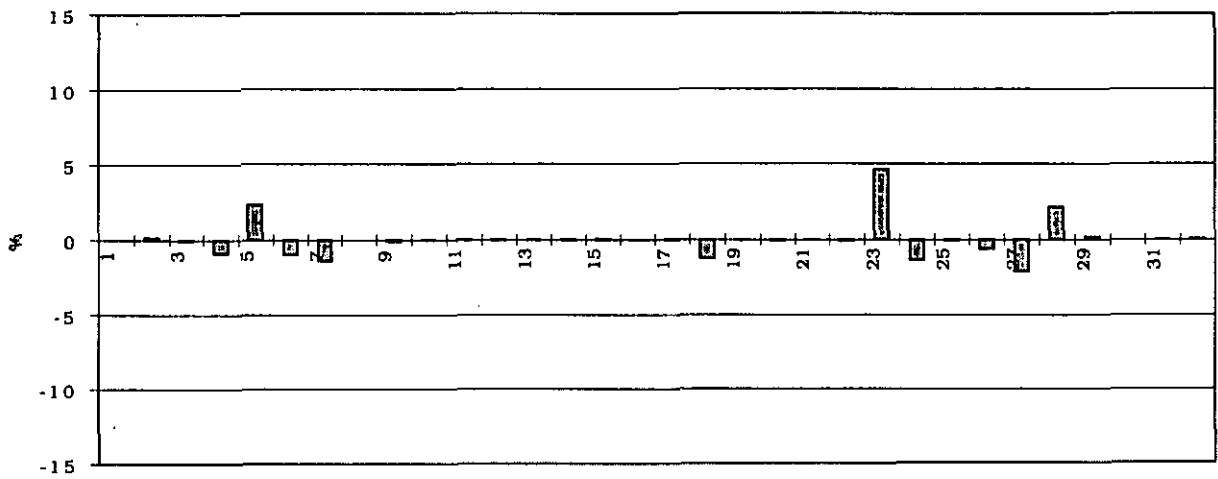


Figure A4.6.54: Main effects for the CO₂-concentration in the bathroom at 01h00. DOORS CLOSED.

For sake of clarity, the scale of the Figures A.4.7.55 and 56 has been taken ten times smaller.

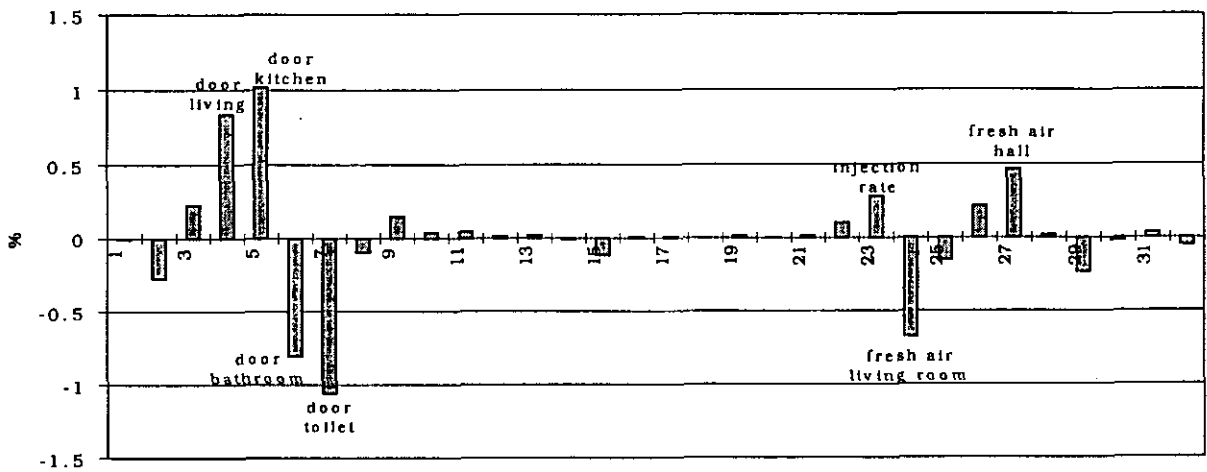


Figure A4.6.55: Main effects for the CO₂-concentration in the living room at 01h00. DOORS CLOSED.

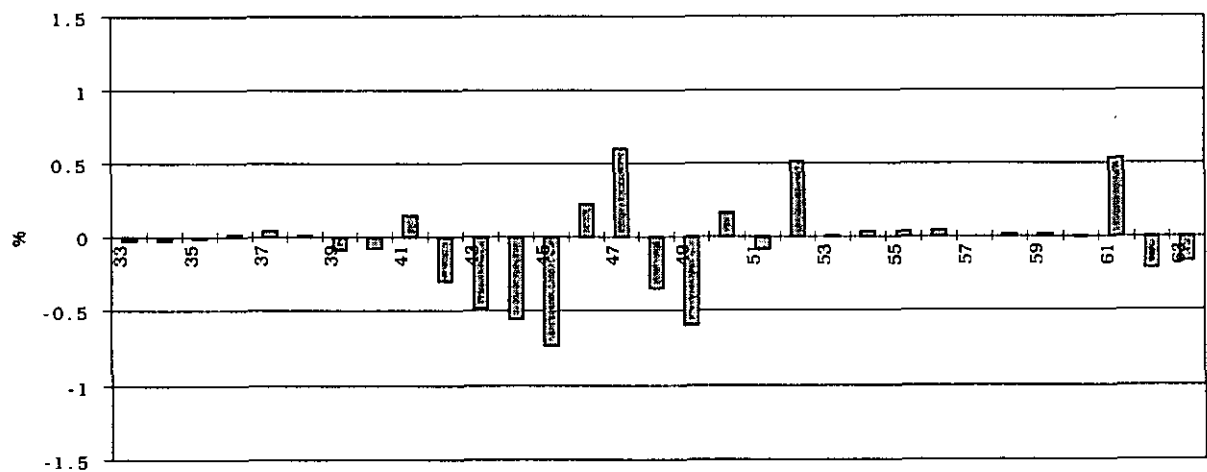


Figure A4.6.56: Effects of the first order for the CO₂-concentration in the living room at 01h00. DOORS CLOSED.

Remarks on these figures:

1. In Figure A4.6.49 to Figure A4.6.51 one can notice that the only parameters with an important influence on the concentration in bedroom 2 are the volume, the injection rate and the fresh air supply.

The influence of the fresh air supply seems to increase significantly during time (Figure A4.6.49 >> Figure A4.6.51), even when the injection has already been stopped.

The direction of the influence of the room's volume seems to change on a certain moment (Figure A4.6.49 >< Figure A4.6.51) (Figure A4.6.57). Injecting the same quantity in a room with a higher volume will initially give a smaller concentration. But, with a higher volume and the same fresh air supply, the room's air change rate will be smaller: this means that the concentration will not decrease so quickly as for a room with a smaller volume (Figure A4.6.58). One can notice in Figure A4.6.58 that on a certain moment the two concentration-lines are crossing. For this point the effect of the volume will be zero in Figure A4.6.57.

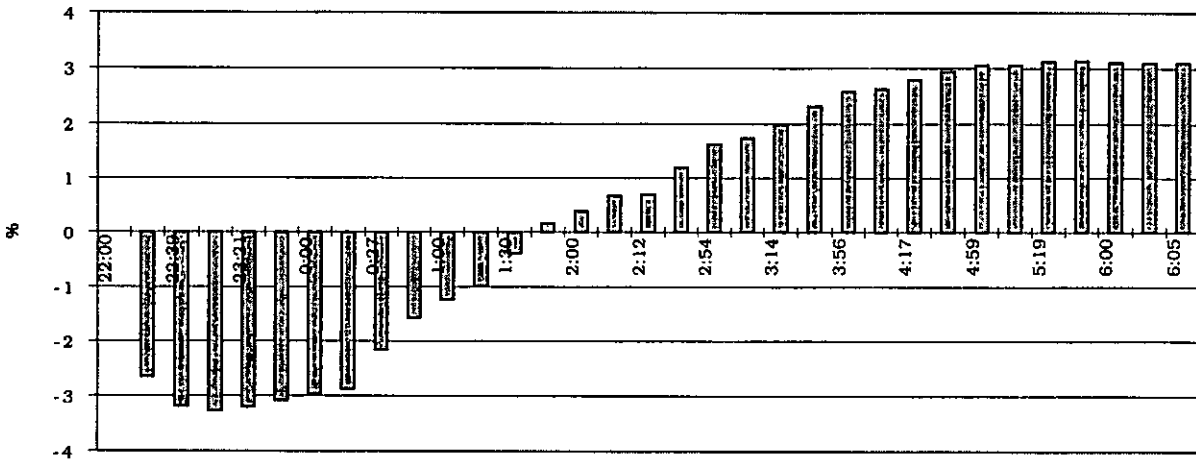


Figure A4.6.57: Variation of the effect of the volume on the CO₂-concentration in bedroom 2. DOORS CLOSED.

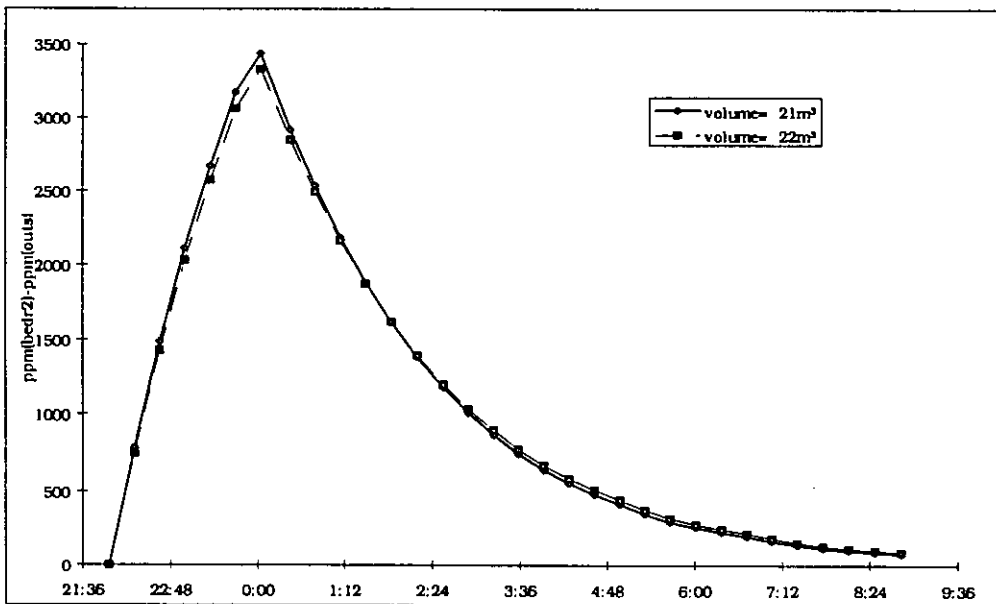


Figure A4.6.58: Influence of the volume (5% difference) on the CO₂-concentration in bedroom 2. DOORS CLOSED.

Figure A4.6.58 is made using the simple model.

It has to be mentioned that one would maybe expect an effect of about -5 % when the injection has just started. In Figure A4.6.57 this is not the case because for the simulation the absolute concentrations were used and thus the concentration before injection is not 0 ppm, but ± 500 ppm (= about the same as the outside concentration).

2. In Figure A4.6.53 and Figure A4.6.54 one can see that the cracks in the doors of the living room, kitchen, toilet and bathroom have an important influence on the concentrations in the hall, the bathroom and the toilet (this figure is not given because it is nearly the same as the one for the bathroom). This illustrates very well what was said in the explanation of Figure A4.6.44. It explains also the difference between the simple model and COMIS in Figure A4.6.48: in the simple model the cracks are not taken into account.

3. In Figure A4.6.55 one notices that for the living room the influence of the crack-values is higher than the influence of the injection rate. This is only true in a relative way: the uncertainty on the cracks (± 50 %) was taken a lot higher (because the value wasn't measured) than the uncertainty on the injection rate (10 %). Nevertheless, one has to wonder for which one of these parameters the value is most easy to determine.

4. In Figure A4.6.56 one sees that the effects of the first order for the concentration in the living room are not negligible in comparison with the main effects. For the other rooms these effects were very small.

Again, each bar in the figure is a combination of 16 effects of the first order (see explanation of Figure A4.6.34).

The effects which are causing the large error bars are normally effects of the first order combining two crack-values, in other words the effects caused by changing the values of the cracks of two doors in the same time.

For example in this case:

- * α_{42} : combined effect of α_4 and α_6 .
- * α_{43} : combined effect of α_5 and α_6 .
- * α_{44} : combined effect of α_4 and α_7 .
- * α_{45} : combined effect of α_5 and α_7 .
- * ...

For a list of the aliases: see [Fürbringer, 1994].

A 4.6.6 Conclusions

The main focus in the study of the apartment building in Namur was concentrated on:

- * the prediction of the air flows through large openings (situation 1: doors open);
- * the prediction of concentrations in the different rooms (situation 1 and 2).

It is important to stress that the purpose of these simulations was not to predict the fresh air supplies, which were entered as known parameters (using fans).

In the situation with the inside doors open (situation 1), the temperature difference between the rooms seemed to be a very important and even critical value, because (as one can see in Figure A4.6.39) choosing wrong values for the temperatures changes totally the final result. The smaller the temperature difference, the higher will be the influence of a fixed error on the final result. This is also illustrated very well in Figures A 4.7.49 to 56, giving the effect of the parameters on the final result.

From this point of view it is very important to mention that performing a simplified simulation with COMIS, for which the temperatures are taken to be the same throughout the whole apartment, will give results which are not at all correct if there are temperature differences between the rooms. In other words, if one wants to do a simulation it is very important to have a good knowledge of the temperatures in the apartment. But, as one could see in the comparisons between the Monte Carlo results and the measurements, a good knowledge of the temperatures is not enough. Indeed, if there are horizontal temperature differences (in other words, not only a vertical gradient) in a room (e.g. due to sunshine, radiators,...), it will be difficult to simulate this in a precise way with COMIS.

From the results of situation 1, it becomes clear that the prediction of pollution levels in multizone buildings with large internal openings, is very much associated with the assumptions for the internal temperature distribution. In practice, one often knows practically nothing about this temperature distribution. Therefore, prediction of the distribution of the pollution from local sources throughout a building is not evident. It must be stressed that this is not a negative appreciation of COMIS but a problem of collecting accurate input data.

For the situation with the inside doors closed the simulations have a good agreement with the measurements. It is interesting to notice that, in this simulation, no two-way flows occur in the internal openings. Given the fact that the fresh air flow rates are input data, it was possible to predict the evolution of the concentrations by means of a number of simple calculations. The level of agreement found with the COMIS results was very good.

MISA is a useful tool with which to perform sensitivity analyses. It is not only possible to examine the influence of certain parameters on the final result but also the influence of combinations of parameters (effects of the first order). Nevertheless, if one wants to examine the effect of one (or a small number of) specific parameter(s) (without the effects of the first order), it is easier to do some runs with COMIS and change the value(s) of the parameter(s) manually, because the construction of large fractional factorial designs takes a reasonable length of time.

A 4.6.7 Acknowledgements

The participation of the Belgian Building Research Institute (WTCB/CSTC) to Annex 23 'Air Flow Modeling' of the Implementing Agreement on Energy Conservation and Community Systems, is made possible with the financial support of the Ministry of the Flemish Community.

A 4.6.8 References

- Fürbringer J.M.: Sensibilité de Modèles et de Mesures en Aéraulique du Bâtiment à l'aide de Plans d'Expériences. *PhD Thesis, EPFL Lausanne, Switzerland, 1994.*
- van der Maas J.: Air Flow through Large Openings in Buildings, Subtask 2, Technical Report. *Annex 20: Air flow Patterns within Buildings, International Energy Agency, 1992.*

A 4.7 PASSYS Cell In Greece

A 4.7.1 Measured Object

The PASSYS Test Cell is a fully equipped outdoor facility for thermal and solar monitoring [Vandaele and Wouters, 1994]. It is divided into two rooms, called the "test room" and the "service room" (Figure A4.8.1). The test room has a floor area of 13.84 m^2 , a width of 2.76 m and a height of 2.75 m . The volume of the room is 38.04 m^3 . The service room has a floor area of 8.6 m^2 , a length of 2.4 m and a height of 3.29 m . Its volume is 28.29 m^3 . An exterior door opening of 2.22 m^2 with a width equal to 1.01 m connects the room with the outdoor environment. The two rooms communicate through a 2.02 m^2 door opening. The height of the interior door is 2 m and its width is 1.01 m . Ventilation experiments were held in the service room.

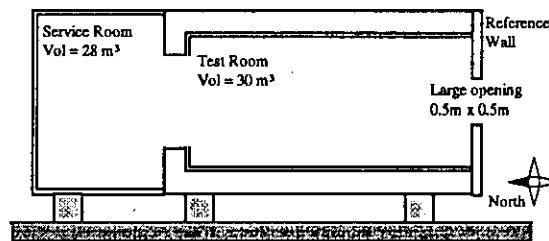


Figure A4.8.1: The PASSYS Test Cell - Sectional view

A 4.7.2 Measurements performed

The thermal behaviour of the cell was constantly monitored. Surface temperatures on all internal and external surfaces were monitored by platinum 100Ω resistors (PT100 sensors). The air temperature in the service room was also measured by an array of various PT100 sensors and T-Fast sensors placed at different heights : $0.29, 0.36, 0.42, 0.59, 0.65, 0.87, 1.05, 1.32, 1.35, 1.6, 1.69, 1.76$ and 2.37 m from the floor.

Outdoor air temperature data were provided by a standard meteorological station very close to the cell as well as by protected sensors located outside the cell. Wind speed and wind direction measurements were taken at a 10 m height and at a height of 1.5 and 2 m respectively, 1 m away from the cell entrance.

The air velocity at various heights in the middle of the opening was measured by an array of five triple hot wires and three DANTEC sensors (accuracy $\pm 0.4\%$). The heights of the hot wires from the floor were $0.33, 0.63, 0.93, 1.43$ and 1.73 m . The heights of the DANTEC sensors from the floor were $0.16, 0.98$ and 1.87 m .

Temperature stratification at the opening was monitored by an array of five PT1000 and five T-Fast sensors (accuracy $\pm 0.1 \text{ }^\circ\text{C}$). The T-fast sensor is a $12.5\text{E-}6 \text{ m}$ platinum wire, wired around an open Plexiglas base. The heights of the PT1000 sensors from the floor were: $0.29, 0.59, 0.87, 1.32$ and 1.60 m . The heights of the T-fast sensors from the floor were: $0.36, 0.65, 1.05, 1.35$ and 1.69 m . The location of the above sensors is shown in Figure A4.8.2.

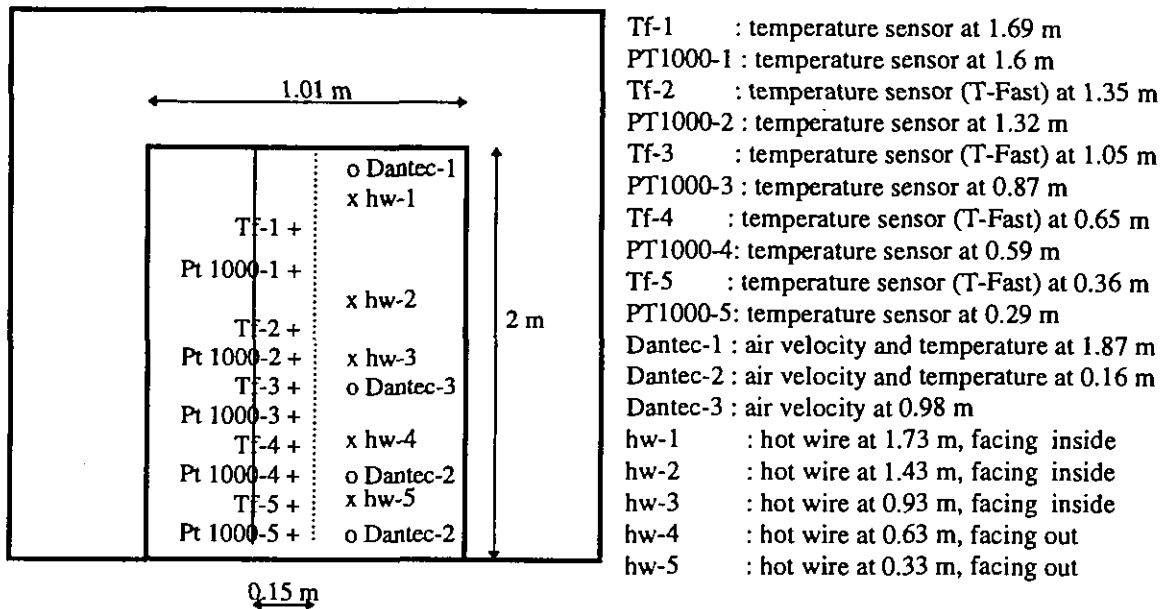


Figure A4.8.2: Location of PT1000, T-fast at the opening (PASSYS Test Cell)

Ventilation measurements were performed according to the single tracer gas decay technique. N₂O was used as a tracer gas. Injection and sampling points were carefully chosen and distributed at various heights inside the space in order to supply the tracer gas homogeneously and also to monitor its spatial variation in the time period of the experiment. The sampling period was 30 s. A BBRI injection-measurement system and an infrared gas analyser were used for this experiment. To establish a uniform concentration of the tracer gas in the room air, a total of six sampling points have been used. They were located at different heights from the floor, in a distance from the entrance door. The location of the injection and measuring points is shown in Figure A4.8.3. During the experiments, N₂O was injected into the room, with the entrance door closed. During the experiments the communication door was kept closed and sealed.

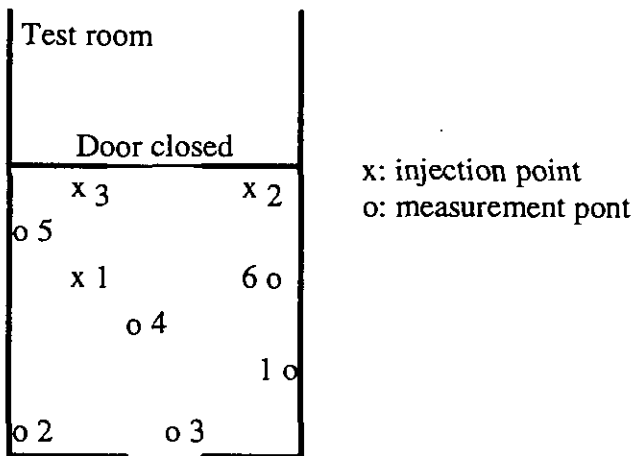


Figure A4.8.3: Location of injection and measurement points in the Service Room of the Test Cell

Measurement point heights from the floor of the Service Room were:

location	o(1)	o(2)	o(3)	o(4)	o(5)	o(6)
height	2.10 m	2.20 m	2.20 m	1.99 m	1.51 m	1.99 m

Wind speed and direction as well as ambient air temperature data at 10 m were provided by a standard meteorological station. Measurements of wind speed and direction were also pro-

vided by a hot wire anemometer and a vane at a height of 1.5 m, 1 m away from the service room entrance door. At the same distance and at a height of 2 m, a PT 1000 was placed to measure ambient temperature. Piezoresistive transducers were used to measure differential pressure at three sides of the test cell (accuracy: $\pm 2.5\%$ in the range 1-10 Pa and $\pm 1\%$ in the range 10Pa - 20kPa). The reference side was the one in the south.

Four experiments have been performed. The mean climatic data measured during the experiments are given in Table A4.8.1.

Table A4.8.1.: Characteristics of the Test Cell experiments

Experiment	Mean Ambient Temperature [°C]	Mean Indoor Temperature [°C]	Mean Wind Speed [ms^{-1}] at a 10 [m] height
Exp. 1	24.1	23.4	3.35
Exp. 2	24.7	24.3	2.51
Exp. 3	25.7	26.2	3.82
Exp. 4	25.6	26.6	3.56

Analysis of the results from these experiments is presented in §A4.9.

A 4.7.3 REFERENCES

Vandaele L. and P. Wouters (1994). The PASSYS Services. *Summary report of the PASSYS Projects. Belgian Building Research Institute, EC DG XII, Brussels.*

A 4.8 Large opening experiment in Greece

A 4.8.1 Measured Object

The Institute of Meteorology and Physics of the Atmospheric Environment is a three-storey, naturally ventilated, office building. A plan of the room is given in Figure A4.59. Each floor is about 4.5 meters high. Ventilation experiments were held on the first floor. The selected office room (zone A) was isolated from the rest of the building and its thermal behaviour was constantly monitored. The room has a 13.59 m^2 floor area, while its length is equal to 3 m. The only external window is on the west wall and is divided in five parts, A1, A2, B1, B2 and C, which can open separately, providing the possibility to vary the opening area (Figure A4.60) by opening different parts. The total window area is 2.5 m^2 . The area of each part is as follows : $A1=0.34 \text{ m}^2$, $A2=0.34 \text{ m}^2$, $B1=0.60 \text{ m}^2$, $B2=0.60 \text{ m}^2$ and $C=0.66 \text{ m}^2$.

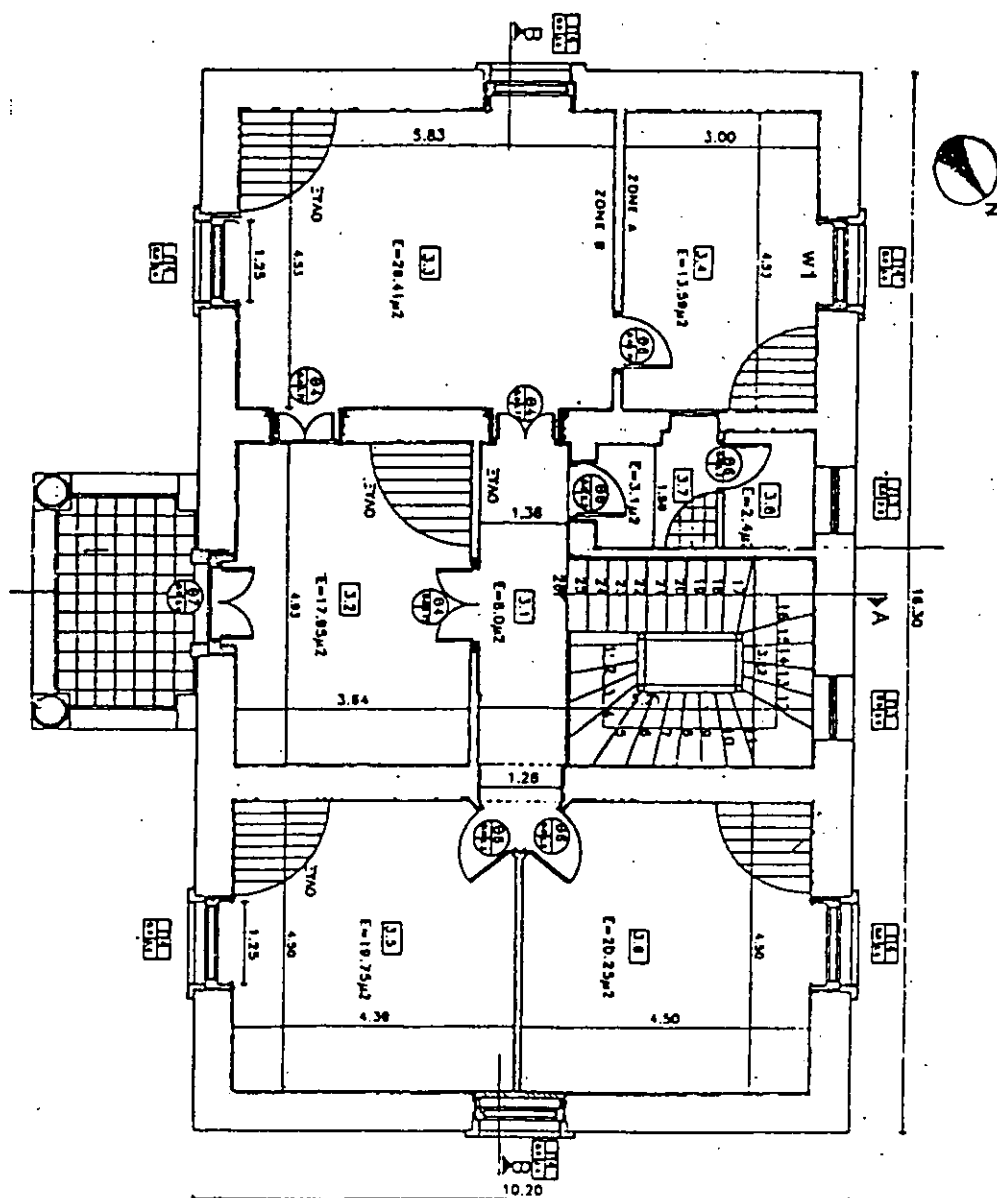


Figure A4.59: Plan of the room

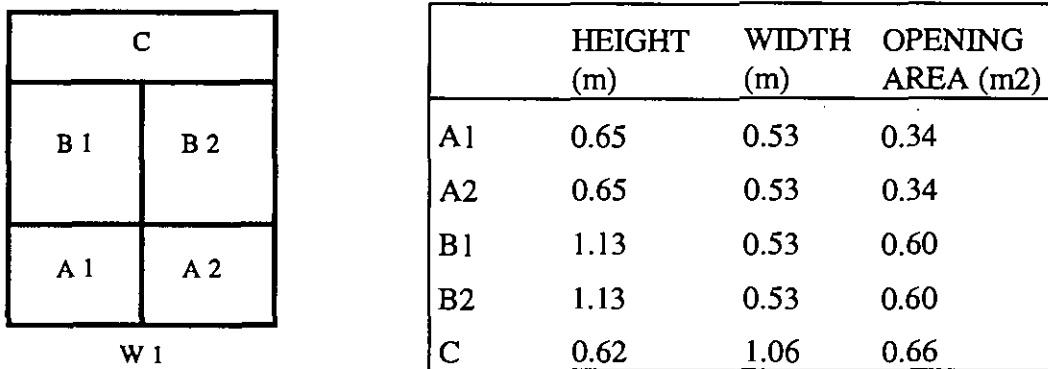


Figure A4.60: Dimensions of the window of the NOA building.

A 4.8.2 Measurements performed

The thermal behaviour of the room, where the ventilation experiments took place, was constantly monitored. Temperature on all internal and external surfaces was monitored by PT100 sensors. Indoor air temperature measurements were taken by an array of three PT100 sensors placed at different heights : 0.3 m, 1.1 m and 2.0 m from the floor. Ambient air temperature data were provided by standard meteorological stations very close to the monitored room, as well as from a protected sensor located outside the opening.

Wind speed and wind direction measurements were taken at heights of 10 m and 18 m at a very close distance from the window. Also, wind speed measurements were taken at the bottom of the opening.

Ventilation measurements were performed according to the single tracer gas decay technique. N₂O was used as a tracer gas. Injection and sampling points were carefully chosen and distributed at various heights inside the space in order to supply the tracer gas homogeneously and also to monitor its spatial variation in the time period of the experiment. The sampling period was 30 s. To establish a uniform concentration of the tracer gas in the room air, a high number of sampling points (5 to 7) have been used, located at different heights from the floor, in a distance from the window. The location of the injection and measuring points is shown in Figure A.4.9.3. During the experiments, N₂O was injected into the room, while the exterior opening was sealed. Small fans were used, in order to achieve good mixing of the gas during the injection period.

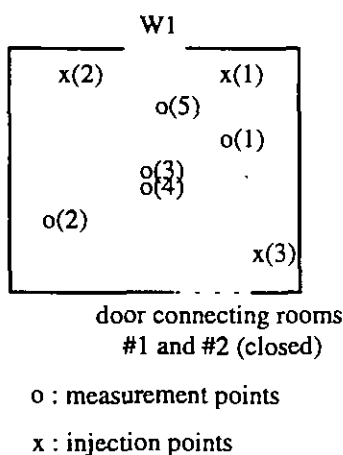


Figure A.4.9.3: Location of the injection and measurement points

The gas concentration in the room increased and when the mixing was satisfactory, the fans were turned off, the injection stopped and the window/door opened. Concentration at every

measuring point was constantly measured throughout each experiment. Fifteen different experiments have been performed. The opening area as well as the mean climatic conditions for each experiment are given in Table A4.8.1

Table A4.8.2 summarises the performed measurements, the used instrumentation followed by their accuracy.

Table A4.8.1: Opening area and mean climatic conditions for single sided ventilation experiments in the NOA building

Experiment	Openings	Mean ambient temperature °C	Mean indoor temperature °C	Mean wind speed at 10 m height m/s
Exp. 1	A1+A2	31.3	31.4	6.8
Exp. 2	B1+B2	32.6	31.8	3.0
Exp. 3	C	30.6	32.1	5.0
Exp. 4	A2+B2	32.5	31.8	6.7
Exp. 5	A1+A2+B1+B2	30.5	31.5	1.7
Exp. 6	B1+B2+C	28.8	29.2	1.6
Exp. 7	ALL	30.2	31.0	3.6
Exp. 8	A1+A2+B1+C	29.6	31.0	3.1
Exp. 9	A1+A2+B2+C	28.2	31.0	3.4
Exp. 10	A2+C	31.2	31.7	5.4
Exp. 11	B2+C	30.7	31.8	4.9
Exp. 12	A1+A2+C	30.8	31.0	4.2
Exp. 13	A1+B1+C	27.6	28.8	2.0
Exp. 14	A2+B2+C	30.1	31.6	5.0
Exp. 15	A2+B1+B2+C	29.4	31.2	4.7

Table A4.8.2: Measured parameters, sensors and accuracy.

Parameter	Sensor	Accuracy
Temperature	PT100 sensors	±0.1 °C
Wind Speed	Dantec Sensors	±0.4 %
Wind Speed	Three cup anemometer	±2.0 %
Wind Direction	Vane	±5 degrees
N20 Concentration	Infrared gas analyzer	±1 %

According to the decay method, the decrease of the tracer gas concentration is given by the following equation :

$$C(t) = C(t_0) \exp(-nt) \quad (\text{A4.9.1})$$

where $C(t)$ and $C(t_0)$ are the tracer gas concentrations at time t and at $t=0$ respectively. Also, n is the ventilation rate. The air changes per hour have been calculated for each sampling point and then the mean value for the whole room was calculated as the mean of all sampling points.

Homogeneity was found to be affected by the infiltration rates, which are sensitive to the variations in the wind speed and direction and by the buoyancy effect, which gets stronger with increasing opening height. When the opening size was small, no significant homogeneity problems were encountered. As the opening size got larger, however, homogeneity was more difficult to achieve especially in cases of low wind speed. Nevertheless, even under the most

difficult conditions, mixing was satisfactory. gives the N2O concentrations, as measured at each measuring point plotted on a semi-log paper for two representative experiments with small and large openings. As shown, the maximum difference between two measuring points is less than 6 per cent for small and 10 % for larger openings.

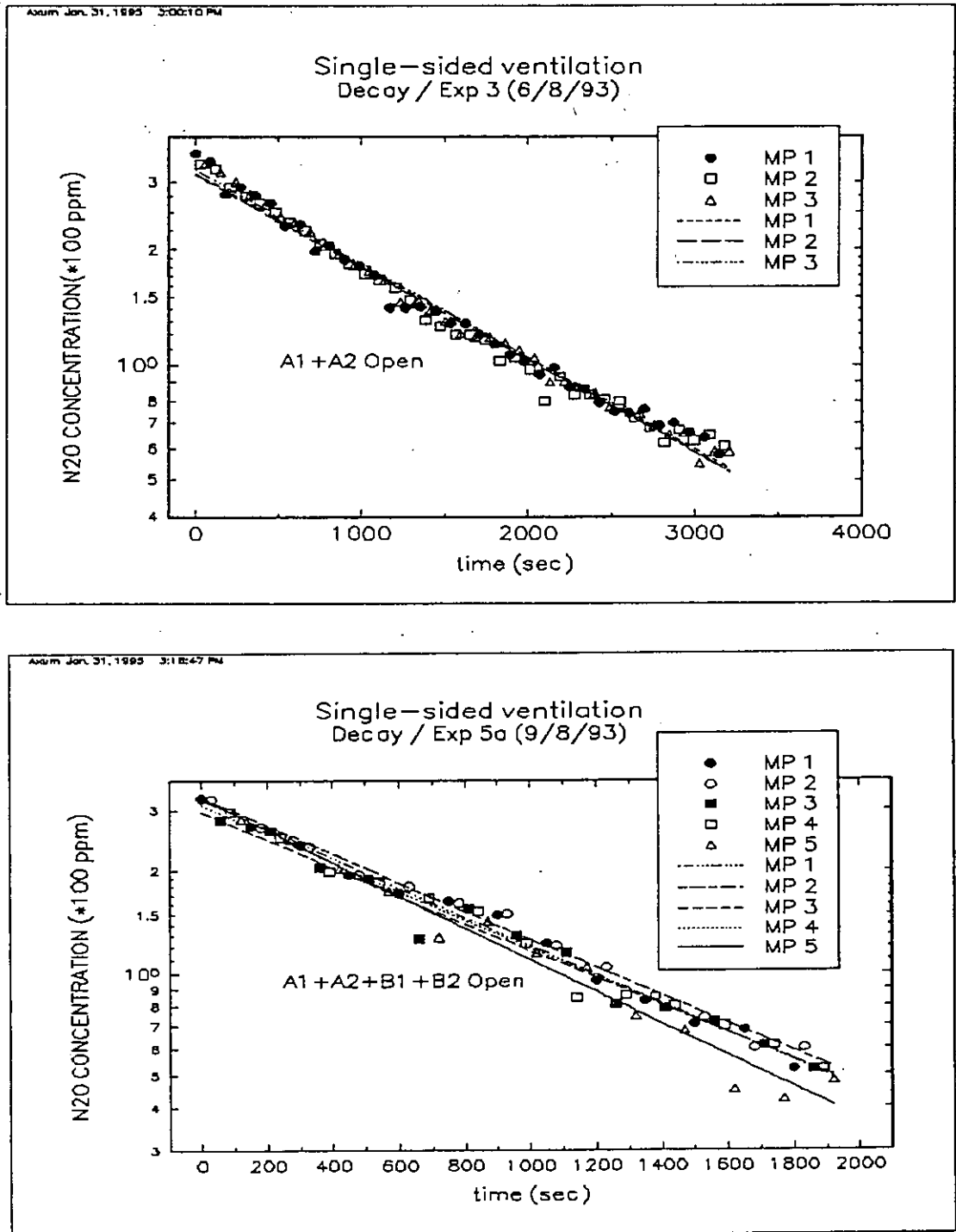


Figure A4.61: Variation of the N2O Concentration

A 4.8.3 Sensitivity Analysis

A sensitivity analysis regarding COMIS predictions for single sided ventilation has been performed. The impact of the following parameters has been examined :

- Wind velocity
- Temperature difference between indoor and outdoor environment
- Surface and height of the opening
- Discharge coefficient.

Wind speed varied from 0 m/s to 5 m/s with a step of 1 m/s. Temperature difference varied from 0 to 5 °C with a step of 1 °C. The surface of the opening varied from 0.5 to 2.5 m² with a step of 0.5 m². Finally, the discharge coefficient varied from 0.4 to 1. All possible combinations have been tried. The results of the sensitivity analysis and the impact of each parameter on the ventilation rate are discussed in the following sections.

The Role of Wind Speed

Air flow simulations have shown, that COMIS' predictions for single sided ventilation configurations are not sensitive to a variation of the wind speed. This is well known for all existing network models. This characteristic of network models is a major source of inaccuracy, because inertia forces are neglected.

The Role of the Temperature Difference

It was found, that the air flow changes as a function of the square root of the absolute value of the temperature difference.

Figure A4.62 shows the variation of the predicted air flow rate with temperature difference for four different values of the discharge coefficient.

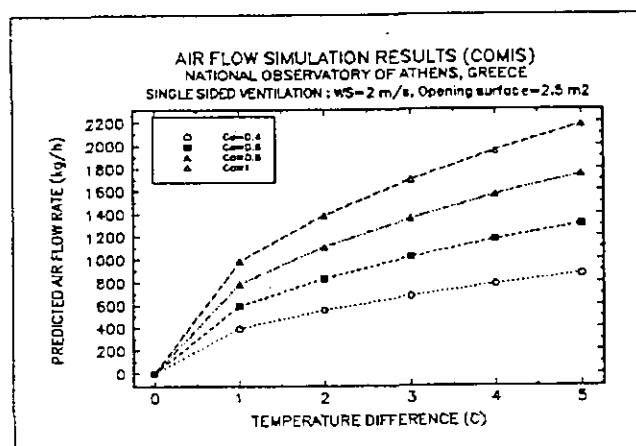


Figure A4.62: *The role of the temperature difference*

The Role of the Opening's Height and Surface

It was found, that the air flow changes as a function of $H^{1.5}$, where H is the height of the opening. The width of the opening remained constant for the simulations. Figure A4.63 shows the variation of the predicted air flow rate with the opening surface for four different values of temperature difference.

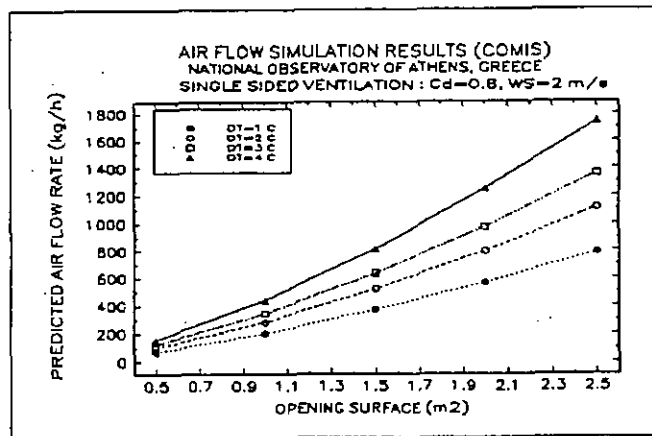


Figure A4.63: The role of the opening surface

The role of the Discharge Coefficient

It was found, that the predicted air flow is a linear function of the discharge coefficient. Figure A4.64 shows the variation of the predicted air flow rate with the discharge coefficient for four different values of temperature difference.

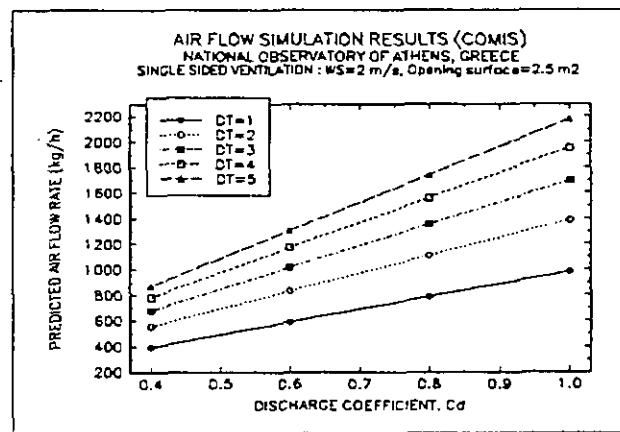


Figure A4.64: The role of the discharge coefficient.

A 4.8.4 Discussion

For all the above experiments COMIS has been used to calculate the air flow rate. A discharge coefficient equal to 1, $Cd = 1$, has been used for all the experiments. Figure A4.65 shows the air flow rate predicted by COMIS as well as the measured values for each experiment. Air flow is expressed in cubic meters per hour. The correlation coefficient between the two set of data is calculated equal to 0.67.

As shown in Figure A4.66, important differences are observed especially for all the experiments with a high opening surface. In order to explain the observed differences, a plot of the obtained differences between the simulated and the measured values as a function of the mean wind speed is given in. Additionally, plots of the prevailing wind direction and absolute

indoor-outdoor air temperature difference during each experiment are given in Figure A4.68 and Figure A4.69.

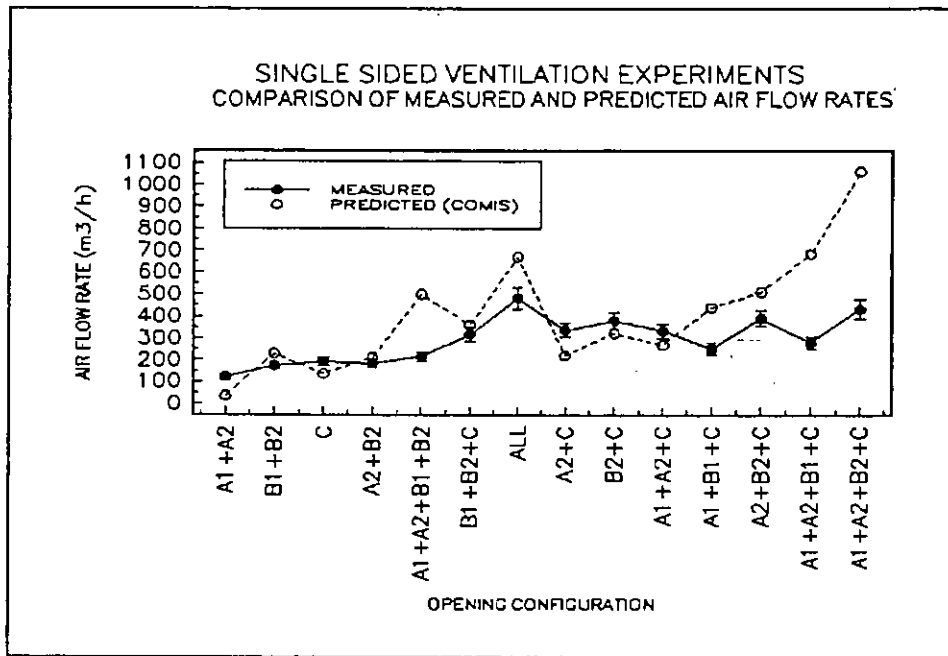


Figure A4.65: Simulated and Measured air flow rates for single sided ventilation experiments

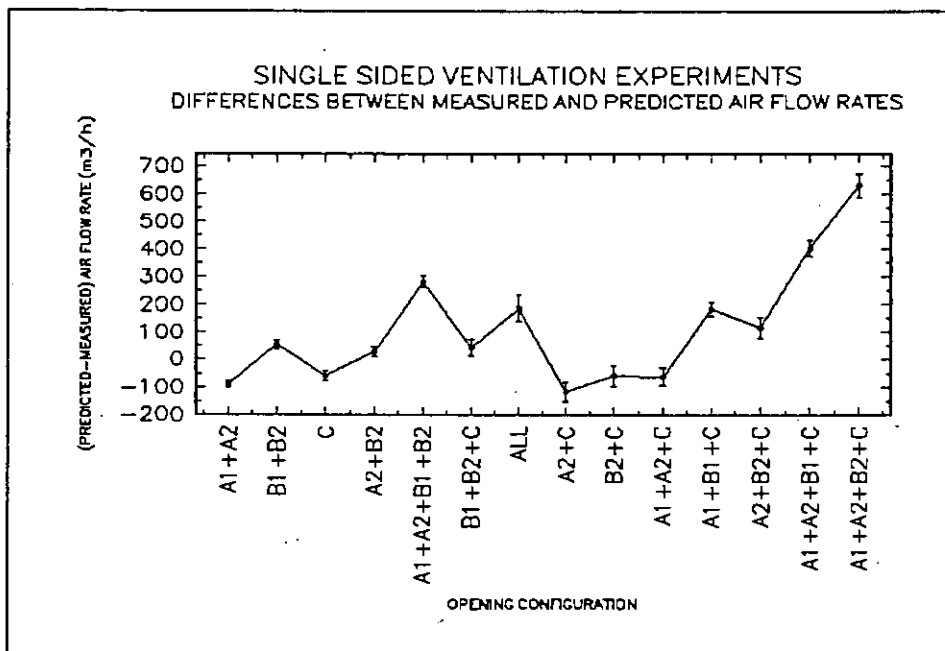


Figure A4.66: Simulated and Measured values for each experiment.

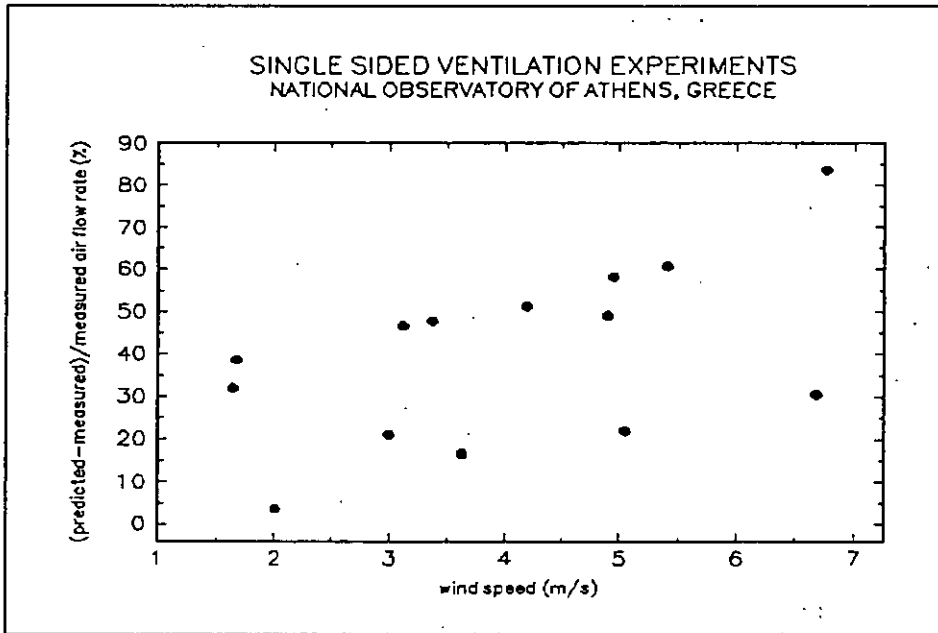


Figure 4.67: Difference between simulated and measured air flow rates as a function of the mean wind speed for each experiment

As shown, there is not a clear relationship between the observed differences and the above parameters. However, when the observed difference between the calculated and the measured values are plotted as a function of the mean wind speed (cf Figure 4.67), it can easily be concluded, that for higher values of the wind speed, the measured values are much higher than the corresponding calculated values.

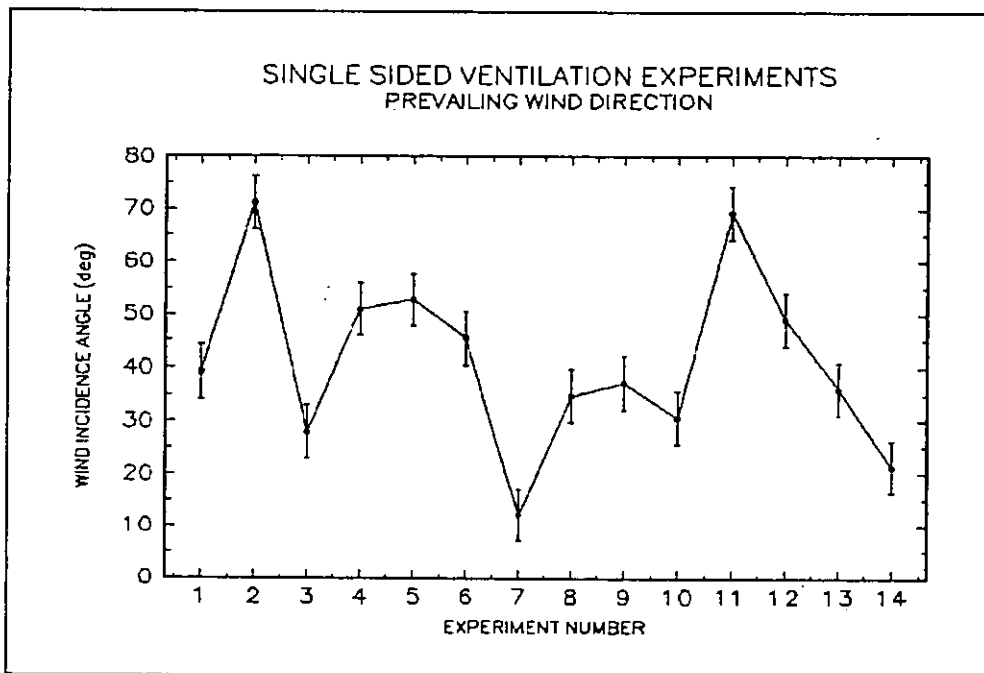


Figure A4.68: Average wind direction for each experiment

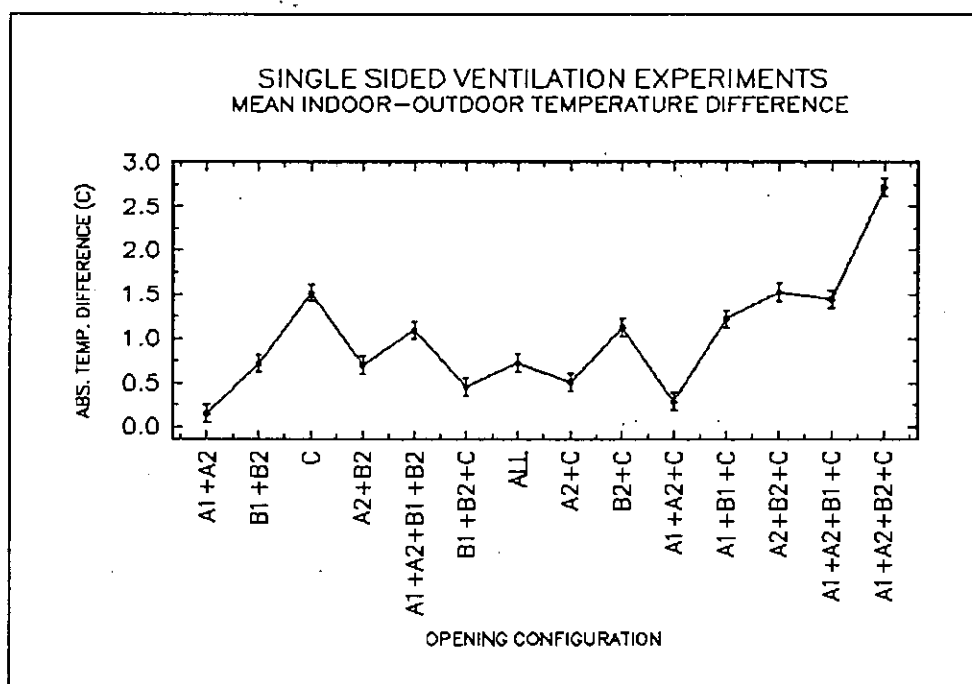


Figure A4.69: Absolute indoor-outdoor temperature difference for each experiment

Analysis of the climatic parameters has shown, that the experiments are characterised by important wind speeds and small temperature differences between the indoor and the outdoor environment, characteristics which are very close to real conditions observed in naturally ventilated buildings in hot climates. Therefore, it should be expected that the reported air flows would be dominated rather by inertia than by gravitational forces.

In order to separate data which are dominated by stack or wind effects the analysis, recommended by Warren [1978], is followed. This is done by plotting a "Warren-plot", where the ventilation parameter F is given as a function of the square root of the Archimedes number, Ar . The ventilation parameter, F , is defined by Warren [1986], and Crommelin and Vriens [1988] and refers to the case of a rectangular opening of area A , where the air flowing in through one half of the opening must flow out through the other half at least when mass conservation is assumed. This dimensionless parameter is given by the following equation :

$$F = \frac{Q}{A V} \quad (\text{A4.9.2})$$

where Q is the ventilation rate and V is the wind velocity. Convection phenomena are classified as natural, mixed or forced using as index the ratio of the Grashof to the square of the Reynolds number. This index is called Richardson number in the field of heat transfer, or Archimedes number, Ar , in ventilation engineering.

$$Ar = \frac{Gr}{Re^2} \quad (\text{A4.9.3})$$

where

$$Gr = \frac{g \Delta T H^3}{T V^2} : \text{the Grashof number}$$

$$Re = \frac{V L}{\nu} : \text{the Reynolds number}$$

ν : viscosity of the air [m^2/s]

H, L : characteristic lengths of the flow [m]

For the calculation of the Reynolds number the mean wind speed, V_{mean} during the experiment measured at a 10 meters height is used:

$$V_{\text{mean}} = \frac{1}{t_1 - t_2} \int_{t_2}^{t_1} V_i dt \quad [\text{m/s}] \quad (\text{A4.9.4})$$

where V_i is the instantaneous velocity component. For $Ar \gg 1$, convection is natural, while for $Ar \ll 1$ convection is forced. For values of Ar close to one, convection is considered as mixed. For the Warren plots the characteristic lengths H and L were taken equal to the vertical dimension of the opening. In this case, equation. A4.9.3 results in:

$$Ar_{(H=L)} = \frac{g \Delta T H}{T V^2} \quad (\text{A4.9.5})$$

where H is the opening height [m] and T is the temperature difference [$^{\circ}\text{K}$].

For large Archimedes number the stack effect will dominate, and taking into account that for stack effect we have that :

$$Q = 0.33 C_d W H \sqrt{\frac{g H \Delta T}{T}}, \quad [\text{m}^3/\text{s}] \quad (\text{A4.9.6})$$

where W is the width of the window. The measured values of the ventilation parameter F should approach an asymptotic value represented by :

$$F = 0.2 \sqrt{Ar} \quad \text{for} \quad C_d = 0.6 \quad (\text{A4.9.7})$$

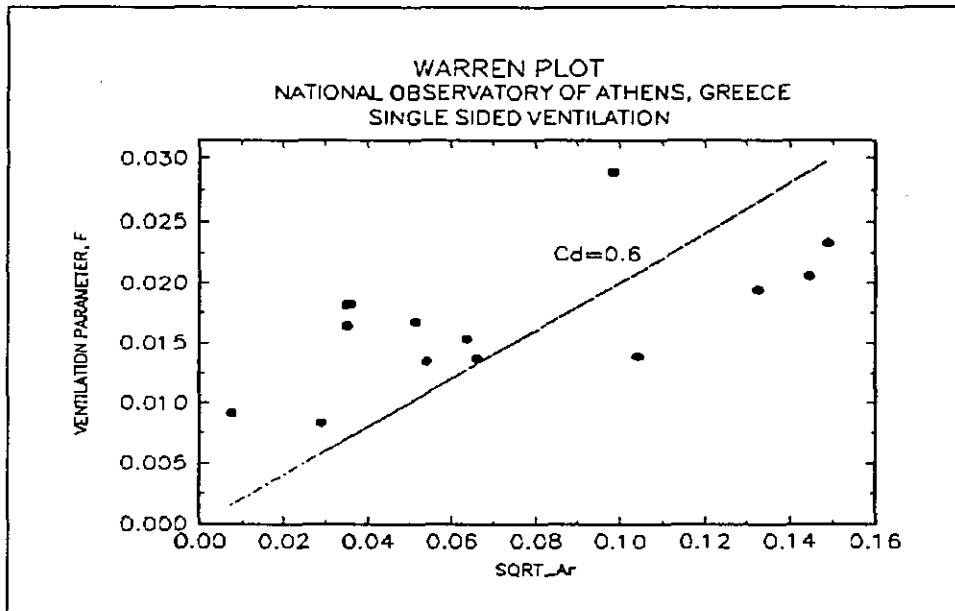


Figure A4.70: Warren Plot for the ventilation experiments carried out at the NOA building and the test cells using decay tracer gas methods.

The asymptote representing stack ventilation is given in the Warren plot in Figure A4.70. To isolate results attributable largely to wind effects, one can discard points lying along or close

to the line. As shown in Figure A4.70, the majority of the present set of data is characterised by the dominance of the wind rather than the stack effect.

The use of Warren-Plots has permitted to show that, for the present set of experiments, inertia forces dominates. However, it does not offer a quantitative evaluation of the relative importance of the phenomena.

Figure A4.71 shows the observed differences between predicted and measured air flow rates as a function of the Archimedes number, Ar , as defined in Equation A4.9.3. The r^2 of the regression is 0.59.

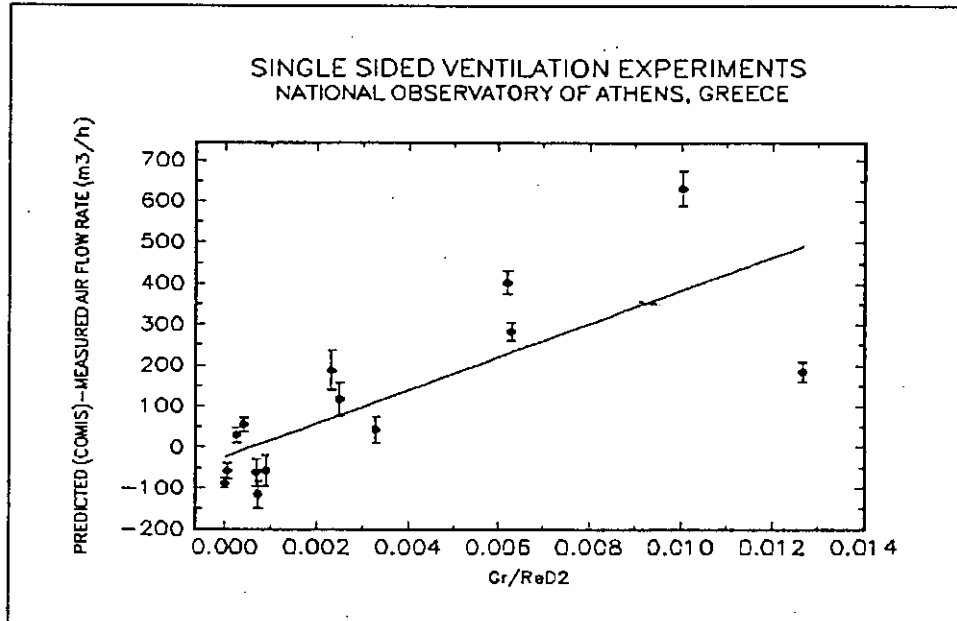


Figure A4.71: Difference between simulated and measured air flow rates as a function of the Gr/ReD^2 ratio for each experiment.

Taking the depth of the room, D , as a characteristic length, L , for the Reynolds number, we define Re_D :

$$Re_D = \frac{V D}{\nu} \tag{A4.9.8}$$

The room depth is defined as the distance between the wall, where the opening(s) is(are) and the wall opposite to it in the single sided ventilated zone. If this expression is used in equation. A4.9.3, the resulting expression for the Archimedes number, Ar_D , becomes:

$$Ar_D = \frac{Gr}{Re^2} = \frac{g H^3 \Delta T}{TV^2 D^2} = Ar_{(H=L)} \left(\frac{H}{D}\right)^2 \tag{A4.9.9}$$

For all the experiments carried out in Athens, Greece, the ratio Gr/ReD^2 is much lower than one and therefore it is evident, that inertia forces are much more important than the gravitational forces. Taking into account that network air flow modeling almost neglects wind speed variations for single sided ventilation configurations, an attempt has been made to study if the observed differences between the experimental and predicted values can be correlated with indices describing the relative importance of the inertia and gravitational forces. This was achieved by the following procedure:

COMIS has been used to predict the air flow for all the single sided ventilation experiments carried out in Greece. For all simulations a discharge coefficient, C_d , equal to 1 has been used. Then, for each experiment, a correction coefficient, CF , is calculated. This coefficient is defined as :

$$CF = \frac{\text{Mean Mesured Air Flow}}{\text{Predicted Air Flow}} \quad (4.9.10)$$

The correction coefficients, CF , as calculated for all the experiments is correlated with the Archimedes number, as previously defined. As shown in Figure 4.9.15, there is a very satisfactory correlation between both parameters and therefore the CF coefficient can be calculated, for single sided ventilation configurations, from the following expression :

$$CF = 0.08 \left(\frac{Gr}{Re_D} \right)^{-0.38} \quad (4.9.11)$$

where Re_D is the Reynolds number defined in eqn. 4.9.8.

The r^2 of the regression is calculated equal to 0.73.

Equation A4.9.11 predicts with sufficient accuracy the correction coefficient, CF , especially for experiments which are not characterised by an important fluctuation of the wind speed and incidence angle during the experiment.

A comparison of the measured air flow rates with values derived from simulations using COMIS with and without the Correction Factor is shown in Figure A4.73. The correlation coefficient between the set of measured air flow rates and the simulation results using the Correction Factor is equal to 0.88.

If the Correction Factor takes values under the limit of 0.6, then CF is taken equal to 0.6.

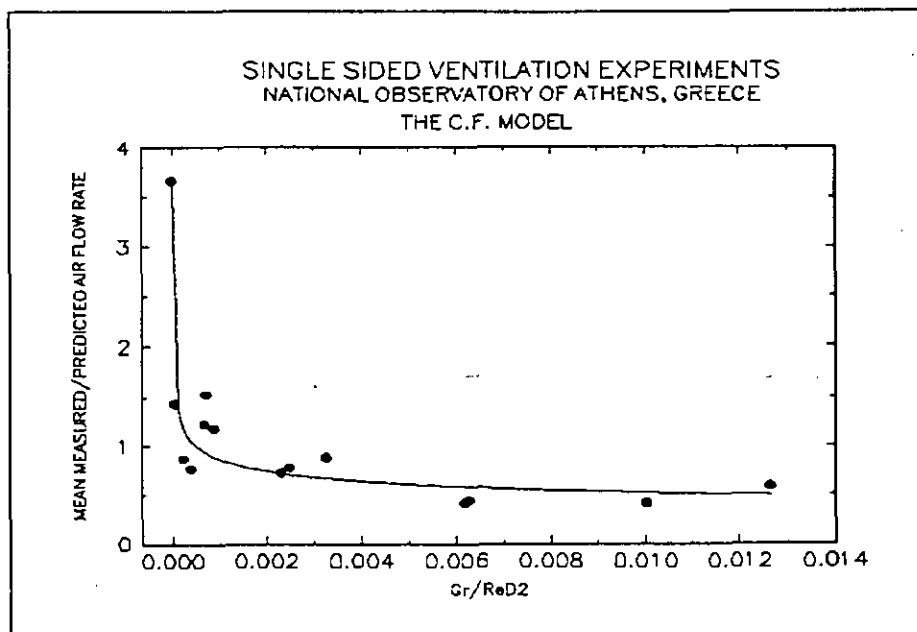


Figure A4.72: Correction coefficients as a function of $Gr/ReD2$.

Equation 4.9.11 can be used to correct the predictions of COMIS as well as those of any network air flow model for single sided configurations. The validity of the formula given by

Equation 4.9.11 should be limited for cases where inertia forces are dominant compared to gravitational forces, i.e. for important wind speeds.

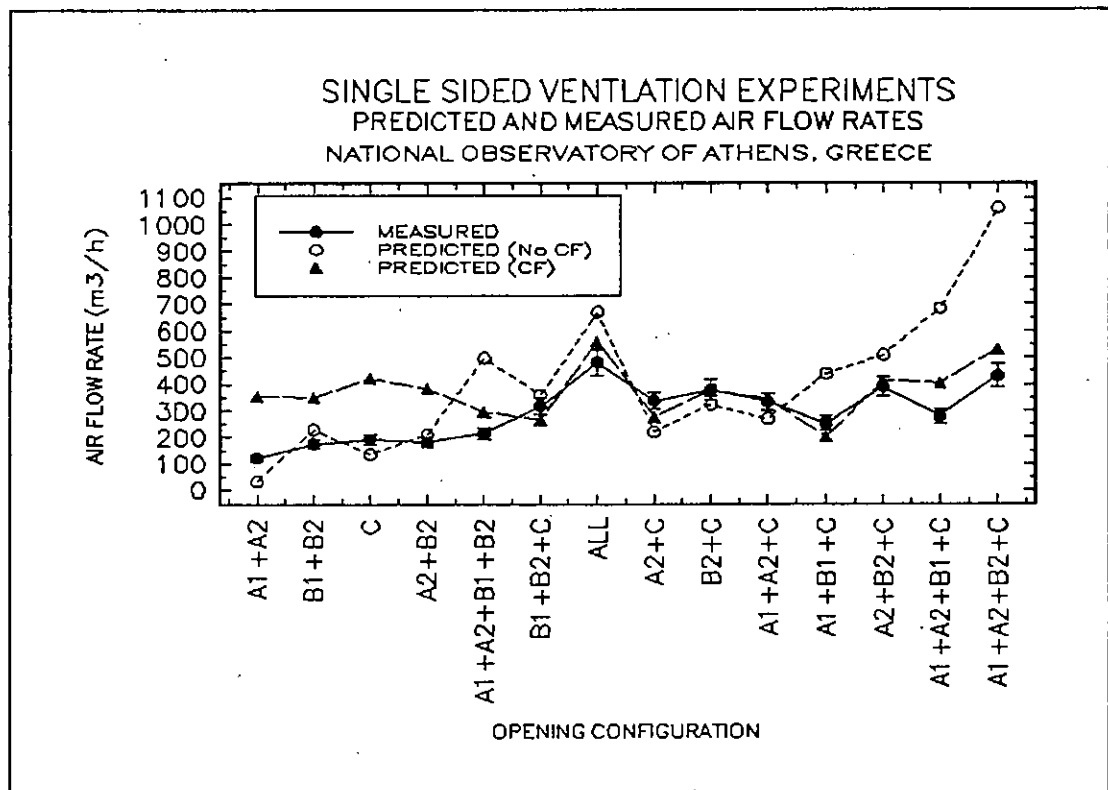


Figure A4.73: Measured air flow rate for each experiment as well as simulated values without the use of any correction factor and the use of the proposed correction factor.

It must be pointed out that the CF model was based on data from experiments with wind speed ranging from 2 to 10 m/s and temperature differences from 0.5-8 °C. The room depth varied from 3-7 m. The prevailing wind direction during the experiments varied from -60 to 60 degrees from the vertical to the opening.

A more extended discussion of single sided ventilation phenomena is given in [Dascalaki 1994].

A 4.8.5 Conclusions

Single sided ventilation configurations are very common in buildings. Prediction of the air flow rates can be achieved using mainly network air flow models like COMIS. Based on an extended experimental program predictions of COMIS have been compared with measured air flow rates. It was found that, for cases where inertia forces are more important than gravitational forces, a systematic difference exists between predicted and experimentally derived values.

A Correction Factor, based on the climatological and geometrical characteristics of each configuration, is proposed in order to consider appropriately the impact of inertia forces to the total air flow. The proposed methodology improves considerably the accuracy of COMIS in predicting the air flow rate in the case of single sided ventilation configurations.

A 4.8.6 References

- Warren P.R. : The analysis of Single Sided Ventilation Measurements. *Air Infiltration Review*, 7, 2, p.p. 3-5, (1986).
- Crommelin R. D. and Vrins E.M.H. : Ventilation Through a Single Opening in a Scale Model. *Air Infiltration Review*, 9,3, p.p. 11-15, (1988).
- Dascalaki E., Santamouris M., Argiriou A., Helmis C., Asimakopoulos D.N., Papadopoulos K. and A. Soilemes : Predicting Single Sided Natural Ventilation Rates in Buildings". *Submitted to J. Solar Energy*, (1994).
- Liddament M.W. (1988). *Air Infiltration Calculation Techniques - An Application Guide*. AIVC, IEA, Coventry, U.K.

A 4.9 Italgas House

A 4.9.1 Measured object: Italgas House

Experimental work on gas appliances can be conducted in different settings, i.e., in the laboratory - a situation which is mostly suitable for characterising the performance of individual systems or components under strictly controllable and repeatable conditions - or in the field, when real installations are examined.

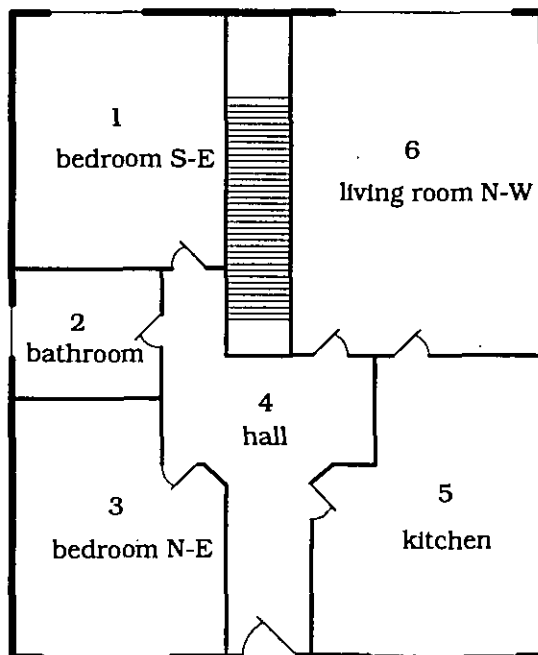


Figure A4.9.1:- Plant view of one Italgas House

Based on past and present experience, acquired both in field and laboratory research, a third intermediate approach has been followed by the Italian gas utility "Italgas": an experimental facility has been built in Venaria (Torino) and put into operation in 1990, which consists of two identical single-family buildings (House A and House B). The buildings - which are realistic examples of current building practice in the residential sector in Italy - are very flexible in terms of thermal systems installation, and are fully instrumented for monitoring relevant parameters such as ambient temperatures, meteorological conditions, combustion analyses, etc.

These buildings consist of two stories: the lower floor hosts the centralised service equipment and the data acquisition and processing system; the ground floor (in which the tests were performed) has a floor area of 114 m², and includes two bedrooms, a living room, a bathroom and a kitchen. If necessary, the attic space

above the ground floor can be heated, so that the test story may also reproduce the thermal condition of an apartment in a multistorey building. A plan view of the test area is shown in Figure A4.9.1

A 4.9.2 Measurements performed

Tracer gas measurements

The experimental apparatus: All the measurements were carried out with the decay technique. The experimental apparatus has been developed at Dipartimento di Energetica of the Politecnico di Torino.

The first version of the apparatus, utilised in March 1991 was a compact and mobile multi-tracer gas system controlled by a PC laptop computer based on an Intel 80C286 12 MHz processor. It utilises two compatible I/O boards and an infrared photometer for the measurement of the nitrogen protoxyde (N₂O) has been included.

In the next measurements (March 1992, October 1992 and January 1994) an upgraded version of the experimental apparatus was utilised. An infrared photometer for the measurement of the sulphur hexafluoride (SF₆) concentration was added. Compactness and portability characteristics have also been improved in this version: the weight was reduced by means of a new type

of solenoid valves, and the valves of each zone are assembled together in a single box that may be removed from the rack at anytime.

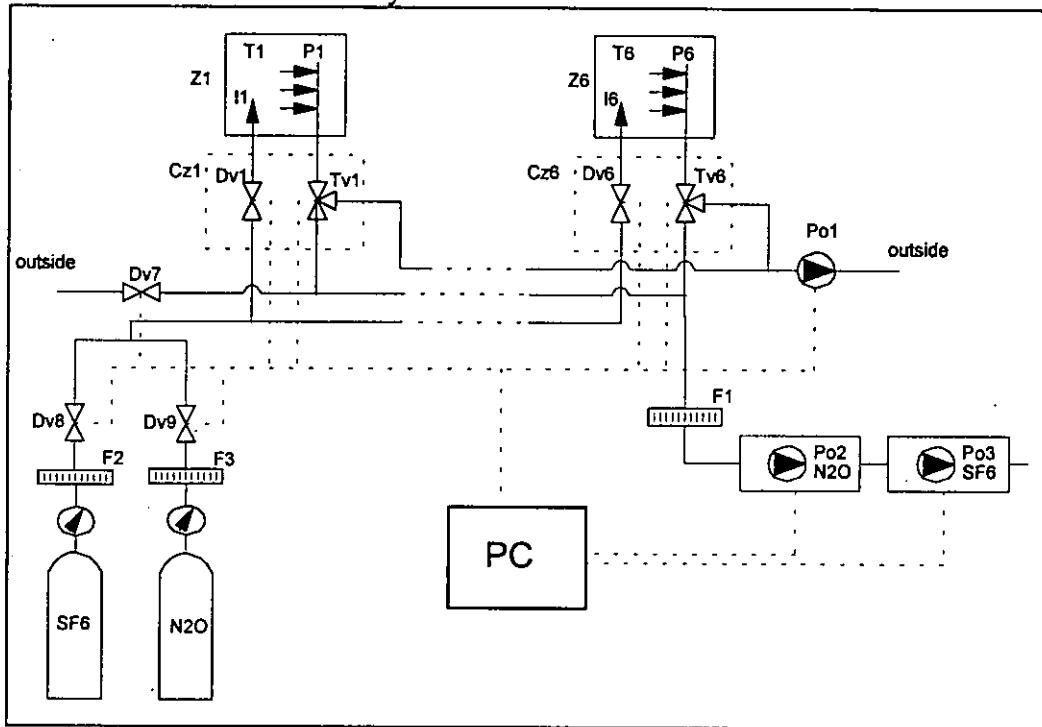


Figure A4.9.2 - Scheme of tracer gases apparatus

Air samples were taken at six different locations throughout the whole house using vertical plastic tubes, radially perforated on the lateral surface. A platinum resistance thermometer, installed inside an aluminium tube connected to the plastic tube for radiation shielding, was used to measure the air temperature. In order to achieve uniform tracer gas mixing, two fans were operated within the room and tracer gas was injected immediately upstream of the fan rotor. As it can be seen in the scheme of Figure A4.9.2, the air sampled at points P1-P6 can be either sent to the analyser or discharged outdoors, depending on the three-ways valve setting. Pump Po1 allows continuous sampling, avoiding the lag time for tube flushing at each change of monitoring zone.

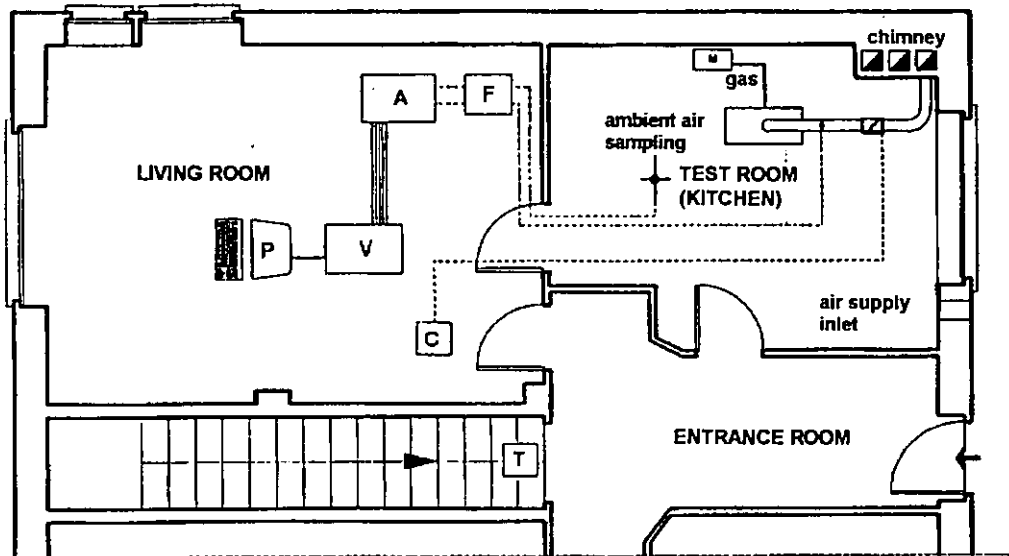
Measurements performed: The tracer gas measurements, analysed here, have been carried out in two different periods: October 1992 and January 1994.

The main characteristics of the measurements are summarised in Table A4.9.3. The first column is the code of the test; the character G means "group" and the next numbers are progressive numbers which start from '1' for every new group. The second column is the date and the third is the time period of the test in seconds. The fourth column is the number of zones while the fifth is the number of tracer gases used in the tests. Finally, in the last column the test characteristics are described.

During the tests on October 1992 (see Table A4.9.3) the air change rate in the dwellings with small gas-fired individual units for space heating and service hot water production, has been measured in order to investigate the influence of purpose-provided ventilation openings (sized according to the national UNI-CIG 7129-72 standard) on air changes and indoor air quality. During these tests, the air supply area of the purpose-provided opening was set respectively to 0%, 50% and 100%; and the chimney cross section was varied from 25% to 100%. In Figure A4.9.3 the plan view of the test area and the instrumentation used during the tests are shown.

Table A4.9.3 - Summary of experimental measurements in the ITALGAS Houses

Test code	Date	Period [s]	Zone Nr	Tracers	Notes
G3-04	07-10 1992		1	SF ₆	- air supply area 100%; - chimney cross section 100%
G3-05	07-10 1992		1	SF ₆	- air supply area 100%; - chimney cross section 50%
G3-06	08-10 1992		1	N ₂ O	- air supply area 100%; - chimney cross section 25%
G3-07	08-10 1992		1	N ₂ O	- air supply area 50%; - chimney cross section 100%
G3-08	08-10 1992		1	N ₂ O	- air supply area 50%; - chimney cross section 50%
G3-09	08-10 1992		1	N ₂ O	- air supply area 50%; - chimney cross section 25%
G3-10	08-10 1992		1	N ₂ O	- air supply area 0%; - chimney cross section 100%
G3-11	08-10 1992		1	N ₂ O	- air supply area 0%; - chimney cross section 50%
G3-12	08-10 1992		1	N ₂ O	- air supply area 0%; - chimney cross section 25%
G3-15	09-10 1992	3809	2	N ₂ O SF ₆	- only internal doors of room 5 are closed; - the air samples in the rooms 1,2,3,4,6 are mixed before reaching the analyser; - N ₂ O is injected in rooms 1,2,3,4,6; - SF ₆ is injected only in room 5; - air supply area 50%; - chimney cross section 50%
G3-16	09-10 1992	4288	2	N ₂ O SF ₆	- only internal doors of room 5 are closed; - the air samples in the rooms 1,2,3,4,6 are mixed before reaching the analyser; - N ₂ O is injected in rooms 1,2,3,4,6; - SF ₆ is injected only in room 5; - air supply area 0%; - chimney cross section 50%
G4-03	14-01 1994	4813	2	N ₂ O SF ₆	- only internal doors of room 5 are closed; - the air samples in the rooms 1,2,3,4,6 are mixed before reaching the analyser; - N ₂ O is injected in rooms 1,2,3,4,6; - SF ₆ is injected only in room 5
G4-04	14-01 1994	4184	2	N ₂ O SF ₆	- only internal doors of room 6 are closed; - the air samples in the rooms 1,2,3,4,5 are mixed before reaching the analyser; - N ₂ O is injected in rooms 1,2,3,4,5; - SF ₆ is injected only in room 6



- | | | | |
|---|-------------------|-------|---|
| M | gas inlet | C | motor driven damper (butterfly valve) control |
| P | personal computer | T | tracer gas apparatus |
| F | gas dryer | ----- | damper control line |
| A | gas analyser | | air/gas sampling line |
| V | voltmeter | | |

Figure A4.9.3 - Plan view of the test area

The networks corresponding to experimental measurements: The experimental measurements are carried out with one or two tracer gases (N_2O and or SF_6). When two tracers have been used the concentration data is analysed with a two zones model whereas in the other test (only one tracer gas) a single zone system has been studied.

In Figure A4.9.4, Figure A4.9.5 and Figure A4.9.6 the networks used for the tests analysis and the calculated air flow rate are shown. Here the word ZONE means a part of the space limited by a boundary fixed only during the test, whereas ROOMS are always fixed for all the tests as shown in Figure A.4.10.1. Therefore a ZONE may be a room or a set of rooms.

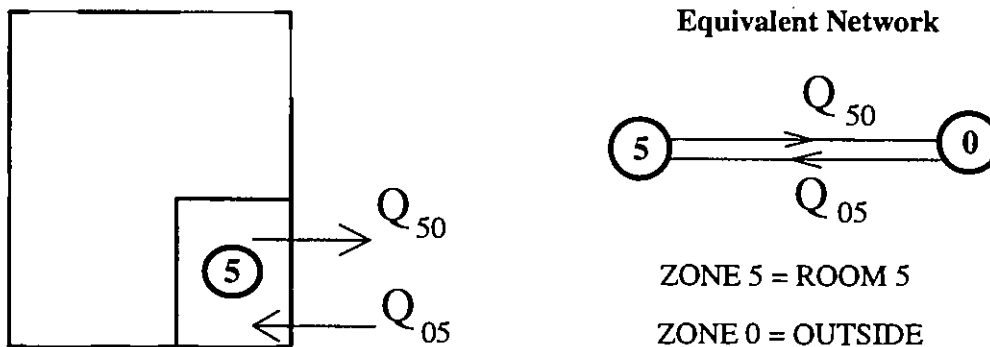


Figure A4.9.4 - Experimental network for the single zone tests from G3-04 to G3-12

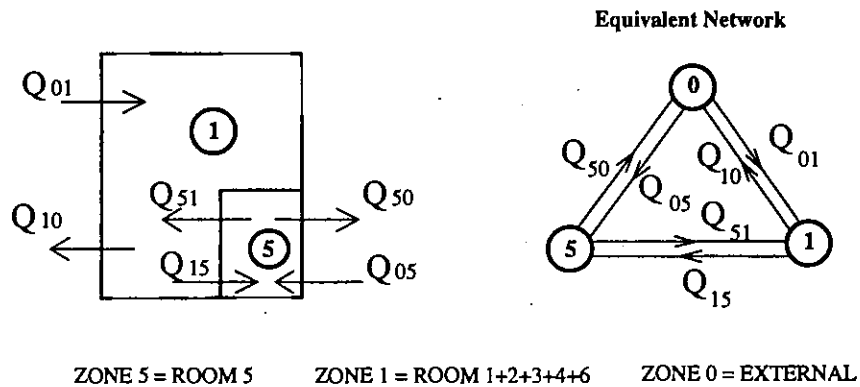


Figure A4.9.5 - Experimental network for the two zone tests G3-15, G3-16 and G4-03

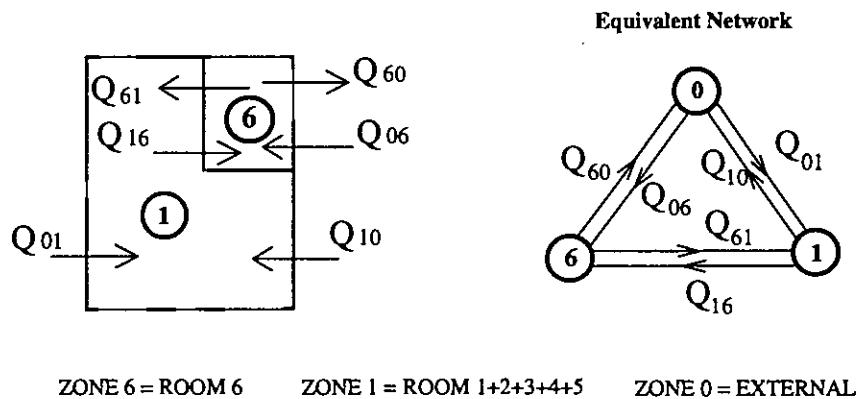


Figure A4.9.6 - Experimental network for the two zone test G4-04

Meteorological Data

The Italgas House has a meteorological station. The data are continuously monitored and saved in a storage unit (i.e. hard disk or tape device). For each time step the following data is recorded:

- 1) External temperature ($^{\circ}\text{C}$).
- 2) Absolute barometer pressure (hPa)
- 3) Relative humidity (%)
- 4) Solar radiation (W/m^2)
- 5) Wind velocity (m/s)
- 6) Wind direction (degree)
- 7) Rain (mm)
- 8) Time (s)

For the measurement of October 1992 the Italgas Data are available only each 15 minutes while for the last measurements (January 1994) the meteorological data was recorded every minute to improve the COMIS comparison.

Air permeability measurements

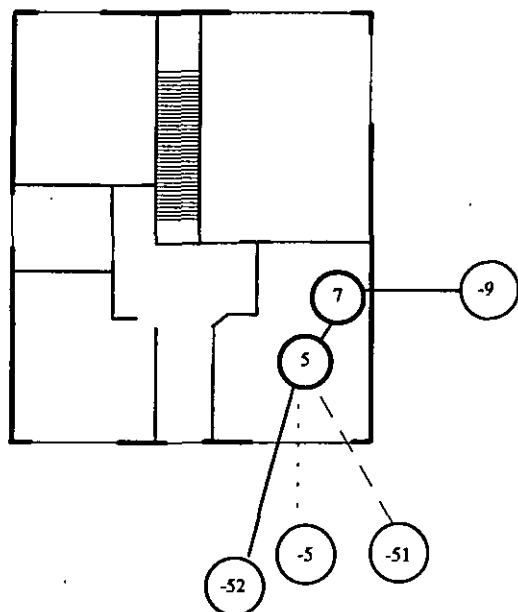
A series of pressurisation tests have been carried out in the Italgas houses in recent years [M. Masoero, V. Fracastoro, D. Vercelli, 1991]. The guarded zone method has been used with two Minneapolis blower doors (the device consists of a variable speed fan and a means of sealing the fan into the doorway). These tests were performed mainly to define the wall per-

meability, that is the characteristic of the crack between inside and outside. For the crack coefficients of the internal doors, the values from the AIVC data base have been used.

A 4.9.3 COMIS simulation

Networks for COMIS input files

The Italgas Houses, and probably all houses, can be described using a lot of different networks. When all doors are open, the user of COMIS could use one node for all rooms or six nodes (one for each room) linked by large openings. The results shown here refer to the first possibility (one node) since the analysis performed using large openings has provided the same numerical values (Borchiellini et al, 1995).



Node 7 has been used for all tests of October '92 for representing the gas fired unit (the boiler); it is connected with the external environment (node -9) by a link that corresponds to the chimney. The link between node 5 and node -52 represents the purpose provided ventilation opening.

The coefficient C_s for closed window and door are divided in two parts: half on top and half on the bottom. So the external nodes are two for each windows and the C_p values are obtained from COMIN C_p routine. In Figure A4.9.7 to Figure A4.9.9, the dotted lines are the lower links and the dashed lines are the upper links.

The internal absolute humidity and the temperature in each room have been measured during the tests. The time variation of the internal temperature was described using the temperature schedule option of

Figure A4.9.7 - COMIS networks for tests from G3-04 to G3-12

COMIS.

The COMVEN version used is 1.2 for MS-DOS and the input files have been written using an editor.

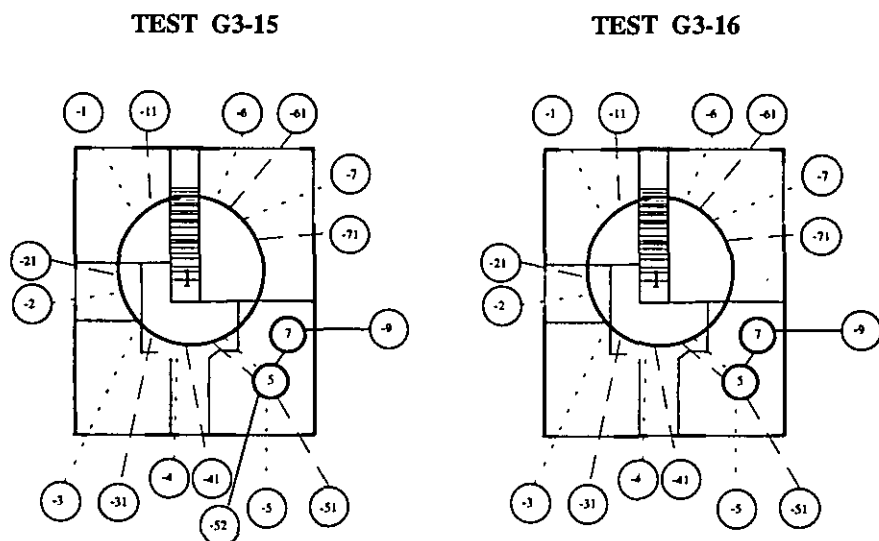


Figure A4.9.8 - COMIS networks for tests G3-15 and G3-16

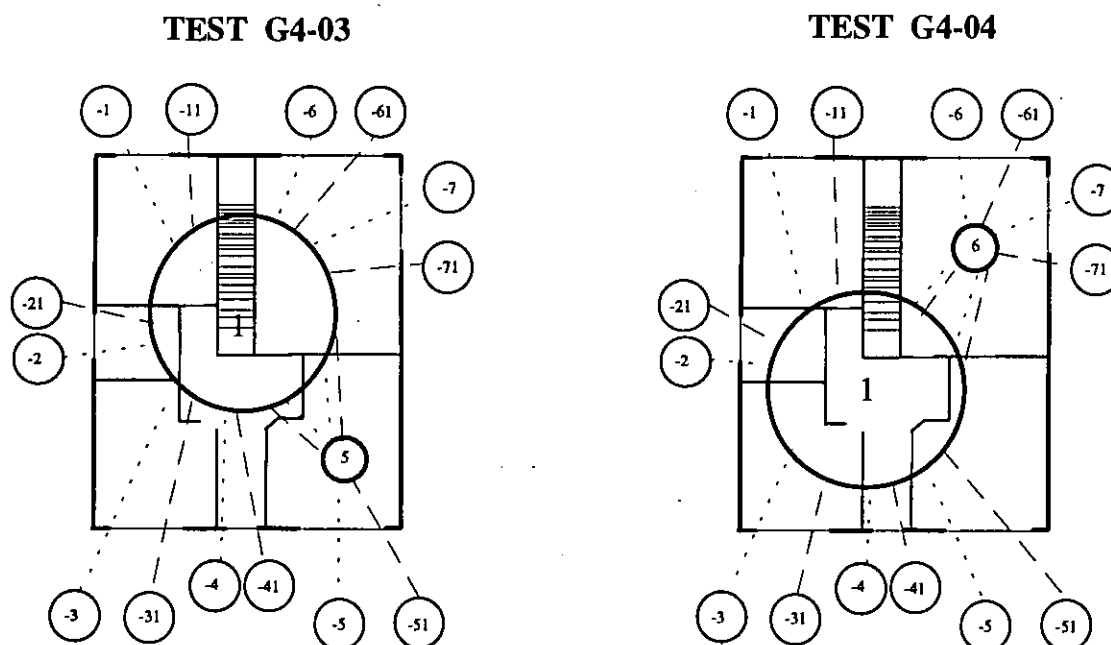


Figure A4.9.9 - COMIS networks for tests G4-03 and G4-04

COMIS results and sensitivity analysis

The first results from sensitivity analysis of the COMIS results for the Italgas Houses are illustrated in Fürbringer et Borchiellini (1993). The complete sensitivity analysis of the COMIS results for each test has been performed using the Monte-Carlo method with the help of MISA (Multirun Interface for Sensitivity Analysis) [Fürbringer, 1994].

For each parameter, the range used for the Monte-Carlo analysis is illustrated in Table A4.9.4; the number of parameters and the number of simulations used for each test is given in Table A4.9.5.

Table A4.9.4 - Parameters range for the Monte-Carlo Analysis

Parameter	Range	Parameter	Range
Crack permeability, [kg/s @ 1 Pa]	±25%	Indoor humidity, [g/kg]	±10%
Crack exponent, [-]t	±10%	Pressure coefficient, [-]	±50%
Duct diameter, [m]	±0.50%	Altitude meteo station, [m]	±1%
Duct roughness, [mm]	±50%	Wind exponent, [-]	±10%
Duct length, [m]	±0.50%	Surrounding build. height, [m]	±10%
Single resistance, [-]	±5%	Outside temperature, [°C]	±1 [°C]
Single resistance butterfly valve, [-]	±25%	Outdoor humidity, [g/kg]	±10%
Zone temperature, [°C]	±1 [°C]	Atmospheric pressure, [kPa]	±0.50%
Zone volume, [m ³]	±5%	Wind speed, [m/s]	±0.3 [m/s]*

* As the wind speed is very close to zero (often the wind speed is zero) in tests analysed here, this error range has been used to take into account the possibility of wind speed fluctuation.

Table A4.9.5 - Number of parameters and simulation used for the Monte-Carlo analysis

Test	Parameters	Simulation
G3-04 ÷ G3-12	32	300
G3-15 and G3-16	58	300
G4-03 and G3-04	40	300

A 4.9.4 Comparison

The compared flows

To compare experimental results and COMIS results the same air flows must be compared. The COMIS flows are more detailed, in fact the number of links in the networks of Figure A4.9.7, Figure A4.9.8 and Figure A4.9.9 are larger than the number of links in Figure A4.9.4, Figure A4.9.5 and Figure A4.9.6.

Table A4.9.6 - The compared flows

Test Code	Experimental flows	COMIS flows *
From G3-04 to G3-12	$Q_{50} = Q_{05}$	$\sum Q_L \cdot \delta_{50} + \sum Q_L \cdot \delta_{70} = \sum Q_L \cdot \delta_{05} + \sum Q_L \cdot \delta_{07}$
G3-15	Q_{51}	$\sum Q_L \cdot \delta_{51}$
G3-16	Q_{15}	$\sum Q_L \cdot \delta_{15}$
and	Q_{05}	$\sum Q_L \cdot \delta_{05} + \sum Q_L \cdot \delta_{07}$ (if zone 7 exist)
G4-03	Q_{01}	$\sum Q_L \cdot \delta_{01}$
G4-04	Q_{61}	$\sum Q_L \cdot \delta_{61}$
	Q_{16}	$\sum Q_L \cdot \delta_{16}$
	Q_{06}	$\sum Q_L \cdot \delta_{06}$
	Q_{01}	$\sum Q_L \cdot \delta_{01}$

* Note:
$$\sum Q_L \delta_{ij} = \sum_{L=1}^{N_L} Q_L \delta_{ij}$$

where: L = L-th link
 N_L = number of links from the i-th zone to the j-th zone.
 Q_L = air flow rate in the L-th link
 δ_{ij} = 1 if Q_L goes from zone i to zone j
 δ_{ij} = 0 if Q_L goes from zone j to zone i

Table A4.9.6 shows the "conversion" of the COMIS flows into the experimental flows. For the single zone tests only the air change rate can be compared, because the internal flows are

not known from the experimental results. Instead, the flows between room 5 (or 6) and the other zone are also compared for the two zone tests (G3-15, G3-16, G4-03 and G4-04).

Comparison

In this paragraph, the comparison between the measured and simulated air flows is illustrated by means of diagrams in which for each value the confidence interval, for 99% probability, is represented.

The measured flows are estimated from the time histories of the tracer concentrations, solving an inverse problem [Roulet and Vandaele 1991]. In the approach used here the air flows are considered to be functions of time. That is for each instant at which the concentrations are measured, a value of the air flow rates is estimated and a standard deviation is associated to this value [Borchiellini and Cali 1992]. The value of standard deviation is related to the experimental uncertainties, to the correlation existing among the estimated flows and to the derivative of the concentration with respect to the air flows [Sherman 1989]. Therefore, the standard deviation may be different for different times of the same air flow function and may also change from one parameter to another, of the parameter set, estimated from the same concentration data.

The simulated flows are the COMIS flows. For tests G3-15, G3-16, G4-03 and G4-04, the air flows have been calculated for many different times, the confidence interval has been calculated for one time only of each test and then used for the remaining times.

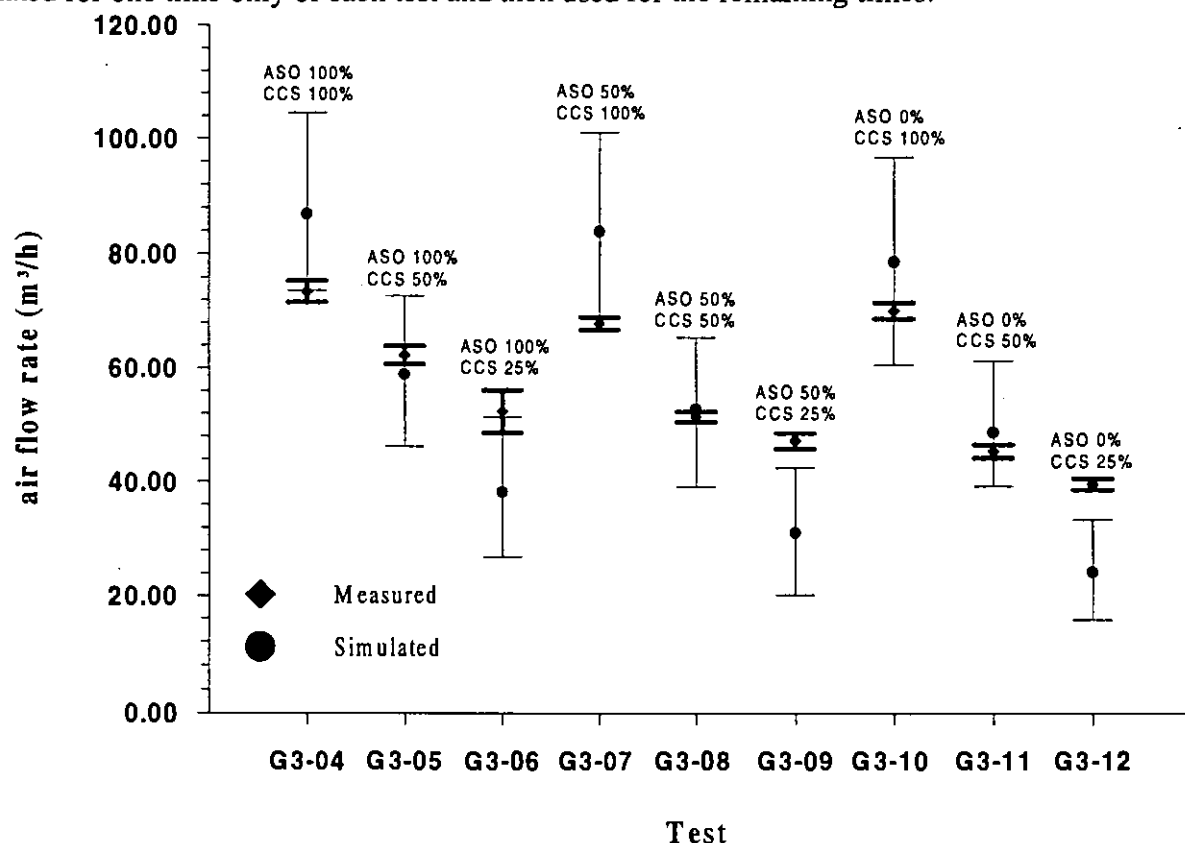


Figure A4.9.10 - Simulated and measured air flow rates for tests G3-04 ÷ G3-12; ASO = Air Supply Opening and CCS = Chimney Cross Section

Figure A4.9.10 refers to the single zone tests (G3-04 ÷ G3-12). The simulated and the measured air flow rate compared in this Figure are the total net flow of zone 5 which, in these tests, corresponds to the air flow from outside to zone 5 (Q_{05}). In the same Figure A4.9.10, for each

test, the Air Supply Opening (ASO) and the Chimney Cross Section (CCS) are specified in order to simplify the understanding of the influence of the purpose-provided ventilation opening and the butterfly valve position on the room ventilation.

When the chimney cross section is 50% one can notice a better agreement between measured and simulated values (differences between 5% and 7%) than those obtained for a chimney cross section of 25% and 100%. The simulated air flows are underestimated by 27% to 39% for a chimney cross section of 25%. Instead for a chimney cross section of 100% the simulated air flows are overestimated by 12% to 24%.

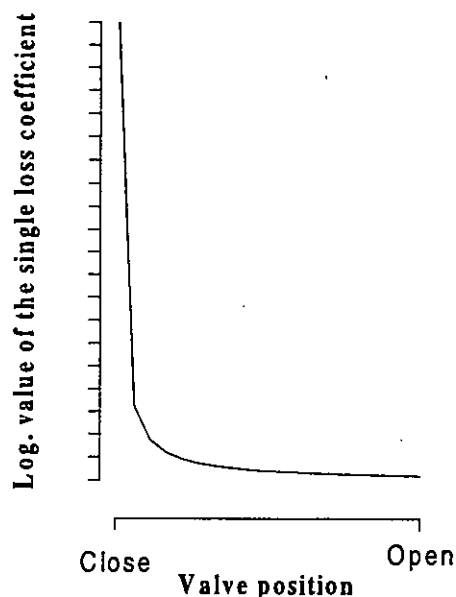


Figure A4.9.11 - Valve single loss coefficient

ing the butterfly valve. Probably for such high values of the single loss coefficient a greater error range than 25% should be used, since when a valve is near to the closed position a high variation of the single loss coefficient, is associated to a small error in the knowledge of the valve position (see Figure A4.9.11).

The last tests of October '92 (G3-15 and G3-16) are two zone tests and the comparison is illustrated in Figures 4.10.15 to 4.10.15. As the information provided by these cases is almost the same, the comparison is analysed here for both cases at the same time. The names used in the diagram for the air flow rates refer to the measured network. See Table A4.9.6 for the equivalence with the simulated flows.

A good agreement is found for the internal flow from zone 5 to zone 1. However, the simulated air flow from zone 1 to zone 5 is about 30% less for G3-15 and 15% less for G3-16 than the measured flow (see Figure A4.9.13 and Figure A4.9.15).

For tests G3-15 and G3-16, in which the chimney cross section is 50%, the simulated flow rates in the chimney (Q_{50}) are very close to the experimental values, as was found in the previously examined single zone tests (see Figure A4.9.10) with a chimney cross section of 50% (G3-05, G3-08 and G3-11)

Both flows between zone 1 and outside (Q_{01} and Q_{10}) are under-evaluated by 67% for G3-15 and 51% for G3-16. This high discrepancy can be explained by taking into account certain clues that indicate an imperfect sealing of some openings (i.e. sink in the bathroom, air ventilation grilles, etc.) that were perfectly sealed during the pressurisation measurements (ageing problems). As these opening are mainly located outside room 5, this imperfect sealing could

The analysis of these results show the strong influence of the chimney stack effect on the room ventilation and therefore special attention should be given to the choice of the single loss coefficient representing the butterfly valve as many different values can be found in literature. An agreement close to that found when the chimney cross section is 50% could, in fact, be reached for the simulation results of the remaining tests by only changing the values of the single loss coefficient of the butterfly valve. For these reasons, a wide error range (25%) was used in the Monte-Carlo analysis for this parameter (see Table A4.9.4).

There are only two tests in which the error range of the simulated value and the error range of the measured value do not overlap (G3-09 and G3-12); in both tests the chimney cross section is 25%. That corresponds to the maximum value of the single loss coefficient representing

be the reason why only for the flows Q_{01} and Q_{10} (and consequently for Q_{total}) the error ranges do not overlap.

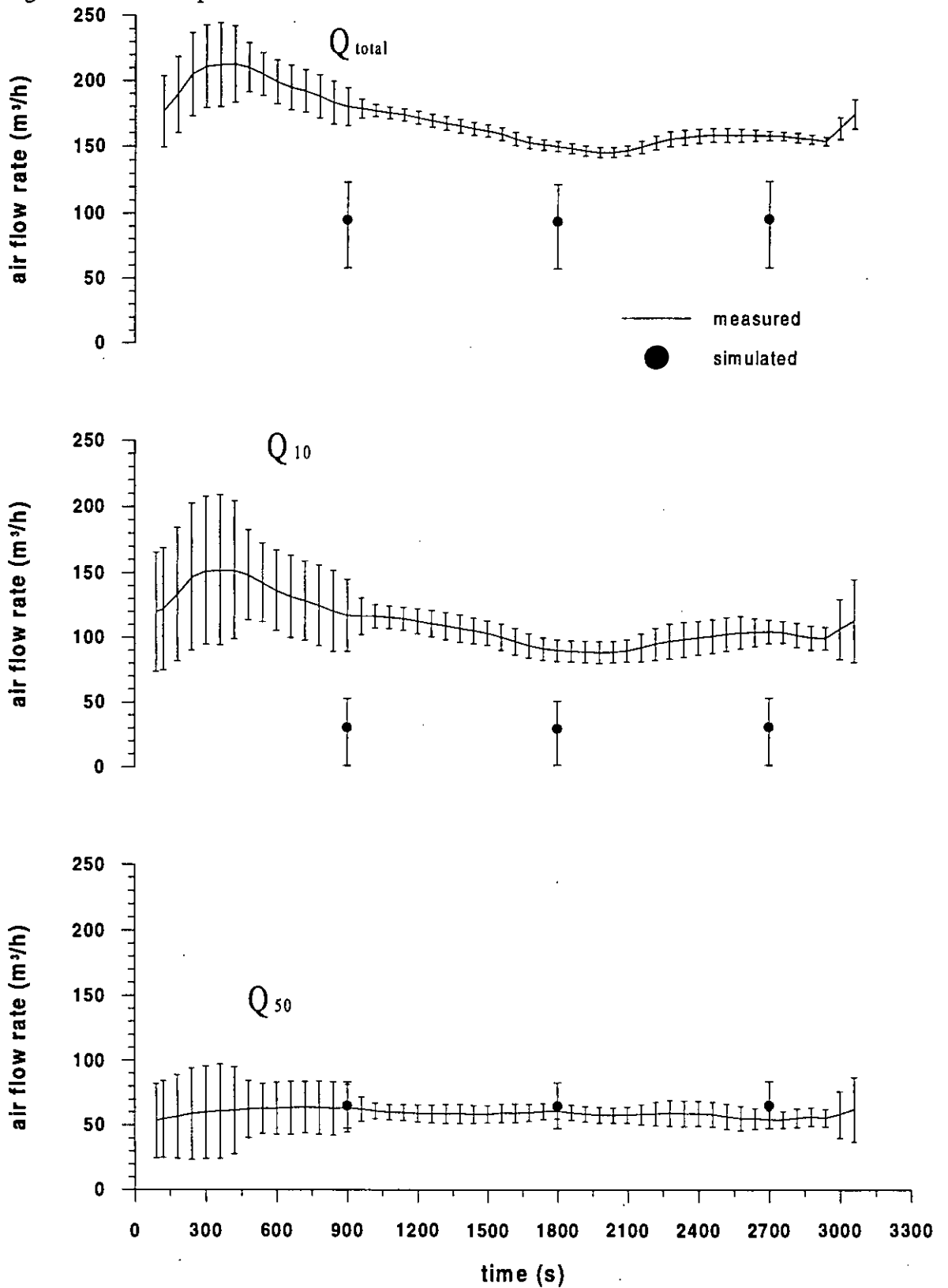


Figure A4.9.12 - Simulated and measured air flow rates Q_{total} , Q_{10} , Q_{50} for test G3-15

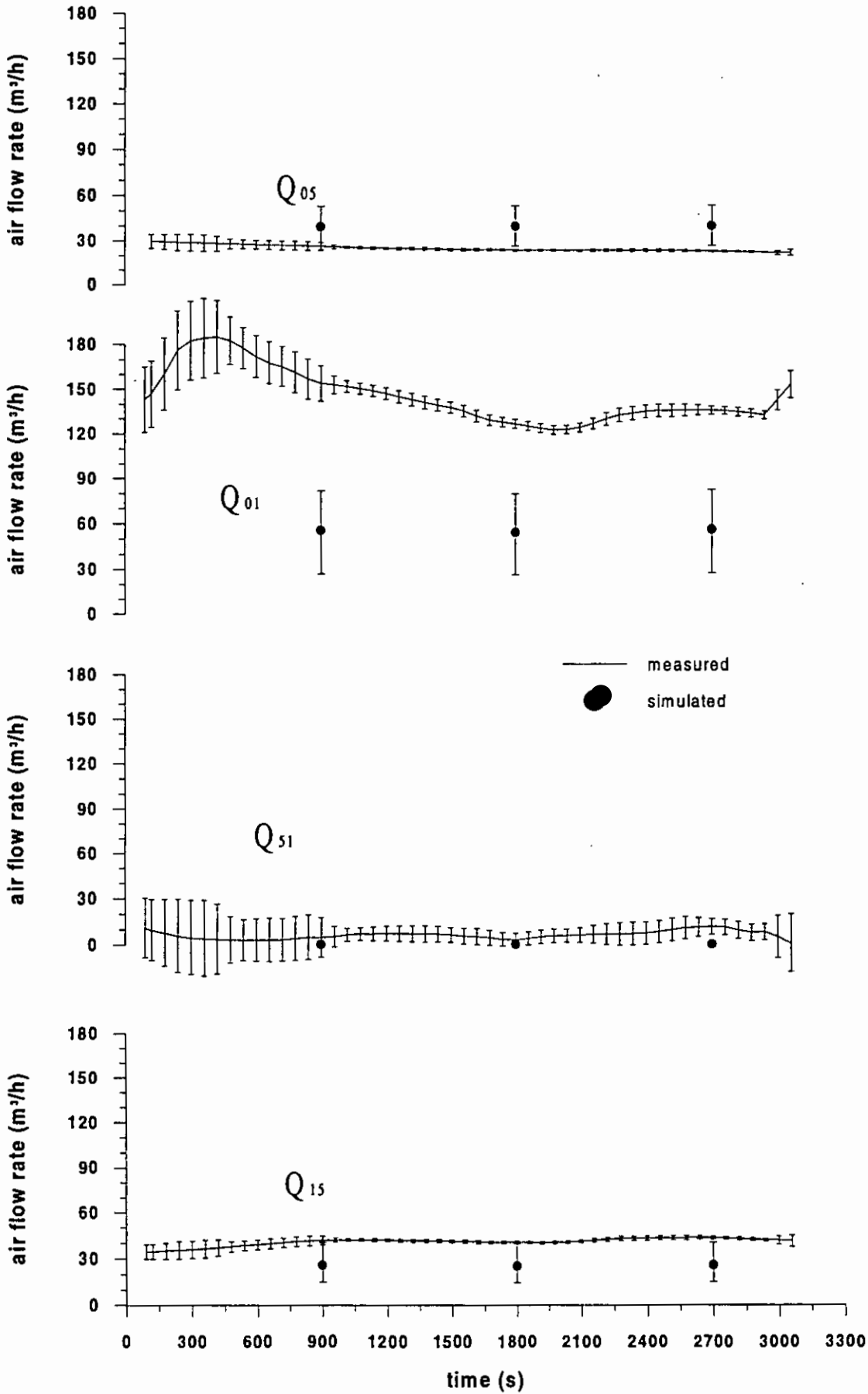


Figure A4.9.13 - Simulated and measured air flow rates Q_{05} , Q_{01} , Q_{51} , Q_{15} for test G3-15

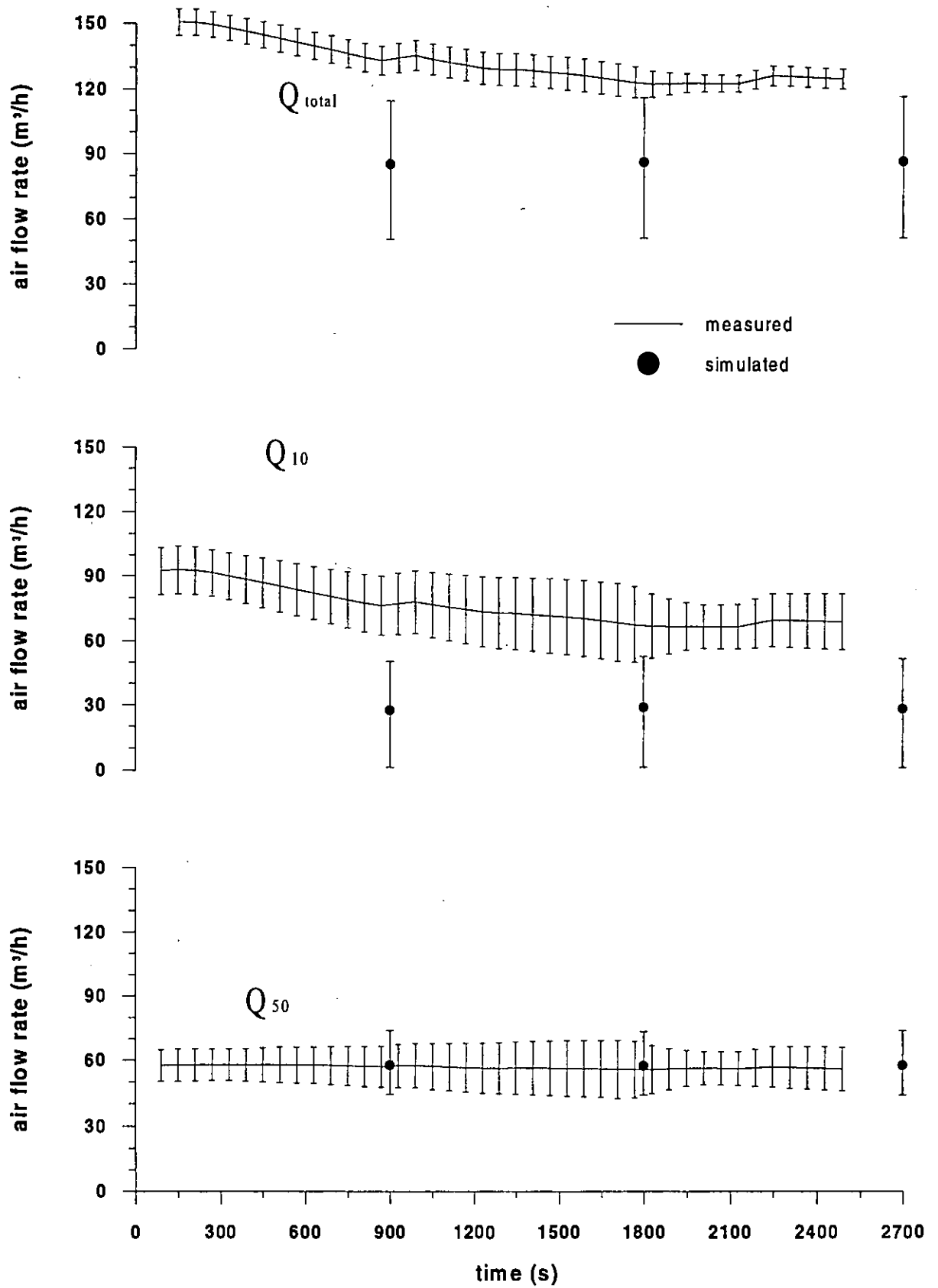


Figure A4.9.14 - Simulated and measured air flow rates Q_{total} , Q_{10} , Q_{50} for test G3-16

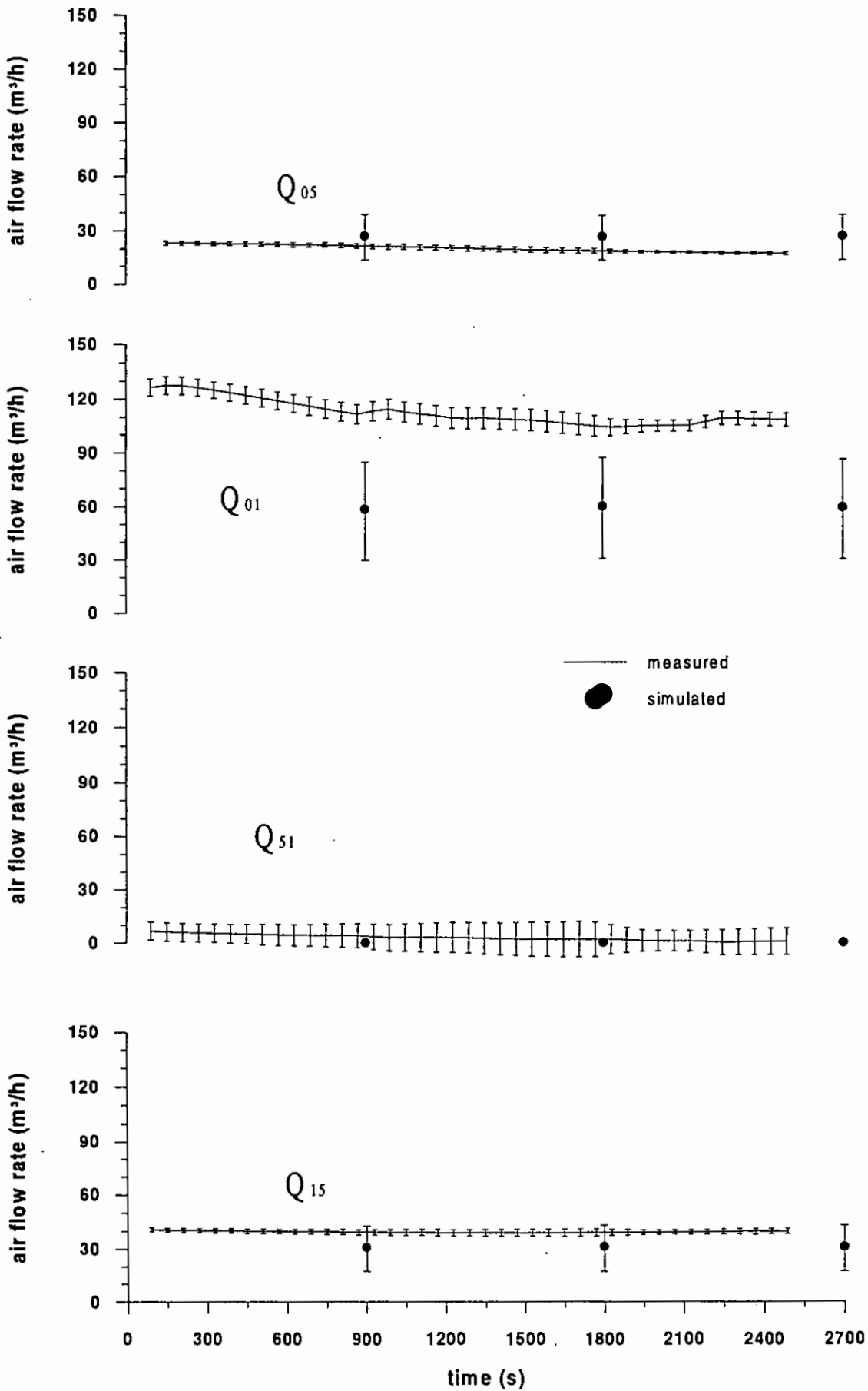


Figure A4.9.15 - Simulated and measured air flow rates Q_{05} , Q_{01} , Q_{51} , Q_{15} for test G3-16

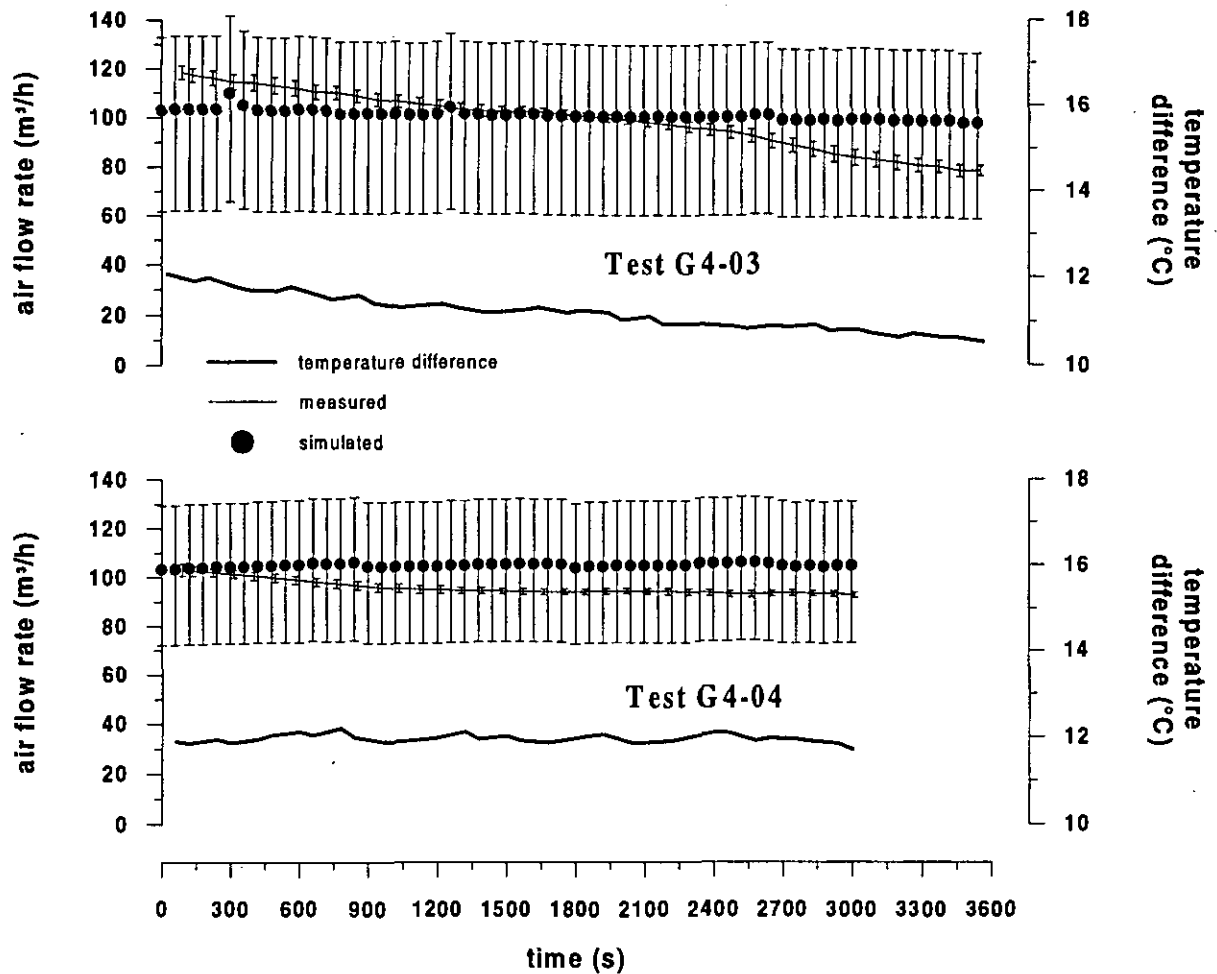


Figure A4.9.16 - Total flow rate for test G4-03 and G4-04

The tests of January '94 have been carried out after a new sealing of the openings which were not characterised during the pressurisation measurements, in order to avoid the previously described ageing problem.

These tests were performed without the gas fired unit and the purpose-provided opening. As for the measurement of October '92, when the wind velocity was very low or zero, these tests refer to a system in which the air flows are mainly driven by the thermal buoyancy due to temperature difference between inside and outside. For this reason, in Figure A4.9.16 the temperature difference is plotted together with the measured and simulated total flow rate for tests G4-03 and G4-04.

For test G4-04 a good agreement is found both between the mean value of the simulated and experimental flows and between the experimental air flow trend and the temperature difference trend; furthermore in both tests the error ranges of the total air flow rate do overlap.

For tests G4-03 the agreement between the flows is very good, the greatest error being in flow Q_{01} (from -10 % to +20%) while in the other flows (Q_{05} , Q_{51} and Q_{15}) the error is smaller. In this test the error range of the simulated flows and of the measured flows always overlap.

For test G4-04 the simulated flows Q_{61} and Q_{01} are very close to the measured flows and the error ranges overlap; Q_{06} is overestimated by more than 100% but the error range of the simulated values includes the measured value for about a half of the measurement period. The mean measured value of the measurement period is within the error range of the mean simulated value.

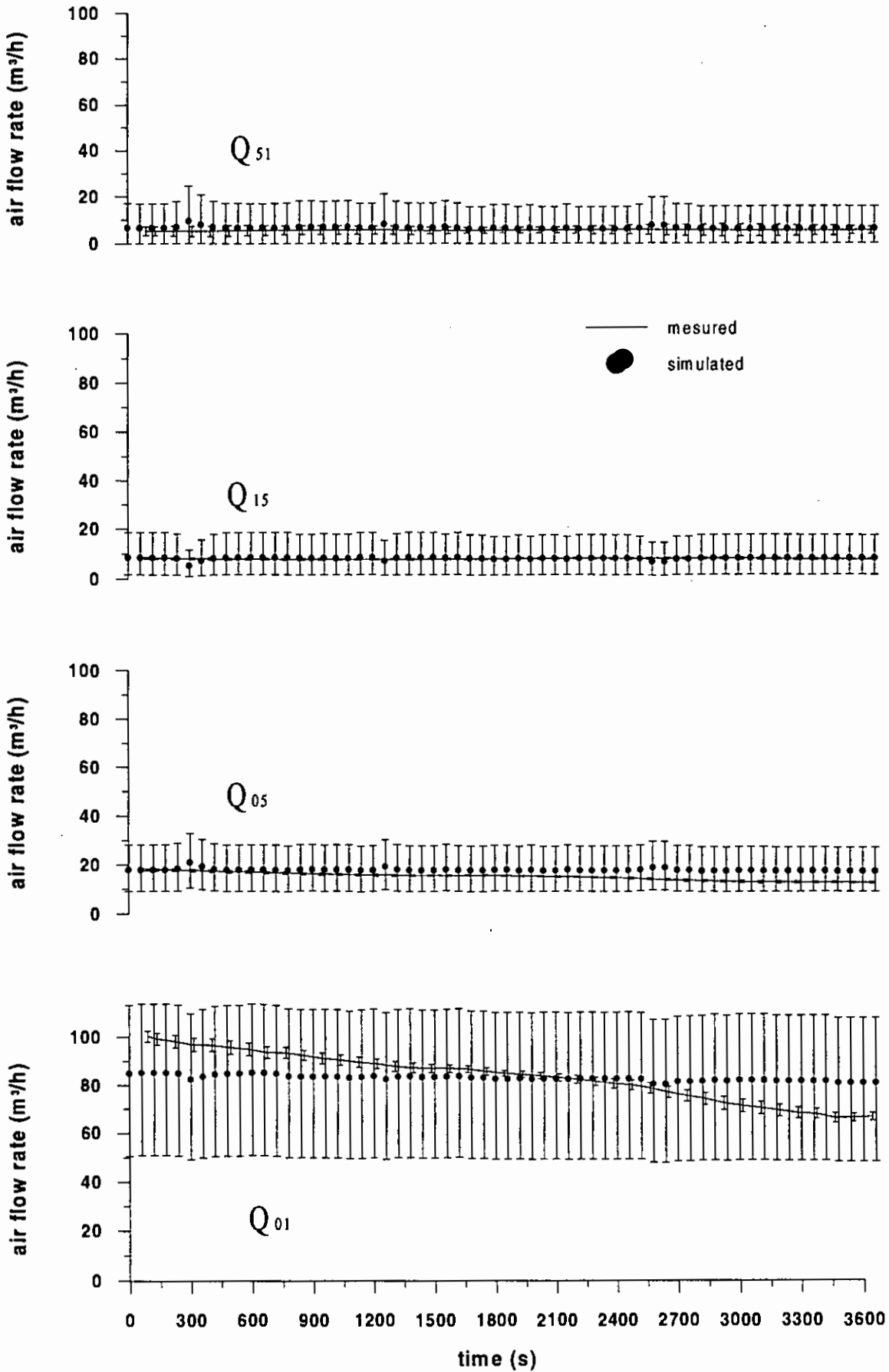


Figure A4.9.17 - Simulated and measured air flow rates Q_{51} , Q_{15} , Q_{05} , Q_{01} for test G4-03

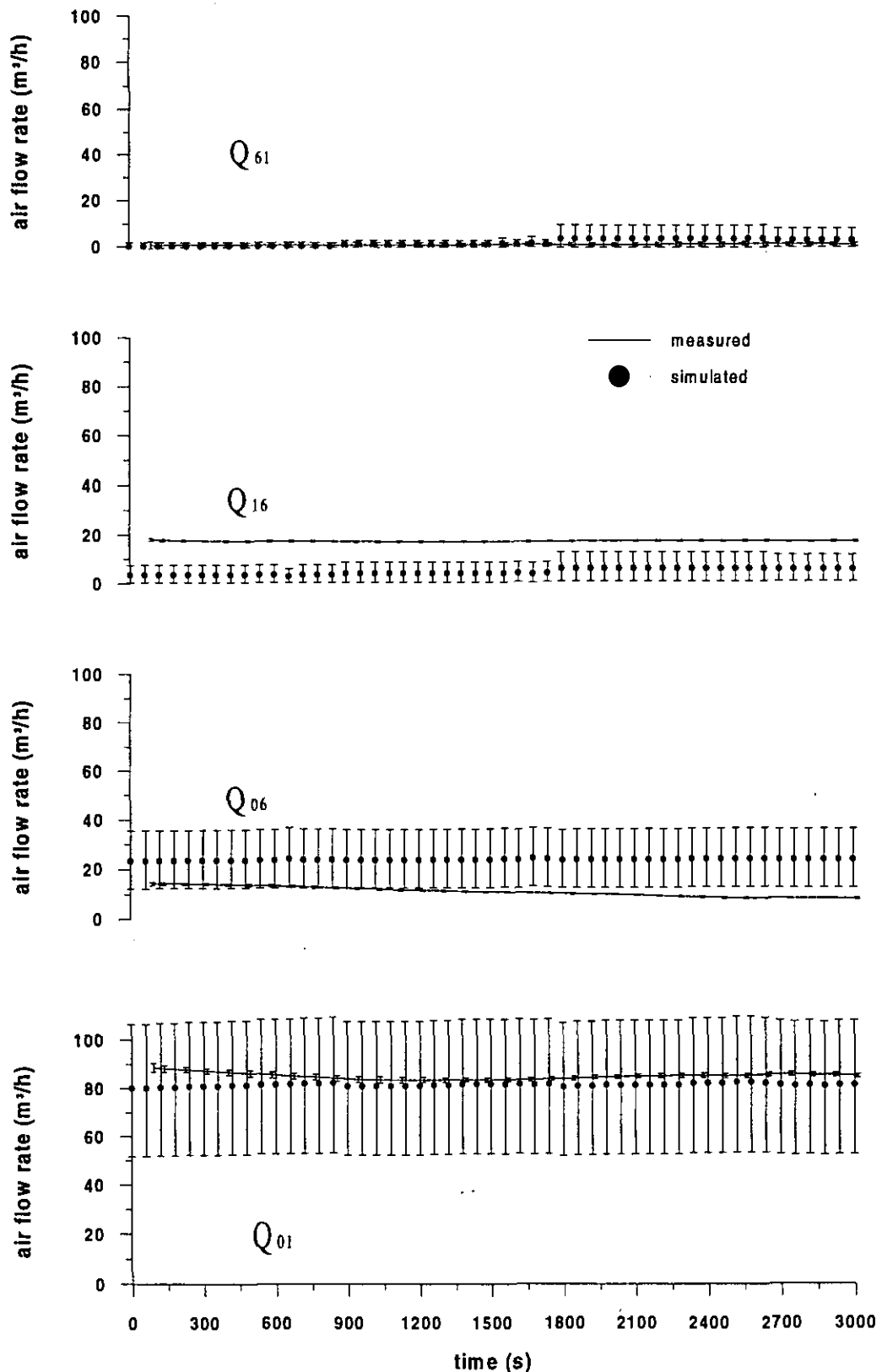


Figure A4.9.18 - Simulated and measured air flow rates Q_{61} , Q_{16} , Q_{06} , Q_{01} for test G4-04

The simulated flow Q_{16} is about 70% less than the measured value and the error ranges in this case never overlap. There are no evident reasons to explain this complete discrepancy. It is only possible to suppose that the literature value used to describe the internal door cracks in this case was not close to the actual value as for test G4-03.

A 4.9.5 Conclusion

COMIS has been used here to simulate the air flow rates inside a detached house and these calculated flows have been compared with the measured values taking into account the error range of each value. This comparison has provided useful information both for COMIS use and for the acquisition of the input data (i.e. crack characteristics).

The possibility of simulating devices (i.e. boiler) which are not included in the COMIS data base has been shown in tests G3-04 ÷ G3-12, but special attention has to be paid to the duct description, especially as far as the single loss coefficients are concerned.

The differences between the simulated total air flow rates and the experimental values in tests G3-15 and G3-16 are greater than the differences found in tests G4-03 and G4-04. This is related to a lack of information on the permeability of the building used for tests G3-15 and G3-16. Therefore, the task of deciding the correct definition of the building permeability is very important in order to achieve an accurate air flow simulation, even if an error range is associated with the simulated value.

Furthermore, the sufficient agreement obtained in tests G4-03 and G4-04, allows one to regard COMIS as a useful tool for analysing the air flow inside a detached house when thermal buoyancy is the main force causing the air flows.

Finally, it is important to remark upon the role of the error range associated with the simulated value in this comparison. Most of the values of simulated air flow rates are quite different from the measured values (even more than 100%) and only the overlapping of the error ranges has allowed any thoughts of reaching an agreement between the measured and the simulated flows. For this reason the use of COMIS in the air flow simulation is strongly related to the knowledge of the associated error range.

A 4.9.6 References

- Borchiellini R., Calì M. Torchio M.: Experimental Evaluation of COMIS Results for Ventilation of a Detached House. *ASHRAE Centennial Meeting 1995, to be published in the ASHRAE TRANS.1995, Vol. 1, Pt.1*
- Borchiellini R., Calì M.: Experimental and Numerical Analysis of Transient Air Changes in Buildings: A Case Study. Proc. of the 3rd International Conference "Air Distribution in Rooms" Roomvent '92, Aalborg Denmark, 2-4 September 1992, pp.417-433
- Fürbringer J.-M.: Sensibilité de modèles et de mesures en aéraulique du bâtiment à l'aide de plans d'expériences. PhD thesis, EPFL, Lausanne, CH, 1994.
- Fürbringer J.M., Borchiellini R.: Air flow simulation of test houses including comparison with measurements and sensitivity analysis - ASHRAE trans. 1993, V 100, Pt. 2.
- Masoero M., Fracastoro G.V., Vercelli D.: Analisi della permeabilità dell'aria degli edifici tramite prove di pressurizzazione. Contratto di ricerca: Analisi di sicurezza, efficienza energetica e qualità dell'aria nell'utilizzazione delle apparecchiature a gas Torino - Italy, settembre 1991.
- Roulet, C.A.; and L. Vandaele : Air Flow Patterns within Buildings; Measurement Techniques. AIVC TN 34, December 1991.
- Sherman, M.H.: Uncertainty in Air Flow Calculations Using Tracer Gas Measurements. Building and Environment Vol. 24, NO. 4, pp. 347-354.

A 5. USER TESTS

A 5.1 Proposals for changes in the User Manual and COMVEN

Changes in the user manual

1. Net Links: present examples of typical cracks, closed and open doors, typical ducts, together with the corresponding part of the input file, and clear explanations of the input values.
2. Net Zones, Meteo: Give a table of typical internal and external air humidity, relating absolute humidity to more usual values such as temperature and relative humidity.
3. Explain more clearly, possibly with a drawing, the reference heights and their influence.
4. Give a list of default values.
5. The term OPTIONAL DATA SECTION is confusing. There are two type of optional sections:
 - a) sections which can be deleted from the input file without changing the result of the calculation (e.g. control section)
 - b) sections which introduce default values when not specified, and which, therefore, may change the result of the calculation (e.g. sections 34 and 35)
6. These two types should be clearly differentiated.
7. Explain more clearly the reasons to define meteorological reference heights at the building and at the meteorological station, and the ways in which these input values are used. Figure 5.7.1 is not clear enough.

Changes in COMVEN

1. Introduce in COMVEN a test and a warning when some zones are not connected directly or indirectly to external nodes.
2. When default values are used, these should automatically appear in a revised copy of the input file.


```
&-NET-AIR flow components
# Allowed prefixes are: *CR *FA *DS *DF *F1 *F2 *F3 *F4 *WI *TD
#
#          | crack | duct | flow-controllers | testdata
points
#          fan      duct-fitting      window(openable)
# keep the KEYWORDS &-CR,...,&-TD in this part &-NET-AIR
&-CR      CRACK
```

1.	Cs (kg/s@1Pa)	Exp n (-)	Lenght [m]	Wall Properties	
				Thickness [m]	U-Value [W/m2 K]

2.	Filter 1 (-)	Filter 2 [-]	Filter 3 [-]	Filter 4 [-]	Filter 5 [-]
----	-----------------	-----------------	-----------------	-----------------	-----------------

```
*CRE1 external crack 1 (bedroom 1)
0.004 0.6
0
*CRE2 external crack 2 (bedroom 2)
0.005 0.6
0
*CRE3 external crack 3 (bedroom 3)
0.0022 0.6
0
*CRE4 external crack 4 (living room)
0.0048 0.6
0
*CRE5 external crack 5 (kitchen)
0.0044 0.6
0
*CRE10 external crack 10 (front door)
0.0015 0.6
0
*CRD internal door
0.01 0.5
0
&-WI Windows and doors
*WIDO Door
0.01 0.5 1 1.0 2.0 0.0
0.0 0.6 0.0 0.0 0.0
1.0 0.6 1.0 1.0 0.0
0.0
&-DS Duct straight
*DSM Main duct
0.23 0.18 0.03 14.4 1.0
0.0
0.0
# Duct leakage can not be simulated with this COMVEN version
*DSW WC duct
0.1 0.1 0.03 0.2 1. 2 20
0.0
0.0
*DSK Kitchen duct
0.23 0.1 0.03 2.5 1. 2 20
0.0
0.0
# Comment: zeta put to 1 since no clear indication is given on the geometry.
```

&-NET-ZONES

18

Zone No (-)	Name [-]	Temp [oC]	Ref. Height [m]	Vol [m3]	Abs. Hum [gr/kg]	Schedule Name [T./H..]
1	Bedroom1	20.	15.	34.5	8.	
2	Bedroom2	20.	15.	32.5	8.	
3	Bedroom3	20.	15.	18.7	8.	
4	Living	20.	15.	77.2	8.	
5	Kitchen	20.	15.	28.4	8.	
6	Hallinterne	20.	15.	17.3	8.	
7	Laundry	20.	15.	6.0	8.	
8	Bathroom	20.	15.	5.3	8.	
9	WC	20.	15.	3.2	8.	
10	Hall	20.	15.	7.6	8.	
11	Ventilation_Box	20.	15.	0.2	8.	

Comment: Reference heighth of zones is put to 15 m, that is on the floor of the room.

&-NET-EXtErnal node data

21

--- OPTIONAL DATASECTION ---

External Node No (-)	Facade Elem No (-)	Outside Conc Factor [-]
1	1	1.
2	2	1.
3	3	1.

&-NET-LINKs

22

Link No (-)	Type Name (-)	Zone No		Height		Own Height [m]	Act. Val. [-]	3Dflow or Press [Pa]	Schedule Name(5char.)	
		From (-)	To (-)	From [m]	To [m]				T-Junct. No [-]	Ref.Link Angle [deg]
11	CRE1	1	-1	1.	16.					
16	CRD	1	6	1.	1.					
22	CRE2	2	-2	1.	16.					
210	CRD	2	10	1.	1.					
31	CRE3	3	-1	1.	16.					
36	CRD	3	6	1.	1.					
41	CRE4	4	-1	1.	16.					
46	WIDO	4	6	1.	1.	1.	1.			
52	CRE5	5	-2	1.	16.					
56	CRD	5	6	1.	1.					
76	CRD	7	6	1.	1.					
78	CRD	7	8	1.	1.					
79	CRD	7	9	1.	1.					
511	DSK	5	11	2.6	2.6					
811	DSW	8	11	2.6	2.6					
911	DSW	9	11	2.6	2.6					
106	CRD	10	6	1.	1.					
102	CRE10	10	-2	1.	16.					
113	DSM	11	-3	2.6	32.					

Comment: Exchange height is put to 1 m. Reference height of external zones is put to 0 m. Extract is therefore at 2.6 (+15) m indoors and goes to 32 (+0) m outdoors, on the roof.

&-CP-BUILDing reference height for Cp data 32 - OPTIONAL DATASECTION ---

Height (m)

30.0

Comment: this is the reference height for wind measurement, which is used as reference height for Cp calculation.

&-CP-VALUes

33

--- OPTIONAL DATASECTION ---

1.	Dataset Name
	UTEST2

2.	Facade	Winddirection					(first line)			
	Elemno	Cp Values					(second and following lines)			
*	(-)	(deg)	[deg]	[deg]	[deg]	[deg]	[deg]	[deg]	[deg]	[deg]
*		0.	90.	180.	270.					
1		0.1	-0.4	-0.2	-0.4					
2		-0.2	-0.4	0.1	-0.4					
3		-0.5	-0.5	-0.5	-0.5					

Comment: The pressure coefficients are taken out of the AIVC calculation handbook, page 6.9. Surrounding buildings are assumed to be at the same heighth.

&-ENV-BUILDing related parameters 34

--- OPTIONAL DATASECTION ---

1.	Altitude	Angle Building	Geographic Position	
	(m)	North to-X-Axis	Latitude +=N	Longitude +=E
		(deg)	[deg] --S	[deg] --W
0.	90.	50.	2.	

Comment: This section should not be optional, since the building orientation has a large influence on the results.

&-ENV-WIND and meteo related parameters 35

--- OPTIONAL DATASECTION ---

1.	Ref. Height	Altitude
	for Wind Speed	Meteo Station
	(m)	(m)
30.	0.	0.32

2.	Wind	Plan Area	Wind	Surrounding
	Direction	Density	Velocity Profile	Buildings Height
	Angle	(-)	Exponent	(m)
	(deg)		(-)	
0.		0.144	0.32	30
270.		0.144	0.32	30

&-SCH-METeo data

36

--- OPTIONAL DATASECTION ---

#-----
METEO DESCRIPTION
#-----

1. Dataset Name						
UTEST2						
2. Time		Wind		Temperature	Humidity	Barometer Pressure Absolute
(-)		Speed (m/sec)	Direction (deg)	(oC)	[g/kg]	[kPa]
1993jan01_00:00		0.	0.	0.	4.	101.3
1993jan02_00:00		1.	0.	0.	4.	101.3
1993jan03_00:00		2.	0.	0.	4.	101.3
1993jan04_00:00		5.	0.	0.	4.	101.3
1993jan05_00:00		10.	0.	0.	4.	101.3
1993jan06_00:00		0.	270.	0.	4.	101.3
1993jan07_00:00		1.	270.	0.	4.	101.3
1993jan08_00:00		2.	270.	0.	4.	101.3
1993jan09_00:00		5.	270.	0.	4.	101.3
1993jan10_00:00		10.	270.	0.	4.	101.3
1993jan11_00:00		0.	0.	10.	4.	101.3
1993jan12_00:00		1.	0.	10.	4.	101.3
1993jan13_00:00		2.	0.	10.	4.	101.3
1993jan14_00:00		5.	0.	10.	4.	101.3
1993jan15_00:00		10.	0.	10.	4.	101.3
1993jan16_00:00		0.	270.	10.	4.	101.3
1993jan17_00:00		1.	270.	10.	4.	101.3
1993jan18_00:00		2.	270.	10.	4.	101.3
1993jan19_00:00		5.	270.	10.	4.	101.3
1993jan20_00:00		10.	270.	10.	4.	101.3
1993jan21_00:00		0.	0.	20.	4.	101.3
1993jan22_00:00		1.	0.	20.	4.	101.3
1993jan23_00:00		2.	0.	20.	4.	101.3
1993jan24_00:00		5.	0.	20.	4.	101.3
1993jan25_00:00		10.	0.	20.	4.	101.3
1993jan26_00:00		0.	270.	20.	4.	101.3
1993jan27_00:00		1.	270.	20.	4.	101.3
1993jan28_00:00		2.	270.	20.	4.	101.3
1993jan29_00:00		5.	270.	20.	4.	101.3
1993jan30_00:00		10.	270.	20.	4.	101.3

